Reconstructing Devonian palaeoatmosphere & palaeoecology using fossil plant traits

A thesis submitted for the degree of master's in science by research,

July 2024,

Bea Jackson (17331160).

Discipline of Botany,

School of Natural Sciences,

Trinity College Dublin.

Supervisor: Prof. Jennifer McElwain

Co-Supervisor: Dr. Carla Harper

Declaration

I declare that this thesis has not been submitted as an exercise for a degree at this or any other university and it is entirely my own work.

I agree to deposit this thesis in the University's open access institutional repository or allow the Library to do so on my behalf, subject to Irish Copyright Legislation and Trinity College Library conditions of use and acknowledgement.

I do not consent to the examiner retaining a copy of the thesis beyond the examining period, should they so wish (EU GDPR May 2018).

Signed: Date: 01/7/2024

Bea Jackson

Summary

This thesis examines the reconstruction of atmospheric CO_2 concentration during the Devonian period and the palaeoecology of Ireland's first fossil forests at the Devonian/Carboniferous boundary. The expansion and diversification of terrestrial plant life during the Devonian period is thought to have had significant consequences for atmospheric CO_2 concentrations via enhanced weathering processes. However, there is a paucity of existing CO_2 proxy data for this period. The advent of mechanistic gas exchange proxies in recent years has provided an opportunity to better constrain changes in atmospheric CO_2. Paired stomatal measurements and carbon isotopic data from *Sawdonia* plant fossils were used to parameterise the gas-exchange-based model of Franks et al. (2014) to reconstruct atmospheric CO_2 concentrations for the Emsian stage of the Devonian (Chapter 2). The results of this chapter indicate atmospheric CO_2 concentrations were approximately 898 ppm (+616/-405 ppm) prior to the emergence of forest ecosystems. A sensitivity analysis of input parameters for the model was used to inform revisions to existing estimates using the same model. The thesis goes on to investigate the leaf morphological diversity and leaf allometry of *Archaeopteris hibernica* in one of Ireland's first fossil forest ecosystem (Chapter 3). Chapter 4 considers the physiological and ecological functioning of *Archaeopteris hibernica* using established methods to estimate the fossil plant functional traits of leaf mass per area and maximum stomatal conductance. The leaf trait analysis of *A. hibernica* was found to indicate that *A. hibernica* had a high leaf mass investment per unit area and a probable stress-tolerant ecological strategy. Finally, future directions for research and the limitations of this study are discussed in Chapter 5. The findings of this thesis highlights the need to further clarify the atmospheric and environmental context and physiological functioning of the first forest ecosystems to understand the evolution of plant-climate and plant-atmosphere interactions.

Acknowledgements

I would like to thank a number of people without whom this thesis would not be possible. First, I would like to thank my supervisor, Jenny McElwain, for her enthusiasm, support and guidance over the past two years. I would also like to thank my co-supervisor, Carla Harper, for her invaluable and practical advice and encouragement during this project. This Research Master's was possible thanks to the funding provided by the ERC Terraform project and a Trinity non-foundational scholarship. I am very fortunate to have had this opportunity to pursue such an interesting research project.

I am grateful for the opportunity to have completed my studies in such a welcoming and supportive environment. A special thank you to Will Matthaeus, for his support and encouragement, his help with R and many helpful discussions. I would also like to thank everyone in the Plant-Climate Interactions lab group over the past two years, for all of the interesting discussions (academic or otherwise), as well as the friendship and encouragement: Christos Chondrogiannis, Katie O'Dea, Kamila Kwasniewska, Midori Yajima, Antonietta Knetge, Catarina Barbosa, Sate Ahmad, Richard Nair, Michelle Murray, Weimu Xu, Danielle Gallagher, Deirdre McClean and Adam Bates. I would also like to thank Thibault Durieux, for interesting discussions and for helping me in photographing fossils from the National Museum of Ireland Collections.

I would also like to thank Patrick Wyse Jackson from TCD Geology Museum, Mike Simms from The National Museum of Northern Ireland and Patrick Roycroft from the National Museum of Ireland for facilitating me accessing the fossils in their collections. Thank you to Cyrille Prestianni, Ed Jarvis and Chris Mays for interesting discussions about *Archaeopteris* and the Kiltorcan flora.

Finally, I would like to thank my family for their love, support and encouragement. Thank you for everything.

Table of Contents

List of Tables

List of Figures

1. Introduction

The Devonian period (419.2 - 358.9 million years ago [Ma]) was a time of great evolutionary transition and diversification in plant history. The emergence of leaves, secondary xylem, arborescence, deep roots and seeds in the Devonian fossil record distinguishes it as a crucial period in plant evolution (Hetherington and Dolan, 2018, Prestianni and Gerrienne, 2010, Shougang et al., 2003, Stein et al., 2007, Stein et al., 2020, Strullu-Derrien et al., 2013). Furthermore, ecosystems developed dramatically over this period from simple ecological communities to the more complex and diverse ecosystems seen in Earth's 'oldest forests' of the Middle Devonian (Stein et al., 2007, Stein et al., 2012).

The diversification and evolutionary innovations of plants during this period had consequences for the long-term carbon cycle as they provided biotic feedbacks on CO_2 sequestration via a number of different direct and indirect impacts on the weathering of calcium and magnesium silicate rocks (Algeo and Scheckler, 1998, Algeo, 2010, Beerling and Berner, 2005, Berner, 1997, Elick et al., 1998, Ibarra et al., 2019, Pawlik et al., 2020, Quirk et al., 2015). The cumulative effect of vascular plant evolution on weathering processes, soil formation and nutrient and carbon cycling has also been proposed as a trigger for widespread ocean anoxia and biotic crises during the Upper Devonian (i.e., the Frasnian-Famennian Kelwasser and the end-Devonian Hangenberg events) (Algeo and Scheckler, 1998, Algeo, 2010, Qie et al., 2023). The "Devonian plant hypothesis" proposes that the expansion of tracheophytes with deeper rooting systems led to enhanced weathering processes, leading to nutrient influx and eventual ocean eutrophication and anoxia (2010, Algeo and Scheckler, 1998, Pawlik et al., 2020, Qie et al., 2023). However, the magnitude of effect of terrestrial plants on these biotic crises is controversial; a number of studies suggest greater importance of abiotic triggers such as volcanism (Racki et al., 2018, Racki, 2020), as the main cause of global change during the Upper Devonian. These effects were likely amplified by other processes (including the effects of root-assisted weathering) in a more complex, multicausal scenario (Bond and Grasby, 2017, Carmichael et al., 2019,

Kaiser et al., 2016). Furthermore, a recent modelling study by D'Antonio et al. (2020) based on carbon mass-balance constraints has suggested that land plant evolution did not increase weathering rates, contradicting the main assumptions of the Devonian plant hypothesis. However, under this alternative hypothesis land plants may have still caused reductions in atmospheric CO_2 via increased weathering feedback strength, as opposed to enhanced weathering rates (D'Antonio et al., 2020).

Existing reconstructions of Devonian atmospheric composition document a decline in CO_2 concentrations as the terrestrial biosphere developed. However, atmospheric CO_2 proxy data for this period is relatively sparse and is associated with significant uncertainty (Dahl et al., 2022, Foster et al., 2017, Witkowski et al., 2018). Therefore, the magnitude of atmospheric CO_2 change over this period is poorly resolved with more recent studies indicating a more gradual decrease than previously thought (Dahl et al., 2022, Witkowski et al., 2018). A study by Dahl et al. (2022) has indicated that atmospheric CO_2 concentrations were low prior to the emergence of deep-rooted forest ecosystems, suggesting that the emergence of these novel evolutionary traits may have had a more limited impact on weathering and therefore atmospheric composition than previously thought. Despite multiple competing hypotheses on the evolution of plant-atmosphere interactions over the Devonian period, the ecophysiological function of the first trees remains poorly quantified.

Plant traits observed from the fossil record provide information on deep-time biosphere processes as they affect and respond to their environment (Brown et al., 2023, Matthaeus et al., 2023, McElwain et al., 2024; see *Appendix 1.1* for author contributions). For example, the stomatal density response of plants to changing atmospheric CO_2 concentrations is well established (Woodward, 1987), and stomatal traits (i.e. stomatal size, density, and different physiological control mechanisms) have been widely researched and used to develop a number of different proxies for atmospheric CO_2 concentrations (Barclay and Wing, 2016, Brodribb and McAdam, 2017, Franks et al., 2014, Jordan, 2011, Konrad et al., 2008, Konrad et al., 2017, Konrad et al., 2021, Kowalczyk et al., 2018, McElwain and Chaloner, 1996, McElwain, 2017, Roth-Nebelsick and Konrad, 2003, Roth-Nebelsick, 2005) which have been

broadly applied over the Phanerozoic (see e.g. the data compilation of Foster et al. (2017)). Stomatal traits have also been used to understand changes in plant transpirational capacity and the hydrological cycle over time (Steinthorsdottir et al., 2012). These same approaches using stomatal traits and isotope geochemistry from plant fossils (Franks et al., 2014) will be used to inform the atmospheric CO_2 reconstruction in this thesis for the Devonian period (Chapter 2).

Fossil plant traits present valuable research potential to develop a better understanding of plant palaeoecological strategies, and the role of land plants in broad scale Earth system processes (Brown et al., 2023, Matthaeus et al., 2023, McElwain et al., 2024). Fossil plant traits have been broadly applied to angiosperm fossil taxa to understand plant strategies and ecophysiological function in the Cenozoic and late Mesozoic (Blonder et al., 2014, Boyce et al., 2010, Brodribb and Feild, 2010, Carvalho et al., 2021, Royer et al., 2007, Royer et al., 2010). However, this palaeo-trait approach has had more limited application to deep-time taxa, particularly during the Palaeozoic (although see Schwendemann (2018), Tanrattana et al. (2019), Wilson et al. (2020) and references therein), where inferences of palaeo-plant function are often based on non-analogue combinations of anatomical and morphological characteristics that existed in vastly different climatic and atmospheric contexts than today (Matthaeus et al., 2023, McElwain et al., 2024). In the context of this thesis, Devonian plant fossils are relatively rare and poorly preserved and often lack clear living analogue taxa, making fossil-based plant trait inferences for the Devonian a challenging, but potentially informative approach to understanding plant function (Chapter 4).

Despite the incomplete nature of the plant fossil record, the Devonian rocks of Ireland's Old Red Sandstone have yielded a rich plant fossil record demonstrating key features of the Devonian plant evolutionary transition. These fossils include some of the earliest seeds (Chaloner et al., 1977), arborescent lycophytes (Klavins, 2004), gymnosperms (Matten et al., 1980) and progymnosperms (Decombeix et al., 2023). Recent palaeobotanical research in Ireland has included a reinvestigation of fossil bearing localities in the south of Ireland, and has yielded new fossils demonstrating evidence of tylosis formation in

archaeopteridalean progymnosperm wood (Decombeix et al., 2022, Decombeix et al., 2023). At this time, Ireland was situated south of the equator on the eastern margin of Euramerica, with the Acadian mountain range to the northwest and west (Graham, 2009, Klavins, 1999). Studies on palaeoclimatically sensitive sediments position Ireland approximately 35 degrees south of the equator, moving gradually closer to the equator over time (Graham, 2009). However, palaeomagnetic reconstructions place Ireland further north - between 5 and 15 degrees south of the equator (Kendall, 2017). Palaeomagnetic reconstructions also show the same northwards shift over time.

Perhaps the most famous Devonian plant fossil locality within Ireland is that of Kiltorcan, Co. Kilkenny, which has yielded a range of plant macrofossils and freshwater fauna, including progymnosperms, arborescent lycophytes, freshwater bivalves, placoderms, eurypterids and peracarid crustaceans (Baily, 1869, Baily, 1872, Carpenter and Swain, 1908, Chaloner, 1968, Chaloner et al., 1977, Johnson, 1911, Ritchie, 1975, Robin et al., 2021). The Kiltorcan Hill outcrops have yielded both LE ('Strunian', latest Famennian) and VI (lowermost Carboniferous) miospore assemblages, therefore the strata of Kiltorcan Hill straddle the Devonian/Carboniferous boundary (Jarvis, 1990). The 'classic' *Archaeopteris-Cyclostigma* assemblage of the Old Plant Quarry has not yielded miospore assemblages to date, but is thought to date to the latest Famennian (Jarvis, 1990). Substantial natural history collections of well-preserved leaf material of *Archaeopteris hibernica* (Forbes) Stur are the result of a number of large-scale excavations of Kiltorcan Hill during the 19th and 20th centuries, and provide extensive material to investigate the ecological function of the first 'modern' trees.

The fossil record can preserve unique trait combinations not seen today with some extinct lineages occupying an intermediate morphospace between extant lineages (Clark et al., 2023). The Progymnospermopsida (progymnosperms) are an example of an extinct lineage which occupies this intermediate morphospace (Clark et al., 2023), with a unique combination of sporophyte reproductive traits and spermatophyte-like vegetative traits. Progymnosperms are a paraphyletic group that are a sister group to the seed plants and are thought to have evolved from the homosporous Trimerophytopsida (Bateman and

DiMichele, 1994, Wang et al., 2021). *Archaeopteris* (Dawson) Stur is a progymnosperm genus that formed a predominant component of Upper Devonian forest ecosystems, with microfossil and macrofossil evidence indicating that they first emerged by the early Givetian (388-383 Ma) (Stein et al., 2020) and last occurred in the fossil record during the Lower Mississippian (Beck, 1962). While arborescence evolved independently in a number of taxa, *Archaeopteris* is particularly notable for its extensive, advanced rooting systems, leafy branch systems and extensive secondary growth (Meyer-Berthaud, 1999, Stein et al., 2020). It is likely that *Archaeopteris* had a far greater impact on Devonian environments and ecosystem processes compared to coeval arborescent taxa which lacked these characteristics (Meyer-Berthaud et al., 1999, Meyer-Berthaud and Decombeix, 2007, Meyer-Berthaud et al., 2010, Stein et al., 2007, Stein et al., 2020). Further understanding of the taxon-specific physiological function and ecology conferred by the combination of traits observed in *Archaeopteris* is needed to try to elucidate the potential of the first forests to impact the environment (in particular weathering rates and atmospheric CO_2 concentration) during the Devonian (Meyer-Berthaud et al., 2010, Stein et al., 2020).

The main aims of this thesis are:

1. To reconstruct atmospheric CO_2 concentrations during the Devonian period and to re-evaluate existing estimates in the context of more recent fossil plant proxies (Chapter 2)
2. To characterise functional diversity within *Archaeopteris* of the Kiltorcan flora using a preliminary study of morphological variation of *Archaeopteris hibernica* (Forbes) Stur fossil leaf material (Chapter 3)
3. To utilise a modern functional trait framework to understand the physiological and ecological functioning of the first modern trees from the Kiltorcan flora (Chapter 4)

References

ALGEO, T. J., & SCHECKLER, S.E. 2010. Land plant evolution and weathering rate changes in the Devonian. *Journal of Earth Science,* 21**,** 75-78.

ALGEO, T. J. & SCHECKLER, S. E. 1998. Terrestrial-marine teleconnections in the Devonian: links between the evolution of land plants, weathering processes, and marine anoxic events. *Philosophical Transactions of the Royal Society of London. Series B: Biological Sciences,* **353,** 113-130.

BAILY, W. H. 1869. Report on fossils obtained at Kiltorcan Quarry, Co. Kilkenny. *Report of the British Association for the Advancement of Science***,** 73-75.

BAILY, W. H. 1872. The Kiltorcan fossils. *Nature,* **5,** 224–225.

BARCLAY, R. S. & WING, S. L. 2016. Improving the ginkgo CO_2 barometer: implications for the early Cenozoic atmosphere. *Earth and Planetary Science Letters,* **439,** 158-171.

BATEMAN, R. M. & DIMICHELE, W. A. 1994. Heterospory: the most iterative key innovation in the evolutionary history of the plant kingdom. . *Biological Reviews,* **69,** 345-417.

BECK, C. B. 1962. Plants of the New Albany Shale. II. *Callixylon arnoldii* Sp. Nov. *Brittonia,* **14,** 322-327.

BEERLING, D. J. & BERNER, R. A. 2005. Feedbacks and the coevolution of plants and atmospheric CO_2. *Proceedings of the National Academy of Sciences of the United States of America,* **102,** 1302-1305.

BERNER, R. A. 1997. The rise of plants and their effect on weathering and atmospheric CO_2. *Science,* **276,** 544-546.

BLONDER, B., ROYER, D. L., JOHNSON, K. R., MILLER, I. & ENQUIST, B. J. 2014. Plant ecological strategies shift across the Cretaceous–Paleogene boundary. *PLoS Biology,* **12,** e1001949.

BOND, D. P. & GRASBY, S. E. 2017. On the causes of mass extinctions. *Palaeogeography, Palaeoclimatology, Palaeoecology,* **478,** 3-29.

BOYCE, C. K., LEE, J.-E., FEILD, T. S., BRODRIBB, T. J. & ZWIENIECKI, M. A. 2010. Angiosperms helped put the rain in the rainforests: the impact of plant physiological evolution on tropical biodiversity. *Annals of the Missouri Botanical Garden,* **97,** 527-540.

BRODRIBB, T. J. & FEILD, T. S. 2010. Leaf hydraulic evolution led a surge in leaf photosynthetic capacity during early angiosperm diversification. *Ecology letters,* **13,** 175-183.

BRODRIBB, T. J. & MCADAM, S. A. 2017. Evolution of the stomatal regulation of plant water content. *Plant physiology,* **174,** 639-649.

BROWN, K. A., BUNTING, M. J., CARVALHO, F., DE BELLO, F., MANDER, L., MARCISZ, K., MOTTL, O., REITALU, T. & SVENNING, J. C. 2023. Trait-based approaches as ecological time machines: developing tools for reconstructing long-term variation in ecosystems. *Functional Ecology***,** 1-18.

CARMICHAEL, S. K., WATERS, J. A., KOENIGSHOF, P., SUTTNER, T. J. & KIDO, E. 2019. Paleogeography and paleoenvironments of the Late Devonian Kellwasser event: a review of its sedimentological and geochemical expression. *Global and Planetary Change,* **183,** 102984.

CARPENTER, G. H. & SWAIN, I. 1908. A new Devonian isopod from Kiltorcan, County Kilkenny. *Proceedings of the Royal Irish Academy. Section B: Biological, Geological, and Chemical Science,* **27,** 61-67.

CARVALHO, M. R., JARAMILLO, C., DE LA PARRA, F., CABALLERO-RODRÍGUEZ, D., HERRERA, F., WING, S., TURNER, B. L., D'APOLITO, C., ROMERO-BÁEZ, M. & NARVÁEZ, P. 2021. Extinction at the end-Cretaceous and the origin of modern Neotropical rainforests. *Science,* **372,** 63-68.

CHALONER, W. G. 1968. The cone of *Cyclostigma kiltorkense* Haughton, from the Upper Devonian of Ireland. *Botanical Journal of the Linnean Society,* **61,** 25-36.

CHALONER, W. G., HILL, A. J. & LACEY, W. S. 1977. First Devonian platyspermic seed and its implications in gymnosperm evolution. *Nature,* **265,** 233-235.

CLARK, J. W., HETHERINGTON, A. J., MORRIS, J. L., PRESSEL, S., DUCKETT, J. G., PUTTICK, M. N., SCHNEIDER, H., KENRICK, P., WELLMAN, C. H. & DONOGHUE, P. C. J. 2023. Evolution of phenotypic disparity in the plant kingdom. *Nature Plants*.

D'ANTONIO, M. P., IBARRA, D. E. & BOYCE, C. K. 2020. Land plant evolution decreased, rather than increased, weathering rates. *Geology,* **48,** 29-33.

DAHL, T. W., HARDING, M. A., BRUGGER, J., FEULNER, G., NORRMAN, K., LOMAX, B. H. & JUNIUM, C. K. 2022. Low atmospheric CO_2 levels before the rise of forested ecosystems. *Nature Communications,* **13,** 7616.

DECOMBEIX, A.-L., HARPER, C. J., PRESTIANNI, C., DURIEUX, T., RAMEL, M. & KRINGS, M. 2023. Fossil evidence of tylosis formation in Late Devonian plants. *Nature Plants,* **9, 1-4**.

DECOMBEIX, A. L., DURIEUX, T., HARPER, C. J., MEYER-BERTHAUD, B., PRESTIANNI, C., MERLIN, R. & MALGORZATA, H.-S. Reinvestigating the Late Devonian plant bearing localities of Co. Kerry and Co. Wexford, Ireland. *In:* MCLOUGHLIN, S., ed. 11th European Palaeobotany and Palynology Conference, 2022 Stockholm, Sweden. Swedish Museum of Natural History.

ELICK, J. M., DRIESE, S. G. & MORA, C. I. 1998. Very large plant and root traces from the Early to Middle Devonian: implications for early terrestrial ecosystems and atmospheric p(CO_2). *Geology,* **26,** 143-146.

FOSTER, G. L., ROYER, D. L. & LUNT, D. J. 2017. Future climate forcing potentially without precedent in the last 420 million years. *Nature communications,* **8,** 14845.

FRANKS, P. J., ROYER, D. L., BEERLING, D. J., VAN DE WATER, P. K., CANTRILL, D. J., BARBOUR, M. M. & BERRY, J. A. 2014. New constraints on atmospheric CO_2 concentration for the Phanerozoic. *Geophysical Research Letters,* **41,** 4685-4694.

GRAHAM, J. R. 2009. Devonian. *In:* HEPWORTH HOLLAND, C. & SANDERS, I. A. (eds.) *The Geology of Ireland.* Edinburgh, Scotland: Dunedin Academic Press ltd.

HETHERINGTON, A. J. & DOLAN, L. 2018. Stepwise and independent origins of roots among land plants. *Nature,* **561,** 235-238.

IBARRA, D. E., RUGENSTEIN, J. K. C., BACHAN, A., BARESCH, A., LAU, K. V., THOMAS, D. L., LEE, J.-E., BOYCE, C. K. & CHAMBERLAIN, C. P. 2019. Modeling the consequences of land plant evolution on silicate weathering. *American Journal of Science,* **319,** 1-43.

JARVIS, D. E. 1990. New palynological data on the age of the Kiltorcan flora of Co. Kilkenny, Ireland. *Journal of micropaleontology,* **9,** 87-94.

JOHNSON, T. 1911. The occurrence of *Archaeopteris tschermaki* Stur. and of other species of *Archaeopteris* in Ireland. *Scientific Proceeding of the Royal Dublin Society,* **13,** 137-141.

JORDAN, G. J. 2011. A critical framework for the assessment of biological palaeoproxies: predicting past climate and levels of atmospheric CO_2 from fossil leaves. *New Phytologist,* **192,** 29-44.

KAISER, S. I., ARETZ, M. & BECKER, R. T. 2016. The global Hangenberg Crisis (Devonian–Carboniferous transition): review of a first-order mass extinction. *In:* BECKER, R. T., KONIGSHOF, P. & BRETT, C. E. (eds.) *Devonian Climate, Sea Level and Evolutionary Events.* London: Geological Society, London, Special Publications.

KENDALL, R. S. 2017. The Old Red Sandstone of Britain and Ireland: a review. *Proceedings of the Geologists' Association,* **128,** 409-421.

KLAVINS, S. D. 1999. *Systematics and paleoecology of three Late Devonian floras of southern Ireland.* PhD Thesis, Southern Illinois University, Carbondale.

KLAVINS, S. D. 2004. Re-interpretation of *Wexfordia hookense* from the Upper Devonian of Ireland as an arborescent lycophyte. *Botanical Journal of the Linnean Society,* **144,** 275-287.

KONRAD, W., KATUL, G., ROTH-NEBELSICK, A. & GREIN, M. 2017. A reduced order model to analytically infer atmospheric CO_2 concentration from stomatal and climate data. *Advances in Water Resources,* **104,** 145-157.

KONRAD, W., ROTH-NEBELSICK, A. & GREIN, M. 2008. Modelling of stomatal density response to atmospheric CO_2. *Journal of theoretical Biology,* **253,** 638-658.

KONRAD, W., ROYER, D. L., FRANKS, P. J. & ROTH-NEBELSICK, A. 2021. Quantitative critique of leaf-based paleo-CO_2 proxies: consequences for their reliability and applicability. *Geological Journal,* **56,** 886-902.

KOWALCZYK, J. B., ROYER, D. L., MILLER, I. M., ANDERSON, C. W., BEERLING, D. J., FRANKS, P. J., GREIN, M., KONRAD, W., ROTH-NEBELSICK, A. & BOWRING, S. A. 2018. Multiple proxy estimates of atmospheric CO_2 from an early Paleocene rainforest. *Paleoceanography and Paleoclimatology,* **33,** 1427-1438.

MATTEN, L. C., LACEY, W. S., MAY, B. I. & LUCAS, R. C. 1980. A megafossil flora from the Uppermost Devonian near Ballyheigue, Co. Kerry, Ireland. *Review of Paleobotany and Palynology,* **29,** 241-251.

MATTHAEUS, W. J., MACAREWICH, S. I., RICHEY, J., MONTAÑEZ, I. P., MCELWAIN, J. C., WHITE, J. D., WILSON, J. P. & POULSEN, C. J. 2023. A systems approach to understanding how plants transformed earth's environment in deep time. *Annual Review of Earth and Planetary Sciences,* **51,** 551-580.

MCELWAIN, J. C., AND STEINTHORSDOTTIR, M. 2017. Paleoecology, ploidy, paleoatmospheric composition, and developmental biology: a review of the multiple uses of fossil stomata. *Plant Physiology,* **174,** 650–664.

MCELWAIN, J. C. & CHALONER, W. G. 1996. The fossil cuticle as a skeletal record of environmental change. *Palaios,* **11,** 376-388.

MCELWAIN, J. C., MATTHAEUS, W. J., BARBOSA, C., CHONDROGIANNIS, C., O'DEA, K., JACKSON, B., KNETGE, A., KWASNIEWSKA, K., NAIR, R., WHITE, J. D., WILSON, J. P., MONTAÑEZ, I. P., BUCKLEY, Y. M., BELCHER, C. M. & NOGUÉ, S. 2024. Functional traits of fossil plants. *New Phytologist,* **242(2),** 392-423.

MEYER-BERTHAUD, B. 1999. *Archaeopteris* is the earliest known modern tree. *Nature,* **398,** 700-701.

MEYER-BERTHAUD, B. & DECOMBEIX, A. L. 2007. A tree without leaves. *Nature,* **446,** 861-862.

MEYER-BERTHAUD, B., SCHECKLER, S. E. & WENDT, J. 1999. *Archaeopteris* is the earliest known modern tree. *Nature,* **398,** 700-701.

MEYER-BERTHAUD, B., SORIA, A. & DECOMBEIX, A. L. 2010. The land plant cover in the Devonian: a reassessment of the evolution of the tree habit. *Geological Society, London, Special Publications,* **339,** 59-70.

PAWLIK, Ł., BUMA, B., ŠAMONIL, P., KVAČEK, J., GAŁĄZKA, A., KOHOUT, P. & MALIK, I. 2020. Impact of trees and forests on the Devonian landscape and weathering processes with implications to the global Earth's system properties-A critical review. *Earth-Science Reviews,* **205,** 103200.

PRESTIANNI, C. & GERRIENNE, P. 2010. Early seed plant radiation: an ecological hypothesis. *Geological Society, London, Special Publications,* **339,** 71-80.

QIE, W., ZHANG, J., LUO, G., ALGEO, T. J., CHEN, B., XIANG, L., LIANG, K., LIU, X., POGGE VON STRANDMANN, P. A. & CHEN, J. 2023. Enhanced continental weathering as a trigger for the End-Devonian Hangenberg crisis. *Geophysical Research Letters,* **50,** e2022GL102640.

QUIRK, J., LEAKE, J. R., JOHNSON, D. A., TAYLOR, L. L., SACCONE, L. & BEERLING, D. J. 2015. Constraining the role of early land plants in Palaeozoic weathering and global cooling. *Proceedings of the Royal Society B: Biological Sciences,* **282,** 20151115.

RACKI, G. 2020. A volcanic scenario for the Frasnian–Famennian major biotic crisis and other Late Devonian global changes: more answers than questions? *Global and Planetary Change,* **189,** 103174.

RACKI, G., RAKOCIŃSKI, M., MARYNOWSKI, L. & WIGNALL, P. B. 2018. Mercury enrichments and the Frasnian-Famennian biotic crisis: a volcanic trigger proved? *Geology,* **46,** 543-546.

RITCHIE, A. 1975. *Groenlandaspis* in Antarctica, Australia and Europe. *Nature,* **254,** 569-573.

ROBIN, N., GUERIAU, P., LUQUE, J., JARVIS, D., DALEY, A. C. & VONK, R. 2021. The oldest peracarid crustacean reveals a Late Devonian freshwater colonization by isopod relatives. *Biology Letters,* **17,** 20210226.

ROTH-NEBELSICK, A. 2005. Reconstructing atmospheric carbon dioxide with stomata: possibilities and limitations of a botanical pCO_2-sensor. *Trees,* **19,** 251-265.

ROTH-NEBELSICK, A. & KONRAD, W. 2003. Assimilation and transpiration capabilities of rhyniophytic plants from the Lower Devonian and their implications for paleoatmospheric CO_2 concentration. *Palaeogeography, Palaeoclimatology, Palaeoecology,* **202,** 153-178.

ROYER, D. L., MILLER, I. M., PEPPE, D. J. & HICKEY, L. J. 2010. Leaf economic traits from fossils support a weedy habit for early angiosperms. *American Journal of Botany,* **97,** 438-445.

ROYER, D. L., SACK, L., WILF, P., LUSK, C. H., JORDAN, G. J., NIINEMETS, Ü., WRIGHT, I. J., WESTOBY, M., CARIGLINO, B., COLEY, P. D., CUTTER, A. D., JOHNSON, K. R., LABANDEIRA, C. C., MOLES, A. T., PALMER, M. B. & VALLADARES, F. 2007. Fossil leaf economics quantified: calibration, Eocene case study, and implications. *Paleobiology,* **33,** 574-589.

SCHWENDEMANN, A. B. 2018. Leaf venation density and calculated physiological characteristics of fossil leaves from the Permian of Gondwana. *In:* KRINGS, M., HARPER, C. J., CÚNEO, N. R. & ROTHWELL, G. W. (eds.) *Transformative Paleobotany.* Academic Press.

SHOUGANG, H., BECK, C. B. & DEMING, W. 2003. Structure of the earliest leaves: adaptations to high concentrations of atmospheric CO_2. *International Journal of Plant Sciences,* **164,** 71-75.

STEIN, W. E., BERRY, C. M., HERNICK, L. V. & MANNOLINI, F. 2012. Surprisingly complex community discovered in the mid-Devonian fossil forest at Gilboa. *Nature,* **483,** 78-81.

STEIN, W. E., BERRY, C. M., MORRIS, J. L., HERNICK, L. V., MANNOLINI, F., STRAETEN, C., LANDING, E., MARSHALL, J. E. A., WELLMAN, C. H., BEERLING, D. J. & LEAKE, J. R. 2020. Mid-Devonian *Archaeopteris* roots signal revolutionary change in earliest fossil forests. *Current Biology,* **30,** 421–431.

STEIN, W. E., MANNOLINI, F., HERNICK, L. V., LANDING, E. & BERRY, C. M. 2007. Giant cladoxylopsid trees resolve the enigma of the Earth's earliest forest stumps at Gilboa. *Nature,* **446,** 904-907.

STEINTHORSDOTTIR, M., WOODWARD, F. I., SURLYK, F. & MCELWAIN, J. C. 2012. Deep-time evidence of a link between elevated CO_2 concentrations and perturbations in the hydrological cycle via drop in plant transpiration. *Geology,* **40,** 815-818.

STRULLU-DERRIEN, C., KENRICK, P., BADEL, E., COCHARD, H. & TAFFOREAU, P. 2013. An overview of the hydraulic systems in early land plants. *Iawa Journal,* **34,** 333-351.

TANRATTANA, M., BARCZI, J. F., DECOMBEIX, A. L., MEYER-BERTHAUD, B. & WILSON, J. 2019. A new approach for modelling water transport in fossil plants. *IAWA Journal,* **40,** 466-487.

WANG, J., HILTON, J., PFEFFERKORN, H. W., WANG, S., ZHANG, Y., BEK, J., PSENICKA, J., SEYFULLAH, L. J. & DILCHER, D. 2021. Ancient noeggerathialean reveals the seed plant sister group diversified alongside the primary seed plant radiation. *Proceedings of the National Academy of Sciences of the United States of America,* **11,** e2013442118.

WILSON, J. P., WHITE, J. D., MONTANEZ, I. P., DIMICHELE, W. A., MCELWAIN, J. C., POULSEN, C. J. & HREN, M. T. 2020. Carboniferous plant physiology breaks the mold. *New Phytologist,* **227,** 667-679.

WITKOWSKI, C. R., WEIJERS, J. W., BLAIS, B., SCHOUTEN, S. & SINNINGHE DAMSTÉ, J. S. 2018. Molecular fossils from phytoplankton reveal secular pCO_2 trend over the Phanerozoic. *Science advances,* **4,** eaat4556.

WOODWARD, F. I. 1987. Stomatal numbers are sensitive to increases in CO_2 from pre-industrial levels. *Nature,* **327,** 617-618.

2. New gas exchange-based atmospheric CO_2 reconstruction using Emsian aged Sawdonia fossils from Gaspé Bay and New Brunswick

Abstract

The Devonian period (419.2-358.9 million years ago) was a key phase in the evolution of plants, distinguished by the appearance of a number of novel traits such as leaves, arborescence, deep roots and seeds, as well as the development of more complex ecosystems. It is known that largescale carbon cycle perturbations occurred during the Devonian, however there is a paucity of estimates for atmospheric CO_2 concentrations for this period. This study uses the mechanistic model of Franks *et al.* (2014) with adjustments of Porter et al. (2017) to estimate palaeo-CO_2 for the Emsian stage of the Devonian. Direct epi-fluorescent microscope observations of *Sawdonia* stems from the Battery Point Fm., Gaspé Peninsula and the Campbellton Fm., New Brunswick were used to obtain stomatal anatomy measurements for fossils with existing carbon isotope data. Predicted palaeo-CO_2 was compared to literature estimates for the Devonian that are derived from application of Frank's model and other proxy methods. Atmospheric CO_2 during the Emsian was found to be approximately 898 ppm and stomatal dimension parameters were found to be particularly critical parameters in the application of the mechanistic model. The results from this study, combined with revisions to existing estimates, indicate that a gradual CO_2 drawdown over the Devonian period, with an approximate decrease from 1300 ppm to 750 ppm. This gradual decreasing trend is consistent with emerging proxy data. Future research is needed to better constrain CO_2 proxies, and to better elucidate atmospheric change during the Devonian and Early Carboniferous periods.

2.1 Introduction

Terrestrial plants play an influential role in biogeochemical cycles and Earth system processes both today and in the deep past (Algeo and Scheckler, 1998, Chen et al., 2021, Coates et al., 2011, Franklin et al., 2016, Le Hir et al., 2011, Maffre et al., 2022, Matthaeus et al., 2023, Poulter et al., 2011, Shukla et al., 2019). In a palaeobotanical context, evolutionary developments in terrestrial plant function are thought to have influenced these systems as early as the Devonian period (419.2-358.9 Ma) (Algeo and Scheckler, 1998, Berner, 1997, Elick et al., 1998, Le Hir et al., 2011, Maffre et al., 2022, Pawlik et al., 2020, Stein et al., 2020, Qie et al., 2023). The earliest unequivocal fossil evidence for the emergence of land plants dates to the Ordovician period (475 Ma) (Wellman et al., 2003), with the origin of vascular plants (tracheophytes) occurring approximately 430 Ma (Kenrick and Crane, 1997). The Devonian period is distinguished as a pivotal period in the development of the biogeosphere by rapid increases in plant richness, biogeographic range and morphological diversification, resulting in increased ecosystem complexity and environmental changes (Capel et al., 2022, Gensel and Edwards, 2001, Pawlik et al., 2020, Stein et al., 2007). When corrected for sampling bias, there are increases in land plant richness during the Pragian and Givetian stages of the Devonian, which are associated with early tracheophyte expansion and the diversification of the first forest ecosystems, respectively (Capel et al., 2022).

Plant evolutionary innovations were both directed by, and engineers of the Earth's physical environment. For example, megaphyll leaf evolution during the Devonian is thought to have been constrained by high temperatures, low stomatal densities and limited water uptake (Beerling et al., 2001, Beerling, 2005, Osborne et al., 2004, Shougang et al., 2003). The atmospheric constraints are thought to have prevented the development of sufficiently high stomatal densities for adequate transpirational cooling to allow the avoidance of lethal overheating of laminate leaves (Beerling et al., 2001, Beerling, 2005, Osborne et al., 2004, Shougang et al., 2003). As a result, it is proposed that large megaphyll leaves did not become common until the late Devonian, when pCO_2 and temperature were lower than during the early Devonian, although the causality of this plant-atmosphere interaction is

unresolved (Beerling et al., 2001, Beerling, 2005, Osborne et al., 2004, Rowe and Speck, 2005, Shougang et al., 2003).

One evolutionary development in the Devonian that contributed to greater vegetative cover of the earth's surface is the evolution of the seed habit. The first seed plants are thought to have been ecological opportunists that evolved in disturbed sub-canopy environments (Prestianni and Gerrienne, 2010). However, the seed habit allowed the eventual exploitation of new ecological niches, such as drier upland areas, facilitating more extensive plant cover of the Earth's surface (Algeo and Scheckler, 1998, Algeo and Scheckler, 2010, Chen et al., 2021, Pawlik et al., 2020). Furthermore, the evolution of deeper, more extensive rooting systems, and the expansion of early forests is thought to have contributed to atmospheric CO_2 drawdown through accelerated weathering processes (Algeo and Scheckler, 1998, Berner, 1997, Elick et al., 1998, Pawlik et al., 2020, Stein et al., 2020, Qie et al., 2023). The Devonian explosion of land plant diversity is also thought to have contributed to enhanced pedogenesis, nutrient transport, organic and inorganic carbon deposition, and possibly marine extinction events in the Late Devonian (Algeo and Scheckler, 1998, Pawlik et al., 2020, Qie et al., 2023). However, the contribution of land plant evolution and diversification to weathering and other earth system processes is difficult to quantify due to limited data and difficulties in its interpretation (Boyce et al., 2023, Carmichael et al., 2019, D'Antonio et al., 2023, Kaiser et al., 2016, Pawlik et al., 2020, Qie et al., 2023). More recent studies have suggested that the timing of these evolutionary events and their impact on the global carbon cycle have been misinterpreted (Boyce et al., 2023, D'Antonio et al., 2023). It is suggested that the evolution of deep rooting systems and the seed habit by themselves occurred too early to be implicated in marine extinction events and largescale carbon 3 cycle perturbations during Late Devonian, but the later evolution of plants that possessed the combination of the two traits (i.e. large, deep rooting, arborescent seed plants) may have played a significant role in these events (Boyce et al., 2023, D'Antonio et al., 2023).

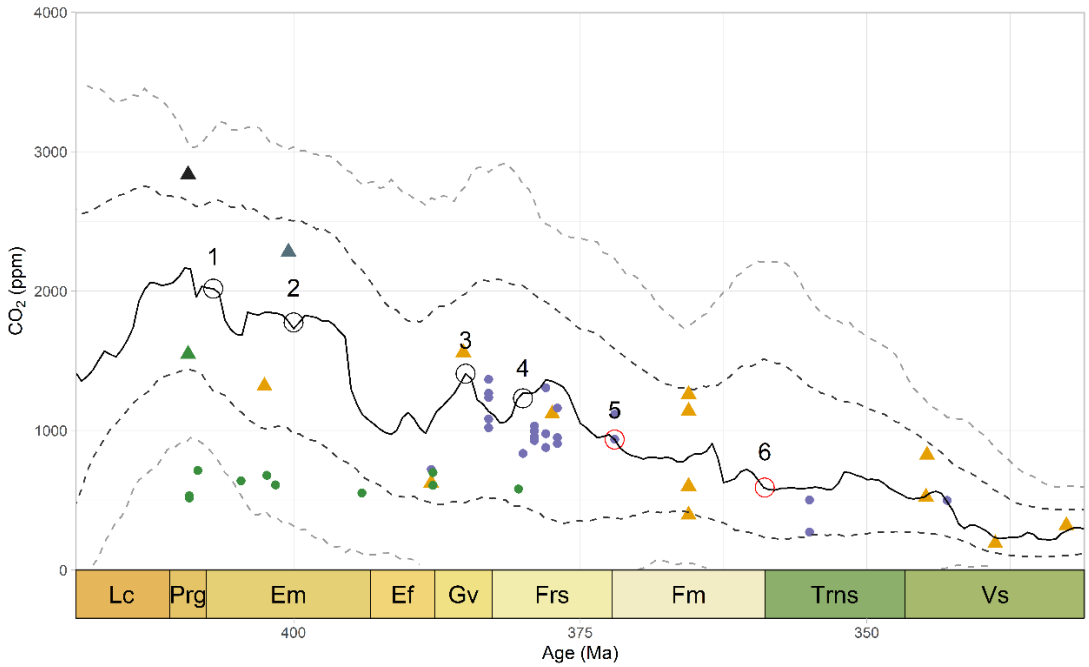

Figure 2.1. Timing of evolutionary innovations during the Devonian period compared with a proxy-based atmospheric CO_2 reconstruction. Modified after Pawlik et al. (2020). The CO_2 record is based on the data compilation of Foster et al. (2017), and from Dahl et al. (2022) and Witkowski et al. (2018). The dark black line indicates the most likely LOESS fit through the palaeo-CO_2 compilation of Foster et al. (2017) (datapoints shown as triangles), with the dark grey and light grey dotted lines showing the 68% and 95% confidence intervals respectively. Points correspond to various atmospheric CO_2 proxies (orange - palaeosol data of Cox et al. (2001), Driese et al. (2000), Ekart et al. (1999), Mora et al. (1996) and Muchez et al. (1993) as used in Foster et al. (2017), green - gas exchange model of Franks et al. (2014) and Dahl et al. (2022), black - gas exchange model of Roth-Nebelsick and Konrad (2003), grey - stomatal ratio proxy of McElwain (1998), purple - phytoplankton data from Witkowski et al. (2018)). The deeptime R package (Gearty, 2021) was used to create the geological scale on the x-axis after Cohen et al. (2013). Numbers correspond to the approximate timing of plant evolutionary innovations (shown with black circles) and environmental crises (shown with red circles) in the Devonian: (1) the first roots (Hetherington and Dolan, 2019) and secondary xylem (Strullu-Derrien et al., 2013); (2) the occurrence of the first megaphyll leaf in the fossil record (Shougang et al., 2003); (3) the first 'modern' forests containing taxa with extensive rooting systems (Stein et al., 2020); (4) the first seed precursors (Prestianni and Gerrienne, 2010) and the more widespread occurrence of megaphyll leaves (Osborne et al., 2004); (5) the Kelwasser event (Carmichael et al., 2019); (6) the Hangenberg event (Kaiser et al., 2016).

While there is evidence for a decline in atmospheric CO_2 concentrations over the Devonian, the large variability and uncertainty associated with palaeo-CO_2 estimates for this period limit certainty regarding the magnitude of Devonian atmospheric CO_2 change and their potential relationship with plant evolutionary innovations through the period. CO_2 concentrations have been found to decrease from a maximum ranging between 6300 and 2100 ppm to minimum values of 1200 to 590 ppm (Berner, 2006, Foster et al., 2017, Le Hir et al., 2011, Lenton et al., 2018, Simon et al., 2007). This CO_2 drawdown is linked to global climatic cooling over the Devonian period. However, there is a discrepancy between temperature proxies and the CO_2 trend, with a temperature increase occurring during the Frasnian (383-375 Ma), despite the overall trend of decreasing atmospheric CO_2 (Algeo and Scheckler, 2010, Joachimski et al., 2009, Girard et al., 2020). It is thought that the surface albedo reduction caused by expanding plant coverage of continental surfaces may have provided a warming feedback effect, counteracting the CO_2 drawdown cooling effect (Le Hir et al., 2011). However, a climate modelling study of Brugger et al. (2019) found that the effect of reduced albedo was likely to be insufficient to fully compensate for CO_2-driven cooling. Further work on Devonian atmospheric evolution has the potential to clarify plant-atmosphere interactions and the resulting climate impacts over this critical interval of plant evolutionary history.

The importance of atmospheric CO_2 in climate forcing has led to the development of numerous CO_2 proxies from biological and geochemical signatures in the geologic record (see *Figure 2.1*). In particular, a variety of CO_2 proxies have been developed from fossil plants, using a combination of stomatal and/or carbon isotope data, and/or leaf gas exchange principles (Cui et al., 2020, Fletcher et al., 2006, Franks et al., 2014, Konrad et al., 2008, Konrad et al., 2017, McElwain and Chaloner, 1996, Roth-Nebelsick and Konrad, 2003, Schubert and Jahren, 2012). Different proxy methods have a number of advantages and limitations. Mechanistic approaches, such as gas exchange models (Franks et al., 2014, Konrad et al., 2017), can account for both physiological and developmental controls of gas exchange (McElwain and Steinthorsdottir, 2017). However, gas exchange approaches require more extensive parameterisation than simpler empirical methods, particularly in relation to dimensions of the stomatal pore, which are not always observable or preserved

in fossils. Furthermore, stable carbon isotope data from fossil plants is also needed for the majority of gas exchange models (excluding e.g. the model of Roth-Nebelsick and Konrad (2003)), and carrying out both stomatal measurements and stable carbon isotope analysis on the same fossil specimen can prove challenging due to the mode of fossil preservation and the need for destructive analysis for carbon isotope data (Dahl et al., 2022). Therefore, gas-exchange approaches to CO_2 reconstruction are not always directly applicable to fossil plant material (Konrad et al., 2021, McElwain and Steinthorsdottir, 2017).

Dahl et al. (2022) approached the issue of infrequent preservation of material from which both carbon isotopic and stomatal data can be directly obtained by exploring the error associated with using unpaired stomatal and stable carbon isotope data from extant plants. This approach was developed to enable the use of unpaired data from literature sources (Edwards et al., 1998, Hueber, 1983, Wan et al., 2019) and their own carbon isotopic analyses, so that variation in local environmental conditions, as well as temporal mismatches between stomatal and carbon isotope data, could be accounted for in model predictions (Dahl et al., 2022). However, for the most robust atmospheric CO_2 estimates both stomatal measurements and stable carbon isotopic analysis need to be carried out on the same fossil specimens. Currently, there are 13 fossil plant-based CO_2 estimates for the Devonian period, from 8 different plant taxa, using a number of different approaches (i.e. the empirical stomatal ratio method (McElwain, 1998) and gas exchange models (Dahl et al., 2022, Franks et al., 2014, Roth-Nebelsick and Konrad, 2003)). Of these estimates, only four of the gas-exchange based estimates use paired stomatal and carbon isotope data, and do not include stomatal dimension parameters from primary data (Dahl et al., 2022).

In this study, for the first time, we present CO_2 estimates from the gas exchange model of Franks et al. (2014) where paired carbon isotope data and detailed stomatal measurements of Emsian aged *Sawdonia* fossils have been used to parameterize the model. This model was applied to measurements obtained from 21 hand specimens, allowing for a detailed sensitivity analysis of the model in the context of a range of stomatal morphological variation observed in the fossil record.

2.2 Materials and Methods

2.2.1 Geological and Palaeoenvironmental setting

The fossil specimens used in this study consisted of well-preserved compression fossils of *Sawdonia* (Dawson) Hueber species from the Battery Point Fm., Gaspé Peninsula and the Campbellton Fm., New Brunswick. The *Sawdonia* material from the Battery Point Formation is from the type locality in the Cap-aux-Os Member of the formation, and falls within the *annulatus-sextantii* spore zone (early to late Emsian) (Hotton et al., 2001). The formation developed on the southern edge of Laurussia, approximately 10° to 20° S of the equator, and was deposited within a low-lying fluvial-deltaic coastal plain (Hotton et al., 2001). *Sawdonia* from the Battery Point Formation is thought to have occupied dysaerobic wetland sites that experienced frequent flooding (Griffing et al., 2000, Hotton et al., 2001). A detailed description of the palaeoenvironment, palaeoecology and sedimentology of the Cap-aux-Os Member of the Battery Point Formation, can be found in Hotton et al. (2001) and Griffing et al. (2000).

The Campbellton Formation spore assemblages span from the *annulatus-sextantii* assemblage zone (mid-Emsian) to the *Grandispora* subzone of the *annulatus-lindlarensis* zone (upper-Emsian). Several formations within the Gaspé Sandstones Group are roughly synchronous with the Campbellton Formation, and *Sawdonia* fossils used in this study from both formations are roughly coeval (Kennedy et al., 2012, Wan et al., 2019). *Sawdonia* specimens from the Campbellton Formation are found in marginal lacustrine and lacustrine facies with restricted circulation and are thought to have been derived from wetland and lakeside growth stands (Kennedy et al., 2012).

2.2.2 Fossil material

Sawdonia is an early zosterophyll that was both geographically and temporally widespread during much of the Devonian, ranging from the Emsian to the late Givetian/early Frasnian (Chaloner et al., 1978, Berry and Gensel, 2019, Gensel and Berry, 2016, Hueber and

Grierson, 1961, Rayner, 1983, Zdebska, 1972). Fossil specimens used in this study were directly observed using epifluorescent microscopy (Leica DM 2500) at 40× and 100× magnification to confirm the generic diagnosis (Gensel and Berry, 2016) and to assess the preservation state of the plant cuticle. Specimens were not identified to species level. Of the 28 hand specimens examined, 21 had sufficient preservation to obtain clear images of the cuticle, epidermal pavement cells and stomatal complex geometry, including guard cells for data collection. However, as *Sawdonia* stomata are slightly sunken (Chaloner et al., 1978, Rayner, 1983), the stomatal pore was often not clearly visible. All specimens used in this study will be curated at the publication stage. A decision still needs to be made with collaborators as to whether to archive them in The Geological Museum, Trinity College Dublin, or in a North American Institution.

2.2.3 Stomatal measurements

Ten cuticle images were taken from each hand specimen (with each hand specimen defined as an individual sample) at 100× magnification using a Leica DM 2500 epifluorescent microscope (filter block A; excitation filter BP 340-380, suppression filter LP 425) with Leica DFC300FX camera (Leica® 312 Microsystems, Wetzlar, Germany) and Syncroscopy Automontage (Syncroscopy Ltd, Cambridge, UK) digital imaging software. Each hand specimen had between 2 and 28 stem fragments preserved (see *Appendix 2.1*) and all stem fragments from an individual hand specimen were considered to have an organic connection. The sample size for stomatal density and size (i.e., guard cell length and width) measurements was determined using a cumulative mean index curve. Stomatal density measurements (n=10) and guard cell length and width measurements (n=20) were taken from randomly selected stem fragments for each sample using ImageJ. In the case where more than 10 stem fragments were preserved, measurements were obtained from 10 randomly selected fragments. As *Sawdonia* stomata are sunken, stomatal pore length, guard cell length and width were not directly observable in the majority of specimens. An example of *Sawdonia* cuticle from which stomatal density measurements and guard cell dimension measurements were taken is illustrated in *Figure 2.2*. In the case where stomatal pore length, guard cell length and width were not directly observable, the stomatal pit

length was measured to estimate guard cell length and stomatal pit width was measured and halved to estimate a single guard cell width following the protocol of Montañez et al. (2016). When directly observable, pore length, guard cell length and guard cell width were measured (see *Figure 2.3*). The directly observable pore length measurements were used in combination with stomatal pore and guard cell length measurements taken from published images of *Sawdonia* stomata to calculate pore length to guard cell length scaling factor (termed S1 in Franks et al. 2014; see *Table A2.2.1*). These direct stomatal observations and measurements were also used to assess the robustness of using stomatal pit dimensions as a proxy for guard cell length and width in fossils where guard cells could not be directly observed (Franks et al., 2014, Montañez et al., 2016). Stomatal number was determined per field of view for each cuticle image. HSB colour thresholding in ImageJ was used to distinguish the cuticle area in each image to exclude tears and obscured areas when present. Stomatal density was then calculated at the number of stomata per mm^2.

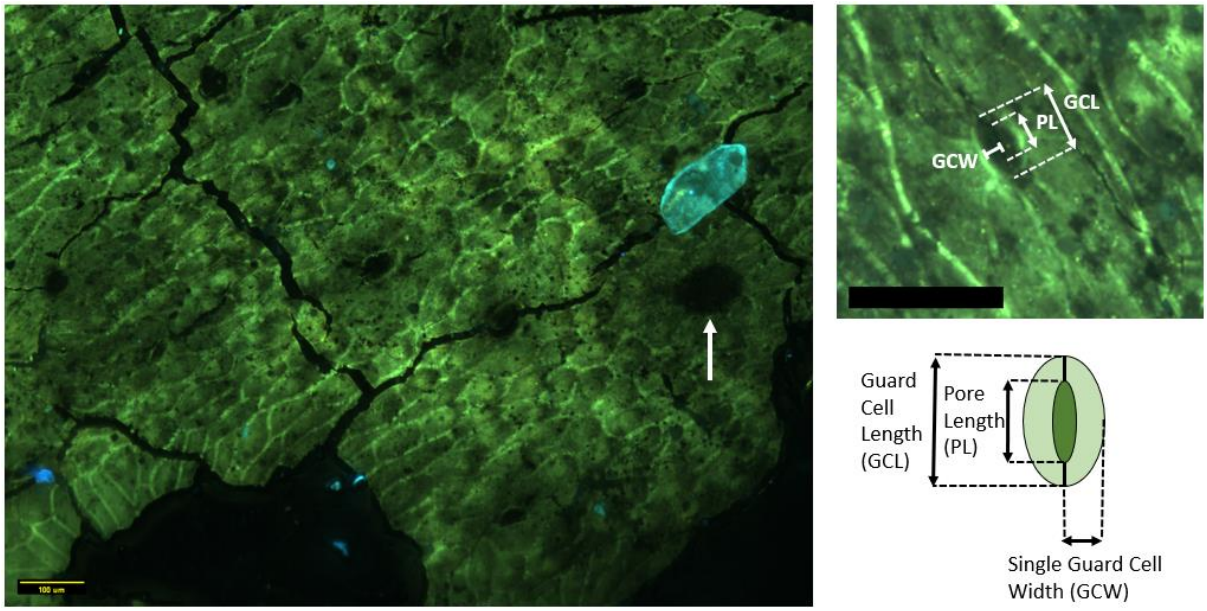

Figure 2.2. Stomatal density and stomatal dimensions of *Sawdonia* fossils were measured from images obtained from epifluorescent microscopy. (Left) A representative image of the fossilized cuticle of *Sawdonia* used to measure stomatal density and size. The fossilized cuticle also showed distinctive papillate epidermal cells and stomata, as well as rosette-shaped aggregations of cells resembling hair bases cuticle (indicated by an arrow). The fossilized cuticle of *Sawdonia* used in this study exhibited strong auto-fluorescence. (Right) When possible, stomatal pore length, guard cell length and guard cell width were measured to calculate the S1 pore length to guard cell length scaling factor and to assess the robustness of using stomatal pit dimensions as a proxy for guard cell length and width in fossils where guard cells could not be directly observed. All scale bars = 100µm.

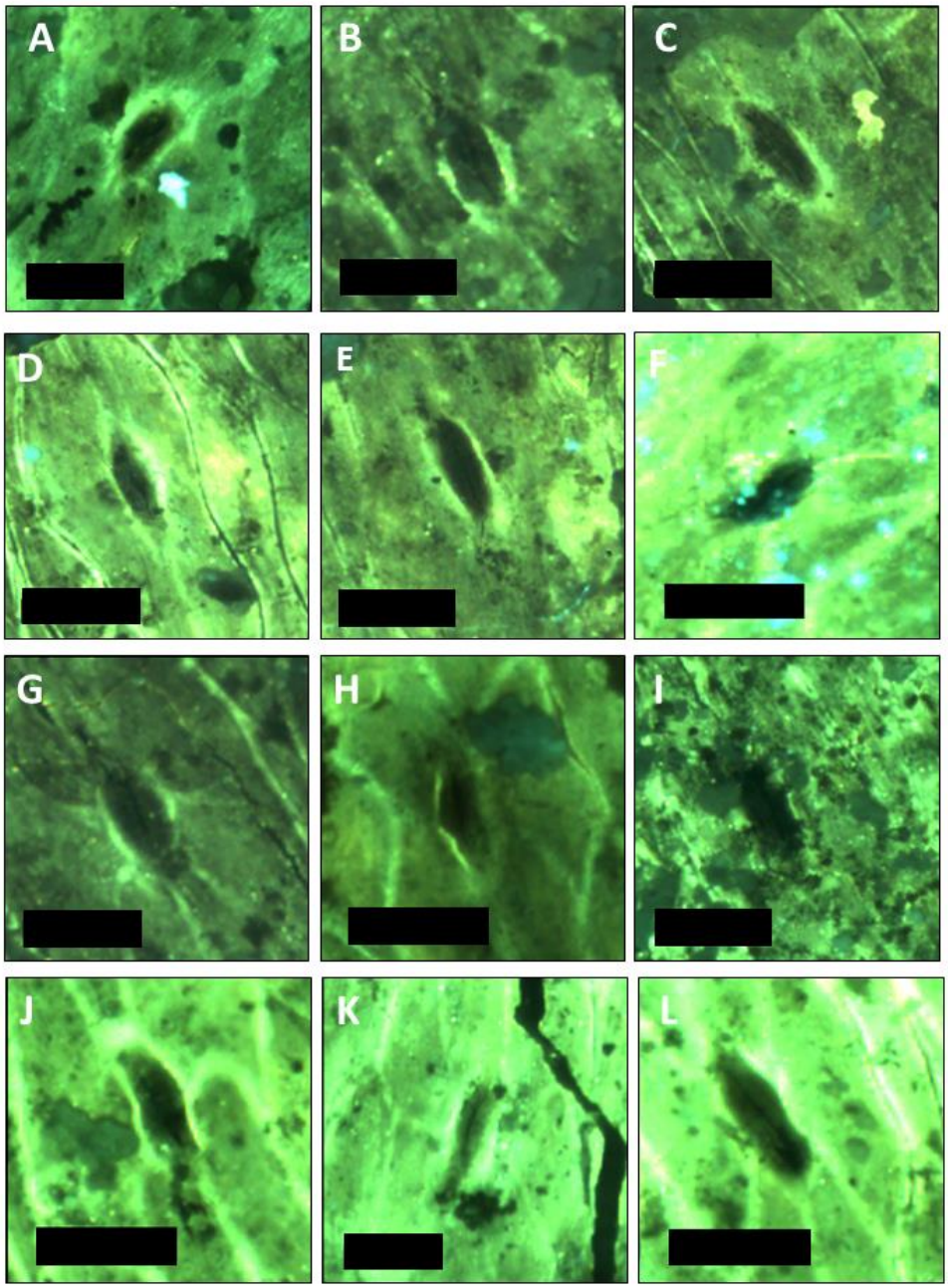

Figure 2.3. Stomatal pore dimensions of *Sawdonia* fossils were measured from images obtained from epifluorescent microscopy when observable. A) Fossil Specimen number SAWD-PG-002-9, Image 1, Pore 1; B) Fossil Specimen number SAWD-PG-002-7, Image 14, Pore 1; C) Fossil Specimen number SAWD-PG-002-7, Image 13, Pore 1; D) Fossil Specimen number SAWD-PG-002-7, Image 13, Pore 2; E) Fossil Specimen number SAWD-PG-002-7, Image 13, Pore 3; F) Fossil Specimen number SAWD-PG-003-4ii, Image 3, Pore 1; G) Fossil Specimen number SAWD-PG-002-7, Image 14, Pore 2; H) Fossil Specimen number SAWD-PG-002-10, Image 8, Pore 1; I) Fossil Specimen number SAWD-PG-002-9, Image 9, Pore 1; J) Fossil Specimen number SAWD-PG-002-10, Image 8, Pore 2. All scale bars = 50µm.

2.2.4 Carbon isotope data and phylogenetic correction

Carbon isotopic composition of *Sawdonia* spp. ($\delta^{13}C_{plant}$) samples used in this study were measured directly from fossil fragments by Wan et al. (2019) from the same hand specimens that stomatal measurements were obtained (see *Appendix 2.1*). Therefore, the isotopic analysis and stomatal measurements are from a 'paired' dataset – i.e., the stomatal and isotope data are from the same hand specimen. However, due to the destructive nature of carbon isotopic analysis are not from the exact same stem fragments and the sample size for isotopic data is smaller than that of the stomatal data. Isotope values obtained from spines rather than stems were excluded, as fossil plant spines are enriched in ^{13}C relative to stems of the same specimen (Wan et al., 2019). Fossil plant $\delta^{13}C$ values were subsequently corrected for phylogenetic effect using the proposed correction factor for lycophytes by Porter et al. (2017) of +2.55 ‰. Palaeo-atmospheric CO_2 carbon isotopic composition ($\delta^{13}C_{atmosphere}$) estimates were based on marine carbonate $\delta^{13}C$ data from Cramer and Jarvis (2020) and Mills et al. (2023), and palaeotemperature data from Joachimski et al. (2009). The midpoint of the values calculated for $\delta^{13}C_{atmosphere}$ within the possible time interval for the Campbellton Formation (405–395 Ma) and Battery Point Formation (410–395 Ma) was used as the final input parameter in the model for $\delta^{13}C_{atmosphere}$ and the error associated with these values was used to account for the age uncertainty of the two formations and temporal variation in $\delta^{13}C_{atmosphere}$ during this period.

2.2.5 Gas exchange model application

The gas exchange model of Franks et al. (2014) was used to estimate atmospheric CO_2 concentration during the Devonian. This model solves two equations simultaneously by iteration for palaeo-atmospheric CO_2 concentration and palaeo-photosynthetic rate. The model was operated in R (v. 4.2.2) as per Franks et al. (2014), using the parameters described below. The original version of the model as published in Franks et al. (2014) was used, as opposed to the model version presented in Kowalczyk et al (2018), as the revised

formulation for solving for A_n from A_0 and CO_2 presented in Kowalczyk et al (2018) requires additional parameterisation with a living relative, which is considered to be less robust for Paleozoic fossils (see Discussion section 2.3.2).

Stomatal size and density measurements were used to calculate maximum stomatal conductance to CO_2 (g_{max}) using the equation of Franks and Farquhar (2001):

$$g_{max} = \frac{dw}{v} \cdot SD \cdot pa_{max} \,/\, (pd + \frac{\pi}{2} \sqrt{pa_{max}/\pi}\ )$$

(1)

where *dw* is the diffusivity of water vapor in air ($m^2\ s^{-1}$), *v* is the molar volume of air, *SD* is stomatal density, pa_{max} is the maximum stomatal pore area and *pd* is pore depth. Operational stomatal conductance (g_{op}) was then calculated from this using a scaling factor of 0.2 (Franks et al., 2014). Total conductance ($g_{c(tot)}$) is estimated by combining g_{op}, with estimated values for boundary layer and mesophyll conductance, which are obtained from literature measurements and modelled from photosynthetic rate respectively.

Paired carbon isotope data from *Sawdonia* fossils (Wan et al., 2019) and coeval proxies of atmospheric $\delta^{13}C$ (Veizer et al., 1999) were used to derive the ratio between leaf internal CO_2 concentration and atmospheric CO_2 concentration (c_i/c_a). Atmospheric CO_2 concentration (C_a) was then be predicted from its relationship with assimilation rate (A_n), which was estimated from an 'initial' assimilation rate of a living equivalent under ambient CO_2 (A_0) and total conductance ($g_{c(tot)}$) (Farquhar and Sharkey, 1982, Von Caemmerer, 2000):

$$C_a = A_n/(g_{c(tot)} * (1 - C_i/C_a))$$

(2)

Robust parameterisation of A_0 is important in the implementation of the Franks model, due to model sensitivity to this value (McElwain et al., 2016). This presents significant issues when applied to extinct taxa in deep time that are non-analogous to extant plants in

function, physiology or ecology. Despite these issues, the Franks model is considered a good compromise between applicability and accuracy when compared to other leaf-based CO_2 proxies (Konrad et al., 2021). Due to this sensitivity, ecologically equivalent lycophyte species (i.e. tropical, sun, terrestrial lycophytes, see *Appendix 2.3*) were used to initialize the model, and a higher value of 3.86 µmol m^{-2} s^{-1} was used, rather than the generic value of 3 µmol m^{-2} s^{-1} from Franks et al. (2014). Tropical, terrestrial lycophytes were chosen as NLEs for this input, due to the tropical-subtropical climate that has been interpreted from palaeoenvironmental studies (Griffing et al., 2000, Hotton et al., 2001, Kennedy et al., 2012). Lycophytes from a closed canopy or shaded environment were excluded, as this was considered a poor ecological analogue for early Devonian environments that *Sawdonia* occupied. All other scaling factors were used as suggested by Franks et al. (2014) (See *Appendix 2.4*).

A sensitivity analysis of the measured fossil input parameters (i.e., stomatal density, guard cell length, guard cell width and $\delta^{13}C_{plant}$), the initial assimilation rate (A_0), and the pore length (S1), pore shape (β; S3) and maximum stomatal conductance to operational stomatal conductance (S4) scaling factors was performed to understand the uncertainty in these parameters and how they affect the model outputs. The sensitivity analysis was undertaken by changing one parameter at a time, maintaining all other input values as used in the final model run constant. The sensitivity analysis assessed the effect of changing the individual fossil input parameters within the full range of values observed from fossil measurements, and a range of values suggested from the available literature for the tested scaling factors.

2.3 Results and Discussion

2.3.1 Variability in fossil measurements

The fossilized cuticle of *Sawdonia* used in this study was exceptionally well preserved and exhibited strong auto-fluorescence (see *Figure 2.2*). The mean stomatal density for each fossil sample (defined here as a single hand specimen with between 2 and 28 stem fragments preserved (see section 2.2.3)) ranged from 3.7 to 8.2 mm^{-2}. The overall mean of the stomatal density measurements from all samples within each formation was significantly different (see *Figure 2.4*). Samples from the Battery Point Formation had a higher median stomatal density (7.0 mm^{-2}) than those from the Campbellton Formation (4.6 mm^{-2}, Wilcoxon W=10244, p=1.483e^{-12}). The samples from the Campbellton Formation had a more similar mean stomatal density (4.9 ± 1.9 stomata mm^{-2}) to that of *Sawdonia* reported by McElwain and Chaloner (1995) of 4.3 ± 1.9 stomata mm^{-2}. *Sawdonia* is thought to have occupied similar wetland environments at both localities (Griffing et al., 2000, Hotton et al., 2001, Kennedy et al., 2012). However, *Sawdonia* from the Battery Point Formation may have been occasionally exposed to brackish conditions due to tidal over wash (Griffing et al., 2000, Hotton et al., 2001). The variation in stomatal density between the two localities is likely due to a combination of genetic variation and growth under different environmental conditions (Clark et al., 2022).

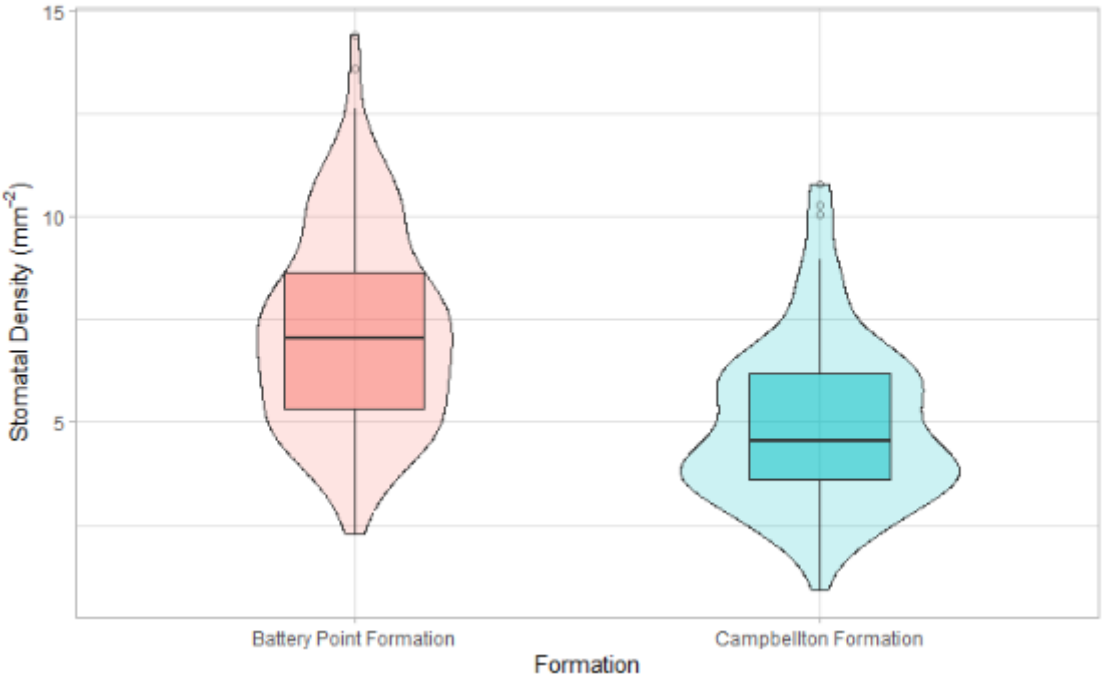

Figure 2.4. Stomatal density measured in *Sawdonia* fossils from the Battery Point Formation and the Campbellton Formation. Measured stomatal density from the Battery Point Formation was higher (i.e., from the overall median of the total number of stomatal counts (n) made on multiple stems from multiple samples; median = 7.03 mm^{-2}, n = 144) than that of the Campbellton Formation (median = 4.55 mm^{-2}, n = 92; Wilcoxon W=10244, p=1.483e^{-12}).

Sawdonia is known to have sunken guard cells (Chaloner et al., 1978, Edwards et al., 1982, Lang, 1933, Rayner, 1983). As a result, stomatal pore length was only directly measurable with confidence on 27 stomata (mean = 33.9 ± 6.4 µm). These measurements were combined with measurements and images from the literature to produce the guard cell length to pore length scaling factor (S1 in Franks et al. (2014), see *Appendix 2.2*). Mean guard cell dimensions for all samples was 46.9 - 69.6 µm long and 10.9 - 14.4 µm wide (single guard cell width was taken as half the width of the stomatal complex (Montañez et al., 2016)). Stomatal size did not vary significantly between the two localities (see *Figure 2.5*; Wilcoxon W = 38173, p-value = 0.2976). These measurements fall within the reported range for stomatal size of cf. *Sawdonia* sp. (i.e., vegetative and fertile axes showing

epidermal features similar to *S. ornata* but lacking clear diagnostic fertile features; (Edwards, 1924, Hueber and Grierson, 1961, Hueber, 1971, Rayner, 1983, Zdebska, 1972). However, measurements in these samples are larger than stomata described from the emended diagnosis of *Sawdonia* of Gensel and Berry (2016) (stomata described as 8 µm wide and 16 µm long).

The mean carbon isotope values ($\delta^{13}C$) for the *Sawdonia* samples from Wan et al. (2019) varied between -25.098 – -28.81 ‰ (mean = -27.52 ± 1.69 ‰). Only isotope values from stem samples were used, as fossil plant spines were found to be enriched in ^{13}C relative to stems of the same specimen (Wan et al., 2019). There is some variation in isotopic values between the two formations, with values from the Battery Point Formation showing a more negative $\delta^{13}C$ (see *Figure 2.5*). However, this may be an artifact of sample size (n=9), as there were far fewer carbon isotope measurements taken from each sample than there were stomatal measurements (see section 2.2.4). One potential outlier sample from the Campbellton Formation had a more positive $\delta^{13}C$ than the rest, causing a skewed data distribution. This value had a large impact on the mean $\delta^{13}C$ from that location.

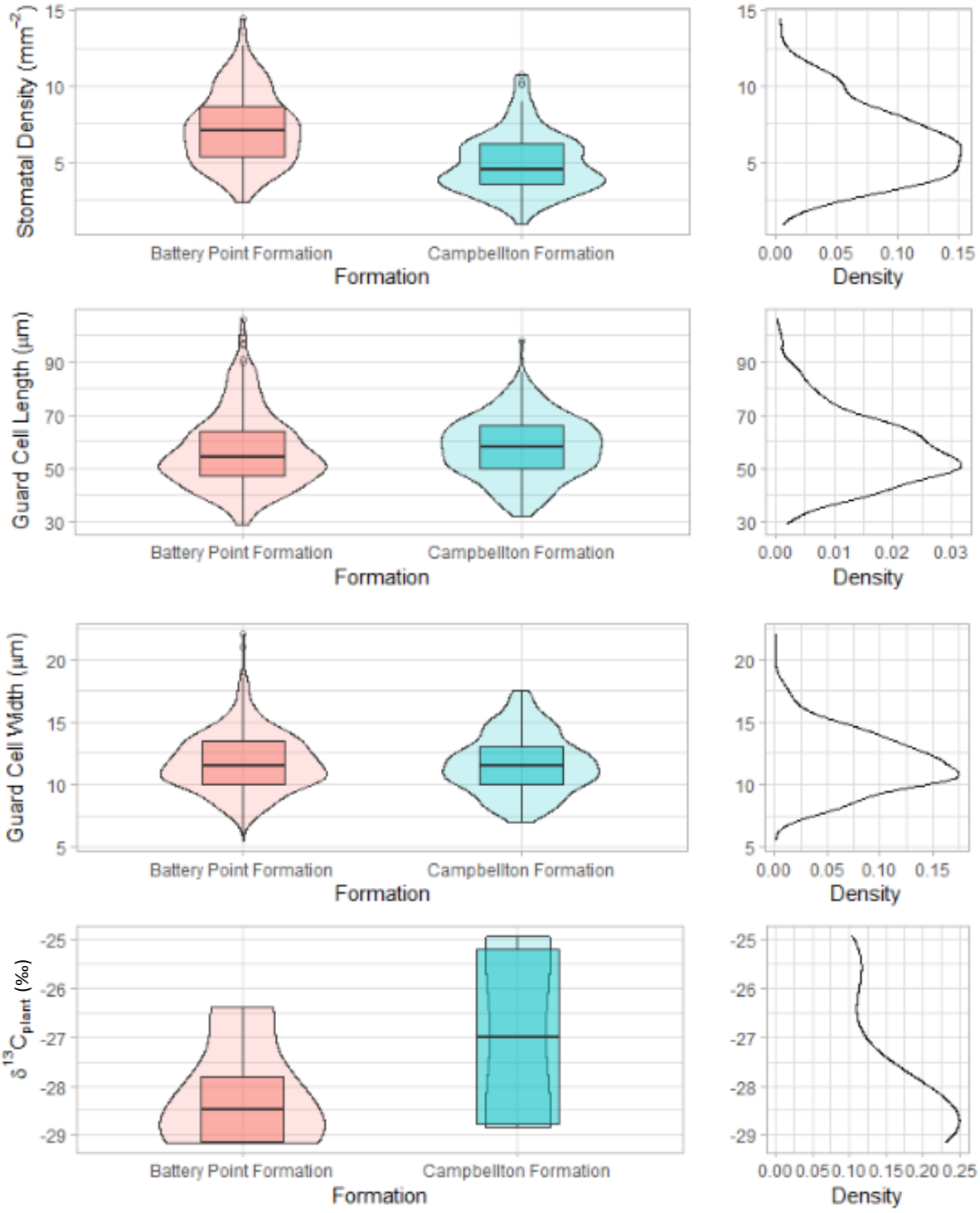

Figure 2.5. Trait value differences in *Sawdonia* fossils between samples from the Battery Point Formation (right) and the Campbellton Formation (left). Overall data distribution for each dataset is shown on the right (kernel density estimates). Stomatal density showed significant differences between the two formations (Wilcoxon W=10244, p=1.483e^{-12}), whereas stomatal size did not show significant differences between the two formations (Wilcoxon W = 38173, p-value = 0.2976).

2.3.2 Early Devonian CO_2 estimates and comparison with published CO_2 estimates

We estimate a median palaeo-atmospheric CO_2 concentration of 898 ppm from application of the Franks model to coupled stomatal and carbon isotopic analyses of Emsian-age *Sawdonia* fossil axes. This is the first time that coupled isotopic and stomatal measurements from the same hand specimen have been achieved for any Devonian gas exchange-based CO_2 estimates. However, there was a large degree of variability in CO_2 estimates between samples, which produced a range between 1695 ppm and 597 ppm (see *Figure 2.6*). The majority of the confidence intervals produced by the model for the individual sample estimates lie between 502-1637 ppm (based on the 16th and 84th percentiles of the resampled CO_2 data). The impact of variation in stomatal traits (i.e., stomatal density, guard cell length, guard cell width and associated scaling factors) and carbon isotope data on variation in CO_2 estimates will be discussed further in section 2.3.3. The CO_2 estimates obtained from this study are significantly lower than those modelled by COPSE, GEOCARBSULF and COMBINE (Lenton et al., 2018, Royer et al., 2014, Simon et al., 2007). However, the median CO_2 estimate from this study does fall within the 95% confidence interval of GEOCARBSULF (Royer et al., 2014).

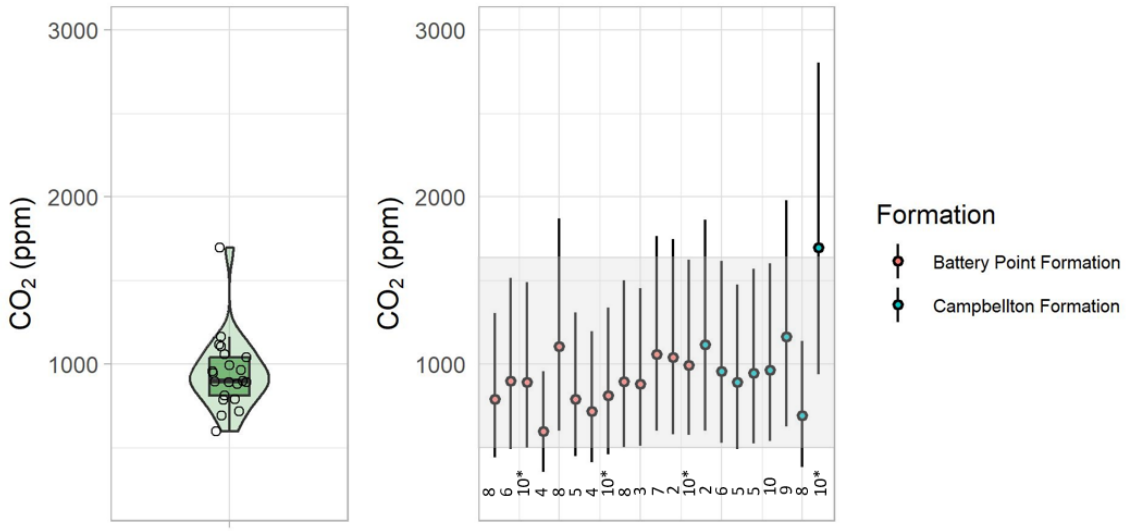

Figure 2.6. Average CO_2 estimates obtained for the Emsian (402.3 Ma) from Sawdonia fossils. (Left) The boxplot shows the median CO_2 estimate (898 ppm), and the first and third quartiles (809 ppm and 1039 ppm respectively). The median estimate from each individual fossil is represented by a point. The mean CO_2 estimate is 946 ± 225 ppm. (Right) Points show Franks model CO_2 estimates from each fossil plotted with the 16th and 84th percentile confidence intervals derived from Monte Carlo simulations of error propagation. The majority of confidence intervals fall between 502 and 1637 ppm (grey shaded area; constructed using the 16th and 84th percentiles of the resampled CO_2 data). The samples from the Battery Point Formation are shown in pink and the samples from the Campbellton Formation are shown in blue. The number of stems from which stomata measurements were obtained from each sample is under each estimate. A star (*) denotes a sample where measurements were obtained from 10 stem fragments, but more than 10 fragments were preserved in that sample.

There are few proxy-based atmospheric CO_2 estimates for the Devonian period. Existing work that has focused on the early Devonian (Pragian-Emsian) using empirical and mechanistic gas exchange stomatal-based proxies (Dahl et al., 2022, Franks et al., 2014, McElwain, 1998), as well as an anatomically-based gas-exchange model (Roth-Nebelsick

and Konrad, 2003) and palaeosol proxies (Driese et al., 2000). More recent work has introduced a CO_2 proxy based on carbon isotope data of marine phytoplankton (Witkowski et al., 2018), although Devonian CO_2 estimates using this proxy are limited to between 388-370 Ma.

Existing proxy-based estimates for CO_2 during the Emsian are very variable. Previous CO_2 estimates based on *Sawdonia ornata* and *Aglaophyton major* fossils using the stomatal ratio method indicate CO_2 concentrations of between 1800-2029 ppm (using the 'Recent standard') and 3000-3382 ppm (using the 'Carboniferous standard') (McElwain, 1998), which is far higher than the CO_2 concentrations obtained from this study. However, the stomatal ratio method requires a comparison with a nearest living relative (NLR) or nearest living equivalent (NLE; i.e. a species that is morphologically and/or ecological comparable) and requires the assumption that the relationship between stomatal density and CO_2 is relatively unchanged over geological time (i.e. it is an evolutionarily conserved relationship) and therefore can be applied in deep time (McElwain and Steinthorsdottir, 2017). The need to compare fossil taxa with a NLR or NLE for the stomatal ratio method presents significant challenges when applied in deep time to enigmatic, extinct taxa. While the Franks model also requires calibration with a NLR or NLE, both in terms of the initialisation of photosynthetic rate and to correct for phylogenetic effects on carbon isotope discrimination, it provides a mechanistic basis for interpreting changes in stomatal density and size and does not require the assumption that the stomatal density-CO_2 relationship is unchanged over geological time (McElwain and Steinthorsdottir, 2017, Porter et al., 2017, Porter et al., 2019). In the case of the mechanistic model, it is recommended to use a species assemblage approach (with representatives of pteridophytes and spermatophytes) to obtain a consensus CO_2 estimate from taxa with differential stomatal behaviour and therefore differential stable carbon isotope discrimination (Porter et al., 2019). This is not always possible due to the incomplete nature of the fossil record and is further complicated in the case of the Devonian period by the scarcity of spermatophyte taxa with sufficient preservation for parameterization of the model, as well as the existence of extinct lineages where possible differences in carbon isotope discrimination is unknown. For example, both stomatal and carbon isotope data exist for *Archaeopteris* (Osborne et al., 2004, Wan et al.,

2019), but the stomatal response behaviour and therefore differential stable carbon isotope discrimination remains unknown.

Revised palaeosol-based estimates for the Emsian indicate CO_2 concentrations of 1320 ppm (+1320/-660 ppm) (Driese et al., 2000, Foster et al., 2017). The CO_2 estimates from this study lie within the confidence interval of the palaeosol proxy. However, palaeosol-based CO_2 estimates are sensitive to the contribution of soil-respired CO_2 (S(z)) used in the model (Montañez, 2013). While the correction to S(z) used by Foster et al. (2017) results in better agreement between palaeosol and other CO_2 proxies, there is still a large degree of uncertainty surrounding this parameter in the absence of an alternative method to derive S(z) (Foster et al., 2017).

The CO_2 estimates reported by Dahl et al. (2022) using Franks model (679 +104/-80 ppm) are closest to the results from this study, with some overlap between the confidence interval reported in this study (i.e. 597 – 1801 ppm) and the results reported therein. While our CO_2 estimates are higher than those reported by Dahl et al. (2022) using stomatal data for *Drepanophycus, Asteroxylon* and *Baragwanathia* fossils, we calculate lower palaeo-CO_2 estimates than those reported using previously published data for *Sawdonia* to parameterize the Franks model (approximately 3000 ppm; supplementary figure 11 of Dahl et al. (2022)). This is likely a result of the use of different stomatal scaling factors (discussed further in section 2.3.3).

2.3.3 Model Sensitivity

The results of the sensitivity analysis indicate that the Franks model is most sensitive to pore length scaling factor (S1), stomatal density, and guard cell length, as these produce the widest range of CO_2 estimates when varied across the range of values measured for each sample, or in the case of the pore length scaling factor, when varied between measured scaling factor (*Appendix 2.2*) and a generic scaling factor from the literature (Franks et al., 2014) (see *Figure 2.7*). The magnitude of model sensitivity caused by stomatal anatomy related parameters is the result of the large stomatal size of Devonian plants which ultimately play a very important role in controlling gas exchange in these ancient taxa. Using the minimum observed stomatal density measurement from each sample (defined here as a single hand specimen with between 2 and 28 stem fragments preserved (see section 2.2.3)) increased the median CO_2 estimate by 757 ppm. Using the minimum observed guard cell length measurement (i.e., the proxy measurement for pore length) from each sample also increased the median CO_2 estimate significantly (+572 ppm). Guard cell width (i.e., the proxy measurement for pore depth) had a smaller effect on CO_2 estimates produced by the model.

The morphological variation observed in this study is within what is expected based on previously published studies (Edwards, 1924, Hueber and Grierson, 1961, McElwain and Chaloner, 1995, Rayner, 1983, Zdebska, 1972). Steinthorsdottir et al. (2022) conducted a study on the potential climatic effects on CO_2 proxy estimates on a global sample of extant *Ginkgo biloba* and found that variability in measured leaf traits resulted in a reasonably wide range of CO_2 estimates (i.e., 290 – 626 ppm). In the case of this study, it is likely that the variability between samples is a result of true variation in *Sawdonia* stomatal anatomy and ecophysiology controlling the plants gas exchange and photosynthetic physiology. This should be confirmed with larger sample sizes in studies using fossils and extant plants, to confidently capture the natural variation in these traits and to obtain convergent CO_2 estimates. The influence of sample preservation quality on CO_2 estimate variation (with samples separated into 'medium' and 'high' quality preservation bins) was not found to have a significant effect on CO_2 estimates produced (Wilcoxon W=34 , p=0.2103).

The pore length scaling factor (S1 in Franks et al. (2014), i.e., scaling pore length from guard cell length) was found to be a critical parameter in the model. Using a generic scaling factor defined by using the generic 'lycophyte' scaling ratios of Franks et al. (2014) results in an increase in the median CO_2 estimate of +2065 ppm. Using this generic scaling factor with our guard cell length data, as opposed to values obtained from direct observations in this study and from published values used here (see *Table A2.2.1*) results in an estimated median pore length of 15µm. The resulting CO_2 estimates from this parameterisation of the pore length scaling factor are similar to those presented by Dahl et al. (2022) using *Sawdonia* fossils in supplementary figure 11 (approximately 3000 ppm). Dahl et al. (2022) used a pore length of 17µm for *Sawdonia* to parameterise the model. However, this value is at the lower end of the range of variation in pore length reported by Rayner (1983) for cf. *Sawdonia* sp. (15-35 µm), and therefore may have underestimated stomatal pore length, and did not fully account for any compensatory effect of pore size on low stomatal density, resulting in a higher CO_2 estimate. The median estimated pore length was found to be 33 µm when using the scaling factor derived from direct observations in this study and from published values (presented in *Table A2.2.1*). This is similar to the median pore length of 31 µm measured from fossils in this study where pore length was directly observable However, the pore length scaling factor may be difficult to fully constrain due to taxonomic uncertainties around some putative *Sawdonia* material (discussed in Berry and Gensel (2019); Gensel and Berry (2016)) and requires further study.

Despite the loose age-constraints on the plant fossil material in this study, and therefore uncertainty in $\delta^{13}C_{atmosphere}$, the model sensitivity analysis does not indicate a high degree of sensitivity to this input factor. The use of the maximum value calculated for $\delta^{13}C_{atmosphere}$ within the possible time interval for the Campbellton Formation (405–395 Ma) and Battery Point Formation (410–395 Ma) results in a modest increase to the median CO_2 estimate of 112 ppm. Similarly, the use of the minimum value calculated for $\delta^{13}C_{atmosphere}$ within the possible time interval for the two formations results in a modest decrease to the median CO_2 estimate of 62 ppm.

Previous studies have indicated a high degree of model sensitivity to the A_0 input parameter (McElwain et al., 2016). The model sensitivity analysis indicates that the use of a generic value of 3 µmol CO_2 m^{-2} s^{-1} (Franks et al., 2014) resulted in a decrease in the median CO_2 estimate of 175 ppm (compared to using an A_0 value of 3.86 µmol m^{-2} s^{-1} based on NLEs described in section 2.2.5).

Other model scaling factors are also a considerable source of sensitivity. Increasing the ratio of operational stomatal conductance to maximum stomatal conductance (ζ) from 0.2 to 0.3 results in a significant decrease in CO_2 estimates of 256 ppm. Recent studies on C3 angiosperms have indicated that the ratio of operational stomatal conductance to maximum stomatal conductance is approximately 0.26 (Murray et al., 2020). However, as there are currently no direct measurements of this scaling factor for lycophytes, and there is no evidence to suggest a high photosynthetic capacity for these fossil taxa (McElwain et al., 2015), the generic value of 0.2 (as recommended by Franks et al. (2014)) was used. Similarly, changing the pore shape parameterisation (β; a fraction of a circle with the diameter equal to stomatal pore length) results in significant changes to CO_2 estimates produced by the model. In this sensitivity analysis, we compared the effect of elongating the pore shape, i.e. decreasing the value of β from 0.6 (the value recommended by Franks et al. (2014) for lycophytes) and 0.4 (calculated by Dahl et al. (2022) from images of *Asteroxylon* fossils). This decrease in β resulted in a significant increase to the median CO_2 estimate by + 293 ppm. A value of 0.6 was used, as it was considered more likely to be robust, as it is based on multiple measurements on extant plants, and there is not sufficient evidence to suggest that *Sawdonia* had much more elongated pores than modern lycophytes. While the Franks model was found to be less sensitive to A_0, and pore shape (β) and operational stomatal conductance scaling factors in this study, they are still a potential source of sensitivity. Further research is recommended to better constrain these parameters, particularly for more ancient plant lineages.

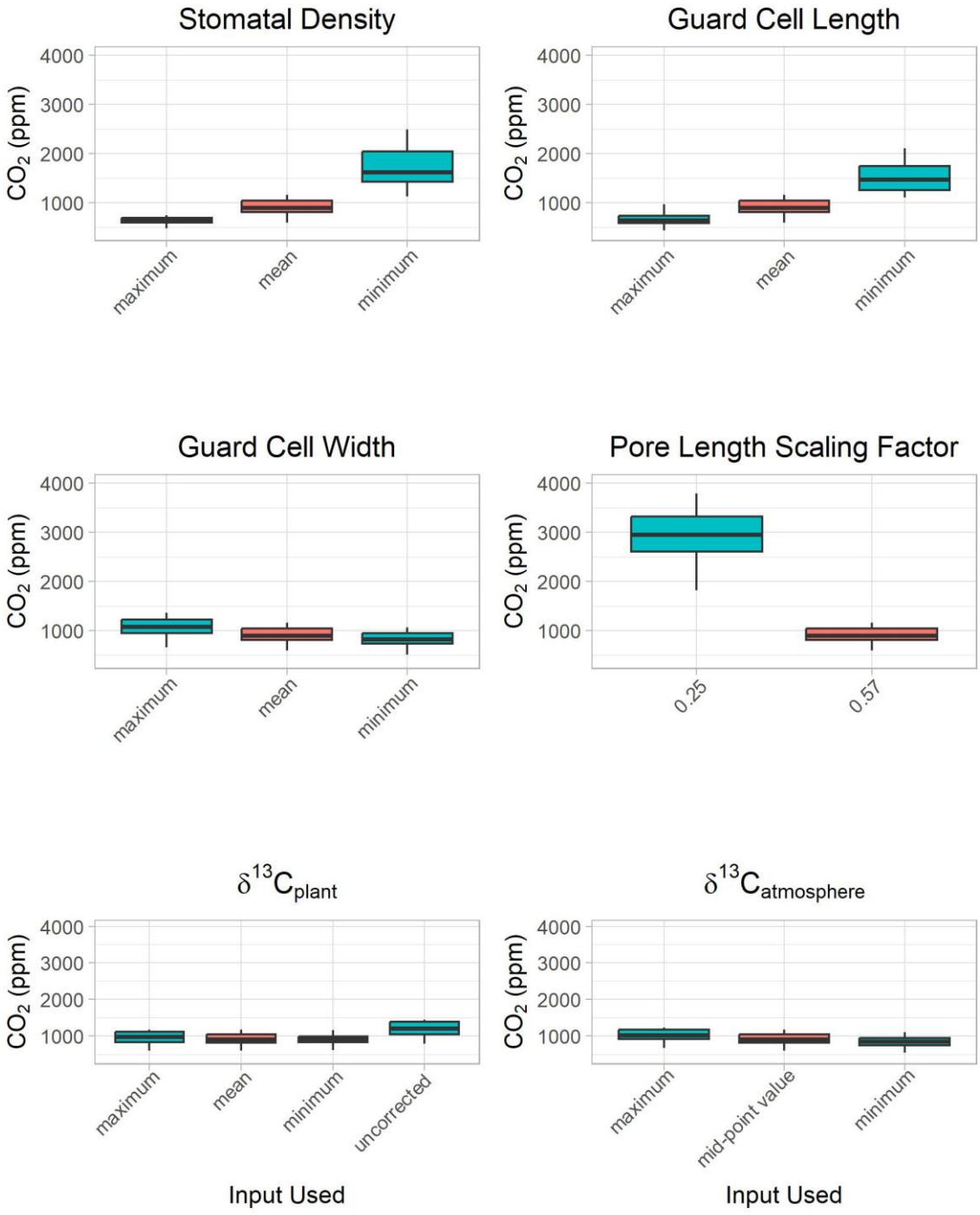

Figure 2.7. Sensitivity of the Franks model CO_2 estimates to different input parameters. Pink box plots denote the final input parameter used and corresponding CO_2 estimate. Input parameters used were the minimum, maximum and mean of fossil measurements obtained for each sample. The effect of initial the pore length (S1 in Franks et al. (2014)) scaling factor was tested for by varying the input parameters within a range of values suggested from the available literature. The effect of using the correction factor of Porter et al. (2017) on $\delta^{13}C_{plant}$ was also analysed. Model sensitivity to $\delta^{13}C_{atmosphere}$ was considered

by using the maximum and minimum values calculated for $\delta^{13}C_{atmosphere}$ within the possible time interval for the Campbellton Formation (405–395 Ma) and Battery Point Formation (410–395 Ma) to account for the age uncertainty of the two formations and temporal variation in $\delta^{13}C_{atmosphere}$ during this period. The midpoint value calculated for $\delta^{13}C_{atmosphere}$ during the time periods in question were used as the final input parameter. Outliers have been removed for ease of comparison. The results of the sensitivity analysis indicate that the Franks model is most sensitive to pore length scaling factor, stomatal density, and guard cell length, as these produced the widest range of CO_2 estimates in this analysis.

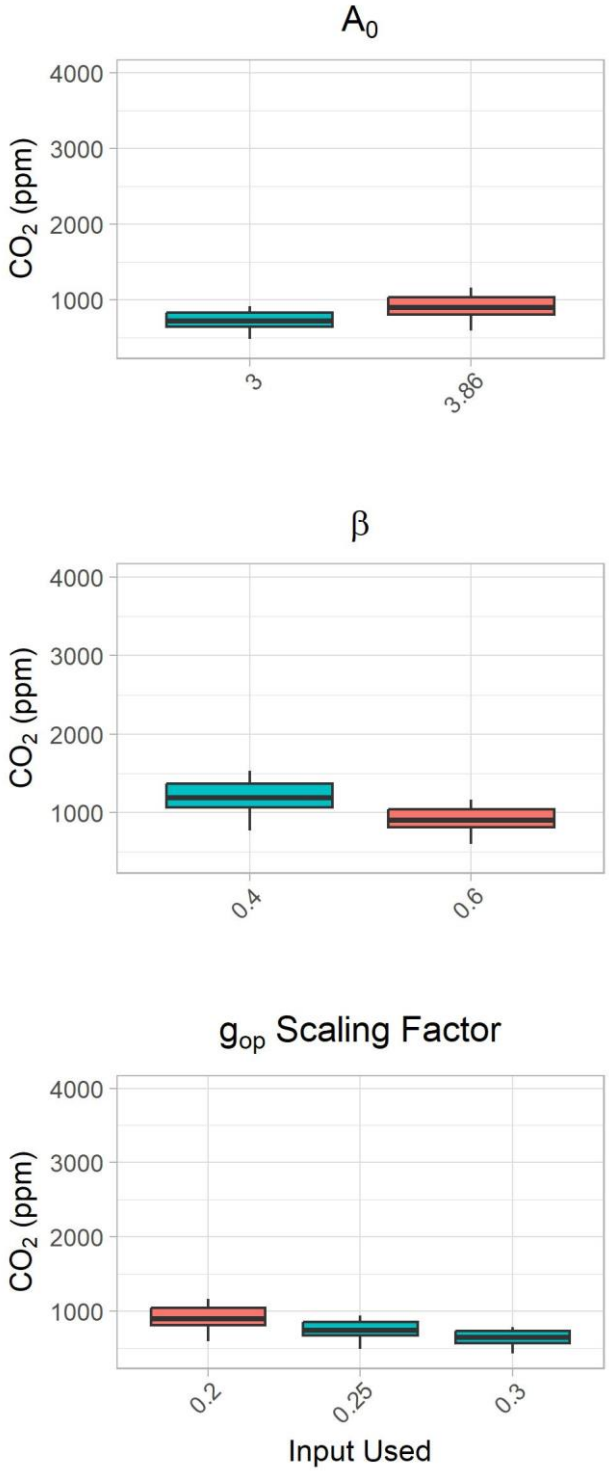

Figure 2.8. Sensitivity of the Franks model CO_2 estimates to different scaling factors. The effect of initial assimilation rate (A_0), pore shape (β, S3 in Franks et al. (2014)) and maximum stomatal conductance to operational stomatal conductance (g_{op}; S4 in Franks et al. (2014)) scaling factors were tested for by varying these input parameters within a range of values suggested from the available literature. Outliers have been removed for ease of comparison.

2.3.4 Further considerations

The Franks model is considered a robust method for palaeo-CO_2 estimates due to its mechanistic basis, and applicability (Konrad et al., 2021). However, recent studies have highlighted uncertainties associated with the use of carbon isotope data in CO_2 reconstructions due to the effects of water availability on plant carbon isotopic signature (Jardine and Lomax, 2021, Lomax et al., 2019). This is primarily an issue for proxies that rely solely on carbon isotope data (e.g. the proxy of Schubert and Jahren (2012)). A recent study by Steinthorsdottir et al. (2022) found that the effect of total annual precipitation on Franks gas exchange model CO_2 estimates was effectively 'dampened' by the inclusion of stomatal parameters, and therefore reconstructed CO_2 well across a range of climate conditions. In the context of this study, it is considered unlikely that water availability had a large effect on plant carbon isotope composition of fossils from the Campbellton formation given their growth in wetland and lakeside environments (Kennedy et al., 2012). However, fossil plants from the Battery Point Formation may have been periodically subject to osmotic stress due to tidal over wash (Griffing et al., 2000, Hotton et al., 2001). Osmotic stress is known to decrease carbon isotope discrimination in C3 plants (i.e. lead to a more positive $\delta^{13}C_p$) (Arens et al., 2000). Further analysis of a larger dataset of carbon isotope data for *Sawdonia* spp. from the Battery Point formation and the Campbellton Formation (Wan et al., 2019) has found that fossils from the Campbellton Formation show a more positive carbon isotope signature (median = -25.49‰) than the Battery Point Formation (-28.17‰, Wilcoxon W=20, p=0.01285). Based on the isotopic data and palaeoenvironmental information available, it is considered unlikely that water availability had a significant impact on the carbon isotopic signature of *Sawdonia*.

The results of our sensitivity analysis indicate that the model is most sensitive to stomatal density, pore length scaling factor and guard cell length within the range of variation measured in these fossil plants than other input parameters (see *Figure 2.7*). However, previous studies have found pore depth to be a critical parameter in the Franks model (Kowalczyk et al., 2018). There are generally two approaches to parameterising pore depth.

Pore depth can be scaled from single guard cell width, assuming that guard cells are circular in cross-section (Franks et al., 2014). This assumption is based on observations of inflated guard cells (Franks and Farquhar, 2007, Franks et al., 2001) and is supported by observations of lycophyte guard cell sections in the literature (Merced and Renzaglia, 2017, Skrodzki, 2017, Sun et al., 2005) (see *Appendix 2.5*). Alternatively other geometric ratios from a nearest living relative can be used (Franks et al., 2014).

To further investigate the sensitivity of the model to pore depth, we ran the Franks model using stomatal measurements of *Asteroxylon* from Edwards et al. (1998), varying the scaling relationship used for pore depth, and comparing it to the result obtained using pore depth as measured from the transverse section of an *Asteroxylon* stomatal complex from Edwards et al. (1998) (*Figure 2.8*). We note that using different scaling factors or assumptions to parameterise pore depth, can result in a large degree of variation in CO_2 estimates produced (ranging from 590 - 1253 ppm). On consideration of the literature supporting pore depth parameterisation, and by comparison of CO_2 estimates obtained using the different pore depth scaling assumptions, we believe that the scaling relationship of *0.4 x pore length* used by Dahl et al. (2022), is unsupported. We recommend a correction to their pore depth parameterisation by using the assumption that guard cells are circular in cross-section. While this is a small adjustment to the scaling relationship used, it results in a significant increase in the CO_2 estimate obtained using *Asteroxylon* of +370 ppm. When this correction to pore depth parameterisation, and the carbon isotope correction factor of Porter et al. (2017) are applied to the dataset of Dahl et al. (2022), the resulting revised upwards CO_2 estimates (see *Table 2.1*) are in better agreement with existing palaeosol and phytoplankton proxies and this study, but still shows a more gradual CO_2 drawdown over the Devonian period than earlier studies (Foster et al., 2017, Lenton et al., 2018, McElwain, 1998, Royer et al., 2014, Simon et al., 2007) (see *Figure 2.9*). Despite growing datasets on stomatal-based CO_2 estimates for the Devonian and increased understanding of the scaling factors which exert the greatest influence on these early land plants gas exchange properties, more research is still needed to better elucidate how atmospheric CO_2 changed during the late Devonian and early Mississippian, a time of profound evolutionary innovation in land plants.

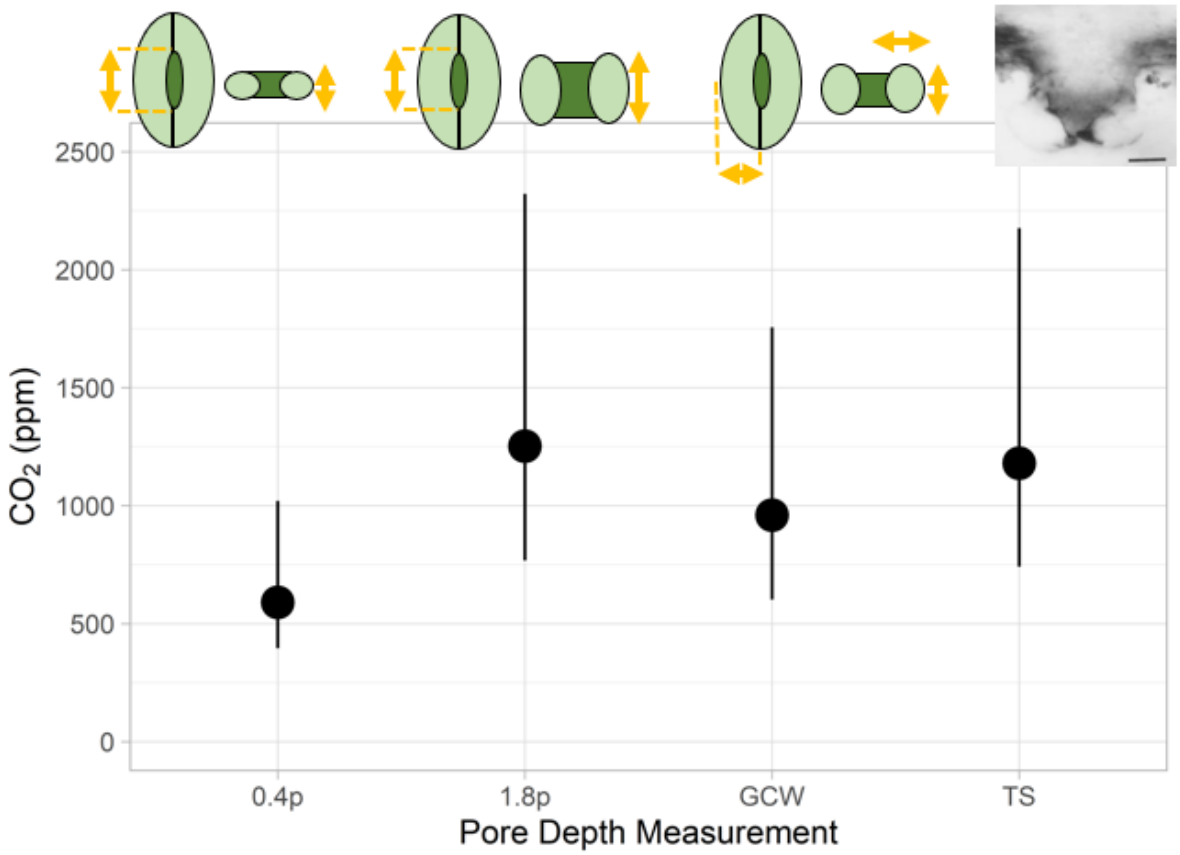

Figure 2.9. Effect of different pore depth parameterisations on CO_2 estimates using *Asteroxylon* stomatal measurements from Edwards *et al.,* (1998). Using pore length to pore depth scaling factor of 0.4 used by Dahl et al. (2022) results in an estimated atmospheric CO_2 concentration of 590 ppm. Using the single guard cell width (as in this study) results in an estimated atmospheric CO_2 concentration of 960 ppm. Using a pore length to pore depth scaling factor of 1.8 (based on Supplemental Table 2 in Franks et al. (2014)) results in an estimated atmospheric CO_2 concentration of 1253 ppm. This is compared to using stomatal depth measured directly from the transverse section of an *Asteroxylon* stoma from Edwards et al. (1998) (resulting in an estimated atmospheric CO_2 concentration of 1180 ppm). These estimates do not use the phylogenetic correction factor to $\delta^{13}C$ of Porter et al. (2017).

Table 2.1. The effect of revisions to pore depth parameterisation and carbon isotope data on CO_2 estimates. Pore depth parameterisation was changed using estimates for single guard cell width based on published data (Edwards et al., 1998, Hueber, 1983) and the phylogenetic carbon isotope correction factor for lycophytes was used (Porter et al., 2017). All other model inputs were kept the same as in Dahl et al. (2022). Error ranges reported represent the 84 and 16 percentiles as per Franks et al. (2014). D represents *Drepanophycus*, B represents *Baragwanathia,* and A represents *Asteroxylon*.

Fossil taxon	**Age**	**0.4 x pore length (µm)**	**Single Guard Cell Width (µm) estimated from Edwards et al. (1998) and Hueber (1983)**	**CO_2 estimates with 0.4 x pore length pore depth parameterisation (ppm +/- error) (Dahl et al., 2022)**	**CO_2 estimates with single guard cell width pore depth parameterisation (ppm +/- error), and correction to carbon isotope data of Porter et al. (2017)**
D	380.46	6.8	25	581 (+79/-64)	**1000 (+565/-349)**
D	387.85	6.8	25	698 (+100/-77)	**1264 (+717/-439)**
D	387.85	6.8	25	607 (+82/-64)	**1120 (+643/-401)**
D	394.05	6.8	25	552 (+90/-82)	**1013 (+666/-386)**
D	401.58	6.8	25	610 (+83/-68)	**1132 (+660/-406)**
D	402.33	6.8	25	679 (+101/-80)	**1258 (+722/-455)**
D	404.59	6.8	25	639 (+89/-69)	**1182 (+686/-429)**
D	408.39	6.8	25	714 (+144/-102)	**1279 (+859/-473)**
B	409.10	11.2	27.5	533 (+77/-76)	**754 (+662/-231)**
A	409.10	7.6	22.5	516 (+136/-95)	**882 (+749/-341)**

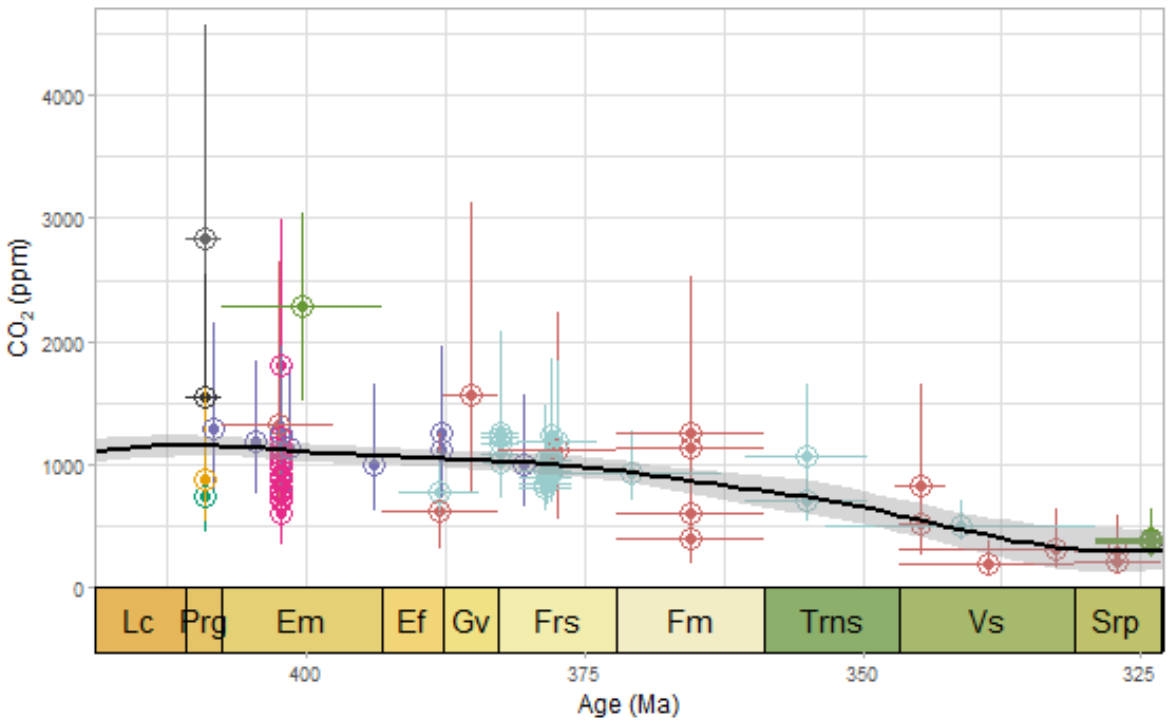

Figure 2.10. Effect of correcting for pore depth parameterisation and phylogenetic effect on carbon isotope discrimination on CO_2 estimates. Using the single guard cell width as a proxy for pore depth and the phylogenetic correction factor of Porter et al. (2017) (as in this study) results in a much better agreement between estimated atmospheric CO_2 concentrations. Points correspond to various atmospheric CO_2 proxies (pink - using the Franks model on *Sawdonia* fossils (this study); purple - using the Franks model on *Drepanophycus* fossils, with modifications to pore depth scaling and $\delta^{13}C$ (modified from Dahl et al. (2022)); dark green - using the Franks model on *Asteroxylon* fossil data, with modifications to pore depth scaling and $\delta^{13}C$ (modified from Dahl et al. (2022)); orange - using the Franks model on *Baragwanathia* fossil data, with modifications to pore depth scaling and $\delta^{13}C$ (modified from Dahl et al. (2022)); red - palaeosol data of Cox et al. (2001), Driese et al. (2000), Ekart et al. (1999), Mora et al. (1996) and Muchez et al. (1993) as used in Foster et al. (2017); light green - stomatal frequency proxies of McElwain (1998) and Beerling (2002); black - gas exchange model of Franks et al. (2014); grey - gas exchange model of Roth-Nebelsick and Konrad (2003); blue - phytoplankton data from Witkowski et al. (2018). The black line shows the loess curve with a span of 0.3 (see *Appendix 2.6*). The deeptime R package (Gearty, 2021) was used for the geological scale on the x-axis after Cohen et al. (2013).

2.3.5 Recommendations

While there is some agreement between the CO_2 estimates produced from this study and other research, there are a number of inconsistencies between estimates. A number of previous multi-proxy-based CO_2 studies show good agreement between gas-exchange models and stomatal frequency-based methods (Kowalczyk et al., 2018, Li et al., 2019, Montañez et al., 2016, Steinthorsdottir et al., 2021, Zhou et al., 2020). However, this is not the case in this study. This may be a result of uncertainty in selection of an appropriate NLR or NLE. While the Franks model is in some ways less sensitive to NLE selection, there are still input parameters which require the use of a NLR or NLE. Therefore, more research is needed to further clarify what groups of extant plants are most appropriate for this purpose, and multi-proxy estimates are crucial to try to gain a better understanding of the evolution of Earth's atmosphere in deep time, and to better evaluate the most likely atmospheric CO_2 concentrations during the Devonian period.

Model sensitivity to pore length and depth scaling factors highlights the importance of trying to better constrain these scaling factors. In the case where these scaling factors cannot be well constrained from the fossil material being studied (e.g., due to lack of preservation), it may be possible to use a scaling factor based on a related, and ecologically similar coeval fossil. In the case where neither is available, the use of a carefully selected NLR or NLE may be appropriate. Further detailed comparisons of fossil and modern material for this purpose are recommended.

2.4 Conclusion

This study presents the first application of the Franks model for Devonian-age fossils where all fossil-based input parameters were measured from the same fossil specimens, thereby minimizing a potential source of error caused by natural genotypic and phenotypic variability in plant photosynthetic biology and gas exchange characteristics. The results indicate elevated atmospheric CO_2 concentrations during the early Devonian (Emsian) of 898 ppm (+616/-405) and, with revisions to existing data, highlights that a more gradual CO_2 drawdown may have occurred during the Devonian period than previously thought. This more gradual decreasing trend is consistent with emerging proxy data (Witkowski et al., 2018). Although our analysis has revised upwards the palaeo-CO_2 estimates by Dahl et al. (2022), a finding of more gradual pCO_2 change during the Devonian is generally consistent with their main conclusion. However, we find that the assertion that CO_2 was low before the rise of forest ecosystems is unsupported. Our detailed study of *Sawdonia* fossil stomatal traits also demonstrates the need for the development of robust constraints on key input parameters to further support the application of gas exchange models for palaeo-CO_2 reconstructions on deep time taxa. Further research is needed to better constrain existing CO_2 proxies and to better account for discrepancies between them. This is especially important during this critical time in Earth history when plants are hypothesised to have evolved the physiological capacity to impact Earth system processes.

References

ALGEO, T. J. & SCHECKLER, S. E. 1998. Terrestrial-marine teleconnections in the Devonian: links between the evolution of land plants, weathering processes, and marine anoxic events. *Philosophical Transactions of the Royal Society of London. Series B: Biological Sciences,* **353,** 113-130.

ALGEO, T. J. & SCHECKLER, S. E. 2010. Land plant evolution and weathering rate changes in the Devonian. *Journal of Earth Science,* **21,** 75-78.

ARENS, N. C., JAHREN, A. H. & AMUNDSON, R. 2000. Can C3 plants faithfully record the carbon isotopic composition of atmospheric carbon dioxide? *Paleobiology,* **26,** 137-164.

BEERLING, D. 2002. Low atmospheric CO_2 levels during the Permo-Carboniferous glaciation inferred from fossil lycopsids. *Proceedings of the National Academy of Sciences,* **99,** 12567-12571.

BEERLING, D. J. 2005. Leaf evolution: gases, genes and geochemistry. *Annals of Botany,* **96,** 345-352.

BEERLING, D. J., OSBORNE, C. P. & CHALONER, W. G. 2001. Evolution of leaf-form in land plants linked to atmospheric CO_2 decline in the Late Palaeozoic era. *Nature,* **410,** 352-354.

BERNER, R. A. 1997. The rise of plants and their effect on weathering and atmospheric CO_2. *Science,* **276,** 544-546.

BERNER, R. A. 2006. GEOCARBSULF: a combined model for Phanerozoic atmospheric O_2 and CO_2. *Geochimica et Cosmochimica Acta,* **70,** 5653-5664.

BERRY, C. M. & GENSEL, P. G. 2019. Late Mid Devonian *Sawdonia* (Zosterophyllopsida) from Venezuela. *International Journal of Plant Sciences,* **180,** 540-557.

BOYCE, C. K., IBARRA, D. E. & D'ANTONIO, M. P. 2023. What we talk about when we talk about the long-term carbon cycle. *New Phytologist,* **237,** 1550-1557.

BRODRIBB, T. J. & HOLBROOK, N. M. 2006. Declining hydraulic efficiency as transpiring leaves desiccate: two types of response. *Plant, Cell & Environment,* **29,** 2205-2215.

BRUGGER, J., HOFMANN, M., PETRI, S. & FEULNER, G. 2019. On the sensitivity of the Devonian climate to continental configuration, vegetation cover, orbital configuration, CO_2 concentration, and insolation. *Paleoceanography and Paleoclimatology,* **34,** 1375-1398.

CAMPANY, C. E., MARTIN, L. & WATKINS JR, J. E. 2019. Convergence of ecophysiological traits drives floristic composition of early lineage vascular plants in a tropical forest floor. *Annals of Botany,* **123,** 793-803.

CAPEL, E., CLEAL, C. J., XUE, J., MONNET, C., SERVAIS, T. & CASCALES-MIÑANA, B. 2022. The Silurian–Devonian terrestrial revolution: diversity patterns and sampling bias of the vascular plant macrofossil record. *Earth-Science Reviews,* **231,** 104085.

CARMICHAEL, S. K., WATERS, J. A., KOENIGSHOF, P., SUTTNER, T. J. & KIDO, E. 2019. Paleogeography and paleoenvironments of the Late Devonian Kellwasser event: A review of its sedimentological and geochemical expression. *Global and Planetary Change,* **183,** 102984.

CARRIQUÍ, M., ROIG-OLIVER, M., BRODRIBB, T. J., COOPMAN, R., GILL, W., MARK, K., NIINEMETS, Ü., PERERA-CASTRO, A. V., RIBAS-CARBÓ, M. & SACK, L. 2019. Anatomical constraints to nonstomatal diffusion conductance and photosynthesis in lycophytes and bryophytes. *New Phytologist,* **222,** 1256-1270.

CHALONER, W., HILL, A. & ROGERSON, C. 1978. Early Devonian plant fossils from a southern England UK borehole *Palaeontology,* **21,** 693-708.

CHEN, B., CHEN, J., QIE, W., HUANG, P., HE, T., JOACHIMSKI, M. M., REGELOUS, M., VON STRANDMANN, P. A. P., LIU, J. & WANG, X. 2021. Was climatic cooling during the earliest Carboniferous driven by expansion of seed plants? *Earth and Planetary Science Letters,* **565,** 116953.

CLARK, J. W., HARRIS, B. J., HETHERINGTON, A. J., HURTADO-CASTANO, N., BRENCH, R. A., CASSON, S., WILLIAMS, T. A., GRAY, J. E. & HETHERINGTON, A. M. 2022. The origin and evolution of stomata. *Current Biology,* **32,** R539-R553.

COATES, J. C., MOODY, L. A. & SAIDI, Y. 2011. Plants and the earth system-past events and future challenges. *The New Phytologist,* **189,** 370-373.

COHEN, K. M., FINNEY, S. C., GIBBARD, P. L. & FAN, J.-X. 2013. The ICS international chronostratigraphic chart. *Episodes Journal of International Geoscience,* **36,** 199-204.

COX, J., RAILSBACK, L. & GORDON, E. 2001. Evidence from Catskill pedogenic carbonates for a rapid Late Devonian decrease in atmospheric carbon dioxide concentrations. *Northeastern Geology and Environmental Sciences,* **23,** 91-102.

CRAMER, B.D. & JARVIS, I. (2020) 'Carbon isotope stratigraphy', in GRADSTEIN, F.M., OGG, J.G., SCHMITZ, M.D. & OGG, G.M. (ed.) *Geologic Time Scale 2020.* Elsevier, pp. 309-343.

CUI, Y., SCHUBERT, B. A. & JAHREN, A. H. 2020. A 23 my record of low atmospheric CO_2. *Geology,* **48,** 888-892.

D'ANTONIO, M. P., IBARRA, D. E. & BOYCE, C. K. 2023. The preservation of cause and effect in the rock record. *Paleobiology,* **49,** 204-214.

DAHL, T. W., HARDING, M. A., BRUGGER, J., FEULNER, G., NORRMAN, K., LOMAX, B. H. & JUNIUM, C. K. 2022. Low atmospheric CO_2 levels before the rise of forested ecosystems. *Nature Communications,* **13,** 7616.

DRIESE, S. G., MORA, C. I. & ELICK, J. M. 2000. The paleosol record of increasing plant diversity and depth of rooting and changes in atmospheric pCO_2 in the Siluro-Devonian. *The Paleontological Society Papers,* **6,** 47-62.

EDWARDS, D. 1993. Cells and tissues in the vegetative sporophytes of early land plants. *New Phytologist,* 125**,** 225-247.

EDWARDS, D., EDWARDS, D. S. & RAYNER, R. 1982. The cuticle of early vascular plants and its evolutionary significance. *In:* CULTER, D. F., ALVIN, K. L. & PRICE, C. E. (eds.) *The plant cuticle.* London: Academic Press.

EDWARDS, D., KERP, H. & HASS, H. 1998. Stomata in early land plants: an anatomical and ecophysiological approach. *Journal of Experimental Botany,* **49,** 255-278.

EDWARDS, W. 1924. On the cuticular structure of the Devonian plant *Psilophyton*. *Botanical Journal of the Linnean Society,* **46,** 377-385.

EKART, D. D., CERLING, T. E., MONTANEZ, I. P. & TABOR, N. J. 1999. A 400 million year carbon isotope record of pedogenic carbonate: implications for paleoatmospheric carbon dioxide. *American Journal of Science,* **299**.

ELICK, J. M., DRIESE, S. G. & MORA, C. I. 1998. Very large plant and root traces from the Early to Middle Devonian: implications for early terrestrial ecosystems and atmospheric $p(CO_2)$. *Geology,* **26,** 143-146.

FARQUHAR, G. D. & SHARKEY, T. D. 1982. Stomatal conductance and photosynthesis. *Annual review of plant physiology,* **33,** 317-345.

FLETCHER, B. J., BRENTNALL, S. J., QUICK, W. P. & BEERLING, D. J. 2006. BRYOCARB: a process-based model of thallose liverwort carbon isotope fractionation in response to CO_2, O_2, light and temperature. *Geochimica et Cosmochimica Acta,* **70,** 5676-5691.

FOSTER, G. L., ROYER, D. L. & LUNT, D. J. 2017. Future climate forcing potentially without precedent in the last 420 million years. *Nature communications,* **8,** 14845.

FRANKLIN, J., SERRA-DIAZ, J. M., SYPHARD, A. D. & REGAN, H. M. 2016. Global change and terrestrial plant community dynamics. *Proceedings of the National Academy of Sciences,* **113,** 3725-3734.

FRANKS, P. J., BUCKLEY, T. N., SHOPE, J. C. & MOTT, K. A. 2001. Guard cell volume and pressure measured concurrently by confocal microscopy and the cell pressure probe. *Plant physiology,* **125,** 1577-1584.

FRANKS, P. J. & FARQUHAR, G. D. 2001. The effect of exogenous abscisic acid on stomatal development, stomatal mechanics, and leaf gas exchange in *Tradescantia virginiana*. *Plant physiology,* **125,** 935-942.

FRANKS, P. J. & FARQUHAR, G. D. 2007. The mechanical diversity of stomata and its significance in gas-exchange control. *Plant physiology,* **143,** 78-87.

FRANKS, P. J., ROYER, D. L., BEERLING, D. J., VAN DE WATER, P. K., CANTRILL, D. J., BARBOUR, M. M. & BERRY, J. A. 2014. New constraints on atmospheric CO_2 concentration for the Phanerozoic. *Geophysical Research Letters,* **41,** 4685-4694.

GEARTY, W. 2021. Deeptime: plotting tools for anyone working in deep time. *R package version 0.0,* 6.

GENSEL, P. G. 1992. Phylogenetic relationships of the zosterophylls and lycopsids: evidence from morphology, paleoecology, and cladistic methods of inference. *Annals of the Missouri Botanical Garden***,** 450-473.

GENSEL, P. G. & BERRY, C. M. 2016. Sporangial morphology of the Early Devonian zosterophyll *Sawdonia ornata* from the type locality (Gaspé). *International Journal of Plant Sciences,* **177,** 618-632.

GENSEL, P. G. & EDWARDS, D. 2001. *Plants invade the land: evolutionary and environmental perspectives*, Columbia University Press.

GIRARD, C., CORNEE, J.-J., JOACHIMSKI, M. M., CHARRUAULT, A.-L., DUFOUR, A.-B. & RENAUD, S. 2020. Paleogeographic differences in temperature, water depth and conodont biofacies during the Late Devonian. *Palaeogeography, Palaeoclimatology, Palaeoecology,* **549,** 108852.

GRIFFING, D. H., BRIDGE, J. S. & HOTTON, C. L. 2000. Coastal-fluvial palaeoenvironments and plant palaeoecology of the Lower Devonian (Emsian), Gaspé Bay, Québec, Canada. *Geological Society, London, Special Publications,* **180,** 61-84.

HETHERINGTON, A. J. & DOLAN, L. 2019. Rhynie chert fossils demonstrate the independent origin and gradual evolution of lycophyte roots. *Current opinion in plant biology,* **47,** 119-126.

HOTTON, C., HUEBER, F., GRIFFING, D. & BRIDGE, J. 2001. Early terrestrial plant environments: an example from the Emsian of Gaspé, Canada. *Plants invade the land: evolutionary and environmental perspectives.* Columbia University Press.

HUEBER, F. M. 1971. *Sawdonia ornata*: a new name for *Psilophyton princeps* var. *ornatum*. *Taxon,* **20,** 641-642.

HUEBER, F. M. 1983. A new species of *Baragwanathia* from the Sextant Formation (Emsian) northern Ontario, Canada. *Botanical Journal of the Linnean Society,* **86,** 57-79.

HUEBER, F. M. & GRIERSON, J. 1961. On the occurrence of *Psilophyton princeps* in the early Upper Devonian of New York. *American Journal of Botany,* **48,** 473-479.

JARDINE, P. E. & LOMAX, B. H. 2021. A 23 my record of low atmospheric CO_2: COMMENT. *Geology,* **49**.

JOACHIMSKI, M., BREISIG, S., BUGGISCH, W., TALENT, J., MAWSON, R., GEREKE, M., MORROW, J., DAY, J. & WEDDIGE, K. 2009. Devonian climate and reef evolution: insights from oxygen isotopes in apatite. *Earth and Planetary Science Letters,* **284,** 599-609.

KAISER, S. I., ARETZ, M. & BECKER, R. T. 2016. The global Hangenberg Crisis (Devonian–Carboniferous transition): review of a first-order mass extinction. *Geological Society, London, Special Publications,* **423,** 387-437.

KENNEDY, K. L., GENSEL, P. G. & GIBLING, M. R. 2012. Paleoenvironmental inferences from the classic Lower Devonian plant-bearing locality of the Campbellton Formation, New Brunswick, Canada. *Palaios,* **27,** 424-438.

KENRICK, P. & CRANE, P. R. 1997. The origin and early evolution of plants on land. *Nature,* **389,** 33-39.

KONRAD, W., KATUL, G., ROTH-NEBELSICK, A. & GREIN, M. 2017. A reduced order model to analytically infer atmospheric CO_2 concentration from stomatal and climate data. *Advances in Water Resources,* **104,** 145-157.

KONRAD, W., ROTH-NEBELSICK, A. & GREIN, M. 2008. Modelling of stomatal density response to atmospheric CO_2. *Journal of theoretical Biology,* **253,** 638-658.

KONRAD, W., ROYER, D. L., FRANKS, P. J. & ROTH-NEBELSICK, A. 2021. Quantitative critique of leaf-based paleo-CO_2 proxies: Consequences for their reliability and applicability. *Geological Journal,* **56,** 886-902.

KOWALCZYK, J. B., ROYER, D. L., MILLER, I. M., ANDERSON, C. W., BEERLING, D. J., FRANKS, P. J., GREIN, M., KONRAD, W., ROTH-NEBELSICK, A. & BOWRING, S. A. 2018. Multiple proxy estimates of atmospheric CO_2 from an early Paleocene rainforest. *Paleoceanography and Paleoclimatology,* **33,** 1427-1438.

LANG, W. 1933. XVII.—Contributions to the study of the Old Red Sandstone flora of Scotland. VIII. On *Arthrostigma*, *Psilophyton*, and some associated plant-remains from the Strathmore beds of the Caledonian Lower Old Red Sandstone. *Earth and Environmental Science Transactions of The Royal Society of Edinburgh,* **57,** 491-521.

LANG, W. H. 1931. On the spines, sporangia, and spores of *Psilophyton princeps*, Dawson, shown in specimens from Gaspé. *Philosophical Transactions of the Royal Society of London. Series B, Containing Papers of a Biological Character***,** 421-442.

LE HIR, G., DONNADIEU, Y., GODDÉRIS, Y., MEYER-BERTHAUD, B., RAMSTEIN, G. & BLAKEY, R. C. 2011. The climate change caused by the land plant invasion in the Devonian. *Earth and Planetary Science Letters,* **310,** 203-212.

LENTON, T. M., DAINES, S. J. & MILLS, B. J. 2018. COPSE reloaded: an improved model of biogeochemical cycling over Phanerozoic time. *Earth-Science Reviews,* 178**,** 1-28.

LI, H., YU, J., MCELWAIN, J. C., YIOTIS, C. & CHEN, Z.-Q. 2019. Reconstruction of atmospheric CO_2 concentration during the late Changhsingian based on fossil conifers from the Dalong Formation in South China. *Palaeogeography, Palaeoclimatology, Palaeoecology,* **519,** 37-48.

LOMAX, B. H., LAKE, J. A., LENG, M. J. & JARDINE, P. E. 2019. An experimental evaluation of the use of $\Delta^{13}C$ as a proxy for palaeoatmospheric CO_2. *Geochimica et Cosmochimica Acta,* **247,** 162-174.

MAFFRE, P., GODDERIS, Y., POHL, A., DONNADIEU, Y., CARRETIER, S. & LE HIR, G. 2022. The complex response of continental silicate rock weathering to the colonization of the continents by vascular plants in the Devonian. *American Journal of Science,* **322,** 461-492.

MATTHAEUS, W. J., MACAREWICH, S. I., RICHEY, J., MONTAÑEZ, I. P., MCELWAIN, J. C., WHITE, J. D., WILSON, J. P. & POULSEN, C. J. 2023. A systems approach to understanding how plants transformed Earth's environment in deep time. *Annual Review of Earth and Planetary Sciences,* **51,** 551-580.

MCELWAIN, J. 1998. Do fossil plants signal palaeoatmospheric carbon dioxide concentration in the geological past? *Philosophical Transactions of the Royal Society of London. Series B: Biological Sciences,* **353,** 83-96.

MCELWAIN, J. C. & CHALONER, W. G. 1995. Stomatal density and index of fossil plants track atmospheric carbon dioxide in the Palaeozoic. *Annals of Botany,* **76,** 389-395.

MCELWAIN, J. C. & CHALONER, W. G. 1996. The fossil cuticle as a skeletal record of environmental change. *Palaios,* **11,** 376-388.

MCELWAIN, J. C., MONTAÑEZ, I., WHITE, J. D., WILSON, J. P. & YIOTIS, C. 2016. Was atmospheric CO_2 capped at 1000 ppm over the past 300 million years? *Palaeogeography, Palaeoclimatology, Palaeoecology,* **441,** 653-658.

MCELWAIN, J. C. & STEINTHORSDOTTIR, M. 2017. Paleoecology, ploidy, paleoatmospheric composition, and developmental biology: a review of the multiple uses of fossil stomata. *Plant Physiology,* **174,** 650-664.

MCELWAIN, J. C., YIOTIS, C. & LAWSON, T. 2015. Using modern plant trait relationships between observed and theoretical maximum stomatal conductance and vein density to examine patterns of plant macroevolution. *New Phytologist,* **209,** 94-103.

MERCED, A. & RENZAGLIA, K. S. 2017. Structure, function and evolution of stomata from a bryological perspective. *Bryophyte Diversity and Evolution,* **39,** 7–20.

MILLS, B.J.W., KRAUSE, A.J., JARVIS, I. & CRAMER, B.D. 2023. Evolution of atmospheric O_2 through the Phanerozoic Revisited. *Annual Review of Earth and PLanetary Sciences,* **51,** 253-276.

MONTAÑEZ, I. P. 2013. Modern soil system constraints on reconstructing deep-time atmospheric CO_2. *Geochimica et Cosmochimica Acta,* **101,** 57-75.

MONTAÑEZ, I. P., MCELWAIN, J. C., POULSEN, C. J., WHITE, J. D., DIMICHELE, W. A., WILSON, J. P., GRIGGS, G. & HREN, M. T. 2016. Climate, pCO_2 and terrestrial carbon cycle linkages during late Palaeozoic glacial–interglacial cycles. *Nature Geoscience,* **9,** 824-828.

MORA, C. I., DRIESE, S. G. & COLARUSSO, L. A. 1996. Middle to Late Paleozoic atmospheric CO_2 levels from soil carbonate and organic matter. *Science,* **271,** 1105-1107.

MUCHEZ, P., PEETERS, C., KEPPENS, E. & VIAENE, W. 1993. Stable isotopic composition of paleosols in the Lower Viséan of eastern Belgium: evidence of evaporation and soil-gas CO_2. *Chemical geology,* **106,** 389-396.

MURRAY, M., SOH, W. K., YIOTIS, C., SPICER, R. A., LAWSON, T. & MCELWAIN, J. C. 2020. Consistent relationship between field-measured stomatal conductance and theoretical maximum stomatal conductance in C3 woody angiosperms in four major biomes. *International Journal of Plant Sciences,* **181,** 142-154.

OSBORNE, C., BEERLING, D., LOMAX, B. & CHALONER, W. 2004. Biophysical constraints on the origin of leaves inferred from the fossil record. *Proceedings of the National Academy of Sciences,* **101,** 10360-10362.

PAWLIK, Ł., BUMA, B., ŠAMONIL, P., KVAČEK, J., GAŁĄZKA, A., KOHOUT, P. & MALIK, I. 2020. Impact of trees and forests on the Devonian landscape and weathering processes with implications to the global Earth's system properties-A critical review. *Earth-Science Reviews,* **205,** 103200.

PORTER, A. S., GERALD, C. E.-F., YIOTIS, C., MONTANEZ, I. P. & MCELWAIN, J. C. 2019. Testing the accuracy of new paleoatmospheric CO_2 proxies based on plant stable carbon isotopic composition and stomatal traits in a range of simulated paleoatmospheric O_2: CO_2 ratios. *Geochimica et Cosmochimica Acta,* 259**,** 69-90.

PORTER, A. S., YIOTIS, C., MONTAÑEZ, I. P. & MCELWAIN, J. C. 2017. Evolutionary differences in $\Delta^{13}C$ detected between spore and seed bearing plants following exposure to a range of atmospheric O_2: CO_2 ratios; implications for paleoatmosphere reconstruction. *Geochimica et Cosmochimica Acta,* **213,** 517-533.

POULTER, B., CIAIS, P., HODSON, E., LISCHKE, H., MAIGNAN, F., PLUMMER, S. & ZIMMERMANN, N. 2011. Plant functional type mapping for earth system models. *Geoscientific Model Development,* **4,** 993-1010.

PRESTIANNI, C. & GERRIENNE, P. 2010. Early seed plant radiation: an ecological hypothesis. *Geological Society, London, Special Publications,* **339,** 71-80.

QIE, W., ZHANG, J., LUO, G., ALGEO, T. J., CHEN, B., XIANG, L., LIANG, K., LIU, X., POGGE VON STRANDMANN, P. A. & CHEN, J. 2023. Enhanced continental weathering as a trigger for the End-Devonian Hangenberg Crisis. *Geophysical Research Letters,* **50,** e2022GL102640.

RAYNER, R. 1983. New observations on *Sawdonia ornata* from Scotland. *Earth and Environmental Science Transactions of The Royal Society of Edinburgh,* **74,** 79-93.

ROTH-NEBELSICK, A. & KONRAD, W. 2003. Assimilation and transpiration capabilities of rhyniophytic plants from the Lower Devonian and their implications for paleoatmospheric CO_2 concentration. *Palaeogeography, Palaeoclimatology, Palaeoecology,* **202,** 153-178.

ROWE, N. & SPECK, T. 2005. Plant growth forms: an ecological and evolutionary perspective. *New phytologist,* **166,** 61-72.

ROYER, D. L., DONNADIEU, Y., PARK, J., KOWALCZYK, J. & GODDERIS, Y. 2014. Error analysis of CO_2 and O_2 estimates from the long-term geochemical model GEOCARBSULF. *American Journal of Science,* **314,** 1259-1283.

SCHUBERT, B. A. & JAHREN, A. H. 2012. The effect of atmospheric CO_2 concentration on carbon isotope fractionation in C3 land plants. *Geochimica et Cosmochimica Acta,* **96,** 29-43.

SHOUGANG, H., BECK, C. B. & DEMING, W. 2003. Structure of the earliest leaves: adaptations to high concentrations of atmospheric CO_2. *International Journal of Plant Sciences,* **164,** 71-75.

SHUKLA, P. R., SKEA, J., CALVO BUENDIA, E., MASSON-DELMOTTE, V., PÖRTNER, H. O., ROBERTS, D., ZHAI, P., SLADE, R., CONNORS, S. & VAN DIEMEN, R. 2019. IPCC, 2019: Climate Change and Land: an IPCC special report on climate change, desertification, land degradation, sustainable land management, food security, and greenhouse gas fluxes in terrestrial ecosystems.

SIMON, L., GODDÉRIS, Y., BUGGISCH, W., STRAUSS, H. & JOACHIMSKI, M. M. 2007. Modeling the carbon and sulfur isotope compositions of marine sediments: climate evolution during the Devonian. *Chemical Geology,* **246,** 19-38.

SKRODZKI, C. 2017. *Lycophyte Huperzia lucidula Morphological, Physiological, and Modelled Response to Paleozoic Environmental Conditions.* Masters, Baylor University.

STEIN, W. E., BERRY, C. M., MORRIS, J. L., HERNICK, L. V., MANNOLINI, F., VER STRAETEN, C., LANDING, E., MARSHALL, J. E., WELLMAN, C. H. & BEERLING, D. J. 2020. Mid-Devonian *Archaeopteris* roots signal revolutionary change in earliest fossil forests. *Current biology,* **30,** 421-431.

STEIN, W. E., MANNOLINI, F., HERNICK, L. V., LANDING, E. & BERRY, C. M. 2007. Giant cladoxylopsid trees resolve the enigma of the Earth's earliest forest stumps at Gilboa. *Nature,* **446,** 904-907.

STEINTHORSDOTTIR, M., JARDINE, P., LOMAX, B. & SALLSTEDT, T. 2022. Key traits of living fossil *Ginkgo biloba* are highly variable but not influenced by climate–Implications for palaeo-pCO_2 reconstructions and climate sensitivity. *Global and Planetary Change,* **211,** 103786.

STEINTHORSDOTTIR, M., JARDINE, P. E. & REMBER, W. C. 2021. Near-future pCO_2 during the hot Mid Miocene Climatic Optimum. *Paleoceanography and Paleoclimatology,* **36,** e2020PA003900.

STRULLU-DERRIEN, C., KENRICK, P., BADEL, E., COCHARD, H. & TAFFOREAU, P. 2013. An overview of the hydraulic systems in early land plants. *Iawa Journal,* **34,** 333-351.

SUN, T.-X., EDWARDS, D. & LI, C.-S. 2005. The stomatal apparatus of *Lycopodium japonicum* and its bearing on the stomata of the Devonian lycophyte *Drepanophycus spinaeformis*. *Botanical journal of the Linnean society,* **149,** 209-216.

VEIZER, J., ALA, D., AZMY, K., BRUCKSCHEN, P., BUHL, D., BRUHN, F., CARDEN, G. A., DIENER, A., EBNETH, S. & GODDERIS, Y. 1999. $^{87}Sr/^{86}Sr$, $\delta^{13}C$ and $\delta^{18}O$ evolution of Phanerozoic seawater. *Chemical geology,* **161,** 59-88.

VON CAEMMERER, S. 2000. *Biochemical models of leaf photosynthesis*, Csiro publishing.

WAN, Z., ALGEO, T. J., GENSEL, P. G., SCHECKLER, S. E., STEIN, W. E., CRESSLER III, W. L., BERRY, C. M., XU, H., ROWE, H. D. & SAUER, P. E. 2019. Environmental influences on the stable carbon isotopic composition of Devonian and Early Carboniferous land plants. *Palaeogeography, Palaeoclimatology, Palaeoecology,* **531,** 109100.

WELLMAN, C. H., OSTERLOFF, P. L. & MOHIUDDIN, U. 2003. Fragments of the earliest land plants. *Nature,* **425,** 282-285.

WITKOWSKI, C. R., WEIJERS, J. W., BLAIS, B., SCHOUTEN, S. & SINNINGHE DAMSTÉ, J. S. 2018. Molecular fossils from phytoplankton reveal secular pCO_2 trend over the Phanerozoic. *Science advances,* **4,** eaat4556.

ZDEBSKA, D. 1972. *Sawdonia ornata* (= *Psilophyton princeps* var. *ornatum*) from Poland. *Acta Palaeobotanica,* **13,** 77-98.

ZHOU, N., WANG, Y., YA, L., PORTER, A. S., KÜRSCHNER, W. M., LI, L., LU, N. & MCELWAIN, J. C. 2020. An inter-comparison study of three stomatal-proxy methods for CO_2 reconstruction applied to early Jurassic Ginkgoales plants. *Palaeogeography, Palaeoclimatology, Palaeoecology,* **542,** 109547.

3. Morphological variation in *Archaeopteris hibernica* leaves from the Fossil Flora of Kiltorcan Quarry, County Kilkenny.

Abstract

The Kiltorcan Hill locality in the southeast of Ireland has been an area of palaeobotanical interest since the 19th century and is famous for the large number of well-preserved ultimate and penultimate branches of *Archaeopteris hibernica* (Forbes) Stur. The morphometric approach of Moreno-Sánchez (2004) was applied to well-preserved leaf fossils to investigate intraspecific variation in leaf morphology and to compare the leaf shape of *A. hibernica* with other *Archaeopteris* species. *A. hibernica* leaves were found to be larger and rounder than *A. halliana,* and sometimes had a crenulate leaf margin. However, there was a degree of overlap in leaf morphological variation between the two species. Future research is needed to revise and clarify differences between different *Archaeopteris* species using both sterile and fertile leaf characteristics. The differences in leaf margin in *A. hibernica*, may be a result of the leaf's light or water environment, or may indicate polyploidy.

3.1 Introduction

The Old Red Sandstone (ORS) is a term used to describe late Silurian to early Carboniferous continental siliclastic strata (Kendall, 2017). These strata were deposited across Laurussia at tropical and sub-tropical latitudes, with extensive deposits occurring in the south and south-west of Ireland (see *Figure 3.1*) (Graham and Sevastopulo, 2021, Kendall, 2017). The ORS deposits in Ireland originated from fluviatile and shallow marine environments (Graham and Sevastopulo, 2021). The majority of the ORS of Ireland is late Devonian in age, with Silurian, Lower Devonian and Middle Devonian rocks restricted to a few areas (Holland, 1977). The Kiltorcan Formation forms the uppermost part of the ORS facies in Southern Ireland and dates to the Upper Devonian/ Lower Carboniferous transition (Colthurst, 1978, Jarvis, 2000). It is characterised by fine non-red sandstones and yellow sandstones, as well as red, yellow and green mudstones and siltstones (Colthurst, 1978, Graham and Sevastopulo, 2021, Jarvis, 2000). These have been interpreted as fluvial deposits from rivers flowing south across a low gradient, coastal plain (Clayton et al., 1977, Graham and Sevastopulo, 2021). The appearance of the white or yellow sandstone of the Kiltorcan Formation is a particularly distinctive change in the Old Red Sandstone sequence, marking both a change in sedimentology and the introduction of large amounts of feldspar detritus (Penney, 1980). This is thought to coincide with the unroofing of the Leinster Granite (Penney, 1980).

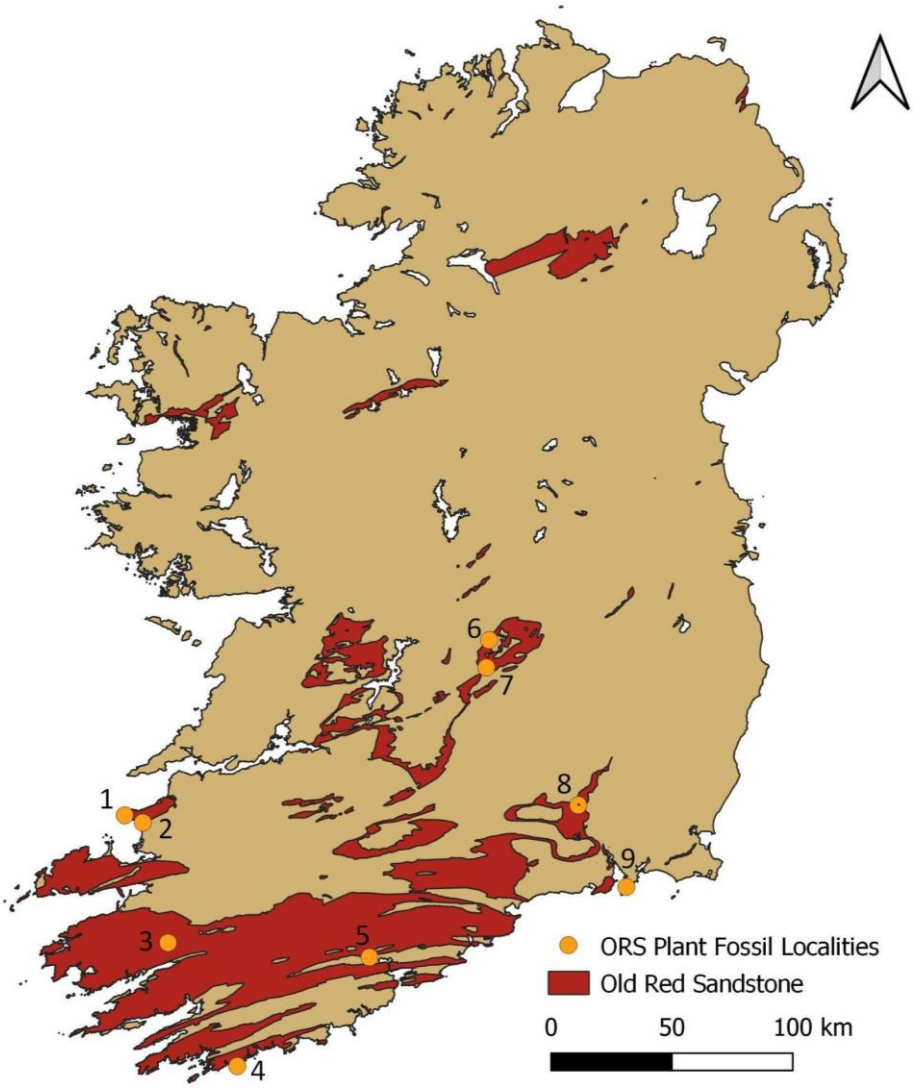

Figure 3.1. Map of Old Red Sandstone outcrops in Ireland (red) and ORS plant fossil localities. Fossil localities are show in orange and are labelled as follows: 1) Kerry Head (Matten et al., 1975); 2) Ballyheigue (Klavins and Matten, 1996); 3) Moll's Gap (Walsh, 1968); 4) Toe Head (Connery, 1999); 5) Tivoli Quarry (Jarvis, 1992); 6) Kinnitty (Feehan, 1979); 7) Ballyduff townland (O'Kelly, 1862); 8) Kiltorcan Quarry (Jarvis, 2000) and 9) Hook Head (Klavins, 2004). Created using QGIS (version 3.22.13) and Geological Survey Ireland Bedrock Geology data, scale 1:1,000,000 (GSI, 2014).

Kiltorcan Hill in Co. Kilkenny (52° 27’ 43" N, 07° 10' 56" W) contains the principal outcrops of the Kiltorcan formation and has been an area of palaeobotanical interest since the mid-nineteenth century, representing fossil floras of latest Devonian to early Carboniferous age (Colthurst, 1978, Graham and Sevastopulo, 2021, Jarvis, 1990). The fossil-containing sediments on Kiltorcan Hill are found in three quarries: the New Quarry, the Old Plant Quarry (referred to as the “Classic Quarry'' in Colthurst (1978) and referred to as “Mr. Patrick Galway’s Quarry” on the Geological Survey of Ireland 6” field sheet), the Roadstone Quarry (referred to as the “Council Quarry'' in Colthurst (1978); see *Figure 3.2*).

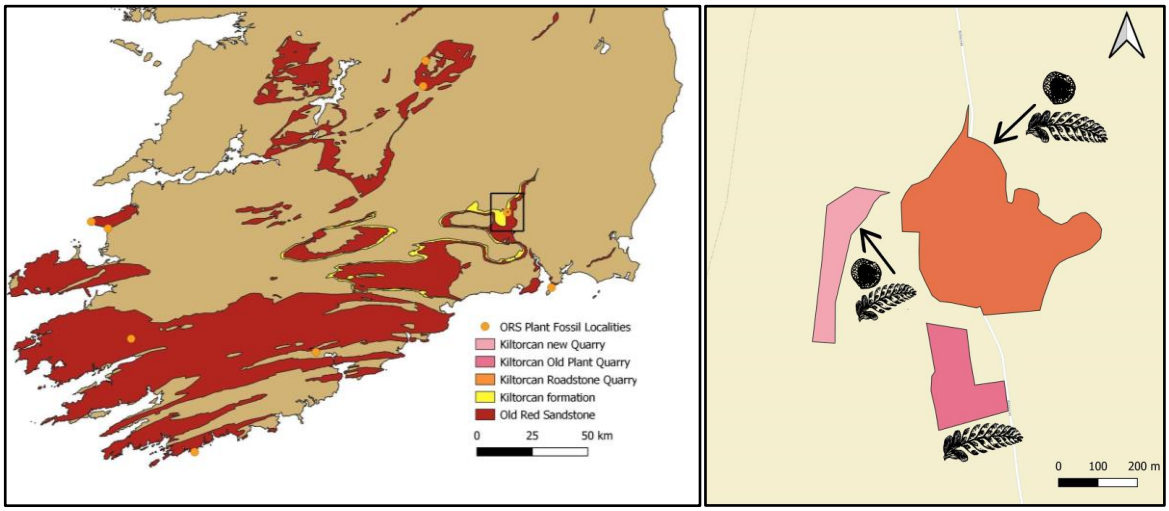

Figure 3.2. Map showing the Kiltorcan formation (left) and quarries on Kiltorcan Hill in relation to each other (right). The Kiltorcan formation is shown in yellow, the Old Red Sandstone is shown in red, and plant fossil localities are shown in orange. A black box is drawn around the location of Kiltorcan Hill (left). This is shown in more detail on the right. The Old Plant Quarry is shown in dark pink, the New Quarry in pale pink and the Roadstone Quarry is shown in orange. Adapted from Jarvis (1990) using QGIS (version 3.22.13), Geological Survey Ireland Bedrock Geology data, scale 1:100,000 (GSI, 2014) and Geological Survey Ireland Geological heritage sites data (Clarke et al., 2007).

The Roadstone Quarry is the youngest of the three quarries, dating to the Lower Carboniferous VI Miospore Biozone (Jarvis, 1990) and was first excavated in the 1960s (Chaloner, 1968). The VI Miospore Biozone was indicated by the presence of the spore taxa *Verrucosisporites nitidus, Spelaeotriletes obtusus* and *Spelaeotriletes resolutus,* and the absence of upper Devonian spore taxa (Jarvis, 1990). The fossiliferous strata lie approximately 5m above the Old Plant Quarry (see *Figure 3.3*) and show a distinct floral assemblage unlike that of the Old Plant Quarry (Jarvis, 1990, Jarvis, 1992). This includes *Lepidodendropsis* spp. aff. *L. hirmeri* (initially misidentified as *Cyclostigma kiltorkense* in Chaloner (1968))*, Sublepidodendropsis* c.f. *isachseni*, cf. *Rhacophyton* spp. and *Bythotrephis* spp. (an alga), with an absence of the *Archaeopteris-Cyclostigma* flora found in the Old Plant Quarry (Chaloner and Meyer-Berthaud, 1983, Jarvis, 1990, Jarvis, 2000). However, the fossils of the Roadstone Quarry have not been formally described (Klavins, 1999). The New Quarry's fossiliferous bed is approximately 25m below that of the Roadstone Quarry (see *Figure 3.3*), and has been dated to the Upper Devonian LE Miospore Biozone (Jarvis, 1990). This was indicated by the presence of the Devonian spore taxa *Retispora lepidophyta, Rugospora flexuosa, Diducites plicabilis* and *Hymenozonotriletes explanatus,* and the absence of *Verrucosisporites nitidus* and *Vallatisporites verrucosus* (Jarvis, 1990). The New Quarry assemblage consists of coalified and permineralized *Cyclostigma kiltorkense* stems (Jarvis, 2000). The Roadstone Quarry and New Quarry sections can be related by a section of intermittent exposure along a track (Jarvis, 1990).

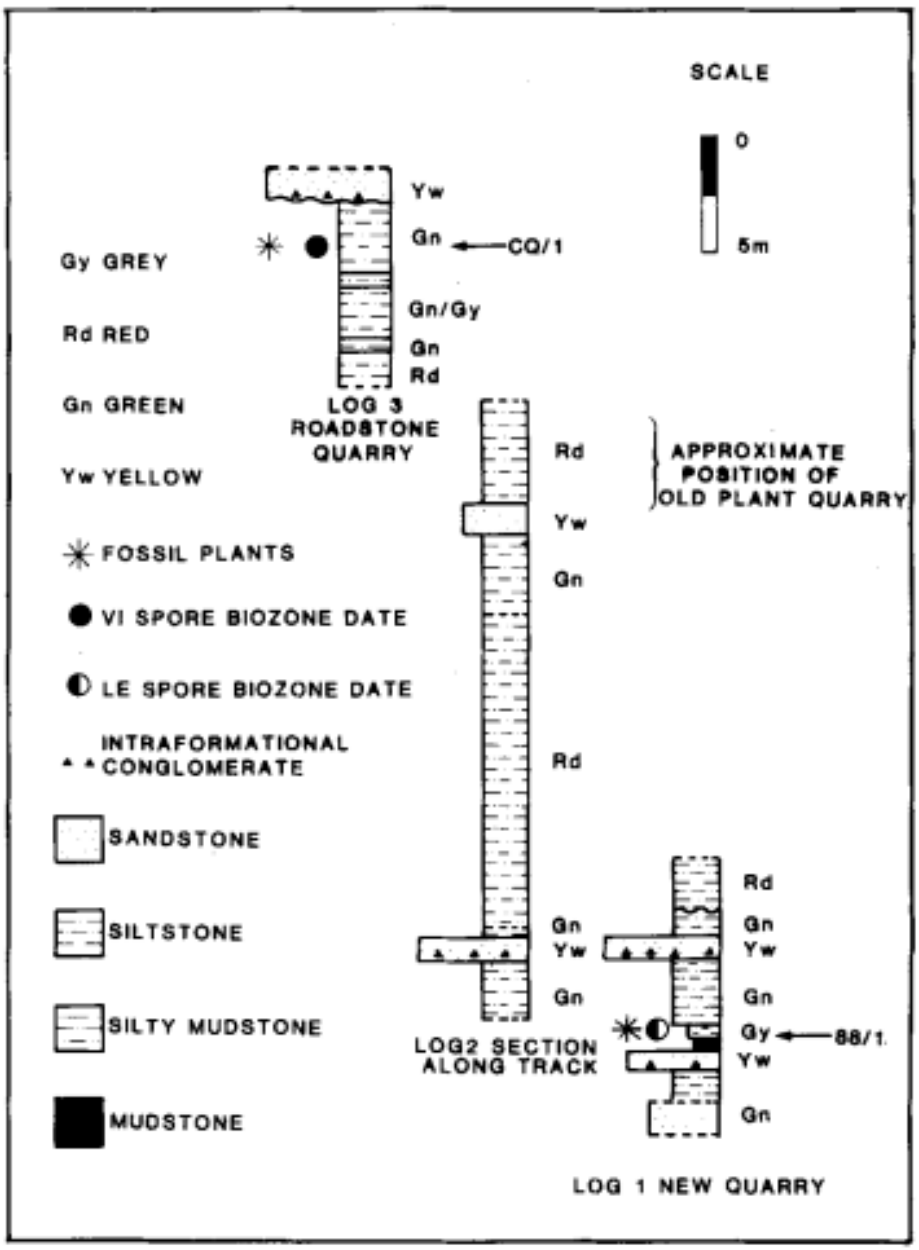

Figure 3.3. Stratigraphic log from Jarvis (1990) showing the succession on Kiltorcan Hill. The location of palynological samples used for biostratigraphy and the approximate position of the Old Plant Quarry in the succession are shown. The Old Plant Quarry lies approximately 5m below that of the Roadstone Quarry, and the New Quarry's fossiliferous bed is approximately 25m below that of the Roadstone Quarry

The majority of palaeobotanical work to date has been carried out on specimens from the Old Plant Quarry and has concentrated on describing the assemblage and determining its age (Baily, 1858, Baily, 1861, Baily, 1869a, Baily, 1869b, Baily, 1872, Baily, 1875b, Baily, 1875a, Brongniart, 1857, Carruthers, 1872, Chaloner, 1968, Chaloner et al., 1977, Chaloner and Meyer-Berthaud, 1983, Forbes, 1853, Griffith and Brongniart, 1857, Haughton, 1855, Haughton, 1860, Heer, 1872, Jarvis, 1990, Jarvis, 1992, Jarvis, 2000, Johnson, 1911a, Johnson, 1911b, Johnson, 1913, Johnson, 1914b, Johnson, 1914a, Johnson, 1917). However, there is some uncertainty on whether the fossiliferous beds of the Old Plant Quarry are Upper Devonian or early Carboniferous in age, as its preservation presents significant challenges to obtaining palynological samples (Brongniart, 1857, Chaloner, 1968, Forbes, 1853, Griffith and Brongniart, 1857, Heer, 1871, Jarvis, 1990, Johnson, 1913). Furthermore, difficulties in accessing the Old Plant Quarry precluded it from being used in more recent palynological studies (Jarvis, 1990, Jarvis, 1992). However, the dating of the Roadstone and New Quarry assemblages suggests that the Old Plant Quarry fossil assemblage dates to between the LE and VI biozones, with a probable range within the LE or LN Biozones (Graham and Sevastopulo, 2021, Jarvis, 1990). While no unequivocal evidence is available due to a lack of samples from the Old Plant Quarry, palynological studies carried out from other localities within the Kiltorcan formation, (including Greywood Quarry, Co. Kilkenny and Tivoli Quarry, Lower Glanmire Road, Co. Cork) further supports this estimate (Jarvis, 1992).

Preservation in the Old Plant Quarry and Roadstone Quarry is by chloritization (Chaloner, 1968, Jarvis, 1990). It is thought that the mineral replacement took place as a result of a chloritization process of kaolinite following the formation of coalified compression fossils (Chaloner, 1968, D.E. Jarvis 2021, personal communication 11 November). As a result of this process, the carbon content of the fossil matrix within the Old Plant Quarry and Roadstone Quarry is thought to be negligible (Chaloner, 1968). However, plant remains in the New Quarry are preserved as coalified compressions (Jarvis, 1990, Jarvis, 1992, Jarvis, 2000). Since 2000, the New Quarry has been further excavated, exposing a change in fossilisation of plant material from coalified compressions to the chloritic preservation seen in the Roadstone and Old Plant Quarries at a higher stratigraphic level (D.E. Jarvis 2021, personal communication 11 November). Further excavation of the New Quarry may be

possible to obtain new plant material and to investigate this taphonomic change using more modern techniques for petrological, mineralogical and chemical analyses (see e.g. Bourdelle et al. (2021) and Edwards et al. (2014)) than when it was last investigated in the late 1960s (Chaloner, 1968).

While there are other important Devonian fossil localities in Ireland such as Ballyheigue and Hook Head (Klavins, 2004, Matten et al., 1980, Decombeix et al., 2023), Kiltorcan has been studied the most extensively and for the longest period of time. The earliest fossil discoveries at Kiltorcan occurred through the work of the Geological Society of Ireland in 1851 in the Old Plant Quarry (Forbes, 1853), with initial excavations resulting in the discovery of *Archaeopteris hibernica, Cyclostigma kiltorkense, Sphenopteris hookeri* and *Sphenopteris humphresiana,* with the latter two occurring less frequently (Baily, 1858, Baily, 1869a, Forbes, 1853, Haughton, 1860). Freshwater bivalve, crustacean and fish remains have also been found from the Old Plant Quarry (Baily, 1869b, Baily, 1872, Carpenter and Swain, 1908, Ritchie, 1975, Robin et al., 2021). Further work was not carried out on the Kiltorcan flora until the early 20th century, when a detailed examination of museum specimens and further excavations of the Old Plant Quarry were carried out by Johnson (1911a, 1911b, 1913, 1914a, 1914b, 1917). This led to a more detailed description and whole plant reconstruction of *Cyclostigma kiltorkense* (then referred to as *Bothodendron*) (Johnson, 1913, Johnson, 1914a), and the identification of three new taxa: *Archaeopteris tschermaki, Kiltorkensia devonica* (initially referred to as *Ginkgophyllum kiltorkense*) and *Spermolithus devonicus* (Johnson, 1911b, Johnson, 1914b, Johnson, 1917). Subsequent work by Chaloner et al. (1977) on new *S. devonicus* material from the Old Plant Quarry led to its identification as one of the oldest platyspermic seeds. A full summary of the macrofloral elements of Kiltorcan, their affinities and former names can be seen in *Appendix 3.1.*

One of the most abundant fossils and best understood plant taxon within the classic Kiltorcan flora is *Archaeopteris hibernica* (Forbes) Stur., which has subsequently been found in a number of different localities both within and outside of Ireland (Tivoli Quarry, Co. Cork (Jarvis, 1992); Toe Head, Co. Cork (Connery, 1999, Graham and Sevastopulo, 2021);

Hampshire formation, West Virginia, USA (Scheckler, 1986); Catskill formation, Pennsylvania, USA (Broussard et al., 2018, Cressler, 2006); South-eastern Mountainous Altay, Russia (Gutak et al., 2011)). While there is an abundance of *Archaeopteris* fossils found at Kiltorcan, to date no *Callixylon* remains have been found at this locality. However, *Callixylon* specimens have been found in Sandeel Bay, Hook Head, Co. Wexford (Decombeix et al., 2023, Klavins, 1999). The identification of different *Archaeopteris* species has often been based on variable characters, and the delineation of separate species can be unclear (Anderson et al., 1995, Arnold, 1939, Carluccio et al., 1966, Fairon-Demaret et al., 2001, Kenrick and Fairon-Demaret, 1991, Kräusel and Weyland, 1941). More work is needed to determine useful characters in delineating species, as the current approach may represent different growth stages or preservational differences of the same species as separate taxa (Carluccio et al., 1966). For example, more recent detailed investigations into the morphological variation of *A. halliana* and *A. roemeriana* found the two species to be synonymous (Fairon-Demaret et al., 2001, Moreno-Sánchez, 2004). A preliminary investigation using leaf morphometrics will be used in this study to try to gain a better understanding of the degree of intraspecific morphological variation in *A. hibernica* leaves.

3.2. Materials and Methods

3.2.1 Palaeoenvironmental setting

The plant fossils from the Old Plant Quarry were mostly found as single layers of plant material on each bedding surface, with occasional pockets of abundant plant debris (Baily, 1861, Colthurst, 1978). Colthurst (1978) suggested that the plant material was buried soon after deposition due to the unfragmented nature of the plant remains and the presence of only a single layer of plant material per bedding plane. Therefore, the assemblage is considered to be parautochthonous and the most likely depositional environment was considered to be a bar-tail in a meandering river channel (Colthurst, 1978). However, the quarry has subsequently become overgrown and inaccessible due to the dumping of building materials in the quarry so further, more detailed analysis of the palaeoenvironment of the Old Plant Quarry has not been possible (Clarke et al., 2007, Jarvis, 2000, Klavins, 1999).

3.2.2 Fossil material

Photos of *Archaeopteris* leaf material from the Kiltorcan flora were obtained from the Trinity College Dublin Geology Museum (TCD), the National Museum of Northern Ireland (NMNI) and the National Museum of Ireland (NMI) fossil collections using a Sony Cybershot DSC-RX100 digital camera and a Canon EOS 1100D camera, with a SIGMA 70MM F2.8 lens. In total, 63 specimens of *Archaeopteris* ultimate and penultimate branch systems with attached sterile leaves were photographed for this study (21 specimens from the TCD collection, 17 specimens from the NMNI collection and 25 specimens were photographed from the NMI collection). Six specimens were photographed under water immersion to increase the contrast between the fossil and the rock matrix (Kerp and Bomfleur, 2011). Water immersion is generally not appropriate for use on clayey sediment and some clay minerals, due to swelling (Kerp and Bomfleur, 2011). The fossil matrix of the Kiltorcan material is mostly fine sand and detrital muscovite, and the fossils themselves are mostly chlorite, so damage from swelling clays in the matrix was not considered to be an issue (P.

Roycroft, 2023 personal communication, 20 April) and other contrast-enhancing immersion fluids such as xylene or ethanol were not used due to poor ventilation and the potential health hazards associated with them. Photographs were processed using Adobe Photoshop (24.7.0 Release) to further enhance the contrast between the fossil and the rock matrix before carrying out measurements. All photographs were a minimum of 2848 x 4272 pixels and 600 dpi.

3.2.3 Leaf Measurements

Leaf measurements were carried out in Adobe Photoshop (24.7.0 Release). Leaf area was measured following the protocol of Peppe et al. (2011). The leaf was selected using the quick selection tools (with a maximum selection size of 10 pixels) and copied to a new layer. Any minor portions of the leaf margin that were damaged were reconstructed when possible to do so as in Peppe et al. (2011). Leaf area, perimeter and length was then measured from extracted leaves that were sufficiently well preserved. 94 leaves from 17 specimens were of sufficiently well preserved for this study. Leaf shape, margin and apex were also categorised using the shape categories used in the Climate Leaf Analysis Multivariate Programme (CLAMP; Wolfe (1993)), and the leaf's position along the ultimate branch and preservation quality was noted.

Leaf area and perimeter were used to calculate the leaf area-perimeter index as described by Moreno-Sánchez (2004), to ensure data compatibility. The leaf area-perimeter index (I_a) was calculated from leaf area (A) and perimeter (P) according to the following equation:

$$I_a = \frac{P^2}{4\pi A} \quad (3)$$

This equation is derived by comparing leaf area to the area of a circle with a perimeter equal to the real leaf perimeter (A_p) (Moreno-Sánchez, 2004). The equation for the

perimeter of a circle can be rearranged to express the radius of the circle (r) being used for comparison, and this can be used to calculate the area of this circle.

$$\frac{P}{2\pi} = r$$

(4)

$$A_p = \frac{P^2}{4\pi}$$

(5)

The leaf area-perimeter index is then calculated as the ratio of the circle A_p to the real leaf area:

$$I_a = \frac{P^2}{4\pi A}$$

(6)

High values of I_a indicate leaves that are dissected or elongated. In the case of a perfectly circular leaf $I_a = 1$ (Moreno-Sánchez, 2004). This index is the inverse of the circularity index (i.e. shape factor) used by Bacon et al. (2013). Leaf perimeter:length index (I_l) was also calculated according to Moreno-Sánchez (2004), where L is leaf length:

$$I_l = \frac{P}{\pi L}$$

(7)

3.3. Results

The *Archaeopteris hibernica* leaf material was found to have variable leaf morphology (see *Table 3.1*). Average leaf area was 102.4 mm^2 (± 53.0 mm^2). Leaf length varied from 9.1 mm to 28.3 mm (mean = 17.5 ± 4.2 mm). Leaf area-perimeter index (I_a) varied between 1.5 (close to round, where I_a = 1) and 7.3 (mean = 3.1 ± 0.8). The gap method was used to determine the optimal number of clusters within the leaf morphology dataset (i.e., the leaf area, length, perimeter, area index (see *Equation 1*) and perimeter: length index (see *Equation 5*) data). This indicated K=1 optimised clustering within the dataset (see *Figure 3.4*) and therefore there were no distinct groupings by leaf morphology.

Table 3.1. **Leaf morphological variables measured for *Archaeopteris hibernica* (n=94).**

Measurement	Mean (± S.D.)	Median	Q1	Q3	Minimum	Maximum
Area (mm^2)	102.4 (± 53.0)	96.0	55.5	141.3	23.6	272.4
Length (mm)	17.5 (± 4.2)	17.7	14.1	20.1	9.9	28.3
Perimeter (mm)	59.5 (± 15.0)	58.9	48.3	72.4	30.2	102.4
I_a	3.1 (± 0.8)	3.0	2.6	3.4	1.5	7.3

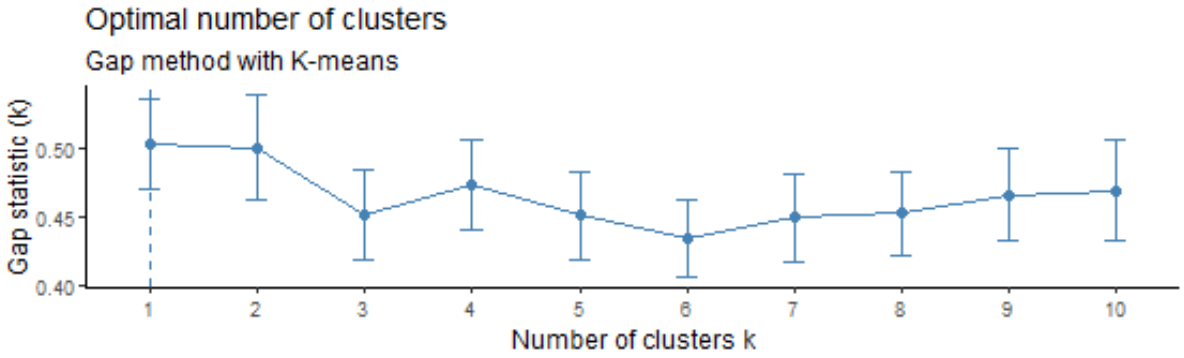

Figure 3.4. Gap statistics for clusters based on leaf morphological variables of *A. hibernica*. The optimal value for K=1 is chosen**,** indicating that there are no distinct groupings of *A. hibernica* within the Kiltorcan flora by leaf morphology.

Leaf area differed depending on branch position (Kruskal-Wallis test; X^2 = 13.34, df = 2, p=0.001), with smaller leaves (median size = 98.4 mm^2) occurring at the end of the branch systems, and larger leaves (median size = 124.7 mm^2) occurring closer to the mid-section and start of the ultimate branch systems. However, post-hoc analysis revealed a significant difference only between the mid-section and end of branches (Pairwise Wilcoxon rank sum test, p=0.0005, Benjamini-Hochberg p-value adjustment method). Leaf area-perimeter index (I_a) was found to differ between leaves of different margin types (Wilcoxon W=366, p=0.001), with more entire margins having lower I_a values (median = 2.8, n = 74) than leaves with crenulate or more dissected margins (median = 3.2, n =19) (see *Figure 3.5*). Grouping by leaf shape descriptors (i.e., shape, margin and apex descriptors) and preservation quality were not found to result in statistically significant differences in all other leaf measurements.

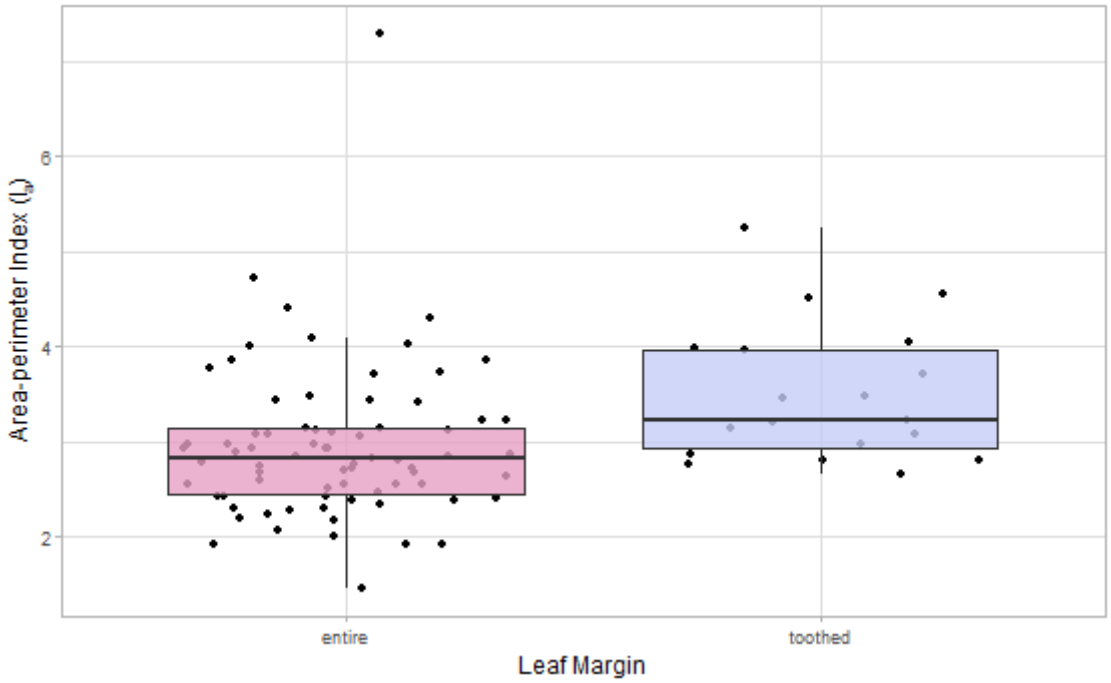

Figure 3.5. Leaf area-perimeter index measured from *Archaeopteris hibernica* leaves from the Kiltorcan flora. Leaves with an entire margin had a lower area-perimeter index value (i.e., had rounder leaves, median I_a = 2.8, n = 74), than those with a toothed (i.e., crenulate) leaf margin (median I_a = 3.2, n =19; Wilcoxon rank sum test, W=366, p=0.001).

Archaeopteris hibernica has a substantially greater leaf area (median = 96.0 mm^2, n = 93) than that reported for *A. halliana* by Moreno-Sánchez (2004) (median = 51.3 mm^2, n = 31; Wilcoxon rank sum test, W=585, p= $2.546e^{-05}$) However, there is some overlap in the range of sterile leaf morphological variation between the two species (see *Figure 3.6*). The two species show a more distinct difference in I_a values calculated, with *A. hibernica* having higher I_a values (median = 2.9, n = 93) than *A. halliana* (median = 1.9, n= 31; Wilcoxon rank sum test, W= 158, p=$5.417e^{-12}$). This indicates the leaf shape of *A. hibernica* was less round than *A. halliana* and likely had a more crenulate leaf margin. By comparison, *A. macilenta* and *A. fissilis* (*Figure 3.6*) both have more deeply dissected leaves and have higher I_a values than the other *Archaeopteris* species (median = 5.6, n = 30 and median = 38.06, n = 11 respectively; pairwise Wilcoxon rank sum test, p<0.05 for all pairings, Benjamini-Hochberg p-value adjustment method).

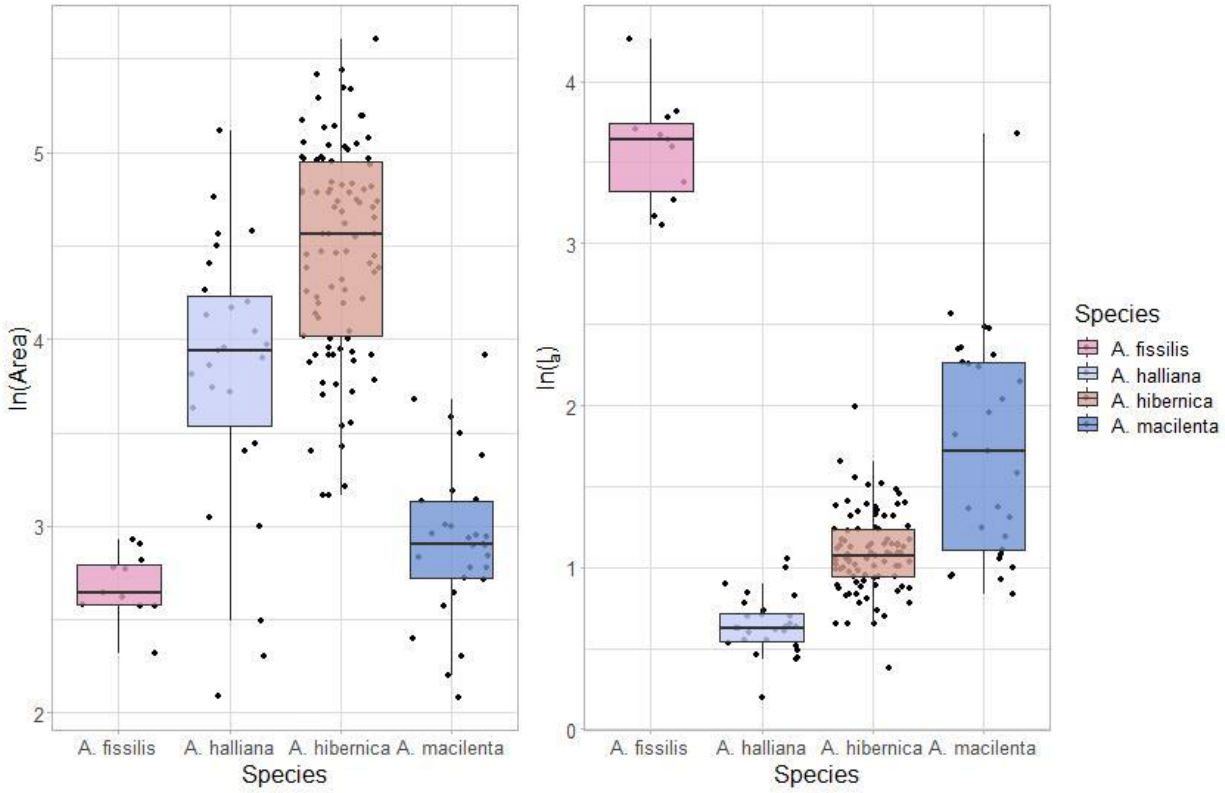

Figure 3.6. Leaf area and area-perimeter index measured from different *Archaeopteris* species. Leaf area and area-perimeter index are log transformed in order to better visualise the data. New measurements are presented for *A. hibernica* from the Kiltorcan flora. Data for *A. halliana, A. fissilis* and *A. macilenta* were digitally extracted from Moreno-Sánchez (2004). Leaf area and area-perimeter index were found to be significantly different between species (Kruskal-Wallis test for leaf area, $X^2 = 90.145$, df = 3, $p<2.2e^{-16}$; Kruskal-Wallis test for area-perimeter index, $X^2 = 89.563$, df = 3, $p<2.2e^{-16}$; pairwise Wilcoxon rank sum test, $p<0.05$ for all pairings, Benjamini-Hochberg p-value adjustment method).

A negative allometric relationship between leaf area and area-perimeter index was found in *Archaeopteris hibernica,* but the model explained only 13% of the variance (p=0.0001; see *Figure 3.7*). This indicates that the leaves became more round as they increased in size, but other factors influence area-perimeter index. This allometric response is similar to that observed for *A. halliana* by Moreno-Sánchez (2004) (R^2=0.26, p=0.004), and contrasts with the positive allometric relationship found for the more dissected leaves of *A. macilenta* (R^2=0.21, p=0.007). The relationship between leaf area and area-perimeter index for *A. fissilis* was not found to be statistically significant (p=0.22).

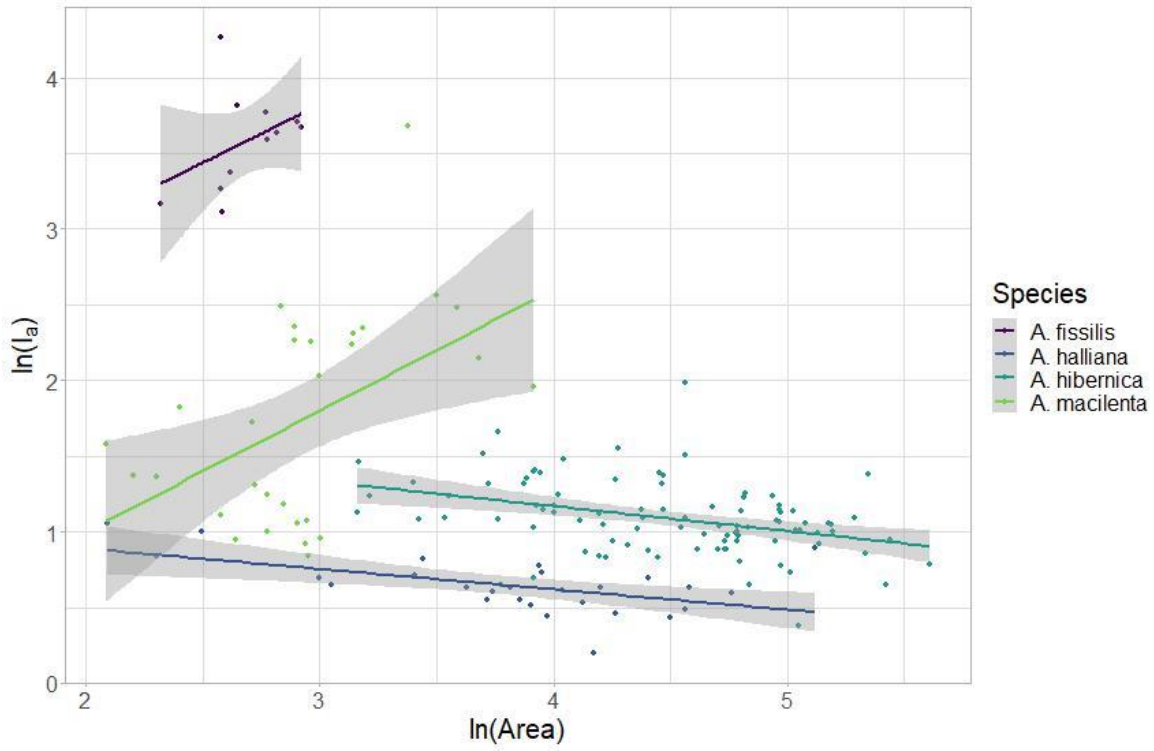

Figure 3.7. The relationship between ln(leaf area) and ln(area-perimeter index) measured from different *Archaeopteris* species. New measurements are presented for *A. hibernica* from the Kiltorcan flora. Data for *A. halliana, A. fissilis* and *A. macilenta* were digitally extracted from Moreno-Sánchez (2004). The relationship between Leaf area and area-perimeter index was statistically significant for *A. hibernica* ($\ln(I_a) = -0.16\ln(Area) + 1.83$; R^2=0.13, p=0.0001), *A. halliana* ($\ln(I_a) = -0.13\ln(Area) + 1.16$; R^2=0.26, p=0.004), and *A. macilenta* ($\ln(I_a) = 0.80\ln(Area) - 0.60$; R^2=0.21, p=0.007).

3.4. Discussion

3.4.1 Leaf morphological variation

The morphological variability of *Archaeopteris hibernica* sterile leaf material is generally consistent with previous published descriptions of Irish and North American material (Arnold, 1939, Johnson, 1911a, Johnson, 1911b, Kräusel and Weyland, 1941, Lesquereux, 1880, Schimper, 1869). Furthermore, cluster analysis did not indicate any distinct groupings on the basis of the leaf morphological variables measured, suggesting the presence of a single species. However, the leaf attachment within the Kiltorcan material was found to be more variable than discussed by Johnson (1911b). While the majority of specimens showed a decurrent leaf attachment to the ultimate branches, one specimen in the NMNI collection (BELUM K12448) appears to have a non-decurrent leaf attachment (see *Figure 3.8*). This may indicate the presence of *A. halliana* in the Kiltorcan flora as sterile leaf material of *A. hibernica* and *A. halliana* differ in leaf base attachment, as well as degree of leaf overlap and size of ultimate and penultimate branches (Johnson, 1911b, Stockmans, 1948). However, this difference may also be an artefact of preservation and leaf position when fossilised, as the leaf lamina and portions of the ultimate branches are not very clearly preserved on this specimen, and leaf attachment can appear decurrent or non-decurrent on the same specimen depending on its position when preserved (Stockmans, 1948; see *Figure 3.8*).

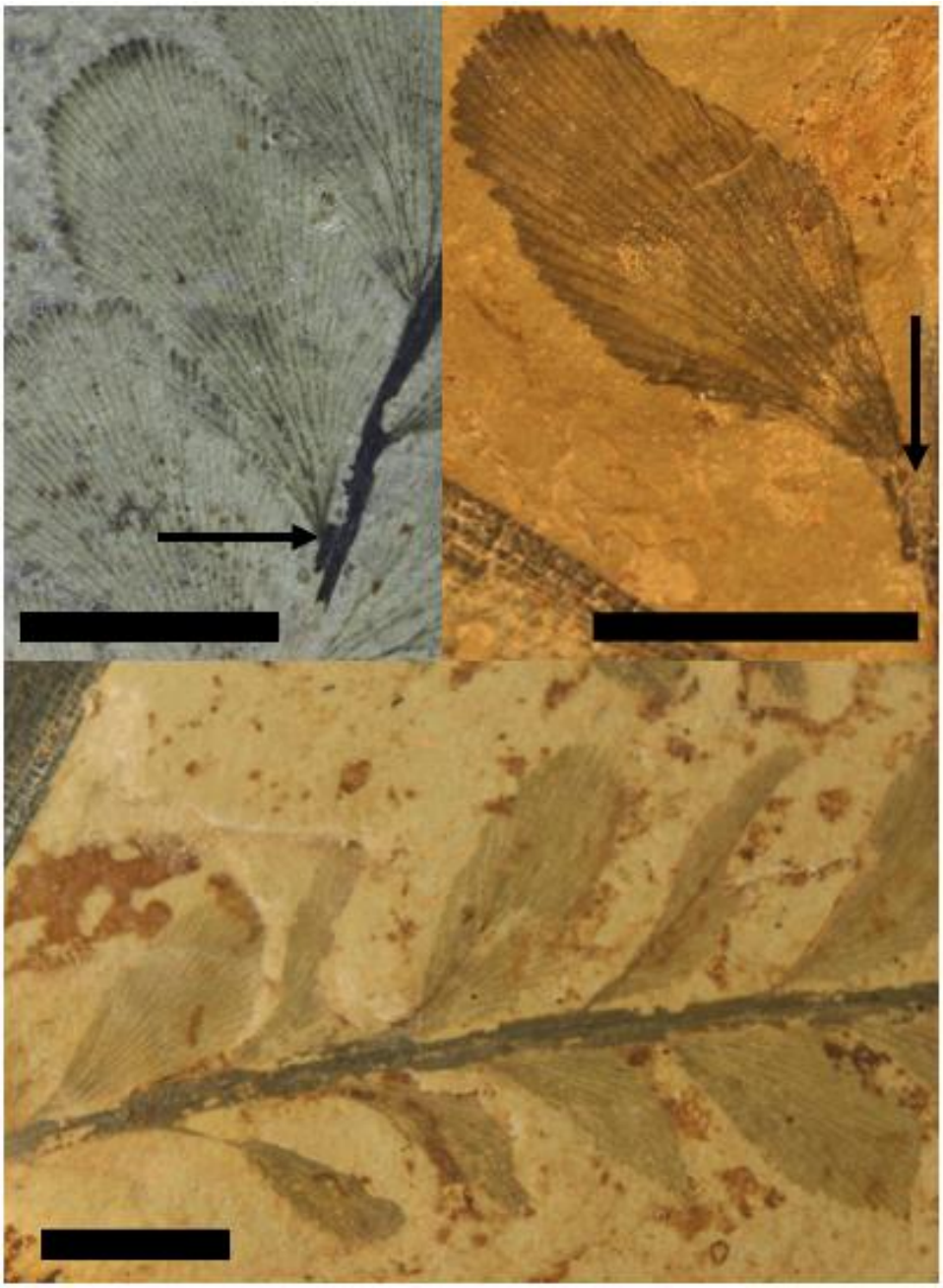

Figure 3.8. Variation in leaf attachment in *Archaeopteris* specimens. Different specimens showed non-decurrent (top right; specimen number BELUM K12488, NMNI collection) and decurrent leaf attachment (top left; specimen number F26194, NMI collection) to the ultimate branches. Leaf phyllotaxy and/or leaf position when fossilised, as well as preservation quality can affect the appearance of leaf attachment (bottom; specimen number TCD-19761, TCD Geology Museum collection). All scale bars = 1cm.

Interpretations of the distinction between *A. hibernica* and *A. halliana* have varied in the past. Arnold (1939) distinguished between *A. hibernica* and *A. halliana* by differences in leaf size and whether fertile ultimate branches are bound exclusively proximally by sterile leaves (*A. halliana*) or proximally and distally (*A. hibernica*). However, later work describes the transition between sterile and fertile leaves on ultimate branches as much more variable in *A. halliana* (Fairon-Demaret et al., 2001, Kenrick and Fairon-Demaret, 1991, Stockmans, 1948). According to these authors, fertile ultimate branches may be bound both proximally and distally by a variable number of vegetative leaves, with transitional zones sometimes observed between the sterile and fertile leaves (Fairon-Demaret et al., 2001, Kenrick and Fairon-Demaret, 1991). Stockmans (1948) further states that the main observable difference between *A. halliana* and *A. hibernica* is the size of the leaves and the penultimate and ultimate branch systems, which are larger in *A. hibernica* than *A. halliana.* Comparison of leaf area and I_a measurements in this study found that *A. hibernica* had larger, less round and more crenulate leaves (indicated by a higher I_a values) than *A. halliana*. However, there was some overlap for these measurements between the two species, despite there being a significant difference in median values (see *Figure 3.6*). Furthermore, considering what is now known about the likely arborescent habit of *Archaeopteris*, the degree of variation in leaf size and the size of ultimate and penultimate branch systems would be expected to be large.

The majority of the taxonomic work on *Archaeopteris* compression fossils (Arnold, 1939, Johnson, 1911a, Johnson, 1911b, Kräusel and Weyland, 1941, Lesquereux, 1880, Schimper, 1869, Stockmans, 1948) was carried out before it was understood to be arborescent, therefore the possible range of variation of a number of vegetative features may have been interpreted incompletely. Further examination of sterile and fertile leaf material from the Kiltorcan flora, and comparison of this material with *A. halliana* is recommended to investigate this further, and to evaluate the utility of different measurements in separating out *Archaeopteris* species on the basis of sterile leaf morphology.

The allometric relationship between leaf area and leaf area-perimeter index (I_a) was found to be significant, indicating a general trend of increasing roundness with greater leaf area.

However, the data were not well fitted by the regression line (R^2=0.13, p<0.01), indicating that the majority of variation in the I_a measurements was not explained by changes in leaf area. Environmental and genetic factors such as water availability, irradiance and ploidy are known to affect intraspecific variation in leaf size and roundness (Boyce, 2009, Niinemets et al., 2004, Šmarda et al., 2018). It may be possible to further investigate hydraulic supply and light environment as factors in leaf morphological variation in *Archaeopteris* through the lens of canopy placement. In sufficiently large assemblages, vein density and number of vein endings per distal leaf perimeter may be used to elucidate former canopy placement of fossilised leaves (Boyce, 2009). Shoot flatness and leaf overlap have also been found to decrease with increasing irradiance in *Nothofagus* spp. (Niinemets et al., 2004). In *Archaeopteris* assemblages, ultimate branch insertion angle may be a useful measure of branch flatness and the ratio of ultimate branch silhouette area per unit length to leaf area may be a useful measure of leaf overlap. Future canopy placement estimates may clarify environmental sources of morphological variation in sterile leaf material of *Archaeopteris.* Sedimentological and palynological data could also be used to consider differences in water availability across broader spatial scales (Fairon-Demaret et al., 2001).

Leaf preservation may also impact variation in leaf margin shape reconstructions, and therefore I_a measurements, through poor preservation of the leaf lamina (see *Figure 3.9*). Additionally, drying has been found to result in significant leaf shrinkage (Blonder et al., 2012). Drying may cause the leaf margin to appear crenulate via differential shrinkage around the vein endings. However, this may arise from projection of the veins at the edge of the leaf margin (Johnson, 1911a) and becomes less pronounced as the leaf develops. Preservation quality was not found to result in a significant difference in leaf roundness (I_a), and compression fossilisation in the absence of leaf drying has not been found to result in significant leaf shrinkage (Blonder et al., 2012), therefore it is more likely that the main source of variation in leaf morphology, including crenulation of the margin, are a combination of environmental and genetic factors.

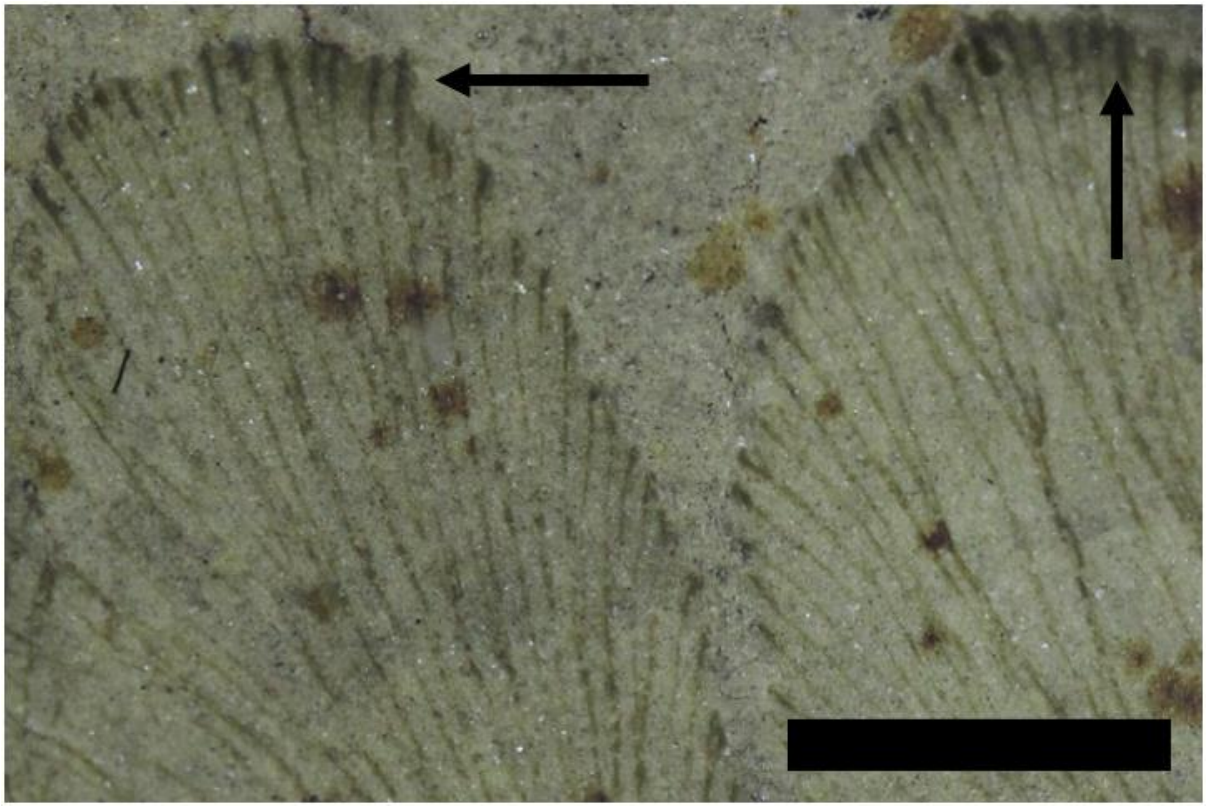

Figure 3.9. *Archaeopteris* leaf margin shape appears different with poorer preservation of the leaf lamina. *Archaeopteris* leaves (specimen number BELUM K12488, NMNI collection) appear crenulate at the distal portion of the leaf margin, with more pronounced crenulation in sections with a better-preserved lamina (indicated with arrows). Scale bar = 5mm.

Genome characteristics can influence leaf size and shape, and guard cell length in extant plants (Beaulieu et al., 2008, Šmarda et al., 2018) and the positive correlation between guard cell length and genome size has been used to estimate changes in genome size in plant taxa across geological time (Beaulieu et al., 2008, Lomax et al., 2014, McElwain and Steinthorsdottir, 2017). Many Devonian plants, including *Archaeopteris* spp.*,* occupy the upper range of guard cell lengths observed in extant plants and therefore may have had a relatively large genome size (Lomax et al., 2014, Osborne et al., 2004). Leaf size and shape is also known to be affected by ploidy in some extant plants. In the case of *Ginkgo biloba*, larger leaves, with more irregularly lobed laciniate margins are a distinct leaf phenotype that has been associated with higher ploidy levels (Šmarda et al., 2018). Therefore variable leaf margins and I_a measurements from *A. hibernica* leaves may be indicative of ploidy

levels. It may be possible to investigate relative genome size in *Archaeopteris* species through comparison of leaf size and margin phenotype (Šmarda et al., 2018), guard cell size (Beaulieu et al., 2008, Lomax et al., 2009, Lomax et al., 2014, McElwain and Steinthorsdottir, 2017) and spore size (Henry et al., 2014, Knight et al., 2010, Kürschner et al., 2013). However, the rarity of sufficient preservation to conduct the suite of measurements needed presents a significant limitation to investigate differences in *Archaeopteris* genome characteristics using these methods.

The Devonian/Carboniferous boundary was a time of significant environmental change (Brezinski et al., 2008, Brezinski et al., 2010, Clayton et al., 1977, Graham and Sevastopulo, 2021, Kaiser et al., 2016, Lakin et al., 2016, Montañez, 2022, Prestianni et al., 2016). Whole genome duplication events have been proposed as a mechanism of enhanced resilience for land plants over mass extinction intervals, allowing better adaptation to drastic environmental changes (Fawcett et al., 2009, Kürschner et al., 2013, McElwain and Steinthorsdottir, 2017). In contrast, spore size decrease and increased spore malformation at the Devonian/Carboniferous boundary may indicate genome size reduction (Henry et al., 2014) in some plant taxa and/or enhanced mutagenesis due to environmental factors (Fields et al., 2020, Marshall et al., 2020, Marshall, 2021, Prestianni et al., 2016).

Palynological assemblages of the uppermost Famennian in Western Europe and Greenland show an increase in abnormal palynomorphs (in particular *Retispora lepidophyta* var. *tener*) close to or potentially coinciding with the end-Devonian Hangenberg event (Jarvis, 1992, Marshall et al., 2020, Marshall, 2021, Maziane et al., 2002, Prestianni et al., 2016, Streel, 1966). Jarvis (1992) found that the diameter of *R. lepidophyta* decreased with time across the south of Ireland across three samples: Araglin, Co. Waterford (LL biozone, mean diameter = 61.5µm), Kiltorcan New Quarry, Co. Kilkenny (LE biozone, mean diameter = 48µm) and Glengorrine Wood, Co. Cork (LN biozone, mean diameter = 44µm). The Kiltorcan New Quarry assemblage contained small *R. lepidophyta* specimens, which fit into the size range of *R. lepidophyta* var. *tener.* However, the lack of reticulum breakdown was taken to indicate a population of small sized *R. lepidophyta,* rather than *R. lepidophyta* var. *tener* (Jarvis, 1992). In the youngest sample (i.e., the sample closest to the

Devonian/Carboniferous boundary; Glengorrine Wood), *R. lepidophyta* var. *tener* was the dominant form of *R. lepidophyta,* showing degradation of the reticulum into a series of crests or verrucae (Jarvis, 1992). However, thickening of the exoexine (observed by Streel (1966) in the Ardenno-Rhenan basin) was rarely observed by Jarvis (1992).

Similar patterns of high levels of spore malformation have also been seen at the end-Permian (Benca et al., 2018, Visscher et al., 2004) and end-Triassic (Lindström et al., 2019) extinction intervals. A number of different environmental causes have been suggested for the increase in spore malformation at the Devonian/Carboniferous boundary such as climatic cooling and drought (Prestianni et al., 2016), enhanced UV-B radiation (Marshall et al., 2020, Marshall, 2021) or supernova explosion (Fields et al., 2020), however, this remains an area of active research. Evidence for enhanced mutagenesis from the palynological record (Jarvis, 1992, Marshall et al., 2020, Marshall, 2021, Maziane et al., 2002, Prestianni et al., 2016, Streel, 1966), combined with the persistence of *Archaeopteris* across the Devonian/Carboniferous boundary before its last occurrence and extinction during the Mississippian (Beck, 1962), provides an interesting context for the consideration of the variable in leaf margin morphology and possible large genome size in *Archaeopteris* based on the suite of measurable traits outlined above.

3.4.2 Other *Archaeopteris* specimens within the Kiltorcan flora

Two putative *Archaeopteris* species have been found in the Old Plant Quarry at Kiltorcan: *Archaeopteris hibernica* and *Archaeopteris* cf. *tschermaki* (Johnson, 1911b). A third possible *Archaeopteris* specimen (labelled as *Noeggerathia foliosa*) is also recorded in the Muséum National d'Histoire Naturelle, Paris (Chagnoux, 2021, Dawson, 1871). However, its taxonomic identity remains unclear. The classification of the *Archaeopteris tschermaki* specimen (Botanical division, National Museum, Dublin, “B.D. 10”, Johnson, 1911b) is also unresolved. Johnson initially identified the specimen as *Archaeopteris tschermaki* (Johnson, 1911b). However, this was later transferred to the genus *Sphenopteridum* Schimper (Johnson, 1917). Potonié, Gothan and Sterzel did not consider *Archaeopteris* a suitable

genus to include *Archaeopteris tschermaki* Stur. and *Archaeopteris dawsoni* Stur., so they were included in the genus *Sphenopteridium* Schimper (Gothan, 1913, Kidston, 1923). However, Kidston (1923) did not consider these species to agree with the genus *Sphenopteridium* as defined by Schimper. Kidston (1923) studied specimens of *Archaeopteris tschermaki* Stur. and *Archaeopteris dawsoni* Stur. and concluded that they represented the same species. Furthermore, both were considered significantly different from the genus *Archaeopteris,* therefore the genus *Archaeopteridium* Kidston was founded as a more suitable taxonomic classification of these specimens (Kidston, 1923). Secondary rachises of *Archaeopteridium tschermaki* resemble the ultimate leafy branches of *Archaeopteris,* however they differ significantly in overall frond architecture and reproductive structures (Kidston, 1923, Rowe, 1992). *Archaeopteridium* fronds are more complex and the frond portions above the bifurcation are more broad-lanceolate than those of *Sphenopteridium* (Hübers et al., 2014). Despite this taxonomic revision, the identity of the Kiltorcan specimen described by Johnson (1911b) remains unresolved. Kidston (1923) considered the photographic plates of the specimen in Johnson (1911b) to be unclear and the associated illustrations were not considered likely to be *Archaeopteridium tschermaki*. The section of the Kiltorcan specimen that is preserved is a simple pinnate frond 10 cm long and 2.5 cm wide and has two fertile segments containing rows of stalked sporangia similar to *A. hibernica* (Johnson, 1911b). However, the Kiltorcan specimen, like *Archaeopteridium,* has a bifurcating frond, which is a feature distinct from the genus *Archaeopteris* (Johnson, 1911b, Rowe, 1992). Kräusel and Weyland (1941) suggested that the identity of *A. tschermaki* from Kiltorcan was *A. hibernica*, and any apparent morphological differences were an artefact of poor preservation. However, this requires reinvestigation.

3.5. Conclusion

The Kiltorcan Hill locality in the southeast of Ireland is famous for the preservation of ultimate and penultimate branches of *Archaeopteris hibernica.* Despite the abundance of well-preserved fossils and the volume of research that has been conducted on this locality, it remains poorly understood. Modern techniques may provide an opportunity to better understand the fossil preservation at this site since it was last investigated in the late 1960s. The Roadstone and New Quarries may also present further opportunities for both taphonomic and taxonomic research. However, this may be limited by preservation quality. Analysis leaf shape of different *Archaeopteris* species using the method of Moreno-Sánchez (2004) in this study resulted in separation of *A. hibernica* from several other *Archaeopteris* species on the basis of sterile leaf morphology alone, although there was some overlap in the range of morphological variation between *A. hibernica* and *A. halliana*. Additional work on fertile leaf material is needed to revise and clarify differences between different *Archaeopteris* species. Both *A. hibernica* and *A. halliana* showed a similar allometric trend of increasing leaf roundness with size. *A. hibernica* was found to have larger, less round leaves, and a variable, sometimes crenulate margin. This variation in leaf morphology may be a result of difference in hydraulic supply, or light environment, or may indicate polyploidy.

References

ANDERSON, H. M., HILLER, N. & GESS, R. W. 1995. *Archaeopteris* (Progymnospermopsida) from the Devonian of southern Africa. *Botanical Journal of the Linnean Society,* **117,** 305-320.

ARNOLD, C. A. 1939. Observations on fossil plants from the Devonian of eastern North America IV. Plant remains from the Catskill delta deposits of Northern Pennsylvania and Southern New York *Contibutions from the museum of Paleontology, University of Michigan,* **5,** 271-314.

BACON, K. L., BELCHER, C. M., HAWORTH, M. & MCELWAIN, J. C. 2013. Increased atmospheric SO_2 detected from changes in leaf physiognomy across the Triassic–Jurassic boundary interval of East Greenland. *PloS one,* **8,** e60614.

BAILY, W. H. 1858. On the fructification of *Cyclopteris hibernica* (Forbes) from the Upper Devonian or Lower Carboniferous strata at Kiltorkan Hill, County Kilkenny. *Transactions of the 28th Meeting of the British Association for the Advancement of Science,* **28,** 75-76.

BAILY, W. H. 1861. *Paleontological notes, explanations to accompany sheets 147 and 157 of the maps of the Geological Survey of Ireland illustrating parts of the Counties of Kilkenny, Carlow, and Wexford*. Dublin: Alexander Thom & Sons.

BAILY, W. H. 1869a. Notes on the fossil from the Old Red Sandstone of Kiltorcan Hill, Co. Kilkenny. *Reports of the British Association for 1868.* Norwich.

BAILY, W. H. 1869b. Report on fossils obtained at Kiltorcan Quarry, Co. Kilkenny. *Report of the British Association for the Advancement of Science***,** 73-75.

BAILY, W. H. 1872. The Kiltorcan Fossils. *Nature,* **5,** 224–225.

BAILY, W. H. 1875a. *Figures of characteristic British fossils (Palaeozoic division) with descriptive remarks,* London, John Van Voorst.

BAILY, W. H. 1875b. On fossils from the Upper Old Red Sandstone of Kiltorcan Hill, in the county of Kilkenny. Report No. 1. *Proceedings of the Royal Irish Academy,* **2,** 45-48.

BEAULIEU, J. M., LEITCH, I. J., PATEL, S., PENDHARKAR, A. & KNIGHT, C. A. 2008. Genome size is a strong predictor of cell size and stomatal density in angiosperms. *New Phytologist,* **179,** 975-986.

BECK, C. B. 1962. Plants of the New Albany shale. II. *Callixylon arnoldii* Sp. Nov. *Brittonia,* **14,** 322-327.

BENCA, J. P., DUIJNSTEE, I. A. & LOOY, C. V. 2018. UV-B–induced forest sterility: Implications of ozone shield failure in Earth's largest extinction. *Science Advances,* **4,** e1700618.

BLONDER, B., BUZZARD, V., SIMOVA, I., SLOAT, L., BOYLE, B., LIPSON, R., AGUILAR-BEAUCAGE, B., ANDRADE, A., BARBER, B. & BARNES, C. 2012. The leaf-area shrinkage effect can bias paleoclimate and ecology research. *American Journal of Botany,* **99,** 1756-1763.

BOURDELLE, F., DUBOIS, M., LLORET, E., DURAND, C., ADDAD, A., BOUNOUA, S., VENTALON, S. & RECOURT, P. 2021. Kaolinite-to-Chlorite Conversion from Si,Al-Rich Fluid-Origin Veins/Fe-Rich Carboniferous Shale Interaction. *Minerals,* **11,** 804.

BOYCE, C. K. 2009. Seeing the forest with the leaves–clues to canopy placement from leaf fossil size and venation characteristics. *Geobiology,* **7,** 192-199.

BREZINSKI, D. K., CECIL, C. B. & SKEMA, V. W. 2010. Late Devonian glacigenic and associated facies from the central Appalachian Basin, eastern United States. *GSA Bulletin,* **122,** 265-281.

BREZINSKI, D. K., CECIL, C. B., SKEMA, V. W. & STAMM, R. 2008. Late Devonian glacial deposits from the eastern United States signal an end of the mid-Paleozoic warm period. *Palaeogeography, Palaeoclimatology, Palaeoecology,* **268,** 143-151.

BRONGNIART, A. 1857. Letter from M. Adolphe Brongniart to Dr. Griffith on the fossil plants which have been discovered in the rocks at the base of the Carboniferous system in Ireland. *Journal of the Geological Society of Dublin,* **2,** 287-293.

BROUSSARD, D. R., TROP, J. M., BENOWITZ, J. A., DAESCHLER, E. B., CHAMBERLAIN JR., J. A. & CHAMBERLAIN, R. B. 2018. Depositional setting, taphonomy and geochronology of new fossil sites in the Catskill Formation (Upper Devonian) of north-central Pennsylvania, USA, including a new early tetrapod fossil. *Palaeogeography, Palaeoclimatology, Palaeoecology,* **511,** 168-187.

CARLUCCIO, L. M., HUEBER, F. M. & BANKS, H. P. 1966. *Archaeopteris macilenta*, anatomy and morphology of its frond. *American Journal of Botany,* **53,** 719-730.

CARPENTER, G. H. & SWAIN, I. 1908. A new Devonian isopod from Kiltorcan, County Kilkenny. *Proceedings of the Royal Irish Academy. Section B: Biological, Geological, and Chemical Science,* **27,** 61-67.

CARRUTHERS, W. 1872. Notes on some fossil plants. *Geological Magazine,* **9,** 49-59.

CHAGNOUX, S. 2021. *The fossil collection (F) of the Muséum National d'Histoire Naturelle (MNHN - Paris). Version 68.231. MNHN - Muséum National d'Histoire Naturelle. Occurrence dataset* [Online]. Available: https://www.gbif.org/occurrence/419306416 [Accessed 8/11/2021].

CHALONER, W. G. 1968. The cone of *Cyclostigma kiltorkense* Haughton, from the Upper Devonian of Ireland. *Botanical Journal of the Linnean Society,* **61,** 25-36.

CHALONER, W. G., HILL, A. J. & LACEY, W. S. 1977. First Devonian platyspermic seed and its implications in gymnosperm evolution. *Nature,* **265,** 233-235.

CHALONER, W. G. & MEYER-BERTHAUD, B. 1983. Leaf and stem growth in the Lepidodendrales. *Botanical Journal of the Linnean Society,* **86,** 135-148.

CLARKE, A., PARKES, M. & GATLEY, S. 2007. The geological heritage of Kilkenny. An audit of county geological sites in Kilkenny.

CLAYTON, G., COLTHURST, J. R. J., HIGGS, K., JONES, G. L. & KEEGAN, J. B. 1977. Tournaisian miospores and conodonts from County Kilkenny. *Bulletin of the Geological Survey of Ireland,* **2,** 99-106.

CLEAL, C. J. & THOMAS, B. A. 2018. Nomenclatural status of the palaeobotanical "artificial taxa" established in Brongniart's 1822 "Classification" paper. *Fossil Imprint,* **74,** 9-28.

COLTHURST, J. R. J. 1978. Old Red Sandstone rocks surrounding the Slievnamon Inlier, Counties Tipperary and Kilkenny. *Journal of Earth Sciences,* **1,** 77-103.

CONNERY, T. 1999. Plant fossils from the Late Devonian Toe Head Sandstone Formation, west Cork, Ireland: a preliminary report. *Acta Palaeobotany, Supplement,,* **2,** 21–25.

CRESSLER, W. L. 2006. Plant palaeoecology of the Late Devonian Red Hill locality, north-central Pennsylvania, an *Archaeopteris*-dominated wetland plant community and early tetrapod site. *In:* S.F. GREB & DIMICHELE, W. A. (eds.) *Wetlands Through Time* Boulder, Colorado: Geological Society of America.

DAWSON, J. W. 1871. *The fossil plants of the Devonian and Upper Silurian formation of Canada, Geological Survey of Canada,* Montreal, Dawson Bros.

DECOMBEIX, A.-L., HARPER, C. J., PRESTIANNI, C., DURIEUX, T., RAMEL, M. & KRINGS, M. 2023. Fossil evidence of tylosis formation in Late Devonian plants. *Nature Plants***, 1-4**.

DOWELD, A. B. 2017a. Proposal to conserve the name *Cyclostigma kiltorkense* against *Lepidodendron griffithii, L. minutum,* and *Sigillaria dichotoma* (fossil Lycopodiophyta: Lepidodendropsida). *Taxon,* **66,** 1481–1482.

DOWELD, A. B. 2017b. A review of the nomenclature of *Cyclostigma* (Cyclostigmatales: Cyclostigmataceae; fossil Isoetophyta). *Taxon,* **66,** 1456-1465.

EDWARDS, N. P., MANNING, P. L., BERGMANN, U., LARSON, P. L., VAN DONGEN, B. E., SELLERS, W. I., WEBB, S. M., SOKARAS, D., ALONSO-MORI, R., IGNATYEV, K. & BARDEN, H. E. 2014. Leaf metallome preserved over 50 million years. *Metallomics,* **6,** 774-782.

FAIRON-DEMARET, M. 1986. 'Some Uppermost Devonian Megafloras: A Stratigraphical Review', Ministry of Economic Affairs, Adm. of Mines, Belgian Geological Survey. *Annales de la Société géologique de Belgique,* **109,** 43–48.

FAIRON-DEMARET, M., LEPONCE, I. & STREEL, M. 2001. *Archaeopteris* from the Upper Famennian of Belgium: heterospory, nomenclature, and palaeobiogeography. *Review of Palaeobotany and Palynology,* **115,** 79-97.

FAWCETT, J. A., MAERE, S. & VAN DE PEER, Y. 2009. Plants with double genomes might have had a better chance to survive the Cretaceous–Tertiary extinction event. *Proceedings of the National Academy of Sciences,* **106,** 5737-5742.

FEEHAN, J. 1979. Plants from the Upper Old Red Sandstone of Slieve Bloom, County Offaly, Eire. *Geological Magazine,* **116,** 403–404.

FIELDS, B. D., MELOTT, A. L., ELLIS, J., ERTEL, A. F., FRY, B. J., LIEBERMAN, B. S., LIU, Z., MILLER, J. A. & THOMAS, B. C. 2020. Supernova triggers for end-Devonian extinctions. *Proceedings of the National Academy of Sciences of the United States of America,* **117,** 21008-21010.

FORBES, E. 1853. On the fossils of the yellow sandstone of the south of Ireland. *Report of the British Association for the Advancement of Science,* **22,** 43.

GOTHAN, W. 1913. *Die Oberschlesische Steinkohlenflora I. Teil Farne und farnähnliche Gewächse (Cycadofilices besw. Pteridospermen),* Berlin, Königlich Preussischen Geologischen Landesanstalt.

GRAHAM, J. R. & SEVASTOPULO, G. D. 2021. The statigraphy of latest Devonian and earliest Carboniferous rocks in Ireland. *Palaeobiodiversity and Palaeoenvironments,* **101,** 515-527.

GRIFFITH, R. & BRONGNIART, A. 1857. On the remains of fossil plants discovered in the yellow sandstone strata, situated at the base of the Carboniferous limestone series of Ireland, in connexion with a communication on that subject received from M. Adolphe Brongniart. *Journal of the Royal Dublin Society,* **1,** 313-325.

GSI 2014. Bedrock Geology 1 Million (scale 1:1,000,000). *In:* DEPARTMENT OF THE ENVIRONMENT, C. A. C. (ed.). https://www.gsi.ie/en-ie/data-and-maps/Pages/Bedrock.aspx#.

GUTAK, J. M., ANTONOVA, V. A. & RUBAN, D. A. 2011. Diversity and richness of the Devonian terrestrial plants in the Southeastern Mountainous Altay (Southern Siberia): Regional versus global patterns. *Palaeogeography, Palaeoclimatology, Palaeoecology,* **299,** 240-249.

HAUGHTON, S. 1855. On the evidence afforded by fossil plants, as to the boundary line between the Devonian and Carboniferous rocks. *Journal of the Geological Society of Dublin,* **6,** 227-241.

HAUGHTON, S. 1860. On *Cyclostigma*, a new genus of fossil plants from the Old Red Sandstone of Kiltorcan, Co. Kilkenny; and on the general law of phyllotaxis in the natural orders Lycopodiaceæ, Equisetaceæ, Filices, &c . *Annals and Magazine of Natural History: Series 3,* **5,** 433-445.

HEER, O. 1871. On the Carboniferous flora of Bear Island (lat. 74° 30'N.). *Quarterly Journal of the Geological Society,* **27,** 1-3.

HEER, O. 1872. On *Cyclostigma*, *Lepidodendron* and *Knorria* from Kiltorkan. *Quarterly Journal of the Geological Society of London,* **28,** 169-172.

HENRY, T. A., BAINARD, J. D. & NEWMASTER, S. G. 2014. Genome size evolution in Ontario ferns (Polypodiidae): evolutionary correlations with cell size, spore size, and habitat type and an absence of genome downsizing. *Genome,* **57,** 555-566.

HERENDEEN, P. S. 2020. Report of the Nomenclature Committee for Fossils: 13. *Taxon,* **69,** 398-402.

HOLLAND, C. H. 1977. Ireland. *In:* HOUSE, M. R., RICHARDSON, J. B., CHALONER, W. G., ALLEN, J. R. L., HOLLAND, C. H. & WESTOLL, T. S. (eds.) *A correlation of Devonian rocks in the British Isles.* Special Reports Geological Society of London.

HÜBERS, M., BOMFLEUR, B., KRINGS, M., POTT, C. & KERP, H. 2014. A reappraisal of Mississippian (Tournaisian and Visean) adpression floras from central and northwestern Europe. *Zitteliana A,* **54,** 39-52.

JARVIS, D. E. 1990. New palynological data on the age of the Kiltorcan flora of Co. Kilkenny, Ireland. *Journal of micropaleontology,* **9,** 87-94.

JARVIS, D. E. 1992. *The stratigraphic palynology, palynofacies and sedimentology of Devonian-Carboniferous Kiltorcan Formation of Southern Ireland.* PhD Thesis, University College Cork.

JARVIS, D. E. 2000. Palaeoenvironment of the plant bearing horizons of the Devonian-Carboniferous Kiltorcan Formation, Kiltorcan Hill, Co. Kilkenny, Ireland. *Geological Society, London, Special Publications,* **180,** 333–341.

JOHNSON, T. 1911a. Is *Archaeopteris* a pteridosperm? *Scientific Proceeding of the Royal Dublin Society,* **13,** 114-136.

JOHNSON, T. 1911b. The occurrence of *Archaeopteris tschermaki* Stur. and of other species of *Archaeopteris* in Ireland. *Scientific Proceeding of the Royal Dublin Society,* **13,** 137-141.

JOHNSON, T. 1913. On *Bothrodendron* (*Cyclostigma*) *kiltorkense*. Haughton sp. *Scientific Proceeding of the Royal Dublin Society,* **13,** 500-528.

JOHNSON, T. 1914a. *Bothrodendron kiltorkense* Haught. sp. its stigmaria and cone. . *Scientific Proceeding of the Royal Dublin Society,* **14,** 211-213.

JOHNSON, T. 1914b. *Ginkgophyllum kiltorkense* sp. nov. *Scientific Proceeding of the Royal Dublin Society,* **14,** 169-178.

JOHNSON, T. 1917. *Spermolithus devonicus* gen. et sp. nov., and other pteridosperms from the Upper Devonian beds at Kiltorcan, Co. Kilkenny. *Scientific Proceeding of the Royal Dublin Society,* **15,** 245-252.

KAISER, S. I., ARETZ, M. & BECKER, R. T. 2016. The global Hangenberg Crisis (Devonian–Carboniferous transition): review of a first-order mass extinction. *In:* BECKER, R. T., KONIGSHOF, P. & BRETT, C. E. (eds.) *Devonian Climate, Sea Level and Evolutionary Events.* London: Geological Society, London, Special Publications.

KENDALL, R. S. 2017. The Old Red Sandstone of Britain and Ireland: a review. *Proceedings of the Geologists' Association,* **128,** 409-421.

KENRICK, P. & FAIRON-DEMARET, M. 1991. *Archaeopteris roemeriana* (Göppert) sensu Stockmans, 1948 from the Upper Famennian of Belgium: anatomy and leaf polymorphism. *Bulletin de l'Institute Royal des Sciences Naturelles de Belgique, Sciences de la Terre,* **61,** 179-195.

KERP, H. & BOMFLEUR, B. 2011. Photography of plant fossils—new techniques, old tricks. *Review of Palaeobotany and Palynology,* **166,** 117-151.

KIDSTON, R. 1923. Fossil plants of the Carboniferous rocks of Great Britain. *Memoirs of the Geological Survey of Great Britain, Palaeontology,* **2,** 1-670.

KLAVINS, S. D. 1999. *Systematics and paleoecology of three Late Devonian floras of southern Ireland.* PhD Thesis, Southern Illinois University, Carbondale.

KLAVINS, S. D. 2004. Re-interpretation of *Wexfordia hookense* from the Upper Devonian of Ireland as an arborescent lycophyte. *Botanical Journal of the Linnean Society,* **144,** 275-287.

KLAVINS, S. D. & MATTEN, L. C. 1996. Reconstruction of the frond of *Laceya hibernica*, a lyginopterid pteridosperm from the uppermost Devonian of Ireland. *Review of Palaeobotany and Palynology,* **93,** 253-268.

KNIGHT, C. A., CLANCY, R. B., GÖTZENBERGER, L., DANN, L. & BEAULIEU, J. M. 2010. On the relationship between pollen size and genome size. *Journal of Botany***,** 612017.

KRÄUSEL, R. & WEYLAND, H. 1941. Pflanzenreste aus dem Devon von Nord-Amerika. I. Vorbemerkung. II. Die oberdevonischen Floren von Elkins, West-Virginien, und Perry, Maine, mit Berücksichtigung einiger Stücke von der Chaleur-Bai, Canada. *Palaeontographica Abteilung B,* **86,** 1-78.

KÜRSCHNER, W. M., BATENBURG, S. J. & MANDER, L. 2013. Aberrant Classopollis pollen reveals evidence for unreduced (2 n) pollen in the conifer family Cheirolepidiaceae during the Triassic–Jurassic transition. *Proceedings of the Royal Society B: Biological Sciences,* **280,** 20131708.

LAKIN, J., MARSHALL, J., TROTH, I. & HARDING, I. 2016. Greenhouse to icehouse: a biostratigraphic review of latest Devonian–Mississippian glaciations and their global effects. *In:* BECKER, R. T., KONIGSHOF, P. & BRETT, C. E. (eds.) *Devonian Climate, Sea Level and Evolutionary Events.* London: Geological Society, London, Special Publications.

LESQUEREUX, L. 1880. *Description of the Coal Flora of the Carboniferous Formation in Pennsylvania and Throughout the United States*, Board of commissioners for the Second geological survey.

LINDSTRÖM, S., SANEI, H., VAN DE SCHOOTBRUGGE, B., PEDERSEN, G. K., LESHER, C. E., TEGNER, C., HEUNISCH, C., DYBKJÆR, K. & OUTRIDGE, P. M. 2019. Volcanic mercury

and mutagenesis in land plants during the end-Triassic mass extinction. *Science advances,* **5,** eaaw4018.

LOMAX, B. H., HILTON, J., BATEMAN, R. M., UPCHURCH, G. R., LAKE, J. A., LEITCH, I. J., CROMWELL, A. & KNIGHT, C. A. 2014. Reconstructing relative genome size of vascular plants through geological time. *New Phytologist,* **201,** 636-644.

LOMAX, B. H., WOODWARD, F. I., LEITCH, I. J., KNIGHT, C. A. & LAKE, J. A. 2009. Genome size as a predictor of guard cell length in *Arabidopsis thaliana* is independent of environmental conditions. *New Phytologist,* **181,** 311-314.

MARSHALL, J. E. A. 2021. A terrestrial Devonian-Carboniferous boundary section in East Greenland. *Palaeobiodiversity and Palaeoenvironments,* **101,** 541-559.

MARSHALL, J. E. A., LAKIN, J., TROTH, I. & WALLACE-JOHNSON, S. M. 2020. UV-B radiation was the Devonian-Carboniferous boundary terrestrial extinction kill mechanism. *Science Advances,* **6,** eaba0768.

MATTEN, L. C., LACEY, W. S. & EDWARDS, D. 1975. Discovery of one of the oldest gymnosperm floras containing cupulate seeds. *Phytologia,* 32**,** 299-303.

MATTEN, L. C., LACEY, W. S., MAY, B. I. & LUCAS, R. C. 1980. A megafossil flora from the Uppermost Devonian near Ballyheigue, Co. Kerry, Ireland. *Review of Paleobotany and Palynology,* **29,** 241-251.

MAZIANE, N., HIGGS, K. T. & STREEL, M. 2002. Biometry and paleoenvironment of *Retispora lepidophyta* (Kedo) Playford 1976 and associated miospores in the latest Famennian nearshore marine facies, eastern Ardenne (Belgium). *Review of Palaeobotany and Palynology,* **118,** 211-226.

MCELWAIN, J. C. & STEINTHORSDOTTIR, M. 2017. Paleoecology, ploidy, paleoatmospheric composition, and developmental biology: a review of the multiple uses of fossil stomata. *Plant Physiology,* **174,** 650-664.

MONTAÑEZ, I. P. 2022. Current synthesis of the penultimate icehouse and its imprint on the Upper Devonian through Permian stratigraphic record. *In:* LUCAS, S. G., SCHNEIDER, J. W., WANG, X. & NIKOLAEVA, S. (eds.) *The Carboniferous Timescale.* London: Geological Society, London, Special Publications.

MORENO-SÁNCHEZ, M. 2004. Graphic approach for morphometric analysis of *Archaeopteris* leaves. *Annales de Paléontologie,* **90,** 161-173.

NIINEMETS, Ü., CESCATTI, A. & CHRISTIAN, R. 2004. Constraints on light interception efficiency due to shoot architecture in broad-leaved Nothofagus species. *Tree Physiology,* **24,** 617-630.

O'KELLY, J. 1862. *Explanations to accompany sheet 127 of the maps of the Geological Survey of Ireland illustrating a portion of the Queen's county (Laois) with palaeontological notes*.

OSBORNE, C. P., BEERLING, D. J., LOMAX, B. H. & CHALONER, W. G. 2004. Biophysical constraints on the origin of leaves inferred from the fossil record. *Proceedings of the National Academy of Sciences,* **101,** 10360-10362.

PENNEY, S. R. 1980. A new look at the Old Red Sandstone Succession of the Comeragh Mountains, County Waterford. *Journal of Earth Sciences,* **3,** 155-178.

PEPPE, D. J., ROYER, D. L., CARIGLINO, B., OLIVER, S. Y., NEWMAN, S., LEIGHT, E., ENIKOLOPOV, G., FERNANDEZ-BURGOS, M., HERRERA, F., ADAMS, J. M., CORREA, E., CURRANO, E. D., ERICKSON, J. M., HINOJOSA, L. F., HOGANSON, J. W., IGLESIAS, A., JARAMILLO, C. A., JOHNSON, K. R., JORDAN, G. J., KRAFT, N. J. B., LOVELOCK, E. C., LUSK, C. H., NIINEMETS, Ü., PEÑUELAS, J., RAPSON, G., WING, S. L. & WRIGHT, I. J. 2011. Sensitivity of leaf size and shape to climate: global patterns and paleoclimatic applications. *New Phytologist,* **190,** 724-739.

PRESTIANNI, C., SAUTOIS, M. & DENAYER, J. 2016. Disrupted continental environments around the Devonian-Carboniferous Boundary: introduction of the *tener* event. *Geologica Belgica,* **19,** 135-145.

RITCHIE, A. 1975. *Groenlandaspis* in Antarctica, Australia and Europe. *Nature,* **254,** 569-573.

ROBIN, N., GUERIAU, P., LUQUE, J., JARVIS, D., DALEY, A. C. & VONK, R. 2021. The oldest peracarid crustacean reveals a Late Devonian freshwater colonization by isopod relatives. *Biology Letters,* **17,** 20210226.

ROWE, N. P. 1992. The gymnosperm *Archaeopteridium tschermaki* and an associated glandular fructification from the Upper Visean Drybrook Sandstone of Great Britain. *Palaeontology,* **35,** 875-900.

SCHECKLER, S. E. 1986. Geology, floristics and palaeoecology of Late Devonian coal swamps from Appalachian Laurentia (USA). *Annales de la Société Géologique de Belgique,* **109,** 206-222.

SCHIMPER, W. P. 1869. *Traité de paléontologie végétale: ou, La flore du monde primitif dans ses rapports avec les formations géologiques et la flore du monde actuel*, JB Baillière et fils.

SCHIMPER, W. P. 1870. *Traité de paléontologie végétale ou la flore du monde primitif,* Paris, J.G. Bailliere.

ŠMARDA, P., HOROVÁ, L., KNÁPEK, O., DIECK, H., DIECK, M., RAŽNÁ, K., HRUBÍK, P., ORLÓCI, L., PAPP, L. & VESELÁ, K. 2018. Multiple haploids, triploids, and tetraploids found in modern-day "living fossil" *Ginkgo biloba*. *Horticulture Research,* **5**.

STOCKMANS, F. 1948. Végétaux du Dévonien Supérieur de la Belgique. *Mémoires du Musée Royal d'Histoire Natuerelle de Belgique,* **110** 1-85.

STREEL, M. 1966. Critères palynologiques pour une stratigraphie détaillée du Tn1a dans les bassins Ardenno-Rhénans. *Annales de la Société géologique de Belgique,* **89,** 65-96.

VISSCHER, H., LOOY, C. V., COLLINSON, M. E. & SEPHTON, M. A. 2004. Environmental mutagenesis during the end-Permian ecological crisis. *Proceedings of the National Academy of Sciences of the United States of America,* **101,** 12952–12956.

WALSH, P. T. 1968. The Old Red Sandstone west of Killarney, Co. Kerry, Ireland. *Proceedings of the Royal Irish Academy. Section B: Biological, Geological, and Chemical Science,* **66,** 9-26.

WANG, Q. 2011. Correct author citation of the Late Devonian plant *Archaeopteris* (Progymnospermopsida). *Paleontological Journal,* **45,** 347-349.

WOLFE, J. A. 1993. *A method of obtaining climatic parameters from leaf assemblages*, US Government Printing Office.

4. A preliminary study on leaf functional traits of *Archaeopteris hibernica* from the Kiltorcan flora, Ireland.

Abstract

Archaeopteris was an ecologically dominant component of Upper Devonian forest ecosystems and is considered one of the first 'modern' trees. The substantial number of functional ecological studies of contemporary plants provides an opportunity to apply a modern understanding of well-established trait trade-offs to extensive natural history collections. A fossil leaf trait analysis was conducted on *Archaeopteris hibernica* (Forbes) Stur foliage from Kiltorcan, Co. Kilkenny, in order to obtain insights into the functioning of Ireland's oldest fossil forests. A preliminary analysis of operational stomatal conductance using the hydraulic constraints of leaf vein density and leaf mass per area are presented for *Archaeopteris hibernica* from the Kiltorcan flora, from the upper Famennian. Operational stomatal conductance was modelled to be between 98-115 mmol m^{-2} s^{-1} using two different vein density-based models. This was higher than operational stomatal conductance modelled from published stomatal morphology data for *Archaeopteris* spp. from the Frasnian (39 mmol m^{-2} s^{-1}). Leaf mass per area was found to be 233 g m^{-2}, which is similar to published values for evergreen gymnosperms, suggesting a slow rate of return on nutrient and dry mass investment in leaves. Although further research is recommended to better constrain LMA and leaf lifespan for *Archaeopteris*, this study suggests that *Archaeopteris* had a slow-lived, stress tolerant life strategy, and was functionally similar to evergreen gymnosperms.

4.1 Introduction

Plant functional traits are defined as morphological, phenological and physiological traits that indirectly impact fitness via effects on growth, reproduction and survival (Violle et al., 2007). Traits and trait trade-offs are considered critical to ecological function at the scale of the individual, community and ecosystem (Díaz et al., 2016, Gomarasca et al., 2023, Maynard et al., 2022, Violle et al., 2007, Wright et al., 2004). Wright et al. (2004) identified six leaf traits (leaf lifespan, leaf mass per area (LMA), photosynthetic assimilation rate, dark respiration rate, leaf nitrogen and leaf phosphorus), which describe the trade-off between resource acquisition and storage strategies (i.e., the leaf economic spectrum). One end of the leaf economic spectrum is represented by 'slow' plants - i.e., slow-growing species that produce long-lived leaves that have 'expensive' (i.e., high LMA) construction, low nutrient concentrations and low rates of dark respiration and photosynthesis (Reich, 2014, Wright et al., 2004). The other end of the spectrum is represented by 'fast' plants, which have high photosynthetic and dark respiration rates, have high nutrient concentrations and have short-lived, 'inexpensive' leaf construction (Wright et al., 2004). More recent studies have found that a small number of leaf economic traits and whole plant traits reflecting plant size also indicate a similar pattern of trait trade-offs and coordination at a global scale (Díaz et al., 2016, Maynard et al., 2022), and that these trait-coordination principles also propagate at ecosystem scales (Gomarasca et al., 2023).

In terms of palaeoecology and palaeobotany, trait ecology presents an exciting opportunity to elucidate plant function and ecosystem processes over evolutionary timescales, and potentially do so across significant periods of environmental upheaval and extinction, at different spatial scales (Blonder et al., 2014, Brown et al., 2023, Currano and Jacobs, 2021, Matthaeus et al., 2023, McElwain et al., 2024, Roth-Nebelsick et al., 2017, Royer et al., 2007, Royer et al., 2010, Soh et al., 2017). Currently, leaf traits are commonly used for palaeoclimatic reconstructions (Peppe et al., 2011, Wolfe, 1993, Kunzmann et al., 2019), and are more rarely used to elucidate plant function and acquisitive strategies. In addition to fossil leaf traits, stem traits and pollen and diaspore traits can also be used in palaeoecological studies, either individually or in combination for this purpose (Adeleye et

al., 2023, Bouda et al., 2022, Kunzmann et al., 2019, Matthaeus et al., 2022, McElwain et al., 2024, Nogué et al., 2022, Wilson et al., 2017, Wilson et al., 2020). A clear constraint of applying functional trait ecology to palaeoecology and palaeobotany is the indirect nature by which the majority of plant functional traits must be assessed. While some functional traits such as leaf area and vein density can be measured directly, other traits, such as leaf mass per area (LMA) or water use efficiency, can only be studied based on fundamental morphological, anatomical or isotopic relationships that have been established using extant plants. Relevant taphonomic factors must also be considered to account for potential over- or under-representation of certain trait syndromes, or potential biases in trait interpretation in the fossil record.

The extensive amount of well-preserved *Archaeopteris hibernica* (Forbes) Stur leaf material from the Famennian aged Kiltorcan flora, Co. Kilkenny, Ireland, presents the possibility of reinvestigating a world-famous fossil locality through the lens of plant functional ecology. The evolution of the arborescent habit in the Devonian occurred independently in a number of taxa, providing plants with an enhanced capacity for propagule dispersal, greater leaf area, and greater access to water and nutrients through deeper rooting systems, over smaller taxa (Boyce et al., 2017, Morris et al., 2015). While not thought to be the earliest arborescent taxon, *Archaeopteris* spp. are known to have become an ecologically significant component of forests by the Famennian (372-359 Ma), with microfossil and macrofossil evidence indicating they first emerged by the early Givetian (388-383 Ma) (Stein et al., 2020) and last occurred during the Lower Mississippian (Beck, 1962). In many ways *Archaeopteris* is considered to be the first 'modern' tree; it had simple laminate leaves, delayed development involving bud-like behaviour, eustelic primary vascular system, bifacial vascular cambium with conifer-like secondary issues, endogenous root production and a highly advanced, extensive root system that is comparable to extant seed plants (Carluccio et al., 1966, Decombeix and Meyer-Berthaud, 2013, Meyer-Berthaud et al., 1999, Meyer-Berthaud et al., 2000, Meyer-Berthaud et al., 2013, Stein et al., 2020). However, it also shows non-analogous combinations of anatomical and reproductive characteristics that are not seen in the modern world (i.e., it is an arborescent spore plant that possesses seed-plant like anatomy) and occupies an intermediate morphospace between extant lineages (Clark et al., 2023).

A number of previous studies have investigated different palaeo-functional traits for different *Archaeopteris* species, such as hydraulic properties (Tanrattana et al., 2019), leaf area (Osborne et al., 2004), stomatal conductance (Osborne et al., 2004), vein density (Boyce et al., 2009) and carbon isotope composition (Wan et al., 2019). Existing collections of well-preserved *Archaeopteris hibernica* leaf material from the Kiltorcan flora presents the opportunity to further investigate *Archaeopteris* through the lens of contemporary trait ecology. However, the preservation of the Kiltorcan material provides a number of constraints on the traits that may be investigated from these collections. The Kiltorcan material lacks organic preservation (Chaloner, 1968), so only leaf traits which can be inferred or measured directly from the chloritic compression-impression fossils can be assessed.

Vein density (total vein length per unit area) is a trait that can be directly measured from well-preserved compression fossils. It shows diverse patterns across different phylogenetic groups and across evolutionary time, applying functional constraints on leaf hydraulic conductance, as well as providing mechanical stability to the leaf (Boyce et al., 2009, Brodribb et al., 2007, Roth-Nebelsick et al., 2001, Sack and Scoffoni, 2013, Scoffoni et al., 2016). Vein density is independent of the leaf economic traits of LMA and leaf lifespan (Sack and Scoffoni, 2013, Sack et al., 2013). However, due to the strong effects of vein density on hydraulic conductance, vein density has a significant effect on stomatal conductance and photosynthetic rate (Boyce et al., 2009, Brodribb et al., 2007, McElwain et al., 2015, Sack et al., 2013) and can be measured on fossils to infer these ecophysiological traits. Throughout plant evolutionary history, vein density in non-angiosperm and early diverging angiosperm lineages remained below 5 mm mm^{-2} (Boyce et al., 2009), with increases in angiosperm vein density occurring at two separate intervals; during the mid-Cretaceous, and the Cretaceous-Paleogene transition (Feild et al., 2011). The evolution of high vein densities in angiosperm lineages is thought to have played a major role in increased precipitation in modern tropical rainforests through changes in plant water cycling (Boyce et al., 2009, Boyce et al., 2010), and provided a photosynthetic advantage over evolutionarily older lineages as atmospheric CO_2 concentrations declined (Boyce et al., 2009, Boyce et al., 2010, Feild et al., 2011, McElwain et al., 2015, Yiotis and McElwain, 2019).

Leaf mass per area (LMA) cannot be measured directly from the fossil record. However, numerous proxies have been developed to try to estimate this important leaf trait in the deep past: cuticle thickness (Soh et al., 2017), adaxial epidermal cell features (Haworth and Raschi, 2014) and petiole width-leaf area relationship (Peppe et al., 2014, Royer et al., 2007, Royer et al., 2010). The most appropriate LMA-proxy for use on *A. hibernica* specimens from the Kiltorcan flora, given its preservation mode, is the petiole width-leaf area relationship, as only leaf morphology is preserved. Royer et al. (2007) investigated the use of the biomechanical and developmental principles to estimate leaf mass per area in the fossil record. Petiole length and cross-sectional area had been previously demonstrated to provide biomechanical support and correlate with leaf mass and area. LMA can thus be estimated from its relationship with petiole width and leaf area, across a range of diverse leaf morphologies from different phylogenetic lineages (Peppe et al., 2014, Royer et al., 2007, Royer et al., 2010).

Within extant plant groups LMA is known to be a variable trait, with most terrestrial plants lying between 30-330 g m^{-2}, with extreme values extending to as low as 3 g m^{-2} (*Myriophyllum* sp.) and as high as over 2000 g m^{-2} (*Agave deserti*) (Poorter et al., 2009). LMA shows strong variance with environmental conditions and has also been found to vary between plant functional groups, with evergreen gymnosperms and succulents having much higher LMA values than deciduous shrubs and tree, herbs, grasses, ferns and aquatic plants (Poorter et al., 2009). This difference in LMA between evergreen and deciduous leaves has been used in palaeobotanical research to interpret the leaf habit of fossil taxa. Royer et al. (2007) used LMA-leaf lifespan relationship described by Wright et al. (2004) to broadly distinguish between taxa that fall into the short-lived (i.e. leaf lifespan < 12 months; LMA < 87 g m^{-2}) and long-lived (i.e. leaf lifespan > 12 months; LMA >129 g m^{-2}) ends of the leaf economic spectrum. The LMA-leaf lifespan axis of plant economic strategies is well known. However, the slope of this relationship differs between evergreen and deciduous species, showing a much steeper relationship for evergreens (Poorter et al., 2009). This may indicate that evergreen leaves can gain higher leaf longevity per unit biomass investment (Poorter et al., 2009). The relationship between LMA and other aspects leaf

economic spectrum have also been found to vary between different phylogenetic groups, with angiosperms showing higher photosynthetic benefits per increase in leaf nitrogen content and LMA than more basal lineages (Gago et al., 2019).

When applied to the fossil record, LMA can reveal different aspects of plant palaeoecology and ecosystem function (Brown et al., 2023, McElwain et al., 2024). A number of studies have correlated LMA and herbivory damage, finding a general trend of increasing herbivory on lower LMA leaves (Poorter et al., 2009, Royer et al., 2007). However, opposite trends have also been observed from fossil-based studies (Wappler et al., 2012), as well as no correlation between herbivory and LMA (Currano et al., 2008). This is likely a result of multiple other factors influencing herbivory, including their representation in the fossil record and influence of taphonomic factors (Currano and Jacobs, 2021). Estimated LMA values from fossil taxa also tend to vary in a predictable way based on known patterns of LMA variation in different habitats (Carvalho et al., 2021, Flynn and Peppe, 2019, Lowe et al., 2018, Royer et al., 2007, Royer et al., 2010), allowing inferences to be made about their palaeoecology.

Inferences about plant ecological strategy from fossil plant functional traits are of particular interest across periods of major environmental change and extinction. However, shifts in ecological strategy have been found to be variable at different intervals. Haworth and Raschi (2014) found that adaxial epidermal cell based LMA values for Ginkgoales increased during the late Triassic and decreased by the early Jurassic. Subsequent work by Soh et al. (2017) using the cuticle-based LMA proxy found that LMA values of Ginkgoales and Bennettitales increased across the Triassic-Jurassic boundary, but did not corroborate the early Jurassic decrease in LMA in Ginkgoales found by Haworth and Raschi (2014). Soh et al. (2017) used both the epidermal-cell and cuticle-LMA proxy methods on Ginkgoales from the same fossil locality and found that they followed the same overall trend, and both proxies were positively correlated with each other. The petiole-based proxy was also used in this study, although the sample size was more limited (Soh et al., 2017). This trend in LMA across the Triassic-Jurassic boundary was interpreted as indicating a shift towards slower growing, stress-tolerant life strategies in the aftermath of the mass extinction

interval (Soh et al., 2017). Variation in LMA values were also found to decline across the Triassic-Jurassic boundary (Soh et al., 2017). Across the Cretaceous-Paleogene boundary the opposite trend in LMA has been observed (Blonder et al., 2014, Lyson et al., 2019), indicating a shift to fast growth strategies during and after global cooling caused by the Chicxulub bolide impact. A more recent study by Butrim et al. (2022) found that there was no significant LMA signal across the Cretaceous-Paleogene boundary, and that any LMA changes were due to a change in local environment, rather than global environmental change. Similarly, Currano et al. (2008) found no change in LMA or ecological strategies across the Palaeocene-Eocene Thermal Maximum. Future studies may reveal more general patterns in community-level plant functional strategies as a response to major environmental change where detailed relative abundance records are available to calculate community-mean LMA values. However, inferences based on relationships between plant functional traits (e.g. LMA) and life history strategy are complex, and context dependent (Kelly et al., 2021).

The aim of this study was to carry a preliminary palaeo-functional trait investigation of *Archaeopteris hibernica* fossil leaves contained within existing museum collections of the Famennian aged Kiltorcan Flora, from Co. Kilkenny, Ireland. LMA and operational stomatal conductance (modelled from vein density) were analysed on fossil leaf specimens of *A. hibernica* to provide an initial assessment of the functional ecology of one of Ireland's oldest fossil forest taxon. Fossil Leaf functional trait data from 17 specimens were then compared to existing modern and fossil trait datasets to explore where *A. hibernica* functioned in relation to modern and fossil plant trait space.

4.2 Materials and Methods

4.2.1 Fossil material

Archaeopteris hibernica chlorite compression fossil leaves from the Kiltorcan flora from the Trinity College Dublin Geology Museum (TCD), the National Museum of Northern Ireland (NMNI) and the National Museum of Ireland (NMI) fossil collections were used for the purposes of this study. In total, 63 specimens of *A. hibernica* branch systems with multiple attached sterile leaves were photographed for this study (21 specimens from the TCD collection, 17 specimens from the NMNI collection and 25 specimens were photographed from the NMI collection). Digital images of the specimens were initially obtained using a Sony Cybershot DSC-RX100 digital camera, with subsequent photographs obtained using a Canon EOS 1100D camera, with a SIGMA 70MM F2.8 lens. Six specimens were photographed under water immersion to increase the contrast between the fossil and the rock matrix (Kerp and Bomfleur, 2011). Other immersion fluids such as xylene or ethanol were not used due to poor ventilation and their associated health hazards. Water immersion is generally not appropriate for use on clayey sediment and some clay minerals, due to swelling (Kerp and Bomfleur, 2011). The fossil matrix of the Kiltorcan material is mostly fine sand and detrital muscovite, and the fossils themselves are mostly chlorite, so damage from swelling clays in the matrix was not considered to be an issue (P. Roycroft, personal communication, 20 April 2023). Photographs were processed using Adobe Photoshop (24.7.0 Release) to further enhance the contrast between the fossil and the rock matrix before carrying out measurements. All photographs were a minimum of 2848 x 4272 pixels and 600 dpi.

4.2.2 Vein density measurements and modelled operational stomatal conductance

Vein density (D_v) was measured directly from fossil leaves of *A. hibernica* using Adobe Photoshop. One square (3 mm x 3 mm) was overlaid onto the image of the leaf and the length of all vein segments within the square were measured (see *Figure 4.1*; Schwendemann, 2018, Uhl and Mosbrugger, 1999). When possible, vein density measurements were taken for six leaves per ultimate or penultimate branch system, with

each intact branch system treated as a separate individual. Vein density measurements were taken as close to the centre of the leaf as possible. More than 1,900 vein segments were measured from 143 leaves from 24 specimens. All D_v measurements were confidence scored based on the quality of preservation.

Maximum theoretical stomatal conductance (g_{max}) was estimated from vein density measurements of *A. hibernica* from the Kiltorcan flora using the following equation (McElwain et al., 2015):

$$g_{max} = 27.574(D_v)^2 - 93.365(D_v) + 512.84;\ r^2 = 0.741 \quad (8)$$

Maximum theoretical stomatal conductance (g_{max}) is defined as per Table 2 in Murray et al. (2019) as the absolute maximum theoretical stomatal conductance based on stomatal density and pore size when fully open. This was then multiplied by 0.2 (Franks et al., 2014, McElwain et al., 2015) to estimate operational stomatal conductance (g_{op}). Higher g_{op}:g_{max} ratios have been recorded in plant taxa with high photosynthetic rates (e.g. g_{op}:g_{max} was found to be 0.26 for C3 woody angiosperms in Murray et al. (2020)), however a value of 0.2 was used to as there is no robust evidence to suggest a high photosynthetic rate for *A. hibernica* (McElwain et al., 2015).

$$g_{op} = 0.2\ g_{max} \quad (9)$$

The leaf hydraulic model of Brodribb et al. (2007) and Brodribb and Feild (2010) was also used to estimate operational stomatal conductance (g_{op}) from the same vein density dataset. The model was tested using empirical gas exchange measurements by Brodribb and Feild (2010), therefore the stomatal conductance modelled is considered to be equivalent to operational stomatal conductance (g_{op}) above. Brodribb et al. (2007) found

that the hydraulic conductance of leaves (K_{leaf}) is proportional to the non-vascular hydraulic pathway from veins to the stomata (D_m) and can be described by the following equation:

$$K_{leaf} = 12670\ {D_m}^{-1.27}$$

(10)

D_m is defined by the equation:

$$Dm = \frac{\pi}{2}(dx^2 + dy^2)^{0.5}$$

(11)

Where d_y is the distance from the vein terminals to the epidermis, and d_x is the longest horizontal distance from the vein terminals to the stomata (Brodribb et al., 2007). Higher vein density yields shorter hydraulic distances, and the relationship between D_v and d_x has been found to be highly conserved across species with reticulate venation and can be described by the following equation:

$$dx = \frac{650}{Dv}$$

(12)

As the *A. hibernica* specimens are preserved as chloritic compressions, measurements for d_x and d_y cannot be obtained directly. Therefore, the above equation was used to estimate d_x, and the value for d_y was obtained using the anatomical measurements for *Nageia nagi* in Brodribb et al. (2007). The anatomical measurements for *Nageia nagi* was used as it is the only multi-veined species that has a dichotomous venation pattern within the dataset. Angiosperm and fern-based values were excluded on the basis of venation pattern.

Operational stomatal conductance (g_{op}) was then derived from the modelled leaf hydraulic conductance using the following equation:

$$g_{op} = (K_{leaf}\Delta\psi_{leaf})/v$$

(13)

Where $\Delta\Psi_{leaf}$ is the water potential gradient within the leaf (MPa) and v is leaf to air vapour pressure deficit (kPa). Typical values for temperate-tropical environments of 2kPa (v) and 0.4MPa ($\Delta\Psi_{leaf}$) were used (Brodribb and Feild, 2010).

Finally, for the purposes of comparison, maximum theoretical stomatal conductance (g_{max}) was modelled using stomatal density and size measurements from Carluccio et al. (1966) and Osborne et al. (2004) for Frasnian-aged *A. macilenta* (from the Oneonta Formation, Schoharie Co. Livingstonville, New York) and *Archaeopteris* spp. (from the Escuminac Formation at Miguasha, Quebec) according to the equation of Franks and Farquhar (2007):

$$g_{max} = \frac{dw}{v} \cdot SD \cdot pa_{max} \,/\, (pd + \frac{\pi}{2}\sqrt{pa_{max}/\pi}\ )$$

(14)

where *dw* is the diffusivity of water vapor in air and *v* is the molar volume of air, *SD* is stomatal density, pa_{max} is the maximum stomatal pore area and *pd* is pore depth. Pore depth is estimated from single guard cell width, with the assumption that guard cells are circular in cross-section (Franks et al., 2001, Franks and Farquhar, 2007, Franks et al., 2014). Maximum stomatal pore area (pa_{max}) is calculated from the following equation:

$$pa_{max} = \beta(\pi p^2/4)$$

(15)

Where p is equal to pore length and β is a geometric constant equal to the scaling from the area of a circle with the diameter of the pore length to $pa_{max.}$ These values were obtained from Franks et al. (2014). β=0.5 was used for *Archaeopteris* spp. (based on extant ferns and gymnosperms) (Franks et al., 2014). Again, the calculated g_{max} values were then multiplied by 0.2 (see above) to estimate operational stomatal conductance (g_{op}) for the purposes of comparison between the three methods. All calculations and data analysis were carried out in R (v 4.2.2).

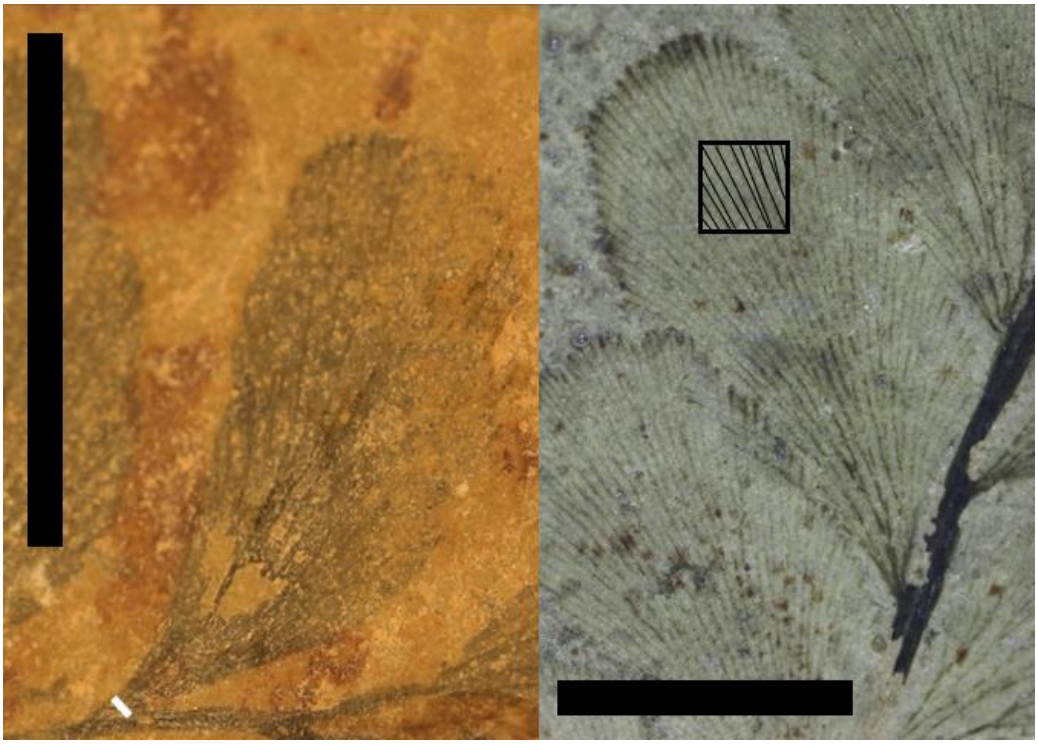

Figure 4.1. Different fossil leaf measurements for LMA (left) and vein density (right) for *Archaeopteris hibernica*. (Left) Petiole width was measured at the point closest to the branch the leaf was attached to, perpendicular to the veins (indicated in white; specimen number F34676, NMI collection). (Right) The length of all vein segments within a 3 mm x 3 mm square were measured from the mid portion of the leaf to obtain vein density measurements (right; specimen number BELUM K12488, NMNI collection). All scale bars = 1cm.

4.2.3 Fossil leaf mass per area estimates

Leaf mass per area (LMA) estimates were obtained from *A. hibernica* specimens from the Kiltorcan flora using the petiole width-leaf area relationship of Royer *et al.* (2007, 2010). Measurements of petiole width and leaf area were carried out in Adobe Photoshop. Petiole width was measured at the point closest to the branch the leaf was attached to, perpendicular to the veins (see *Figure 4.1*). Leaf area was measured following the protocol of Peppe et al. (2011). The leaf was selected using the quick selection tools (with a maximum selection size of 10 pixels) and copied to a new layer. Any minor portions of the leaf margin that were damaged were reconstructed when possible to do so following Peppe et al. (2011). Leaf area was then measured from digitally extracted leaves that were sufficiently well preserved. The petiole width and leaf area measurements were then used to estimate LMA from the following equation, based on the gymnosperm calibration of Royer et al. (2010):

$$log_{10}(LMA_{gymnosperm}) = 0.3076\, log_{10}(\frac{PW^2}{A}) + 3.015$$

(16)

Where PW = petiole width, and A = leaf area. The $LMA_{gymnosperm}$ estimates obtained were further compared to LMA estimates obtained using the angiosperm petiole width-leaf area calibration dataset of Royer et al. (2007) and the *Ginkgo* petiole width-leaf area calibration dataset of Haworth and Raschi (2014) (see *Appendix 4.1*). The fern petiole width-leaf area calibration of Peppe et al. (2014) was not used, as *Archaeopteris* had simple leaves (Carluccio et al., 1966). A total of 82 leaves from 17 specimens were used to estimate palaeo-LMA. Each LMA estimate was categorised as having either 'high' or 'medium' confidence based on preservation quality. 'High' confidence measurements (11 leaves) were those where the leaf lamina and petiole were intact and appeared to be preserved completely flat. 'Medium' confidence measurements (71 leaves) were those where either the leaf attachment appeared to be partially obscured by the branch due to phyllotaxy, or

where the leaf lamina was partially reconstructed due to incomplete leaf preservation. All calculations and data analysis were carried out in R (v 4.2.2).

4.2.4 Processing of leaf mass per area data of extant plants

LMA data from extant plants were obtained from the TRY database (Kattge et al., 2020) for the purpose of comparison with fossil LMA estimates. The inverse of TRY trait IDs 4083, 3116 and 3117 were used (leaf area per leaf dry mass (specific leaf area, SLA or 1/LMA) of total leaf area; leaf area per dry mass (specific leaf area, SLA or 1/LMA) petiole included; leaf area per dry mass (specific leaf area, SLA or 1/LMA) undefined if petiole is in- or excluded). The mean LMA value was calculated when multiple measurements existed for a single species. The LMA data was combined with the TRY - Categorical Traits Dataset (TRY File Archive ID = 3) to categorise species occurring in both dataset by leaf phenology type, phylogenetic group and plant growth form. The following plant growth form categories were excluded: graminoids, mosses, herbs and herb/shrubs, as they were not considered to be a useful comparison based on existing knowledge on the growth habit of *A. hibernica.* Plants that were categorised as 'without leaves' or as having 'evergreen/deciduous' leaf phenology were also excluded for simplicity. All calculations and data analysis were carried out in R (v 4.2.2). A summary table of LMA data obtained from the TRY database (Kattge et al., 2020) can be found in *Appendix 4.2.*

4.3 Results

4.3.1 Estimated operational stomatal conductance from leaf vein density

Mean *A. hibernica* leaf vein density was found to be 3.0 mm mm^{-2} (± 0.6 mm mm^{-2}). This resulted in a median modelled operational stomatal conductance to water of 97 mmol m^{-2} s^{-1} using the vein density - stomatal conductance relationship described in McElwain et al. (2015). This modelled value is lower than estimates obtained using the model of Brodribb et al. (2007) and Brodribb and Feild (2010) (115 mmol m^{-2} s^{-1}; Wilcoxon rank sum test, W=17047, $p<2.2e^{-16}$). The operational stomatal conductance values obtained using vein density-based models were higher than the values obtained using published stomatal data for Frasnian-aged *Archaeopteris macilenta* (Carluccio et al., 1966, Osborne et al., 2004) and *Archaeopteris sp*. (Osborne et al., 2004) (see *Figure 4.2*; median = 39 mmol m^{-2} s^{-1}). However, the stomatal data were obtained from fossils of different species of *Archaeopteris* that predate the Kiltorcan flora by approximately 20 million years, and are based on a much smaller sample size (n=3; see *Table 4.1*).

Table 4.1. Summary of modelled operational stomatal conductance (g_{op}) and maximum stomatal conductance (g_{max}) using all three methods. All values are reported in units of mmol m^{-2} s^{-1}.

Method	n	**Median g_{op}**	Q1	Q3	**Median g_{max}**	Taxa	Approximate Age (Ma)
McElwain et al.	143	**95.6**	91.1	101.1	**478**	*A. hibernica*	360
Brodribb et al.	143	**114.9**	102.2	125.4	**511**	*A. hibernica*	360
Stomatal data	3	**38.7**	31.1	38.7	**193.5**	*A. macilenta* and *Archaeopteris* sp.	380

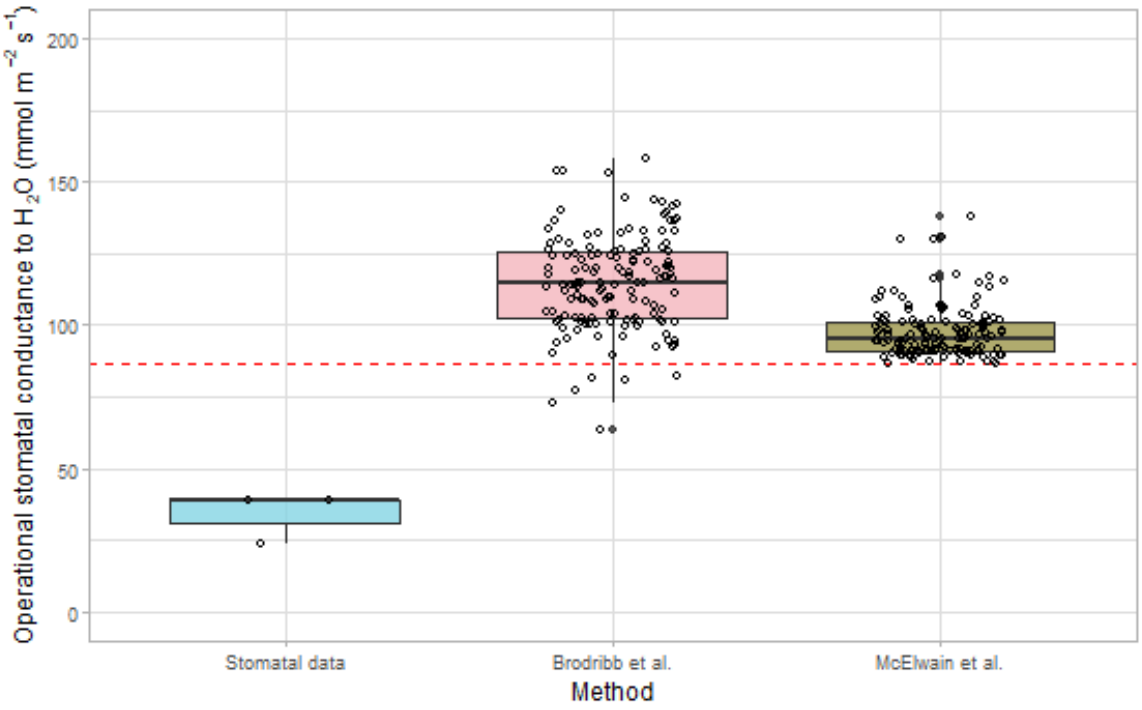

Figure 4.2. Differences in modelled operational stomatal conductance to water for *Archaeopteris*. Operational stomatal conductance estimates produced using vein density - stomatal conductance relationship described in McElwain et al. (2015) for *A. hibernica* (brown; median = 96.6 mmol m^{-2} s^{-1}) were lower than those produced using the model of Brodribb et al. (2007) and Brodribb and Feild (2010) for the same species (pink; median = 114.9 mmol m^{-2} s^{-1}; Wilcoxon rank sum test, W=17047, $p<2.2e^{-16}$). Operational stomatal conductance as modelled based on anatomical stomatal measurements for Frasnian-aged *A. macilenta* and *Archaeopteris* sp. from Carluccio et al. (1966) and Osborne et al. (2004) are shown in blue for comparison (maximum = 38.7 mmol m^{-2} s^{-1} and minimum = 23.4 mmol m^{-2} s^{-1}). The dotted red line corresponds to the minimum possible value that can produced using vein density - stomatal conductance relationship described in McElwain et al. (2015).

4.3.2 Estimated Leaf Mass per Area

Mean leaf mass per area ($LMA_{gymnosperm}$) for *A. hibernica* was found to be 244 g m^{-2} (± 83 g m^{-2}, n=82). LMA estimates produced a wide range of values from a minimum of 114 g m^{-2} to a maximum of 456 g m^{-2}. These estimates are considered to be maximum LMA estimates, due to the possible effects of taphonomic processes on leaf morphology (Royer et al., 2010). Leaf preservation quality was not found to result in a statistically significant difference in median LMA estimates (Wilcoxon rank sum test, W=283, p=0.145).

The gymnosperm calibration dataset resulted in higher LMA estimates (median=233 g m^{-2}) than those using the angiosperm-based (median = 185 g m^{-2}; Pairwise Wilcoxon rank sum test, p=0.00028, Benjamini-Hochberg p-value adjustment method) or *Ginkgo*-based calibration datasets (median = 192 g m^{-2}; Pairwise Wilcoxon rank sum test, p=0.00038, Benjamini-Hochberg p-value adjustment method; see *Figure 4.3*). No significant difference was found between LMA estimates using the angiosperm and *Ginkgo*-based calibration datasets (Pairwise Wilcoxon rank sum test, p=0.39524, Benjamini-Hochberg p-value adjustment method). The gymnosperm calibration dataset was selected as the more appropriate model for *A. hibernica,* as the majority (87%) of species within the gymnosperm dataset have short petioles or subsessile leaves (Soh et al., 2017), which is similar to the leaf attachment of *A. hibernica*.

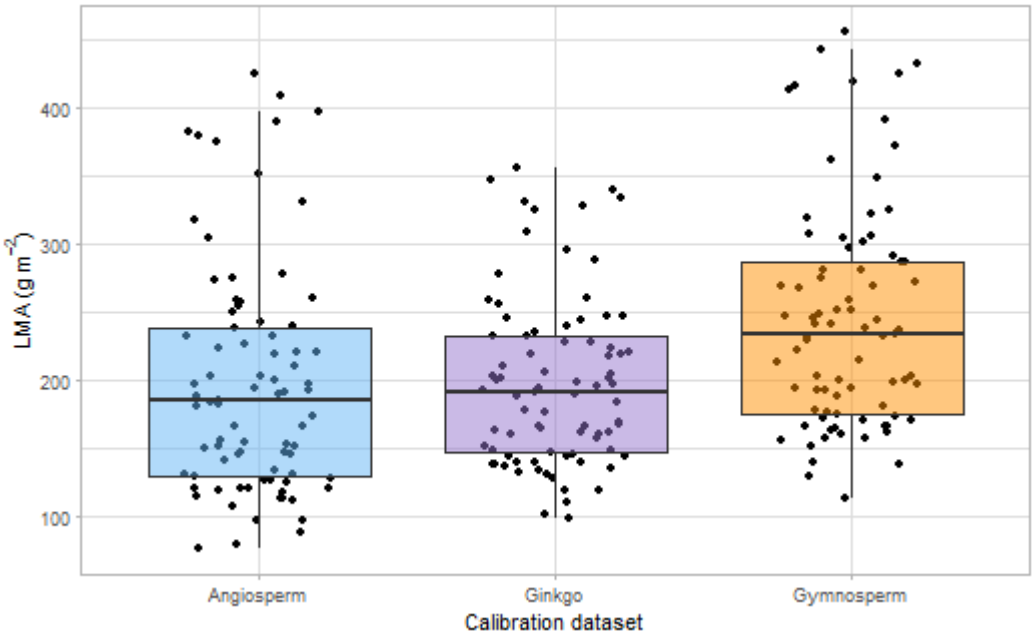

Figure 4.3. Differences in LMA estimates produced using different calibration datasets. LMA estimates produced using the gymnosperm calibration dataset of Royer et al. (2010) resulted in higher LMA estimates (orange, median = 233.1 g m^{-2}) than those produced using the woody angiosperm calibration dataset of Royer et al. (2007) (blue, median = 184.5 g m^{-2}; Pairwise Wilcoxon rank sum test, p=0.00028, Benjamini-Hochberg p-value adjustment method) and the *Ginkgo* calibration dataset of Haworth and Raschi (2014) (purple, median =191.5 g m^{-2}; Pairwise Wilcoxon rank sum test, p=0.00038, Benjamini-Hochberg p-value adjustment method). No significant difference was found between LMA estimates using the angiosperm and *Ginkgo*-based calibration datasets (Pairwise Wilcoxon rank sum test, p=0.39524, Benjamini-Hochberg p-value adjustment method).

The range of resultant $LMA_{gymnosperm}$ estimates for *Archaeopteris hibernica* fall within the range of values that would be expected for plants with a long leaf lifespan (i.e. with a leaf lifespan of longer than 12 months, LMA>129 g m^{-2}) (Royer et al., 2007, Wright et al., 2004). The median $LMA_{gymnosperm}$ of *A. hibernica* (233 g m^{-2}) lies above the median LMA values recorded for all modern plant functional groups within the TRY database (Kattge et al., 2020) (see *Figure 4.4*).

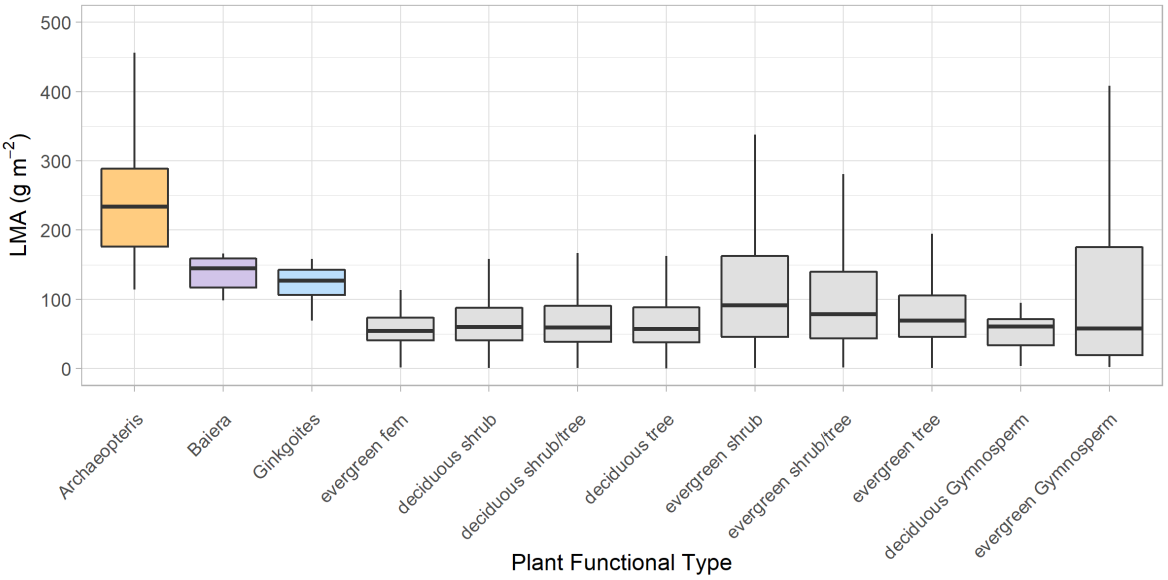

Figure 4.4. LMA estimates produced from fossil taxa using the petiole width-leaf area scaling relationship compared to LMA values reported in the TRY database. LMA estimates produced using the petiole width-leaf area scaling relationship of Royer et al. (2007) and Royer et al. (2010) indicate that *Archaeopteris hibernica* (orange) had high LMA values relative to the median LMA values of modern plant functional types. Petiole-based LMA estimates for *Baeira* (purple; median = 145.0 g m^{-2}, n=7) and *Ginkgoites* (blue; median = 126.8 g m^{-2}, n=25) reported by Soh et al. (2017) are included for comparison to other fossil-based estimates during periods of high CO_2. A summary table of LMA data obtained from the TRY database (Kattge et al., 2020) can be found in *Appendix 4.2*.

4.4 Discussion

4.4.1 Vein density and estimated operational stomatal conductance for *Archaeopteris hibernica*

Mean *A. hibernica* leaf vein density (3.0 ± 0.6 mm mm^{-2}) was found to be higher than that reported by Boyce et al. (2009) for *A. hibernica* (1.3 mm mm^{-2}, n=1), but comparable with values reported for *A. halliana* (3.1 - 3.7 mm mm^{-2}, n=2). The mean vein density reported in this study is considered a more accurate representation of venation architecture for *A. hibernica* due to the larger sample size (i.e., 143 leaves measured from 24 specimens). Both vein density-based methods (i.e., those of McElwain et al., (2015; *Equations 1* and *2*; median = 98 mmol m^{-2} s^{-1}) and Brodribb et al. (2007) and Brodribb and Field (2010; *Equations 3-6*; median = 115 mmol m^{-2} s^{-1}) resulted in differences in modelled operational stomatal conductance (g_{op}). However, there was some overlap between estimates produced using the two methods (see *Figure 4.2*). The similarity between the g_{op} estimates obtained from the leaf-hydraulic capacity model (Brodribb et al., 2007, Brodribb and Feild, 2010) and the g_{max}-D_v relationship established by McElwain et al. (2015) suggests that the likely operational stomatal conductance of *A. hibernica* was between 98-115 mmol m^{-2} s^{-1}. However, both vein density-based methods produced significantly higher g_{op} values than the anatomically based stomatal conductance model (*Equations 7* and *2*; median = 39 mmol m^{-2} s^{-1}). This may be a result of the limited sample size for the stomatal data (n = 3), species difference and atmospheric CO_2 change that occurred in the 20-million-year age difference between the Frasnian and Uppermost Famennian. Atmospheric CO_2 concentrations declined over the Devonian period (Berner, 2006, Dahl et al., 2022, Foster et al., 2017, Le Hir et al., 2011, Lenton et al., 2018, Simon et al., 2007, Witkowski et al., 2018), therefore it would be expected that plants would exhibit increasing stomatal conductance in response to decreases in atmospheric CO_2 concentration (Franks and Beerling, 2009, Wilson et al., 2020). However, there is a paucity of CO_2 proxy data for the Upper Devonian and the Devonian-Carboniferous transition (see Chapter 2), so understanding the significance of atmospheric CO_2 change in explaining these differences in modelled g_{op} is limited.

While there is relatively good agreement between both vein density-based g_{op} estimates, there are several limitations to both vein density-based methods that need to be

considered. The g_{max}-D_v relationship of McElwain et al. (2015) is described by a second order polynomial (*Equation 1*), and therefore has a global minimum value (i.e., it cannot model g_{max} below 433.8 mmol m^{-2} s^{-1} and therefore it also cannot model g_{op} below 86.8 mmol m^{-2} s^{-1}). The plants used to obtain the g_{max}-D_v dataset for the model were also grown under ambient environmental conditions for the stomatal conductance and maximum stomatal conductance measurements (McElwain et al., 2015), which would result in higher values for maximum stomatal conductance than for plants grown under high atmospheric CO_2 concentrations (Franks and Beerling, 2009). Therefore, it is possible that the g_{max}-D_v relationship established by McElwain et al. (2015) is less robust to model maximum stomatal conductance during periods of high atmospheric CO_2, as the expected stomatal parameter space would be different than that observed under ambient or low CO_2 concentrations (Franks and Beerling, 2009, Wilson et al., 2020). However, this remains a useful relationship for fossil plants during periods of lower atmospheric CO_2 concentrations such as the Carboniferous. It is also worth noting that the g_{max}-D_v relationship established by McElwain et al. (2015) was developed to estimate maximum photosynthetic rate (A_{max}) from D_v and g_{max}, rather than g_{max} from D_v. More CO_2 estimates are needed for the Upper Devonian (see Chapter 2) to better assess the utility of the g_{max}-D_v relationship for the Uppermost Devonian.

The leaf hydraulic capacity-based model requires parameterisation with a number of unknown environmental and anatomical measurements. The values used for $\Delta\Psi_{leaf}$ (the water potential gradient within the leaf) and v (leaf to air vapour pressure deficit) were based on typical values for modern temperate-tropical environments (Brodribb and Feild, 2010). This was considered appropriate for *A. hibernica*, which would have lived in a tropical-subtropical environment (Graham, 2009, Graham and Sevastopulo, 2021, Kendall, 2017). The value used for d_y (distance from the vein terminals to the epidermis) was limited to a single species (*Nageia nagi*) on the basis of its venation pattern. In addition, the relationship between D_v (vein density) and d_x (the longest horizontal distance from the vein terminals to the stomata) used is defined based on species with reticulate venation patterns (Brodribb and Feild, 2010), rather than dichotomous venation (seen in *Archaeopteris*). Further research into these measurements in species with dichotomous venation patterns (e.g., *Ginkgo biloba*) is recommended to investigate whether these

relationships are robust to use for fossil species with different venation patterns. Despite the limitations to both vein density-based methods, the similarities in modelled g_{op} produced by both methods suggests that they both provide a useful alternative framework to investigate leaf gas exchange capacity in the absence of stomatal preservation.

Stomatal conductance provides a strong functional constraint on photosynthetic capacity (Brodribb et al., 2007, Brodribb and Feild, 2010, McElwain et al., 2015, Sack et al., 2013). Modelled g_{op} for *Archaeopteris* spp. from vein density and stomatal morphology-based models lies within the bottom 21% of stomatal conductance values from the large dataset of extant angiosperms, gymnosperms and ferns of Maire et al. (2015), and the vein-density based estimates show similar to g_{op} values of extant gymnosperms such as *Agathis australis* (64 mmol m^{-2} s^{-1}) and *Ginkgo biloba* (114 mmol m^{-2} s^{-1}) (McElwain et al., 2015). Furthermore, estimated g_{max} values (see *Table 4.1*) are more similar to those modelled for sphenopsids, tree ferns and some cordaitaleans in the Carboniferous than taxa with a modelled high transpirational and photosynthetic capacity, such as the medullosans (Wilson et al., 2017, Wilson et al., 2020). Therefore, it seems likely that *Archaeopteris* had low photosynthetic rates relative to some Carboniferous and modern plant taxa (Maire et al., 2015, McElwain et al., 2015, Veromann-Jürgenson et al., 2020b, Wilson et al., 2017, Wilson et al., 2020). This is generally consistent with what would be expected from the modelled high LMA values for *Archaeopteris* in this study (Reich, 2014, Sack et al., 2013, Wright et al., 2004).

Under higher atmospheric CO_2 concentrations, the diffusional limitation of stomatal conductance on assimilation rate is reduced (McElwain et al., 2015, Yiotis and McElwain, 2019). Therefore the low vein density of *Archaeopteris* (3 mm mm^{-2}) may have been adequate to saturate leaf photosynthetic capacity at approximately 900 ppm CO_2 (Brodribb and Feild, 2010). Furthermore, mesophyll conductance is also known to play a significant role in the diffusional limitations to photosynthesis in ancient plant lineages (Flexas et al., 2012, Gago et al., 2019, Tosens et al., 2016, Veromann-Jürgenson et al., 2017, Veromann-Jürgenson et al., 2020a, Yiotis and McElwain, 2019). Simulations of photosynthetic physiology over geologic time indicate that the photosynthetic penalty incurred by low

stomatal and mesophyll conductance of more ancient plant lineages (i.e. monilophytes and gymnosperms) under ambient CO_2 concentrations would be greatly reduced during periods of elevated atmospheric CO_2 (Yiotis and McElwain, 2019). More specifically, gymnosperm taxa are modelled to have attained a higher photosynthetic rate than monilophytes under periods of high atmospheric CO_2, conferring a competitive advantage, and ecological dominance (Yiotis and McElwain, 2019). Considering the atmospheric CO_2 context, conifer-like wood and ecological dominance of *Archaeopteris* in Upper Devonian ecosystems it seems plausible that they had comparable photosynthetic physiology to gymnosperms. However, there is significant uncertainty regarding other potential limiting factors (e.g. biochemical) on photosynthetic rate in extinct plant groups, and the presence of plants capable of high productivity in the geologic past remains a matter of significant debate within palaeobotany (Boyce and DiMichele, 2016, Boyce et al., 2017, Boyce et al., 2023, Boyce and Zwieniecki, 2012, Boyce and Zwieniecki, 2019, Wilson et al., 2015, Wilson et al., 2017, Wilson et al., 2020).

4.4.2 *Archaeopteris hibernica* leaf mass per area estimates

The LMA values reconstructed for *Archaeopteris hibernica* were relatively high compared to modern plant functional groups reported in Poorter et al. (2009) and the TRY database (Kattge et al., 2020), and ranged from 114-456 g m^{-2}, with a median value of 233 g m^{-2}. High LMA leaves are strongly associated with leaf longevity, low nitrogen content, low photosynthetic rate and low rate of dark respiration (Díaz et al., 2016, Gomarasca et al., 2023, Wright et al., 2004). This suggests that *A. hibernica* had a slow rate of return on nutrient and dry mass investment in leaves (Wright et al., 2004) and may have had a slow-growing, stress-tolerant life strategy (Adler et al., 2014, Rüger et al., 2018). This interpretation may be further supported by the arborescent, woody habit of *Archaeopteris* (Beck, 1971, Decombeix and Meyer-Berthaud, 2013, Díaz et al., 2016, Maynard et al., 2022, Meyer-Berthaud et al., 1999, Meyer-Berthaud et al., 2000, Scheckler, 1978, Trivett, 1993), its occurrence in periodically dry riparian environments (Retallack and Huang, 2011, Stein et al., 2020) and its inferred hydraulic plasticity, which potentially allowed growth in a range of environmental conditions (Tanrattana et al., 2019). Furthermore, its relative abundance

in the fossil record may support the high LMA values, as higher LMA leaves likely have higher preservation potential than leaves with lower LMA (Bacon et al., 2016).

During the Late Famennian, stress tolerance is thought to have played a role in the differential biogeography of *A. halliana* and *A. macilenta, with A. halliana* persisting during periods of low water-table, due to stress-adapted morphological traits such as anisophylly and non-laminated sporophylls (Fairon-Demaret et al., 2001). However, comparatively little is known of the anatomy, palaeoenvironment or architecture of *A. hibernica* (Decombeix et al., 2023, Jarvis, 2000, Klavins, 1999), and the extrapolation of life history strategies from single leaf functional traits must be interpreted with caution (Matthaeus et al., 2023, McElwain et al., 2024, Rüger et al., 2018). The predictive power of individual leaf traits on demography is low, and individual leaf traits vary considerably with environmental conditions (Adler et al., 2014, Kelly et al., 2021, Poorter et al., 2009, Rüger et al., 2018). Similar life history strategies can also be achieved by species with different growth forms (Kelly et al., 2021, Salguero-Gómez et al., 2016).

The LMA values of *A. hibernica* from this study are similar to the LMA values reported by Poorter et al. (2009) for evergreen gymnosperms (median = 227 g m^{-2}; n=70). However, it is greater than median LMA value (76 g m^{-2}) and interquartile range (47-171 g m^{-2}) obtained for evergreen gymnosperms using the TRY database (n=279). Analysis of variance after ln-transformation of the TRY data (as per Poorter et al. (2009)) indicated that while there was a significant difference in LMA values between groups ($p<2.2e^{-16}$), a much smaller proportion of variation in the LMA data was explained by plant functional groups shown in *Figure 4.4* (R^2=0.02), than reported from the smaller dataset used by Poorter et al. (2009) (R^2=0.35). This suggests that LMA has weaker predictive power for plant functional groups than previously thought, although this interpretation may be limited by confounding environmental factors not screened for in the TRY data. Comparison with modern plant groups suggests that *A. hibernica* occupied a similar plant functional group to that of evergreen gymnosperms and suggests an evergreen habit (Royer et al., 2007, Wright et al., 2004). However, architectural analysis of *Callixylon* specimens have found that *Archaeopteris* possessed both long-lived ('type B') and deciduous, short-lived ('type A')

branches (Beck, 1971, Meyer-Berthaud et al., 1999, Meyer-Berthaud et al., 2000, Scheckler, 1978, Trivett, 1993). Long-lived organs are interpreted to have produced larger branches with greater complexity than the penultimate branches of *Archaeopteris,* and similar long-lived and short-lived branch types were interpreted from architectural analysis of both *Callixylon whiteanum* and *Callixylon erianum* (Meyer-Berthaud et al., 2000, Trivett, 1993). The short-lived type A organs are considered homologous to leaves, but are more likely to be radially symmetrical ultimate branches (Meyer-Berthaud et al., 2000). These branches are thought to have shed seasonally as units in response to periodic stress or seasonality, resulting in a thinned crown, and comprised a major photosynthetic component of the tree (Meyer-Berthaud et al., 2000, Scheckler, 1978, Trivett, 1993).

The evidence for differential lifespans of *Archaeopteris* organs complicates the LMA-based interpretation of leaf lifespan and leaf economics for *A. hibernica*. It is not known what branch type the branches from the Kiltorcan flora correspond to, and therefore whether the assemblage consists of long or short-lived branch types, or both. While there is strong evidence that branch shedding occurred in other *Archaeopteris* species*,* leaf abscission is not thought to have occurred prior to the shedding of ultimate branch systems (Beck, 1971). Furthermore there is no anatomical evidence that branch shedding was an active process, and was likely a passive mechanical process (Trivett, 1993). Some *Archaeopteris* specimens from the Kiltorcan flora display pronounced swelling at the branch base (see *Figure 4.5*), which is characteristic of the active abscission morphotype described by Looy (2013) for early Permian conifers. However, the branch base does not appear to have a smooth separation face, which is also an important characteristic of active abscission (cladoptosis) (Looy, 2013). Therefore, the branch morphotypes seen in the Kiltorcan flora are unlikely to be a result of cladoptosis and are more likely a result of a broad attachment to the trunk or branch. The presence or absence of active abscission morphotypes may be an area for potential future investigation in the Kiltorcan flora. Cladoptosis is not thought to have evolved until the late Pennsylvanian to early Permian, and cladoptosis of penultimate and/or ultimate branch systems is relatively rare in both modern and fossil plants (Looy, 2013).

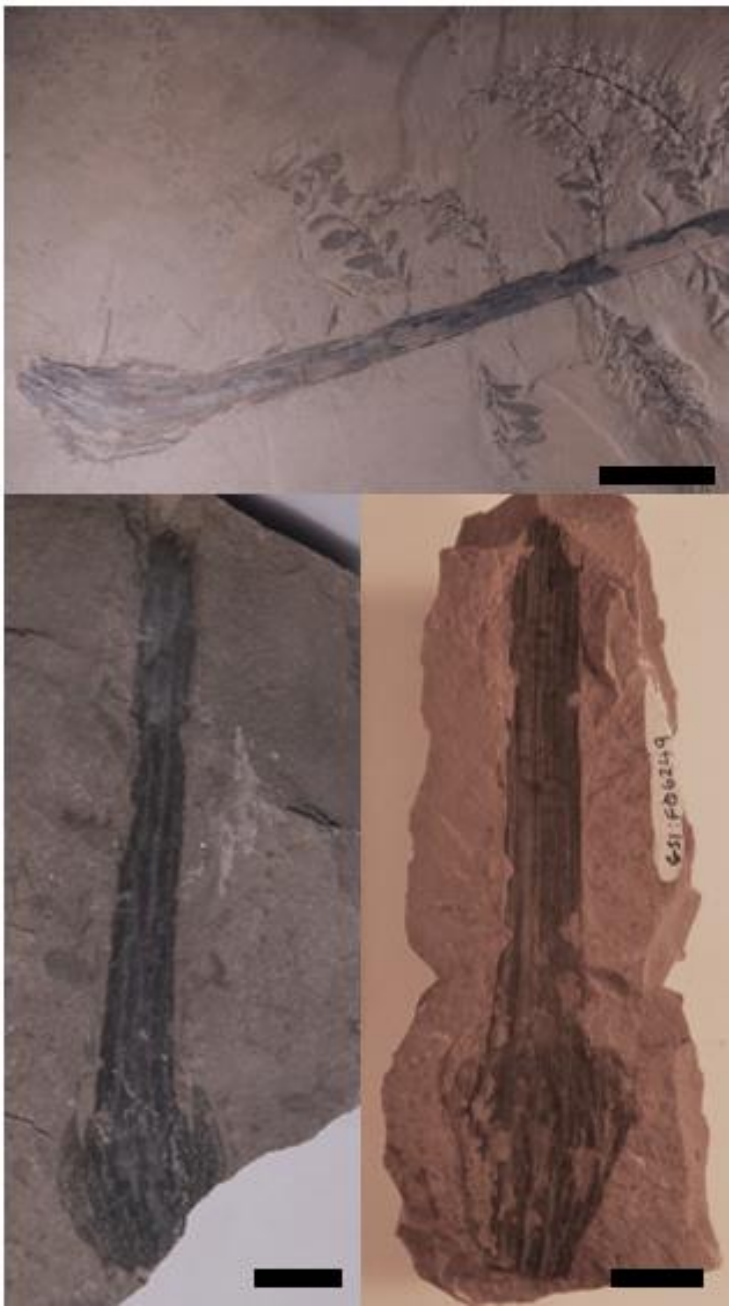

Figure 4.5. Penultimate branch and putative branch bases of *A. hibernica* from the Kiltorcan flora. Photographs of the penultimate branch (top, scale bar = 5 cm; specimen number F14836) and branch bases (bottom left, scale bar = 2 cm; specimen number F26241; bottom right, scale bar = 2 cm; specimen number F06249) were taken from the NMI collection by Bernsunkayeva (2018). Note the bulbous-shaped branch bases, but lack of a smooth abscission surface on the penultimate branch of *A. hibernica* (top). Putative branch bases of *A. hibernica* (bottom left and right) appear to show a smooth abscission surface, although their taxonomic identity is less certain.

While the leaf lifespan - LMA relationship in modern plants is significant, it is also noisy, showing shallower responses along environmental gradients (Poorter et al., 2009, Wright et al., 2004). Therefore, this may be an important factor in the lack of agreement between the morphological LMA-based evidence for leaf longevity and anatomical evidence of branch shedding (Beck, 1971, Meyer-Berthaud et al., 1999, Meyer-Berthaud et al., 2000, Scheckler, 1978, Trivett, 1993). Increased light intensity, low temperature, nutrient stress, water stress, and increased CO_2 concentration have all been found to increase LMA in modern taxa (Bacon et al., 2016, Poorter et al., 2009). It is possible that a number of these environmental factors played a role in the high LMA of *A. hibernica*. Furthermore, leaf lifespan may show an inverse correlation with LMA within a single species due to differences in these traits with regard to canopy placement (Poorter et al., 2009).

The upper Famennian was a time of significant environmental change, with evidence for glaciation occurring in the upper Famennian during the LN Biozone, and possibly through the LL-LN Biozones (Brezinski et al., 2008, Brezinski et al., 2010, Graham and Sevastopulo, 2021, Kaiser et al., 2016, Lakin et al., 2016, Montañez, 2022). This is thought to be coincident with the probable age of the Kiltorcan flora (see Chapter 3) (Jarvis, 1990). Evidence for marine incursions within the Kiltorcan Formation does not occur until the Tournaisian (Clayton et al., 1977). Climate may have been strongly seasonal at times during the Tournaisian/Visean in Ireland. The Kiltorcan flora is thought to be a parautochthonous assemblage, with a probable depositional environment of a bar-tail in a meandering river channel (Colthurst, 1978, Jarvis, 2000). Therefore *A. hibernica* from the Kiltorcan flora is thought to have grown in a near riverside environment. However, *A. hibernica* may have experienced significant seasonal variation in water availability, which could result in selection for drought tolerant traits such as high LMA. However, this interpretation is limited by the lack of more robust, detailed palaeoenvironmental evidence (Jarvis, 2000).

Palynological evidence that suggests increased UV-B radiation may have occurred at the Devonian-Carboniferous boundary, resulting in increased spore malformation (see Chapter 3) (Marshall et al., 2020), and therefore this may have also played a role in the high LMA

of *A. hibernica.* However, there is disagreement over the causes of spore malformation over this period, and other factors such as climatic fluctuation, drought (Prestianni et al., 2016) and supernova explosion (Fields et al., 2020) have all been suggested as alternative drivers of spore malformation. A significant environmental factor that likely influenced LMA of *A. hibernica* is the elevated atmospheric CO_2 concentrations during the Devonian period relative to today. High CO_2 concentrations have been found to result in increased LMA in the short term, due to the accumulation of non-structural carbohydrates, such as starch (Ainsworth and Long, 2005, Bacon et al., 2016, Poorter et al., 2009, Temme et al., 2013). Longer-term effects of CO_2 on LMA values are more indirect, and are due to resulting environmental stress (e.g. high temperature) due to increased CO_2 (Soh et al., 2017). Comparing the *Archaeopteris* LMA data with that obtained by Soh et al. (2017) for *Baeira* and *Ginkgoites* species at the Triassic-Jurassic boundary indicates that *Archaeopteris* did have high LMA values (see *Figure 4.4*) compared to other species that existed during periods of elevated CO_2, and therefore likely fell on the 'slow' side of the leaf economic spectrum.

While there is a lack of congruence between anatomical evidence and LMA-based leaf lifespan estimates, high LMA values seem more likely considering the environmental and atmospheric context. However, much of the environmental evidence is poorly constrained. In addition, the predictive power of the petiole width-leaf area scaling relationship for gymnosperms is relatively low (R^2 = 0.44) (Royer et al., 2010). Future research may be possible to better constrain LMA estimates for *Archaeopteris* species using the cuticle thickness proxy of Soh et al. (2017) on material such as that used by Osborne et al. (2004). It may also be possible to better constrain leaf lifespan using alternative proxies. There are a number of proxies that have been developed to interpret leaf lifespan and leaf economics in polar forests from fossil wood and fossilised leaf material (Diefendorf et al., 2011, Diefendorf et al., 2015, Falcon-Lang, 2000, Falcon-Lang, 2000, Falcon-Lang and Cantrill, 2001). As *Archaeopteris* had conifer-like wood, it may be possible to use growth ring markedness to investigate whether *Archaeopteris* had a deciduous or evergreen habit. However, the presence of growth rings in *Callixylon* fossils is variable (Trivett, 1993), and this method may not be more broadly applicable. It may also be possible to apply the leaf area-petiole proxy (Royer et al., 2007, Royer et al., 2010) to a broader range of

Archaeopteris specimens throughout the Devonian, and to other leafy taxa within the Kiltorcan flora (e.g. *Kiltorkensia devonica* and *Sphenopteris* spp.), which would provide a more robust framework to interpret the data obtained for *A. hibernica*.

4.5. Conclusions

Modern trait functional ecology provides a promising framework to better understand the function of extinct plant taxa. This study, although preliminary in nature, suggests that *A. hibernica* had a high leaf mass per unit area and a slow rate of return on nutrient and dry mass investment in leaves. Vein density and stomatal data suggests low rates of operational stomatal conductance, resulting in low photosynthetic rates at the leaf level. However, this remains speculative due to the difference in relative importance of diffusional limitations to photosynthetic rate under elevated CO_2 conditions. The LMA estimates for *A. hibernica* suggest that it had a slow-growing, stress-tolerant life strategy. This is generally consistent with the existing knowledge of its environmental and architectural context of other *Archaeopteris* species. However, interpretation of leaf lifespan based solely on LMA may not be appropriate and further research is recommended to constrain LMA and leaf lifespan more robustly for *A. hibernica* and for other leafy taxa within the Kiltorcan flora.

References

ADELEYE, M. A., HABERLE, S. G., GALLAGHER, R., ANDREW, S. C. & HERBERT, A. 2023. Changing plant functional diversity over the last 12,000 years provides perspectives for tracking future changes in vegetation communities. *Nature Ecology & Evolution,* **7,** 224-235.

ADLER, P. B., SALGUERO-GÓMEZ, R., COMPAGNONI, A., HSU, J. S., RAY-MUKHERJEE, J., MBEAU-ACHE, C. & FRANCO, M. 2014. Functional traits explain variation in plant life history strategies. *Proceedings of the National Academy of Sciences,* **111,** 740-745.

AINSWORTH, E. A. & LONG, S. P. 2005. What have we learned from 15 years of free-air CO_2 enrichment (FACE)? A meta-analytic review of the responses of photosynthesis, canopy properties and plant production to rising CO_2. *New Phytologist,* **165,** 351-372.

BACON, K. L., HAWORTH, M., CONROY, E. & MCELWAIN, J. C. 2016. Can atmospheric composition influence plant fossil preservation potential via changes in leaf mass per area? A new hypothesis based on simulated palaeoatmosphere experiments. *Palaeogeography, Palaeoclimatology, Palaeoecology,* **464,** 51-64.

BECK, C. B. 1962. Plants of the new albany shale. II. *Callixylon arnoldii* Sp. Nov. *Brittonia,* **14,** 322-327.

BECK, C. B. 1971. On the anatomy and morphology of lateral branch systems of *Archaeopteris*. *American Journal of Botany,* **58,** 758-784.

BERNER, R. A. 2006. GEOCARBSULF: a combined model for Phanerozoic atmospheric O_2 and CO_2. *Geochimica et Cosmochimica Acta,* **70,** 5653-5664.

BERNSUNKAYEVA, Y. 2018. *Estimation of aboveground carbon biomass in Archaeopteris using architecture modelling.* Unpublished Masters Thesis, University College Dublin.

BLONDER, B., ROYER, D. L., JOHNSON, K. R., MILLER, I. & ENQUIST, B. J. 2014. Plant Ecological Strategies Shift Across the Cretaceous–Paleogene Boundary. *PLoS Biology,* **12,** e1001949.

BOUDA, M., HUGGETT, B. A., PRATS, K. A., WASON, J. W., WILSON, J. P. & BRODERSEN, C. R. 2022. Hydraulic failure as a primary driver of xylem network evolution in early vascular plants. *Science,* **378,** 642-646.

BOYCE, C. K., BRODRIBB, T. J., FIELD, T. S. & ZWIENIECKI, M. A. 2009. Angiosperm leaf vein evolution was physiologically and environmentally transformative. *Proceedings of the Royal Society B,* **276,** 1771-1776.

BOYCE, C. K. & DIMICHELE, W. A. 2016. Arborescent lycopsid productivity and lifespan: constraining the possibilities. *Review of Palaeobotany and Palynology,* **227,** 97-110.

BOYCE, C. K., FAN, Y. & ZWIENIECKI, M. A. 2017. Did trees grow up to the light, up to the wind, or down to the water? How modern high productivity colors perception of early plant evolution. *New Phytologist,* **215,** 552-557.

BOYCE, C. K., IBARRA, D. E., NELSEN, M. P. & D'ANTONIO, M. P. 2023. Nitrogen-based symbioses, phosphorus availability, and accounting for a modern world more productive than the Paleozoic. *Geobiology,* **21,** 86-101.

BOYCE, C. K., LEE, J.-E., FEILD, T. S., BRODRIBB, T. J. & ZWIENIECKI, M. A. 2010. Angiosperms helped put the rain in the rainforests: the impact of plant physiological evolution on tropical biodiversity. *Annals of the Missouri Botanical Garden,* **97,** 527-540.

BOYCE, C. K. & ZWIENIECKI, M. A. 2012. Leaf fossil record suggests limited influence of atmospheric CO_2 on terrestrial productivity prior to angiosperm evolution. *Proceedings of the National Academy of Sciences,* **109,** 10403-10408.

BOYCE, C. K. & ZWIENIECKI, M. A. 2019. The prospects for constraining productivity through time with the whole-plant physiology of fossils. *New Phytologist,* **233,** 40-49.

BREZINSKI, D. K., CECIL, C. B. & SKEMA, V. W. 2010. Late Devonian glacigenic and associated facies from the central Appalachian Basin, eastern United States. *GSA Bulletin,* **122,** 265-281.

BREZINSKI, D. K., CECIL, C. B., SKEMA, V. W. & STAMM, R. 2008. Late Devonian glacial deposits from the eastern United States signal an end of the mid-Paleozoic warm period. *Palaeogeography, Palaeoclimatology, Palaeoecology,* **268,** 143-151.

BRODRIBB, T. J. & FEILD, T. S. 2010. Leaf hydraulic evolution led a surge in leaf photosynthetic capacity during early angiosperm diversification. *Ecology letters,* **13,** 175-183.

BRODRIBB, T. J., FEILD, T. S. & JORDAN, G. J. 2007. Leaf maximum photosynthetic rate and venation are linked by hydraulics. *Plant physiology,* **144,** 1890-1898.

BROWN, K. A., BUNTING, M. J., CARVALHO, F., DE BELLO, F., MANDER, L., MARCISZ, K., MOTTL, O., REITALU, T. & SVENNING, J. C. 2023. Trait-based approaches as ecological time machines: Developing tools for reconstructing long-term variation in ecosystems. *Functional Ecology***,** 1-18.

BUTRIM, M. J., ROYER, D. L., MILLER, I. M., DECHESNE, M., NEU-YAGLE, N., LYSON, T. R., JOHNSON, K. R. & BARCLAY, R. S. 2022. No consistent shift in leaf dry mass per area across the Cretaceous—Paleogene Boundary. *Frontiers in Plant Science,* **13,** 894690.

CARLUCCIO, L. M., HUEBER, F. M. & BANKS, H. P. 1966. *Archaeopteris macilenta*, anatomy and morphology of its frond. *American Journal of Botany,* **53,** 719-730.

CARVALHO, M. R., JARAMILLO, C., DE LA PARRA, F., CABALLERO-RODRÍGUEZ, D., HERRERA, F., WING, S., TURNER, B. L., D'APOLITO, C., ROMERO-BÁEZ, M. & NARVÁEZ, P. 2021. Extinction at the end-Cretaceous and the origin of modern neotropical rainforests. *Science,* **372,** 63-68.

CHALONER, W. G. 1968. The cone of *Cyclostigma kiltorkense* Haughton, from the Upper Devonian of Ireland. *Botanical Journal of the Linnean Society,* **61,** 25-36.

CLARK, J. W., HETHERINGTON, A. J., MORRIS, J. L., PRESSEL, S., DUCKETT, J. G., PUTTICK, M. N., SCHNEIDER, H., KENRICK, P., WELLMAN, C. H. & DONOGHUE, P. C. J. 2023. Evolution of phenotypic disparity in the plant kingdom. *Nature Plants*.

CLAYTON, G., COLTHURST, J., HIGGS, K., JONES, G. & KEEGAN, J. 1977. Tournaisian miospores and conodonts from County Kilkenny. *Geol. Surv. Ireland Bull,* **2,** 99-106.

COLTHURST, J. 1978. Old Red Sandstone rocks surrounding the Slievenamon inlier, counties Tipperary and Kilkenny. *Journal of Earth Sciences,* **1,** 77-103.

CURRANO, E. D. & JACOBS, B. F. 2021. Bug-bitten leaves from the early Miocene of Ethiopia elucidate the impacts of plant nutrient concentrations and climate on insect herbivore communities. *Global and Planetary Change,* **207,** 103655.

CURRANO, E. D., WILF, P., WING, S. L., LABANDEIRA, C. C., LOVELOCK, E. C. & ROYER, D. L. 2008. Sharply increased insect herbivory during the Paleocene–Eocene Thermal Maximum. *Proceedings of the National Academy of Sciences,* **105,** 1960-1964.

DAHL, T. W., HARDING, M. A., BRUGGER, J., FEULNER, G., NORRMAN, K., LOMAX, B. H. & JUNIUM, C. K. 2022. Low atmospheric CO_2 levels before the rise of forested ecosystems. *Nature Communications,* **13,** 7616.

DECOMBEIX, A.-L., HARPER, C. J., PRESTIANNI, C., DURIEUX, T., RAMEL, M. & KRINGS, M. 2023. Fossil evidence of tylosis formation in Late Devonian plants. *Nature Plants,* **9, 1-4**.

DECOMBEIX, A. L. & MEYER-BERTHAUD, B. 2013. A *Callixylon* (Archaeopteridales, Progymnospermopsida) trunk with preserved secondary phloem from the Late Devonian of Morocco. *American Journal of Botany,* **100,** 2219-2230.

DÍAZ, S., KATTGE, J., CORNELISSEN, J. H. C., WRIGHT, I. J., LAVOREL, S., DRAY, S., REU, B., KLEYER, M., WIRTH, C., PRENTICE, I. C., GARNIER, E., BÖNISCH, G., WESTOBY, M., POORTER, H., REICH, P. B., MOLES, A. T., DICKIE, J., GILLISON, A. N., ZANNE, A. E., CHAVE, J., WRIGHT, S. J., SHEREMET'EV, S. N., JACTEL, H., BARALOTO, C., CERABOLINI, B., PIERCE, S., SHIPLEY, B., KIRKUP, D., CASANOVES, F., JOSWIG, J. S., GÜNTHER, A., FALCZUK, V., RÜGER, N., MAHECHA, M. D. & GORNÉ, L. D. 2016. The global spectrum of plant form and function. *Nature,* **529,** 167-171.

DIEFENDORF, A. F., FREEMAN, K. H., WING, S. L. & GRAHAM, H. V. 2011. Production of n-alkyl lipids in living plants and implications for the geologic past. *Geochimica et Cosmochimica Acta,* **75,** 7472-7485.

DIEFENDORF, A. F., LESLIE, A. B. & WING, S. L. 2015. Leaf wax composition and carbon isotopes vary among major conifer groups. *Geochimica et Cosmochimica Acta,* **170,** 145-156.

FAIRON-DEMARET, M., LEPONCE, I. & STREEL, M. 2001. *Archaeopteris* from the Upper Famennian of Belgium: heterospory, nomenclature, and palaeobiogeography. *Review of Palaeobotany and Palynology,* **115,** 79-97.

FALCON-LANG, H. & CANTRILL, D. 2001. Leaf phenology of some mid-Cretaceous polar forests, Alexander Island, Antarctica. *Geological Magazine,* **138,** 39-52.

FALCON-LANG, H. J. 2000. The relationship between leaf longevity and growth ring markedness in modern conifer woods and its implications for palaeoclimatic studies. *Palaeogeography, Palaeoclimatology, Palaeoecology,* **160,** 317-328.

FALCON-LANG, H. J. 2000. A method to distinguish between woods produced by evergreen and deciduous coniferopsids on the basis of growth ring anatomy: a new palaeoecological tool. *Palaeontology,* **43,** 785-793.

FEILD, T. S., BRODRIBB, T. J., IGLESIAS, A., CHATELET, D. S., BARESCH, A., UPCHURCH JR, G. R., GOMEZ, B., MOHR, B. A., COIFFARD, C. & KVACEK, J. 2011. Fossil evidence for Cretaceous escalation in angiosperm leaf vein evolution. *Proceedings of the National Academy of Sciences,* **108,** 8363-8366.

FIELDS, B. D., MELOTT, A. L., ELLIS, J., ERTEL, A. F., FRY, B. J., LIEBERMAN, B. S., LIU, Z., MILLER, J. A. & THOMAS, B. C. 2020. Supernova triggers for end-Devonian extinctions. *Proceedings of the National Academy of Sciences,* **117,** 21008-21010.

FLEXAS, J., BARBOUR, M. M., BRENDEL, O., CABRERA, H. M., CARRIQUÍ, M., DÍAZ-ESPEJO, A., DOUTHE, C., DREYER, E., FERRIO, J. P., GAGO, J. & GALLÉ, A. 2012. Mesophyll diffusion conductance to CO_2: an unappreciated central player in photosynthesis. *Plant Science,* **193,** 70-84.

FLYNN, A. G. & PEPPE, D. J. 2019. Early Paleocene tropical forest from the Ojo Alamo Sandstone, San Juan Basin, New Mexico, USA. *Paleobiology,* **45,** 612-635.

FOSTER, G. L., ROYER, D. L. & LUNT, D. J. 2017. Future climate forcing potentially without precedent in the last 420 million years. *Nature communications,* **8,** 14845.

FRANKS, P. J. & BEERLING, D. J. 2009. Maximum leaf conductance driven by CO_2 effects on stomatal size and density over geologic time. *Proceedings of the National Academy of Sciences,* **106,** 10343-10347.

FRANKS, P. J., BUCKLEY, T. N., SHOPE, J. C. & MOTT, K. A. 2001. Guard cell volume and pressure measured concurrently by confocal microscopy and the cell pressure probe. *Plant physiology,* **125,** 1577-1584.

FRANKS, P. J. & FARQUHAR, G. D. 2007. The mechanical diversity of stomata and its significance in gas-exchange control. *Plant physiology,* **143,** 78-87.

FRANKS, P. J., ROYER, D. L., BEERLING, D. J., VAN DE WATER, P. K., CANTRILL, D. J., BARBOUR, M. M. & BERRY, J. A. 2014. New constraints on atmospheric CO_2 concentration for the Phanerozoic. *Geophysical Research Letters,* **41,** 4685-4694.

GAGO, J., CARRIQUÍ, M., NADAL, M., CLEMENTE-MORENO, M. J., COOPMAN, R. E., FERNIE, A. R. & FLEXAS, J. 2019. Photosynthesis optimized across land plant phylogeny. *Trends in Plant Science,* **24,** 947-958.

GOMARASCA, U., MIGLIAVACCA, M., KATTGE, J., NELSON, J. A., NIINEMETS, Ü., WIRTH, C., CESCATTI, A., BAHN, M., NAIR, R. & ACOSTA, A. T. 2023. Leaf-level coordination principles propagate to the ecosystem scale. *Nature Communications,* **14,** 3948.

GRAHAM, J. R. 2009. Devonian. *In:* HEPWORTH HOLLAND, C. & SANDERS, I. A. (eds.) *The Geology of Ireland.* Edinburgh, Scotland: Dunedin Academic Press Ltd.

GRAHAM, J. R. & SEVASTOPULO, G. D. 2021. The stratigraphy of latest Devonian and earliest Carboniferous rocks in Ireland. *Palaeobiodiversity and Palaeoenvironments,* **101,** 515-527.

HAWORTH, M. & RASCHI, A. 2014. An assessment of the use of epidermal micro-morphological features to estimate leaf economics of Late Triassic–Early Jurassic fossil Ginkgoales. *Review of Palaeobotany and Palynology,* **205,** 1-8.

JARVIS, D. 2000. Palaeoenvironment of the plant bearing horizons of the Devonian-Carboniferous Kiltorcan Formation, Kiltorcan Hill, Co. Kilkenny, Ireland. *Geological Society, London, Special Publications,* **180,** 333-341.

JARVIS, E. 1990. New palynological data on the age of the Kiltorcan Flora of Co. Kilkenny, Ireland. *Journal of Micropalaeontolgy,* **9,** 87-94.

KAISER, S. I., ARETZ, M. & BECKER, R. T. 2016. The global Hangenberg Crisis (Devonian–Carboniferous transition): review of a first-order mass extinction. *In:* BECKER, R. T., KONIGSHOF, P. & BRETT, C. E. (eds.) *Devonian Climate, Sea Level and Evolutionary Events.* London: Geological Society, London, Special Publications.

KATTGE, J., BÖNISCH, G., DÍAZ, S., LAVOREL, S., PRENTICE, I. C., LEADLEY, P., TAUTENHAHN, S., WERNER, G. D., AAKALA, T. & ABEDI, M. 2020. TRY plant trait database–enhanced coverage and open access. *Global change biology,* **26,** 119-188.

KELLY, R., HEALY, K., ANAND, M., BAUDRAZ, M. E., BAHN, M., CERABOLINI, B. E., CORNELISSEN, J. H., DWYER, J. M., JACKSON, A. L. & KATTGE, J. 2021. Climatic and evolutionary contexts are required to infer plant life history strategies from functional traits at a global scale. *Ecology Letters,* **24,** 970-983.

KENDALL, R. 2017. The old red sandstone of Britain and Ireland—a review. *Proceedings of the Geologists' Association,* **128,** 409-421.

KERP, H. & BOMFLEUR, B. 2011. Photography of plant fossils—new techniques, old tricks. *Review of Palaeobotany and Palynology,* **166,** 117-151.

KLAVINS, S. D. 1999. *Systematics and paleoecology of three Late Devonian floras of southern Ireland.* PhD, Southern Illinois University at Carbondale.

KUNZMANN, L., MORAWECK, K., MÜLLER, C., SCHRÖDER, I., WAPPLER, T., GREIN, M. & ROTH-NEBELSICK, A. 2019. A Paleogene leaf flora (Profen, Sachsen-Anhalt,

Germany) and its potentials for palaeoecological and palaeoclimate reconstructions. *Flora,* **254,** 71-87.

LAKIN, J., MARSHALL, J., TROTH, I. & HARDING, I. 2016. Greenhouse to icehouse: a biostratigraphic review of latest Devonian–Mississippian glaciations and their global effects. *In:* BECKER, R. T., KONIGSHOF, P. & BRETT, C. E. (eds.) *Devonian Climate, Sea Level and Evolutionary Events.* London: Geological Society, London, Special Publications.

LE HIR, G., DONNADIEU, Y., GODDÉRIS, Y., MEYER-BERTHAUD, B., RAMSTEIN, G. & BLAKEY, R. C. 2011. The climate change caused by the land plant invasion in the Devonian. *Earth and Planetary Science Letters,* **310,** 203-212.

LENTON, T. M., DAINES, S. J. & MILLS, B. J. 2018. COPSE reloaded: an improved model of biogeochemical cycling over Phanerozoic time. *Earth-Science Reviews,* 178**,** 1-28.

LOOY, C. V. 2013. Natural history of a plant trait: branch-system abscission in Paleozoic conifers and its environmental, autecological, and ecosystem implications in a fire-prone world. *Paleobiology,* **39,** 235-252.

LOWE, A. J., GREENWOOD, D. R., WEST, C. K., GALLOWAY, J. M., SUDERMANN, M. & REICHGELT, T. 2018. Plant community ecology and climate on an upland volcanic landscape during the Early Eocene Climatic Optimum: McAbee Fossil Beds, British Columbia, Canada. *Palaeogeography, Palaeoclimatology, Palaeoecology,* **511,** 433-448.

LYSON, T. R., MILLER, I., BERCOVICI, A., WEISSENBURGER, K., FUENTES, A., CLYDE, W., HAGADORN, J., BUTRIM, M., JOHNSON, K. & FLEMING, R. 2019. Exceptional continental record of biotic recovery after the Cretaceous–Paleogene mass extinction. *Science,* **366,** 977-983.

MAIRE, V., WRIGHT, I. J., PRENTICE, I. C., BATJES, N. H., BHASKAR, R., VAN BODEGOM, P. M., CORNWELL, W. K., ELLSWORTH, D., NIINEMETS, Ü. & ORDONEZ, A. 2015. Global effects of soil and climate on leaf photosynthetic traits and rates. *Global Ecology and Biogeography,* **24,** 706-717.

MARSHALL, J. E., LAKIN, J., TROTH, I. & WALLACE-JOHNSON, S. M. 2020. UV-B radiation was the Devonian-Carboniferous boundary terrestrial extinction kill mechanism. *Science Advances,* **6,** eaba0768.

MATTHAEUS, W. J., MACAREWICH, S. I., RICHEY, J., MONTAÑEZ, I. P., MCELWAIN, J. C., WHITE, J. D., WILSON, J. P. & POULSEN, C. J. 2023. A systems approach to understanding how plants transformed earth's environment in deep time. *Annual Review of Earth and Planetary Sciences,* **51,** 551-580.

MATTHAEUS, W. J., MONTAÑEZ, I. P., MCELWAIN, J. C., WILSON, J. P. & WHITE, J. D. 2022. Stems matter: xylem physiological limits are an accessible and critical improvement to models of plant gas exchange in deep time. *Frontiers in Ecology and Evolution,* **10,** 955066.

MAYNARD, D. S., BIALIC-MURPHY, L., Z., C.M., , AVERILL, C., VAN DEN HOOGEN, J., MA, H., MO, L., SMITH, G. R., ACOSTA, A. T. R., AUBIN, I., BERENGUER, E., BOONMAN, C. C. F., CATFORD, J. A., CERABOLINI, B. E. L., DIAS, A. S., GONZÁLEZ-MELO, A., HIETZ, P., LUSK, C. H., MORI, A. S., NIINEMETS, Ü., PILLAR, V. D., PINHO, B. X., ROSELL, J. A., SCHURR, F. M., SHEREMETEV, S. N., DA SILVA, A. C., SOSINSKI, Ê., VAN BODEGOM, P. M., WEIHER, E., BÖNISCH, G., KATTGE, J. & CROWTHER, T. W. 2022. Global relationships in tree functional traits. *Nature Communications,* **13,** 3185.

MCELWAIN, J. C., MATTHAEUS, W. J., BARBOSA, C., CHONDROGIANNIS, C., O'DEA, K., JACKSON, B., KNETGE, A., KWASNIEWSKA, K., NAIR, R., WHITE, J. D., WILSON, J. P., MONTAÑEZ, I. P., BUCKLEY, Y. M., BELCHER, C. M. & NOGUÉ, S. 2024. Functional traits of fossil plants. *New Phytologist,* **242(2),** 392-423.

MCELWAIN, J. C., YIOTIS, C. & LAWSON, T. 2015. Using modern plant trait relationships between observed and theoretical maximum stomatal conductance and vein density to examine patterns of plant macroevolution. *New Phytologist,* **209,** 94-103.

MEYER-BERTHAUD, B., DECOMBEIX, A.-L. & ERMACORA, X. 2013. Archaeopterid root anatomy and architecture: new information from permineralized specimens of Famennian age from Anti-Atlas (Morocco). *International Journal of Plant Sciences,* **174,** 364-381.

MEYER-BERTHAUD, B., SCHECKLER, S. E. & WENDT, J. 1999. *Archaeopteris* is the earliest known modern tree. *Nature,* **398,** 700-701.

MEYER-BERTHAUD, B., SCHECKLER, S. E. & BOUSQUET, J. L. 2000. The development of *Archaeopteris*: new evolutionary characters from the structural analysis of an Early Famennian trunk from southeast Morocco. *American Journal of Botany,* **87,** 456-468.

MONTAÑEZ, I. P. 2022. Current synthesis of the penultimate icehouse and its imprint on the Upper Devonian through Permian stratigraphic record. *In:* LUCAS, S. G., SCHNEIDER, J. W., WANG, X. & NIKOLAEVA, S. (eds.) *The Carboniferous Timescale.* London: Geological Society, London, Special Publications.

MORRIS, J. L., LEAKE, J. R., STEIN, W. E., BERRY, C. M., MARSHALL, J. E. A., WELLMAN, C. H., MILTON, J. A., HILLIER, S., MANNOLINI, F., QUIRK, J. & BEERLING, D. J. 2015. Investigating Devonian trees as geo-engineers of past climates: linking palaeosols to palaeobotany and experimental geobiology. *Palaeontology,* **58,** 787-801.

MURRAY, M., SOH, W. K., YIOTIS, C., BATKE, S., PARNELL, A. C., SPICER, R. A., LAWSON, T., CABALLERO, R., WRIGHT, I. J. & PURCELL, C. 2019. Convergence in maximum stomatal conductance of C3 woody angiosperms in natural ecosystems across bioclimatic zones. *Frontiers in Plant Science,* **10, 558**.

MURRAY, M., SOH, W. K., YIOTIS, C., SPICER, R. A., LAWSON, T. & MCELWAIN, J. C. 2020. Consistent relationship between field-measured stomatal conductance and theoretical maximum stomatal conductance in C3 woody angiosperms in four major biomes. *International Journal of Plant Sciences,* **181,** 142-154.

NOGUÉ, S., DE NASCIMENTO, L., GRAHAM, L., BROWN, L. A., GONZÁLEZ, L. A. G., CASTILLA-BELTRÁN, A., PEÑUELAS, J., FERNÁNDEZ-PALACIOS, J. M. & WILLIS, K. J. 2022. The spatiotemporal distribution of pollen traits related to dispersal and desiccation tolerance in Canarian laurel forest. *Journal of Vegetation Science,* **33,** e13147.

OSBORNE, C. P., BEERLING, D. J., LOMAX, B. H. & CHALONER, W. G. 2004. Biophysical constraints on the origin of leaves inferred from the fossil record. *Proceedings of the National Academy of Sciences,* **101,** 10360-10362.

PEPPE, D. J., LEMONS, C. R., ROYER, D. L., WING, S. L., WRIGHT, I. J., LUSK, C. H. & RHODEN, C. H. 2014. Biomechanical and leaf–climate relationships: a comparison of ferns and seed plants. *American Journal of Botany,* **101,** 338-347.

PEPPE, D. J., ROYER, D. L., CARIGLINO, B., OLIVER, S. Y., NEWMAN, S., LEIGHT, E., ENIKOLOPOV, G., FERNANDEZ-BURGOS, M., HERRERA, F., ADAMS, J. M., CORREA, E., CURRANO, E. D., ERICKSON, J. M., HINOJOSA, L. F., HOGANSON, J. W., IGLESIAS, A., JARAMILLO, C. A., JOHNSON, K. R., JORDAN, G. J., KRAFT, N. J. B., LOVELOCK, E. C., LUSK, C. H., NIINEMETS, Ü., PEÑUELAS, J., RAPSON, G., WING, S. L. & WRIGHT, I. J. 2011. Sensitivity of leaf size and shape to climate: global patterns and paleoclimatic applications. *New Phytologist,* **190,** 724-739.

POORTER, H., NIINEMETS, Ü., POORTER, L., WRIGHT, I. J. & VILLAR, R. 2009. Causes and consequences of variation in leaf mass per area (LMA): a meta-analysis. *New Phytologist,* **182,** 565-588.

PRESTIANNI, C., SAUTOIS, M. & DENAYER, J. 2016. Disrupted continental environments around the Devonian-Carboniferous Boundary: introduction of the tener event. *Geologica Belgica,* **19,** 135-145

REICH, P. B. 2014. The world-wide 'fast–slow'plant economics spectrum: a traits manifesto. *Journal of ecology,* **102,** 275-301.

RETALLACK, G. J. & HUANG, C. 2011. Ecology and evolution of Devonian trees in New York, USA. *Palaeogeography, Palaeoclimatology, Palaeoecology,* **299,** 110-128.

ROTH-NEBELSICK, A., GREIN, M., TRAISER, C., MORAWECK, K., KUNZMANN, L., KOVAR-EDER, J., KVAČEK, J., STILLER, S. & NEINHUIS, C. 2017. Functional leaf traits and leaf economics in the Paleogene - a case study for Central Europe. *Palaeogeography, Palaeoclimatology, Palaeoecology,* **472,** 1-14.

ROTH-NEBELSICK, A., UHL, D., MOSBRUGGER, V. & KERP, H. 2001. Evolution and function of leaf venation architecture: a review. *Annals of Botany,* **87,** 553-566.

ROYER, D. L., MILLER, I. M., PEPPE, D. J. & HICKEY, L. J. 2010. Leaf economic traits from fossils support a weedy habit for early angiosperms. *American Journal of Botany,* **97,** 438-445.

ROYER, D. L., SACK, L., WILF, P., LUSK, C. H., JORDAN, G. J., NIINEMETS, Ü., WRIGHT, I. J., WESTOBY, M., CARIGLINO, B., COLEY, P. D., CUTTER, A. D., JOHNSON, K. R., LABANDEIRA, C. C., MOLES, A. T., PALMER, M. B. & VALLADARES, F. 2007. Fossil leaf economics quantified: calibration, Eocene case study, and implications. *Paleobiology,* **33,** 574-589.

RÜGER, N., COMITA, L. S., CONDIT, R., PURVES, D., ROSENBAUM, B., VISSER, M. D., WRIGHT, S. J. & WIRTH, C. 2018. Beyond the fast–slow continuum: demographic dimensions structuring a tropical tree community. *Ecology letters,* **21,** 1075-1084.

SACK, L. & SCOFFONI, C. 2013. Leaf venation: structure, function, development, evolution, ecology and applications in the past, present and future. *New Phytologist,* **198,** 983-1000.

SACK, L., SCOFFONI, C., JOHN, G. P., POORTER, H., MASON, C. M., MENDEZ-ALONZO, R. & DONOVAN, L. A. 2013. How do leaf veins influence the worldwide leaf economic spectrum? Review and synthesis. *Journal of experimental botany,* **64,** 4053-4080.

SALGUERO-GÓMEZ, R., JONES, O. R., JONGEJANS, E., BLOMBERG, S. P., HODGSON, D. J., MBEAU-ACHE, C., ZUIDEMA, P. A., DE KROON, H. & BUCKLEY, Y. M. 2016. Fast–slow continuum and reproductive strategies structure plant life-history variation worldwide. *Proceedings of the National Academy of Sciences,* **113,** 230-235.

SCHECKLER, S. E. 1978. Ontogeny of progymnosperms. II. Shoots of upper Devonian Archaeopteridales. *Canadian Journal of Botany,* **56,** 3136-3170.

SCHWENDEMANN, A. B. 2018. Leaf venation density and calculated physiological characteristics of fossil leaves from the Permian of Gondwana. *In:* KRINGS, M., HARPER, C. J., CÚNEO, N. R. & ROTHWELL, G. W. (eds.) *Transformative Paleobotany.* Academic Press.

SCOFFONI, C., CHATELET, D. S., PASQUET-KOK, J., RAWLS, M., DONOGHUE, M. J., EDWARDS, E. J. & SACK, L. 2016. Hydraulic basis for the evolution of photosynthetic productivity. *Nature plants,* **2,** 1-8.

SIMON, L., GODDÉRIS, Y., BUGGISCH, W., STRAUSS, H. & JOACHIMSKI, M. M. 2007. Modeling the carbon and sulfur isotope compositions of marine sediments: climate evolution during the Devonian. *Chemical Geology,* **246,** 19-38.

SOH, W. K., WRIGHT, I. J., BACON, K. L., LENZ, T. I., STEINTHORSDOTTIR, M., PARNELL, A. C. & MCELWAIN, J. C. 2017. Palaeo leaf economics reveal a shift in ecosystem function associated with the end-Triassic mass extinction event. *Nature Plants,* **3,** 17104.

STEIN, W. E., BERRY, C. M., MORRIS, J. L., VANALLER HERNICK, L., MANNOLINI, F., VER STRAETEN, C., LANDING, E., MARSHALL, J. E. A., WELLMAN, C. H., BEERLING, D. J. & LEAKE, J. R. 2020. Mid-Devonian *Archaeopteris* roots signal revolutionary change in earliest fossil forests. *Current Biology,* **30**.

TANRATTANA, M., BARCZI, J. F., DECOMBEIX, A. L., MEYER-BERTHAUD, B. & WILSON, J. 2019. A new approach for modelling water transport in fossil plants. *IAWA Journal,* **40,** 466-487.

TEMME, A., CORNWELL, W., CORNELISSEN, J. & AERTS, R. 2013. Meta-analysis reveals profound responses of plant traits to glacial CO_2 levels. *Ecology and Evolution,* **3,** 4525-4535.

TOSENS, T., NISHIDA, K., GAGO, J., COOPMAN, R. E., CABRERA, H.M.,, CARRIQUÍ, M., LAANISTO, L., MORALES, L., NADAL, M., ROJAS, R. & TALTS, E. 2016. The photosynthetic capacity in 35 ferns and fern allies: mesophyll CO_2 diffusion as a key trait. *New Phytologist,* **209,** 1576-1590.

TRIVETT, M. L. 1993. An architectural analysis of *Archaeopteris,* a fossil tree with pseudomonopodial and opportunistic adventitious growth. *Botanical Journal of the Linnean Society,* **111,** 301-329.

UHL, D. & MOSBRUGGER, V. 1999. Leaf venation density as a climate and environmental proxy: a critical review and new data. *Palaeogeography Palaeoclimatology Palaeoecology,* **149,** 15-26.

VEROMANN-JÜRGENSON, L.-L., BRODRIBB, T. J., NIINEMETS, Ü. & TOSENS, T. 2020a. Pivotal role of mesophyll conductance in shaping photosynthetic performance across 67 structurally diverse gymnosperm species. *International Journal of Plant Sciences,* **181,** 116-128.

VEROMANN-JÜRGENSON, L. L., BRODRIBB, T. J., LAANISTO, L., BRUUN-LUND, S., NIINEMETS, Ü., NUNO, S. L., RINNAN, R., PUGLIELLI, G. & TOSENS, T. 2020b. Predictability of leaf morphological traits for paleoecological reconstruction: the case of leaf cuticle and leaf dry mass per area. *International Journal of Plant Sciences,* **181,** 129-141.

VEROMANN-JÜRGENSON, L. L., TOSENS, T., LAANISTO, L. & NIINEMETS, Ü. 2017. Extremely thick cell walls and low mesophyll conductance: welcome to the world of ancient living! *Journal of Experimental Botany,* **68,** 1639-1653.

VIOLLE, C., NAVAS, M.-L., VILE, D., KAZAKOU, E., FORTUNEL, C., HUMMEL, I. & GARNIER, E. 2007. Let the concept of trait be functional! *Oikos,* **166,** 882-892.

WAN, Z., ALGEO, T. J., GENSEL, P. G., SCHECKLER, S. E., STEIN, W. E., CRESSLER III, W. L., BERRY, C. M., XU, H., ROWE, H. D. & SAUER, P. E. 2019. Environmental influences on the stable carbon isotopic composition of Devonian and Early Carboniferous land plants. *Palaeogeography, Palaeoclimatology, Palaeoecology,* **531,** 109100.

WAPPLER, T., LABANDEIRA, C. C., RUST, J., FRANKENHÄUSER, H. & WILDE, V. 2012. Testing for the effects and consequences of mid Paleogene climate change on insect herbivory. *PloS one,* **7,** e40744.

WILSON, J. P., MONTAÑEZ, I. P., WHITE, J. D., DIMICHELE, W. A., MCELWAIN, J. C., POULSEN, C. J. & HREN, M. T. 2017. Dynamic Carboniferous tropical forests: new views of plant function and potential for physiological forcing of climate. *New Phytologist,* **215,** 1333-1353.

WILSON, J. P., WHITE, J. D., DIMICHELE, W. A., HREN, M. T., POULSEN, C. J., MCELWAIN, J. C. & MONTAÑEZ, I. P. 2015. Reconstructing extinct plant water use for understanding vegetation–climate feedbacks: methods, synthesis, and a case study using the Paleozoic-era medullosan seed ferns. *The Paleontological Society Papers,* **21,** 167-196.

WILSON, J. P., WHITE, J. D., MONTANEZ, I. P., DIMICHELE, W. A., MCELWAIN, J. C., POULSEN, C. J. & HREN, M. T. 2020. Carboniferous plant physiology breaks the mold. *New Phytologist,* **227,** 667-679.

WITKOWSKI, C. R., WEIJERS, J. W., BLAIS, B., SCHOUTEN, S. & SINNINGHE DAMSTÉ, J. S. 2018. Molecular fossils from phytoplankton reveal secular pCO_2 trend over the Phanerozoic. *Science advances,* **4,** eaat4556.

WOLFE, J. A. 1993. *A method of obtaining climatic parameters from leaf assemblages*, US Government Printing Office.

WRIGHT, I. J., REICH, P. B., WESTOBY, M., ACKERLY, D. D., BARUCH, Z., BONGERS, F., CAVENDER-BARES, J., CHAPIN, T., CORNELISSEN, J. H. C., DIEMER, M., FLEXAS, J., GARNIER, E., GROOM, P. K., GULIAS, J., HIKOSAKA, K., LAMONT, B. B., LEE, T., LEE, W., LUSK, C., MIDGLEY, J. J., NAVAS, M.-L., NIINEMETS, Ü., OLEKSYN, J., OSADA, N., POORTER, H., POOT, P., PRIOR, L., PYANKOV, V. I., ROUMET, C., THOMAS, S. C., TJOELKER, M. G., VENEKLAAS, E. J. & VILLAR, R. 2004. The worldwide leaf economic spectrum. *Nature,* **428,** 821-827.

YIOTIS, C. & MCELWAIN, J. C. 2019. A novel hypothesis for the role of photosynthetic physiology in shaping macroevolutionary patterns. *Plant physiology,* **181,** 1148-1162.

5. Discussion

The main aim of this thesis was to investigate atmospheric CO_2 change and plant functional ecology during the Devonian period (419.2-358.9 Ma) - a critical period in plant evolution - using CO_2-proxy and functional trait analysis of Emsian (407.6-393.3 Ma) and Famennian (372.2-358.9 Ma) leaf and stem fossils from classic localities in North America and Ireland. First, stomatal and carbon isotope data from *Sawdonia* compression fossils from the Battery Point Formation, Quebec and the Campbellton Formation, New Brunswick were used to reconstruct atmospheric CO_2 concentrations during the Emsian (407.6-393.3 Ma) using the gas-exchange model of Franks et al. (2014) (Chapter 2). Current understanding of Devonian palaeo-atmospheric CO_2 levels using the same model (Dahl et al., 2022) were re-evaluated using a sensitivity analysis of measured stomatal parameters from the *Sawdonia*-based estimates. Second, the diversity of sterile leaf morphology of *Archaeopteris hibernica* from the Kiltorcan flora of the Upper Famennian was investigated using the morphometric method of Moreno-Sánchez (2004). This was then evaluated in the context of existing literature to compare the leaf shape of *A. hibernica* with other *Archaeopteris* species and consider possible factors influencing both inter- and intraspecific variation in sterile leaf morphology (Chapter 3). Finally, a functional leaf trait analysis was conducted on *A. hibernica* from the Kiltorcan flora (i.e., leaf mass per area and vein density) to elucidate the physiological and ecological functioning of the first 'modern' trees (Chapter 4). Here, I will summarise the main findings of this thesis (see *Figure 5.1*), highlight areas of connection between the primary themes and chapters and point out future research opportunities and explore the limitations of this study.

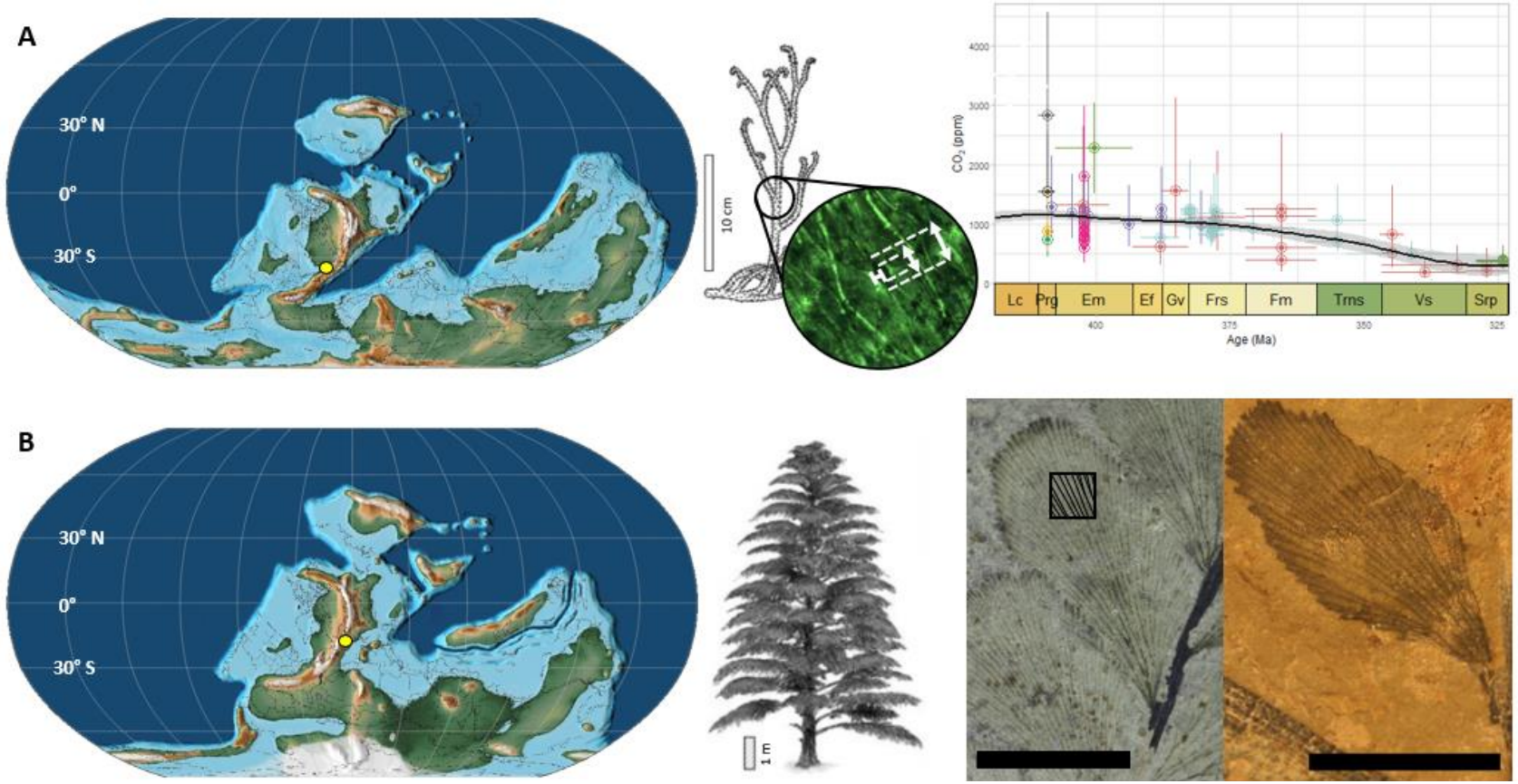

Figure 5.1. Graphical summary. The main aims of this thesis were (A) to reconstruct atmospheric CO_2 concentrations using stomatal and carbon isotope data from Emsian-aged *Sawdonia* fossils from the Battery Point Formation, Quebec and the Campbellton Formation, New Brunswick, (shown as a yellow circle, map A) in the gas-exchange model of Franks et al. (2014) (Chapter 2). (B) Extensive natural history collections of *Archaeopteris hibernica* leaf fossils from the Famenian aged Kiltorcan formation (shown as a yellow circle, map B) were studied to investigate inter- and intraspecific variation in sterile leaf morphology (Chapter 3) and to investigate leaf functional traits (i.e., leaf mass per area and vein density) to elucidate the physiological and ecological functioning of the first 'modern' trees (Chapter 4). Maps were created using GPlates (Müller et al., 2018), and fossil reconstructions are from Wan et al. (2019).

5.1. Summary and synthesis

Chapter 2 applied a mechanistic gas exchange model (Franks et al., 2014) to reconstruct atmospheric CO_2 during the Emsian stage of the Devonian. Atmospheric CO_2 was found to be approximately 898 ppm (+ 616/- 405 ppm). This is higher than the estimates of Dahl et al. (2022) obtained using the same model, but lower than other existing proxies for the same stage of the Devonian (Driese et al., 2000, Foster et al., 2017, McElwain, 1998). A major finding from the sensitivity analysis in Chapter 2 was that stomatal dimensions (i.e., pore length and depth) are critical parameters in this model and are currently the greatest source of error in Devonian CO_2 reconstructions using this proxy. Therefore, gas exchange models should be parameterized with careful observation and direct measurement of the stomatal complex to achieve the most robust palaeo-CO_2 estimates. Preservation quality and stomatal encryption can preclude the use of direct measurements of stomatal geometry and morphology, however, existing gas-exchange based CO_2 estimates should be updated as new data on stomatal dimensions emerges (e.g. Wilson et al. (2020) and references therein). Published stomatal data measured from Devonian plant fossils (see data compilation of Franks and Beerling (2009)) indicate that stomatal density values (i.e. 1-42 mm^{-2}) were restricted to the lowest range of the known parameter space for the entire Phanerozoic, whereas stomatal size values for these taxa (i.e. guard cell length multiplied by total width of the closed guard cell pair; 900-20,700 μm^2) encompasses almost the full range of values observed in extant plants (Franks and Beerling, 2009, Lomax et al., 2014). Gas exchange-based CO_2 reconstructions are more sensitive to the effects of stomatal size when stomatal density is low and during periods of high atmospheric CO_2 (e.g. Franks and Beerling (2009)), highlighting the need to better constrain pore length and depth parameterisation for the Devonian, and for other periods with a similar stomatal size and density parameter space.

Revision of stomatal size parameterisation used by Dahl et al. (2022) presented in Chapter 2 results in an atmospheric CO_2 reconstruction for the Devonian which no longer supports their conclusion that atmospheric CO_2 was low prior to the rise of forested ecosystems. However, this study supports recent findings (Dahl et al., 2022, Witkowski et al., 2018) indicating that decreases in atmospheric CO_2 concentration over this period were more

gradual than previously thought. The impact of deep-rooting vascular plants on atmospheric CO_2 concentrations may have been relatively limited until the evolution of deep rooting in combination with seeds which allowed for the spread of vascular plants across the broader landscape (Boyce and Lee, 2017, Boyce et al., 2023, D'Antonio et al., 2023). However, CO_2 proxy data for the Devonian and early Carboniferous are still relatively sparse compared to more intensively studied periods (Foster et al., 2017, Wilson et al., 2020), making more detailed understanding of the link between plant and atmosphere evolution more difficult to elucidate at this important time in Earth history. Furthermore, a better understanding of the ecophysiology, environmental constraints and spatial distribution of Famennian and Tournaisian floras is also needed (Decombeix et al., 2011, Pawlik et al., 2020). For example, the published guard cell width data used in the revision to the existing CO_2 estimates of Dahl et al. (2022) presented in Chapter 2 is not reported over a temporal range, and therefore possible changes in stomatal pore depth and length are unknown. Therefore reinvestigation of all published Devonian cuticle material (e.g. Li et al. (2000), Rayner (1984) and Stubblefield and Banks (1978)) are now needed to obtain robust estimates of variation in stomatal pore length and width over the Devonian period to minimize the substantial error in palaeo-atmospheric CO_2 estimates that are generated by imprecise stomatal pore length and depth measurements and to better resolve the tempo of atmospheric CO_2 evolution in the Devonian.

The appearance of novel plant evolutionary innovations seen in the Devonian fossil record indicate a drastic change in macroevolutionary patterns of plant functional diversity from the earliest assemblages of small (often leafless) plants, to more complex forested ecosystems (Capel et al., 2022, Gensel and Edwards, 2001, Pawlik et al., 2020, Stein et al., 2007). A plant functional trait approach was applied to fossil leaves in this thesis to try to understand the ecophysiological function of the first 'modern' trees. Chapter 4's maximum stomatal conductance estimates for *Archaeopteris* species appear to support the gradual decline of CO_2 over the Devonian period discussed above. It would be expected that plants would exhibit increasing stomatal conductance in response to decreases in atmospheric CO_2 concentration (Franks and Beerling, 2009, Wilson et al., 2020). Maximum stomatal conductance was found to be greater in *Archaeopteris hibernica* from the Uppermost Famennian using vein density-based methods (Chapter 4 (Brodribb et al., 2007, Brodribb

and Feild, 2010, McElwain et al., 2015)) than that modelled for Frasnian-aged *Archaeopteris* spp. using stomatal density and dimension data (Chapter 4) (see *Figure 5.2*). However, this difference could be a result of the limitations of the vein-density based estimates in modelling stomatal conductance during periods of high CO_2 (see Chapter 4). Comparing stomatal conductance estimates using the same anatomy-based biophysical stomatal conductance model (Franks and Farquhar, 2007, Franks et al., 2014), indicates that the early axial plants of the Devonian (i.e., *Sawdonia* and the Drepanophycales, see Chapter 2) had a theoretical maximum stomatal conductance that was 2-3 times lower than that of Frasnian-aged *Archaeopteris* (Chapter 4) (see *Figure 5.2, Table 5.1*), which seems to be consistent with the proposed gradual decline of CO_2 over the Devonian period. However, uncertainty in stomatal behaviour and therefore an appropriate correction factor for carbon isotope data (Porter et al., 2017) precludes *Archaeopteris* from being used for CO_2 reconstruction using the gas exchange model as per Chapter 2.

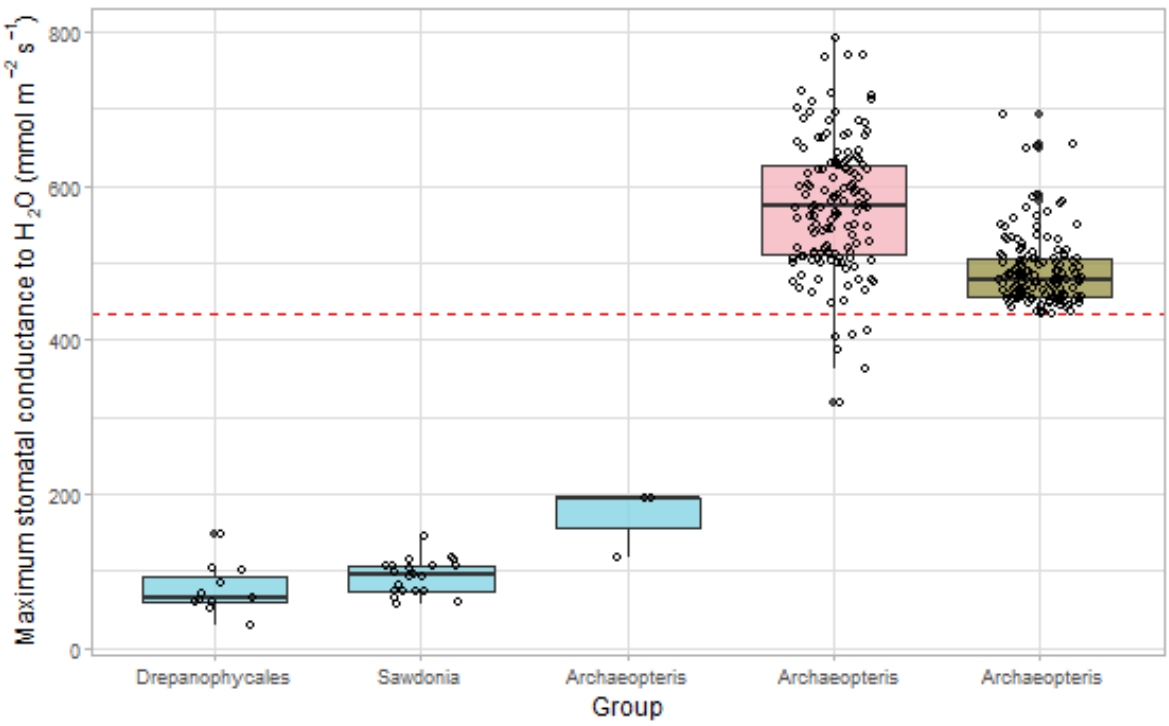

Figure 5.2. Differences in modelled maximum stomatal conductance to water for different Devonian taxa. Maximum stomatal conductance estimates for *Archaeopteris* spp. produced using all three methods (described in Chapter 4) were significantly higher than those obtained using stomatal data from Drepanophycales and *Sawdonia* spp. (Chapter 2; Pairwise Wilcoxon rank sum test, $p<0.05$ for all pairings, Benjamini-Hochberg p-value adjustment method). Blue boxes indicate stomatal conductance modelled from anatomical stomatal measurements, pink indicates the model of Brodribb et al. (2007) and Brodribb and Feild (2010), and brown indicates the model of McElwain et al. (2015). The dotted red line corresponds to the minimum possible value that can be produced using vein density - stomatal conductance relationship described in McElwain et al. (2015). Median estimates for maximum stomatal conductance are 65.9 mmol m^{-2} s^{-1} (Drepanophycales), 95.4 mmol m^{-2} s^{-1} (*Sawdonia* spp.), 193.6 mmol m^{-2} s^{-1} (*Archaeopteris* spp.; stomatal data), 574.7 mmol m^{-2} s^{-1} (*A. hibernica*; Brodribb et al. (2007) and Brodribb and Feild (2010)) and 477.8 mmol m^{-2} s^{-1} (*A. hibernica*; McElwain et al. (2015)).

Table 5.1. Summary of estimated maximum stomatal conductance (g_{max}) for different Devonian taxa. All estimates are expressed in units of mmol m^{-2} s^{-1}. g_{max} estimates for *Sawdonia* are based on stomatal measurements presented in Chapter 2 and estimates for the Drepanophycales are based on stomatal density and dimension data from Edwards et al. (1998) and Hueber (1983) (used in Chapter 2) and Cheng-Sen and Edwards (1995) and Guo and Wang (2016). All estimates for *Archaeopteris* are presented in Chapter 4.

Taxon (n)	Mean (± S.D.)	Median	Q1	Q3	Minimum	Maximum
Drepanophycales (11)	76.2 (± 32.0)	65.9	60.5	93.0	30.1	147.9
Sawdonia spp. (21)	93.0 (± 22.3)	95.4	73.2	106.7	56.6	145.0
Archaeopteris spp. (stomatal data) (3)	168.0 (± 44.2)	193.6	155.3	193.6	117.0	193.6
Archaeopteris hibernica (Brodribb *et al.* model) (143)	574.4 (± 83.9)	574.7	511.2	627.2	317.0	790.8
Archaeopteris hibernica (McElwain *et al.* model) (143)	489.1 (± 45.7)	477.8	455.5	505.4	434.0	691.3

The morphometric methods of Moreno-Sánchez (2004) showed that sterile leaf morphology of *A. hibernica* was different to that of *A. halliana, A. macilenta* and *A. fissilis* in Chapter 3. However, there was a degree of overlap in leaf morphological variation between *A. hibernica* and *A. halliana.* Furthermore, there is a lack of agreement in the literature about the importance of leaf characteristics, such as leaf attachment, in delineating separate *Archaeopteris* species (Arnold, 1939, Kräusel and Weyland, 1941, Stockmans, 1948), indicating the need for detailed taxonomic revision of *Archaeopteris.*

Archaeopteris hibernica was found to have larger, less round leaves than *A. halliana*, and a variable, sometimes crenulate margin. This variation in leaf morphology may be a result of difference in hydraulic supply, or light environment, or may indicate a difference in genome size. Future research could investigate this hypothesis through guard cell size (Beaulieu et al., 2008, Lomax et al., 2009, Lomax et al., 2014, McElwain and Steinthorsdottir, 2017) and spore size (Henry et al., 2014, Knight et al., 2010, Kürschner et al., 2013) measurements. Environmental factors, such as water availability and light environment, should also be investigated through the use of canopy placement proxies (Boyce, 2009) and sedimentological and palynological data (Fairon-Demaret et al., 2001). However, the rarity of sufficient preservation to carry out the suite of measurements needed presents a significant limitation to investigate this further.

Application of a plant functional trait approach to the fossil plant record has high potential to inform the functioning of past ecosystems (see for example Schwendemann (2018), Tanrattana et al. (2019), Wilson et al. (2020) and references therein). However, plant functional traits are rarely studied for Palaeozoic floras. Estimation of leaf functional traits from *A. hibernica* compression fossils in Chapter 4 indicates that *Archaeopteris* had a high leaf mass per unit area and a slow rate of return on investment in leaves. Vein density and stomatal data suggest low maximum stomatal conductance, and therefore low photosynthetic rates. This trait combination is consistent with what would be expected based on the relationships within the leaf economic spectrum (Wright et al., 2004). However, stomatal and mesophyll conductance are less important to photosynthetic capacity under elevated atmospheric CO_2 conditions (the details of which also require more research) (McElwain et al., 2015, Yiotis and McElwain, 2019), complicating leaf economic inferences. Future research on photosynthetic physiology of non-angiosperms and spore bearing plants under a range of CO_2 concentrations is needed to better understand the effects of atmospheric change on palaeo-plant function.

High LMA reconstructed for *A. hibernica* suggests a long leaf lifespan, and a slow-growing, stress tolerant growth strategy. Environmental and atmospheric context previously inferred for *A. hibernica*, as well as plant size, appear to support the same life strategy.

Modelling of wood hydraulic properties of *Archaeopteris* based on anatomical data has found that *Archaeopteris* may have had a broader environmental tolerance than previously thought due to hydraulic plasticity (Tanrattana et al., 2019). Furthermore, evidence of tylosis formation in *Callixylon* indicates that *Archaeopteris* was capable of protecting its vascular system from biotic or abiotic stress (Decombeix et al., 2023). By contrast, the interpretation of *Archaeopteris* leaf lifespan is complicated somewhat by anatomical evidence for branch shedding, and by extension, a probable short leaf lifespan on short-lived branch types (Beck, 1971, Meyer-Berthaud et al., 1999, Meyer-Berthaud et al., 2000, Scheckler, 1978, Trivett, 1993). However, a number of modern taxa within the Araucariaceae have both a high LMA and experience branch shedding (Looy, 2013, Soh et al., 2017), therefore these traits are not necessarily mutually exclusive. Future work on *Archaeopteris* cuticle material to independently investigate LMA is recommended. This may help to elucidate both leaf nutrient investment strategy and leaf lifespan for the earliest modern trees and may prove useful for providing a potential phenological dimension to future modelling of Devonian ecosystems.

5.2 Limitations

Preservation of fossil material precluded the inclusion of more primary stomatal and stable carbon isotopic data over a broader temporal range needed to increase the temporal resolution of atmospheric CO_2 concentrations through the Devonian (Chapter 2). While there are some examples of exceptional fossil preservation during the Devonian period, more generally speaking, fossil preservation of material that can be used for gas-exchange based CO_2 reconstruction is rare. Future efforts should focus on the investigation of existing cuticle material to refine changing stomatal dimension data over time and the application of a multi-proxy approach for the Upper Devonian and Lower Carboniferous, where plant-based proxy CO_2 estimates are sparse (e.g., there are five existing studies that use stomatal-based CO_2 proxies for the Devonian and Mississippian (419.2- 323.2 Ma; Dahl et al., (2022), Foster et al. (2017) and references therein) compared to 14 stomatal-based CO_2 proxy studies for the Jurassic period (201.4-145 Ma; Foster et al. (2017) and references therein, Sun et al. (2018), Zhou et al. (2020)).

Archaeopteris leaf material from Kiltorcan lacks organic preservation (Chaloner, 1968), therefore applying the cuticle-based LMA estimates of Soh et al. (2017) to this material was not possible for this study. However, existing material in museum collections (e.g. Carluccio et al. (1966) and Osborne et al. (2004)) may provide an opportunity to investigate this further. Future comparison to other leafy taxa within the Kiltorcan flora would also provide a within-ecosystem or -deposit context.

The leaf hydraulic model of Brodribb et al. (2007) and Brodribb and Feild (2010) provides a useful method to estimate the physiological characteristics of fossil plants from leaf vein density (Schwendemann, 2018). However, the model used is based on the relationship between vein density and the longest horizontal distance from the vein terminals to the stomata for leaves with reticulate venation, which is highly conserved in angiosperms (Brodribb and Feild, 2010). *Archaeopteris* lacks this venation architecture, introducing uncertainty into modelled stomatal conductance. Furthermore, the distance from the vein terminals to the epidermis of *Archaeopteris* is unknown, therefore this was estimated based on measurements from living plants (see Chapter 4). The vein density- theoretical maximum stomatal conductance (g_{max}) relationship established by McElwain et al. (2015) also has some limitations, as the plants used to obtain the dataset for the model were grown under ambient environmental conditions, therefore it is possible that this model is less robust to model maximum stomatal conductance during periods of high atmospheric CO_2 (see Chapter 4). Furthermore, the model has a global minimum, which lies above that of modelled theoretical stomatal conductance values of some Devonian plants (see *Figure 5.2*). Despite these uncertainties, modelled stomatal conductance using both vein density-based methods were relatively similar to one another, supporting their application in this study.

5.3 Conclusion

The Devonian period was a time of atmospheric change and evolutionary innovation for land plants. This study has demonstrated that atmospheric CO_2 was high (898 ppm +616/-405) prior to the appearance of the first forest ecosystems in the fossil record. Sensitivity analysis and subsequent re-evaluation of existing gas-exchange-based CO_2 estimates have demonstrated the importance of stomatal dimension parameters in these CO_2 estimates during a time when stomatal density was universally low relative to subsequent periods in geologic time. Reinvestigation of fossilised leaves of the first 'modern' trees presented here has indicated a possible leaf growth pattern of increasing roundness with greater leaf area. Sterile leaf morphology may be insufficient to separate out *Archaeopteris* species, highlighting the need for future taxonomic work on the genus. The use of a leaf functional trait framework in the same fossil collection has indicated that *Archaeopteris hibernica* had a high leaf mass investment per unit area and a probable stress-tolerant ecological strategy. This interpretation is partly supported by modelled hydraulic conductance and architectural analysis of anatomically preserved fossils from the same genus, although future work is needed to corroborate this. To conclude, plant functional traits may provide an opportunity to interpret the physiology and ecological tolerance of fossil taxa at a finer scale. However, clarification of the atmospheric and environmental context of these taxa using other methods (e.g., sedimentology and geochemistry) is crucial for robust interpretation of traits and trait syndromes. This study provides a working hypothesis for the palaeo-ecophysiological functioning of *Archaeopteris hibernica*, an extinct woody species that dominated the oldest forested ecosystems in Ireland at a time of globally elevated but declining atmospheric CO_2 at the close of the Devonian Period.

References

ARNOLD, C. A. 1939. Observations on fossil plants from the Devonian of eastern North America IV. Plant remains from the Catskill delta deposits of Northern Pennsylvania and Southern New York *Contibutions from the museum of Paleontology, University of Michigan,* **5,** 271-314.

BEAULIEU, J. M., LEITCH, I. J., PATEL, S., PENDHARKAR, A. & KNIGHT, C. A. 2008. Genome size is a strong predictor of cell size and stomatal density in angiosperms. *New Phytologist,* **179,** 975-986.

BECK, C. B. 1971. On the anatomy and morphology of lateral branch systems of *Archaeopteris*. *American Journal of Botany,* **58,** 758-784.

BEERLING, D. 2002. Low atmospheric CO_2 levels during the Permo-Carboniferous glaciation inferred from fossil lycopsids. *Proceedings of the National Academy of Sciences,* **99,** 12567-12571.

BOYCE, C. K. 2009. Seeing the forest with the leaves–clues to canopy placement from leaf fossil size and venation characteristics. *Geobiology,* **7,** 192-199.

BOYCE, C. K., IBARRA, D. E. & D'ANTONIO, M. P. 2023. What we talk about when we talk about the long-term carbon cycle. *New Phytologist,* **237,** 1550-1557.

BOYCE, C. K. & LEE, J.-E. 2017. Plant evolution and climate over geological timescales. *Annual Review of Earth and Planetary Sciences,* **45,** 61-87.

BRODRIBB, T. J. & FEILD, T. S. 2010. Leaf hydraulic evolution led a surge in leaf photosynthetic capacity during early angiosperm diversification. *Ecology letters,* **13,** 175-183.

BRODRIBB, T. J., FEILD, T. S. & JORDAN, G. J. 2007. Leaf maximum photosynthetic rate and venation are linked by hydraulics. *Plant physiology,* **144,** 1890-1898.

CAPEL, E., CLEAL, C. J., XUE, J., MONNET, C., SERVAIS, T. & CASCALES-MIÑANA, B. 2022. The Silurian–Devonian terrestrial revolution: diversity patterns and sampling bias of the vascular plant macrofossil record. *Earth-Science Reviews,* **231,** 104085.

CARLUCCIO, L. M., HUEBER, F. M. & BANKS, H. P. 1966. *Archaeopteris macilenta*, anatomy and morphology of its frond. *American Journal of Botany,* **53,** 719-730.

CHALONER, W. G. 1968. The cone of *Cyclostigma kiltorkense* Haughton, from the Upper Devonian of Ireland. *Botanical Journal of the Linnean Society,* **61,** 25-36.

CHENG-SEN, L. & EDWARDS, D. 1995. A re-investigation of Halle's *Drepanophycus spinaeformis* Göpp. from the Lower Devonian of Yunnan Province, southern China. *Botanical Journal of the Linnean Society,* **118,** 163-192.

D'ANTONIO, M. P., IBARRA, D. E. & BOYCE, C. K. 2023. The preservation of cause and effect in the rock record. *Paleobiology,* **49,** 204-214.

DAHL, T. W., HARDING, M. A., BRUGGER, J., FEULNER, G., NORRMAN, K., LOMAX, B. H. & JUNIUM, C. K. 2022. Low atmospheric CO_2 levels before the rise of forested ecosystems. *Nature Communications,* **13,** 7616.

DECOMBEIX, A.-L., HARPER, C. J., PRESTIANNI, C., DURIEUX, T., RAMEL, M. & KRINGS, M. 2023. Fossil evidence of tylosis formation in Late Devonian plants. *Nature Plants,* **9, 1-4**.

DECOMBEIX, A.-L., MEYER-BERTHAUD, B. & GALTIER, J. 2011. Transitional changes in arborescent lignophytes at the Devonian–Carboniferous boundary. *Journal of the Geological Society,* **168,** 547-557.

DRIESE, S. G., MORA, C. I. & ELICK, J. M. 2000. The paleosol record of increasing plant diversity and depth of rooting and changes in atmospheric pCO_2 in the Siluro-Devonian. *The Paleontological Society Papers,* **6,** 47-62.

EDWARDS, D., KERP, H. & HASS, H. 1998. Stomata in early land plants: an anatomical and ecophysiological approach. *Journal of Experimental Botany,* **49,** 255-278.

FAIRON-DEMARET, M., LEPONCE, I. & STREEL, M. 2001. *Archaeopteris* from the Upper Famennian of Belgium: heterospory, nomenclature, and palaeobiogeography. *Review of Palaeobotany and Palynology,* **115,** 79-97.

FOSTER, G. L., ROYER, D. L. & LUNT, D. J. 2017. Future climate forcing potentially without precedent in the last 420 million years. *Nature communications,* **8,** 14845.

FRANKS, P. J. & BEERLING, D. J. 2009. Maximum leaf conductance driven by CO_2 effects on stomatal size and density over geologic time. *Proceedings of the National Academy of Sciences,* **106,** 10343-10347.

FRANKS, P. J. & FARQUHAR, G. D. 2007. The mechanical diversity of stomata and its significance in gas-exchange control. *Plant physiology,* **143,** 78-87.

FRANKS, P. J., ROYER, D. L., BEERLING, D. J., VAN DE WATER, P. K., CANTRILL, D. J., BARBOUR, M. M. & BERRY, J. A. 2014. New constraints on atmospheric CO_2 concentration for the Phanerozoic. *Geophysical Research Letters,* **41,** 4685-4694.

GENSEL, P. G. & EDWARDS, D. 2001. *Plants invade the land: evolutionary and environmental perspectives*, Columbia University Press.

GUO, Y. & WANG, D. 2016. Studies on plant cuticles from the Lower–Middle Devonian of China. *Review of Palaeobotany and Palynology,* **227,** 42-51.

HENRY, T. A., BAINARD, J. D. & NEWMASTER, S. G. 2014. Genome size evolution in Ontario ferns (Polypodiidae): evolutionary correlations with cell size, spore size, and habitat type and an absence of genome downsizing. *Genome,* **57,** 555-566.

HUEBER, F. M. 1983. A new species of *Baragwanathia* from the Sextant Formation (Emsian) northern Ontario, Canada. *Botanical Journal of the Linnean Society,* **86,** 57-79.

KNIGHT, C. A., CLANCY, R. B., GÖTZENBERGER, L., DANN, L. & BEAULIEU, J. M. 2010. On the relationship between pollen size and genome size. *Journal of Botany*, 612017.

KRÄUSEL, R. & WEYLAND, H. 1941. Pflanzenreste aus dem Devon von Nord-Amerika. I. Vorbemerkung. II. Die oberdevonischen Floren von Elkins, West-Virginien, und Perry, Maine, mit Berücksichtigung einiger Stücke von der Chaleur-Bai, Canada. *Palaeontographica Abteilung B,* **86,** 1-78.

KÜRSCHNER, W. M., BATENBURG, S. J. & MANDER, L. 2013. Aberrant *Classopollis* pollen reveals evidence for unreduced (2 n) pollen in the conifer family Cheirolepidiaceae during the Triassic–Jurassic transition. *Proceedings of the Royal Society B: Biological Sciences,* **280,** 20131708.

LI, C.-S., HUEBER, F. & HOTTON, C. 2000. A neotype for *Drepanophycus spinaeformis* Göppert 1852. *Canadian Journal of Botany,* **78,** 889-902.

LOMAX, B. H., HILTON, J., BATEMAN, R. M., UPCHURCH, G. R., LAKE, J. A., LEITCH, I. J., CROMWELL, A. & KNIGHT, C. A. 2014. Reconstructing relative genome size of vascular plants through geological time. *New Phytologist,* **201,** 636-644.

LOMAX, B. H., WOODWARD, F. I., LEITCH, I. J., KNIGHT, C. A. & LAKE, J. A. 2009. Genome size as a predictor of guard cell length in *Arabidopsis thaliana* is independent of environmental conditions. *New Phytologist,* **181,** 311-314.

LOOY, C. V. 2013. Natural history of a plant trait: branch-system abscission in Paleozoic conifers and its environmental, autecological, and ecosystem implications in a fire-prone world. *Paleobiology,* **39,** 235-252.

MCELWAIN, J. 1998. Do fossil plants signal palaeoatmospheric carbon dioxide concentration in the geological past? *Philosophical Transactions of the Royal Society of London. Series B: Biological Sciences,* **353,** 83-96.

MCELWAIN, J. C. & STEINTHORSDOTTIR, M. 2017. Paleoecology, ploidy, paleoatmospheric composition, and developmental biology: a review of the multiple uses of fossil stomata. *Plant Physiology,* **174,** 650-664.

MCELWAIN, J. C., YIOTIS, C. & LAWSON, T. 2015. Using modern plant trait relationships between observed and theoretical maximum stomatal conductance and vein density to examine patterns of plant macroevolution. *New Phytologist,* **209,** 94-103.

MEYER-BERTHAUD, B., SCHECKLER, S. E. & WENDT, J. 1999. *Archaeopteris* is the earliest known modern tree. *Nature,* **398,** 700-701.

MEYER-BERTHAUD, B., SCHECKLER, S. E. & BOUSQUET, J. L. 2000. The development of *Archaeopteris*: new evolutionary characters from the structural analysis of an Early Famennian trunk from southeast Morocco. *American Journal of Botany,* **87,** 456-468.

MORENO-SÁNCHEZ, M. 2004. Graphic approach for morphometric analysis of *Archaeopteris* leaves. *Annales de Paléontologie,* **90,** 161-173.

MÜLLER, R. D., CANNON, J., QIN, X., WATSON, R. J., GURNIS, M., WILLIAMS, S., PFAFFELMOSER, T., SETON, M., RUSSELL, S. H. J. & ZAHIROVIC, S. 2018. GPlates: Building a virtual Earth through deep time. *Geochemistry, Geophysics, Geosystems,* **19,** 2243-2261.

OSBORNE, C. P., BEERLING, D. J., LOMAX, B. H. & CHALONER, W. G. 2004. Biophysical constraints on the origin of leaves inferred from the fossil record. *Proceedings of the National Academy of Sciences,* **101,** 10360-10362.

PAWLIK, Ł., BUMA, B., ŠAMONIL, P., KVAČEK, J., GAŁĄZKA, A., KOHOUT, P. & MALIK, I. 2020. Impact of trees and forests on the Devonian landscape and weathering processes with implications to the global Earth's system properties - a critical review. *Earth-Science Reviews,* **205,** 103200.

PORTER, A. S., YIOTIS, C., MONTAÑEZ, I. P. & MCELWAIN, J. C. 2017. Evolutionary differences in $\Delta^{13}C$ detected between spore and seed bearing plants following exposure to a range of atmospheric O_2: CO_2 ratios; implications for paleoatmosphere reconstruction. *Geochimica et Cosmochimica Acta,* **213,** 517-533.

RAYNER, R. 1984. New finds of *Drepanophycus spinaeformis* Göppert from the Lower Devonian of Scotland. *Earth and Environmental Science Transactions of The Royal Society of Edinburgh,* **75,** 353-363.

SCHECKLER, S. E. 1978. Ontogeny of progymnosperms. II. Shoots of upper Devonian Archaeopteridales. *Canadian Journal of Botany,* **56,** 3136-3170.

SCHWENDEMANN, A. B. 2018. Leaf venation density and calculated physiological characteristics of fossil leaves from the Permian of Gondwana. *In:* KRINGS, M., HARPER, C. J., CÚNEO, N. R. & ROTHWELL, G. W. (eds.) *Transformative Paleobotany.* Academic Press.

SOH, W. K., WRIGHT, I. J., BACON, K. L., LENZ, T. I., STEINTHORSDOTTIR, M., PARNELL, A. C. & MCELWAIN, J. C. 2017. Palaeo leaf economics reveal a shift in ecosystem function associated with the end-Triassic mass extinction event. *Nature Plants,* **3,** 17104.

STEIN, W. E., MANNOLINI, F., HERNICK, L. V., LANDING, E. & BERRY, C. M. 2007. Giant cladoxylopsid trees resolve the enigma of the Earth's earliest forest stumps at Gilboa. *Nature,* **446,** 904-907.

STOCKMANS, F. 1948. Végétaux du Dévonien Supérieur de la Belgique. *Mémoires du Musée Royal d'Histoire Natuerelle de Belgique,* **110** 1-85.

STUBBLEFIELD, S. & BANKS, H. P. 1978. The cuticle of *Drepanophycus spinaeformis*, a long-ranging Devonian lycopod from New York and eastern Canada. *American Journal of Botany,* **65,** 110-118.

SUN, C.-L., TAN, X., DILCHER, D. L., WANG, H., NA, Y.-L., LI, T. & LI, Y.-F. 2018. Middle Jurassic *Ginkgo* leaves from the Daohugou area, Inner Mongolia, China and their implication for palaeo-CO_2 reconstruction. *Palaeoworld,* **27,** 467-481.

TANRATTANA, M., BARCZI, J. F., DECOMBEIX, A. L., MEYER-BERTHAUD, B. & WILSON, J. 2019. A new approach for modelling water transport in fossil plants. *IAWA Journal,* **40,** 466-487.

TRIVETT, M. L. 1993. An architectural analysis of *Archaeopteris,* a fossil tree with pseudomonopodial and opportunistic adventitious growth. *Botanical Journal of the Linnean Society,* **111,** 301-329.

WAN, Z., ALGEO, T. J., GENSEL, P. G., SCHECKLER, S. E., STEIN, W. E., CRESSLER III, W. L., BERRY, C. M., XU, H., ROWE, H. D. & SAUER, P. E. 2019. Environmental influences on the stable carbon isotopic composition of Devonian and Early Carboniferous land plants. *Palaeogeography, Palaeoclimatology, Palaeoecology,* **531,** 109100.

WILSON, J. P., WHITE, J. D., MONTANEZ, I. P., DIMICHELE, W. A., MCELWAIN, J. C., POULSEN, C. J. & HREN, M. T. 2020. Carboniferous plant physiology breaks the mold. *New Phytologist,* **227,** 667-679.

WITKOWSKI, C. R., WEIJERS, J. W., BLAIS, B., SCHOUTEN, S. & SINNINGHE DAMSTÉ, J. S. 2018. Molecular fossils from phytoplankton reveal secular pCO_2 trend over the Phanerozoic. *Science advances,* **4,** eaat4556.

WRIGHT, I. J., REICH, P. B., WESTOBY, M., ACKERLY, D. D., BARUCH, Z., BONGERS, F., CAVENDER-BARES, J., CHAPIN, T., CORNELISSEN, J. H. C., DIEMER, M., FLEXAS, J., GARNIER, E., GROOM, P. K., GULIAS, J., HIKOSAKA, K., LAMONT, B. B., LEE, T., LEE, W., LUSK, C., MIDGLEY, J. J., NAVAS, M.-L., NIINEMETS, Ü., OLEKSYN, J., OSADA, N., POORTER, H., POOT, P., PRIOR, L., PYANKOV, V. I., ROUMET, C., THOMAS, S. C., TJOELKER, M. G., VENEKLAAS, E. J. & VILLAR, R. 2004. The worldwide leaf economic spectrum. *Nature,* **428,** 821-827.

YIOTIS, C. & MCELWAIN, J. C. 2019. A novel hypothesis for the role of photosynthetic physiology in shaping macroevolutionary patterns. *Plant physiology,* **181,** 1148-1162.

ZHOU, N., WANG, Y., YA, L., PORTER, A. S., KÜRSCHNER, W. M., LI, L., LU, N. & MCELWAIN, J. C. 2020. An inter-comparison study of three stomatal-proxy methods for CO_2 reconstruction applied to early Jurassic Ginkgoales plants. *Palaeogeography, Palaeoclimatology, Palaeoecology,* **542,** 109547.

Appendices

Appendix 1.1

Statement of contribution to referenced manuscript:

Bea Jackson participated in discussion of the manuscript, contributed to editing the manuscript and drafted the manuscript sections ‘Leaf lifespan and duration of green foliage’, ‘Vein Density’, ‘Mesophyll Conductance’, ‘Life history and Maximum plant lifespan’ and ‘Area of a Leaf’ (supplemental)**.**

Jennifer McElwain and Sandra Nogué conceived the review. Jennifer McElwain and Will Matthaeus designed the review structure and approach. Jennifer McElwain, Will Matthaeus, Bea Jackson, Antonietta Knetge, Christos Chondrogiannis, Sandra Nogué, Catarina Barbosa, Katie O’Dea, Kamila Kwasniewska and Richard Nair drafted the manuscript. Jennifer McElwain, Will Matthaeus, Christos Chondrogiannis and Sandra Nogué prepared the figures and tables. Kamila Kwasniewska, Antonietta Knetge, Katie O’Dea and Catarina Barbosa prepared the bibliography. All authors participated in discussion and editing of the manuscript, figures and tables.

The final published version of the paper can be found https://doi.org/10.1111/nph.19622 and is attached to the end of this thesis.

Appendix 2.1

Table A2.1.1. Number of fossil stem fragments and preservation quality of each hand specimen. Each hand specimen was treated as a separate sample. Up to 10 stem fragments were subsampled for all hand specimens with a number of stem fragments greater than 10 (*). The number of paired stable carbon isotope measurements associated with each sample from Wan et al. (2019) is also reported.

Sample	Number of stem fragments	Number of paired carbon isotope measurements associated with the sample	Preservation Quality
SAWD-PG-002-(3)	8	2	Medium
SAWD-PG-002-(5)	6	2	Medium
SAWD-PG-002-(6)	18*	2	Good
SAWD-PG-002-(7)	4	2	Medium
SAWD-PG-002-(9)	8	2	Medium
SAWD-PG-002-(10)	5	2	Medium
SAWD-PG-002-(11)	4	2	Medium
SAWD-PG-006	13*	2	Medium
SAWD-PG-003-(1)	8	1	Medium
SAWD-PG-003-(2)	3	1	Good
SAWD-PG-003-(3)	7	1	Good
SAWD-PG-003-(4)	2	1	Good
SAWD-PG-003-(4ii)	28*	1	Good
SAWD-PG-003-(5)	2	1	Good
SAWD-PG-003-(6)	6	1	Good
SAWD-PG-003-(7)	5	1	Good
SAWD-PG-005-(1)	5	2	Good
SAWD-PG-005-(2)	10	2	Good

Sample	Number of stem fragments	Number of paired carbon isotope measurements associated with the sample	Preservation Quality
SAWD-PG-005-(3)	9	2	Good
SAWD-PG-005-(4)	8	2	Good
SAWD-WS-009	11*	2	Good

Appendix 2.2.

Table A2.2.1. Summary of images and data used to define the pore length to guard cell length scaling factor.

Pore length / Guard cell length	Reference / Sample number	Notes
0.362	SAWD-PG-002-7	Image 13, pore 1
0.565	SAWD-PG-002-7	Image 13, pore 2
0.557	SAWD-PG-002-7	Image 13, pore 3
0.628	SAWD-PG-002-7	Image 14, pore 1
0.66	SAWD-PG-002-7	Image 14, pore 2
0.631	SAWD-PG-002-7	Image 21, pore 1
0.61	SAWD-PG-002-7	Image 21, pore 2
0.52	SAWD-PG-003-3	Image 10, pore 1
0.782	SAWD-PG-002-3	Image 5, pore 1
0.674	SAWD-PG-002-3	Image 6, pore 1
0.68	SAWD-PG-002-5	Image 7, pore 1
0.554	SAWD-PG-002-5	Image 10, pore 1
0.628	SAWD-PG-002-5	Image 10, pore 2
0.703	SAWD-PG-002-5	Image 16, pore 1
0.571	SAWD-PG-002-11	Image 18, pore 1

	Pore length / Guard cell length	Reference / Sample number	Notes
	0.791	SAWD-PG-002-9	Image 1, pore 1
	0.5	SAWD-PG-002-9	Image 1, pore 2
	0.551	SAWD-PG-002-9	Image 9, pore 1
	0.673	SAWD-PG-002-9	Image 9, pore 2
	0.597	SAWD-PG-002-10	Image 1, pore 1
	0.525	SAWD-PG-002-10	Image 2, pore 1
	0.692	SAWD-PG-002-10	Image 5, pore 1
	0.636	SAWD-PG-002-10	Image 8, pore 1
	0.742	SAWD-PG-002-10	Image 8, pore 2
	0.521	SAWD-PG-002-10	Image 11, pore 1
	0.585	SAWD-PG-003-4ii	Image 3, pore 1
	0.31	SAWD-PG-003-6	Image 9, pore 1
	0.649	Chaloner et al. (1978)	Plate 76, Figure 1; cf. *Sawdonia* sp. (Gensel and Berry, 2016)
	0.621	Chaloner et al. (1978)	Plate 76, Figure 2; cf. *Sawdonia* sp. (Gensel and Berry, 2016)

Pore length / Guard cell length	Reference / Sample number	Notes
0.695	Chaloner et al. (1978)	Plate 76, Figure 3; cf. *Sawdonia* sp. (Gensel and Berry, 2016)
0.538	Edwards (1924)	Plate 37, Figure 6; cf. *Sawdonia* sp. (Gensel and Berry, 2016)
0.467	Edwards (1993)	Figure 35
0.476	Edwards et al. (1998)	Figure 10 A; cf. *Sawdonia* sp. (Gensel and Berry, 2016)
0.52	Gensel (1992)	Figure 7 F
0.544	Hueber and Grierson (1961)	Figure 12; cf. *Sawdonia* sp. (Gensel and Berry, 2016)
0.502	Lang (1931)	Plate 27, Figure 2; cf. *Sawdonia* sp. (Gensel and Berry, 2016)
0.464	Lang (1933)	Figure 66; cf. *Sawdonia* sp. (Gensel and Berry, 2016)

	Pore length / Guard cell length	Reference / Sample number	Notes
	0.481	Lang (1933)	Figure 70; cf. *Sawdonia* sp. (Gensel and Berry, 2016)
	0.446	Rayner (1983)	Midpoint value of range (Normal distribution assumed.); cf. *Sawdonia* sp. (Gensel and Berry, 2016)
	0.405	Rayner (1983)	Minimum value of range reported; cf. *Sawdonia* sp. (Gensel and Berry, 2016)
	0.467	Rayner (1983)	Maximum value of range reported; cf. *Sawdonia* sp. (Gensel and Berry, 2016)
	0.426	Zdebska (1972)	Plate VI, Figure 1; cf. *Sawdonia* sp. (Gensel and Berry, 2016)
Mean (± S.D.)	**0.57 (± 0.12)**		

Appendix 2.3

Table A2.3.1. Summary of species used for calibration of the A_0 input parameter.

	Species	Climate	Light Environment	A_n (µmol CO_2 m^{-2} s^{-1})	Reference
	Selaginella pallescens	Tropical	Sun	6.15	Brodribb and Holbrook (2006)
	Selaginella martensii	Subtropical to tropical	Sun to Partial Shade	3.69	Carriquí et al. (2019)
	Selaginella sp.	Tropical	Open Canopy	2.1	Campany et al. (2019)
	Selaginella umbrosa	Tropical	Open Canopy	3.5	Campany et al. (2019)
Mean				**3.86**	
(± S.D.)				**(± 1.68)**	

Appendix 2.4

Table A2.4.1 Summary of inputs used in the Franks model.

Input	Description	Range of values	Justification
D_{ab}	Stomatal density (m^2) on abaxial surface	3.70 to 8.17 mm^{-2}	Measured on fossil cuticles
eD_{ab}	Error in D_{ab} (m^2)	0.29 to 0.99 mm^{-2}	Standard error of mean of D_{ab} measurements
D_{ad}	Stomatal density (m^2) on adaxial surface	0	hypostomatous
eD_{ad}	Error in D_{ad} (m^2)	0	hypostomatous
GCL_{ab}	Guard cell length (m) on abaxial surface	46.9 to 69.55 µm	Measured directly from cuticles. Where guard cell length could not be directly measured because stomata were sunken the stomatal pit length was measured
$eGCL_{ab}$	Error in GCL_{ab}	0.94 to 3.58 µm	Standard error of mean of GCL_{ab} measurements
GCL_{ad}	Guard cell length (m) on adaxial surface	0	hypostomatous
$eGCL_{ad}$	Error in GCL_{ad}	0	hypostomatous
GCW_{ab}	Single guard cell width (m) on abaxial surface	10.9 to 14.4 µm	The width of both guard cells in a stomatal complex was measured and halved to estimate a single guard cell width.

Input	Description	Range of values	Justification
$eGCW_{ab}$	Error in GCW_{ab}	0.225 to 0.648 µm	Standard error of mean of GCW_{ab} measurements
GCW_{ad}	Single guard cell width (m) on adaxial surface	0	hypostomatous
$eGCW_{ad}$	Error in GCW_{ad}	0	hypostomatous
$\delta^{13}C_p$	$\delta^{13}C_p$ of leaf material relative to that in the PDB standard (‰)	-22.548 to -26.26 ‰	Obtained from supplementary data of Wan et al. (2019) with phylogenetic correction factor for lycophytes of Porter et al. (2017) (Phylogenetically independent $\delta^{13}C_{leaf}$ = observed value + 2.55)
$e\delta^{13}C_p$	Error in $\delta^{13}C_p$	0.06 to 1	Standard deviation of carbon isotope measurements. When only one measurement was obtained the suggested error of Franks et al. (2014) was used.
$\delta^{13}C_{atm}$	Ratio of $\delta^{13}C$ in the palaeoatmosphere relative to that in the PDB standard (‰)	-7.67 to -8.14 ‰	Values from marine carbonate $\delta^{13}C$ data of Jarvis and Cramer (2020) and Mills et al. (2023), and palaeotemperature data from Joachimski et al. (2009).
$e\delta^{13}C_{atm}$	Error in $\delta^{13}C_{atm}$	0.66-1.13	Error associated with $\delta^{13}C_{atm}$ data
CO_{2_0}	Atmospheric CO_2 associated with A_0 (ppm)	400	Suggested value from Franks et al. (2014)

Input	Description	Range of values	Justification
A_0	Photosynthetic rate at CO_{2_0} (μmol m^{-2} s^{-1})	3.86	Measured value for tropical, full-sun, terrestrial lycophytes (Brodribb and Holbrook, 2006, Campany et al., 2019, Carriquí et al., 2019)
eA_0	Error of A_0	1.68	Standard deviation of A_0 values
g_b	Boundary layer conductance to CO_2 (mol m^{-2} s^{-1})	2	Suggested value from Franks et al. (2014)
eg_b	Error in g_b	0.1	Suggested value from Franks et al. (2014)
s1	Scaling from guard cell length to stomatal pore length	0.57	Scaling relationship determined by direct measurements from fossil cuticles and images from the literature.
es1	Error in s1	0.12	Standard deviation of scaling relationship from measured images
s2	Scaling from single guard cell width to stomatal depth	1	Assumed *Sawdonia* guard cells have a circular cross section. Suggested value from Franks et al. (2014)
es2	Error in s2	0.05	Suggested value from Franks et al. (2014)
s3	Scaling from the area of a circle with the diameter of pore length to a_{max} (maximum area of stomatal pore).	0.6	Suggested value from Franks et al. (2014)

es3	Error in s3	0.025	Suggested value from Franks et al. (2014)

Input	Description	Range of values	Justification
s4	Scaling from maximum conductance to CO_2 (gc_{max}) to operational conductance CO_2 (gc_{op})	0.2	Suggested value from Franks et al. (2014)
es4	Error in s4	0.02	Suggested value from Franks et al. (2014)
s5	Scaling from photosynthetic rate (A) to mesophyll conductance to CO_2 (g_m).	0.013	Suggested value from Franks et al. (2014)
es5	Error in s5	0.00065	Suggested value from Franks et al. (2014)

Table A2.4.2 Summary of measured inputs for each fossil sample used in the Franks model. See *Table A2.4.1* for a summary of all scaling factors used.

Sample	Stomatal Density (mm^{-2})	Guard Cell Length (µm)	Single Guard Cell Width (µm)	$\delta^{13}C_{plant}$ (‰)	$\delta^{13}C_{atm}$ (‰)	CO_2 (ppm)
SAWD-PG-002-(3)	3.72 (± 0.49)	62.2 (± 2.3)	10.9 (± 0.5)	-22.548	-8.14	**1116 (+746/-515)**
SAWD-PG-002-(5)	5.74 (± 0.60)	51.6 (± 2.4)	11.9 (± 0.5)	-22.548	-8.14	**954 (+661/-427)**
SAWD-PG-002-(6)	4.46 (± 0.45)	67.5 (± 1.8)	12.9 (± 0.6)	-22.548	-8.14	**889 (+584/-398)**
SAWD-PG-002-(7)	4.84 (± 0.31)	58.0 (± 1.5)	11.3 (± 0.3)	-22.548	-8.14	**945 (+625/-421)**
SAWD-PG-002-(9)	5.02 (± 0.53)	56.7 (± 1.6)	12.0 (± 0.6)	-22.548	-8.14	**964 (+638/-426)**
SAWD-PG-002-(10)	3.70 (± 0.52)	60.4 (± 2.5)	11.0 (± 0.5)	-22.548	-8.14	**1163 (+817/-536)**
SAWD-PG-002-(11)	7.84 (± 0.69)	53.5 (± 2.8)	11.8 (± 0.6)	-22.548	-8.14	**690 (+448/-307)**
SAWD-PG-006	4.40 (± 0.30)	52.0 (± 2.8)	12.8 (± 0.3)	-26.255	-8.14	**1695 (+1109/-756)**

Sample	Stomatal Density (mm^{-2})	Guard Cell Length (µm)	Single Guard Cell Width (µm)	$\delta^{13}C_{plant}$ (‰)	$\delta^{13}C_{atm}$ (‰)	CO_2 (ppm)
SAWD-PG-003-(1)	7.17 (± 0.66)	58.6 (± 1.6)	12.5 (± 0.5)	-23.84	-7.67	**787 (+516/-345)**
SAWD-PG-003-(2)	5.30 (± 0.52)	64.8 (± 3.6)	11.1 (± 0.2)	-23.84	-7.67	**898 (+616/-405)**
SAWD-PG-003-(3)	7.95 (± 0.54)	46.9 (± 0.9)	11.8 (± 0.3)	-23.84	-7.67	**890 (+599/-391)**
SAWD-PG-003-(4)	8.17 (± 0.65)	65.1 (± 1.9)	11.6 (± 0.5)	-23.84	-7.67	**597 (+360/-245)**
SAWD-PG-003-(4ii)	5.68 (± 0.49)	51.2 (± 1.9)	11.2 (± 0.3)	-23.84	-7.67	**1105 (+766/-505)**
SAWD-PG-003-(5)	8.15 (± 0.86)	51.4 (± 1.7)	10.9 (± 0.3)	-23.84	-7.67	**790 (+519/-344)**
SAWD-PG-003-(6)	7.49 (± 0.83)	58.1 (± 2.6)	14.4 (± 0.7)	-23.84	-7.67	**717 (+479/-305)**
SAWD-PG-003-(7)	5.69 (± 0.44)	69.6 (± 2.5)	12.0 (± 0.4)	-23.84	-7.67	**809 (+528/-351)**
SAWD-PG-005-(1)	7.56 (± 0.90)	58.3 (± 2.1)	12.0 (± 0.3)	-25.928	-7.67	**894 (+605/-390)**
SAWD-PG-005-(2)	7.70 (± 0.57)	58.0 (± 2.3)	11.6 (± 0.5)	-25.928	-7.67	**881 (+573/-373)**

Sample	Stomatal Density (mm^{-2})	Guard Cell Length (µm)	Single Guard Cell Width (µm)	$\delta^{13}C_{plant}$ (‰)	$\delta^{13}C_{atm}$ (‰)	CO_2 (ppm)
SAWD-PG-005-(3)	6.46 (± 0.63)	56.6 (± 1.7)	12.1 (± 0.6)	-25.928	-7.67	**1058 (+709/-457)**
SAWD-PG-005-(4)	7.98 (± 0.99)	50.0 (± 1.9)	12.2 (± 0.6)	-25.928	-7.67	**1039 (+706/-461)**
SAWD-WS-009	7.01 (± 0.52)	58.3 (± 2.8)	12.4 (± 0.4)	-26.26	-7.67	**992 (+633/-417)**

Appendix 2.5.

Table A2.5.1. A summary of the stomatal pore depth to guard cell width ratio in living lycophytes. Mean pore depth to guard cell width ratio was found to be 1.03 ± 0.7. In some figures cited, guard cells may be deflated as a result of preparation for sectioning, so may be more oval in cross section.

Species	Guard Cell Width (µm)	Pore Depth (µm)	Pore Depth/ Guard Cell Width	Reference
Lycopodium japonicum	22	20	1.10	Figure 4a (Sun et al., 2005)
Lycopodium japonicum	20	20	1	Figure 4b (Sun et al., 2005)
Lycopodium japonicum	30	29	1.03	Figure 4c (Sun et al., 2005)
Selaginella sp.	8.5	9	0.94	Figure 3c (Left) (Merced and Renzaglia, 2017)
Selaginella sp.	8.5	9	0.94	Figure 3c (Right) (Merced and Renzaglia, 2017)
Huperzia prolifera	30	27	1.11	Figure 2b (Franks and Farquhar, 2007)
Huperzia lucidula	26	27	1.03	Figure C1 (Skrodzki, 2017)
Huperzia selago	20	22	1.1	This study (Figure A2.5.1)
Mean			**1.03 ± 0.7**	

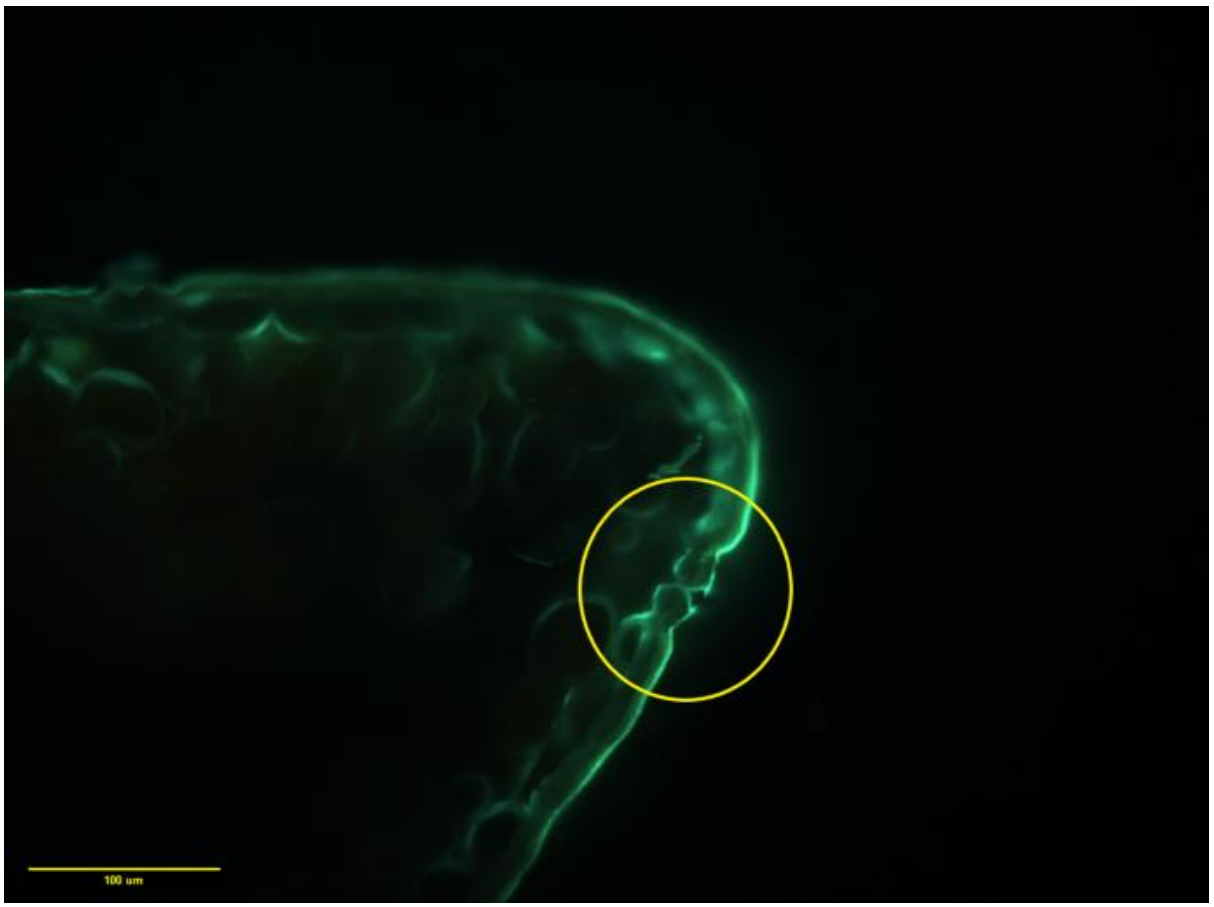

Figure A2.5.1. Transverse section of *Huperzia selago* guard cells. Sample obtained from Trinity College Dublin Botanic Gardens. Section photographed using epifluorescence microscopy. Stomatal complex is circled in yellow. Scale bar = 100µm.

Appendix 2.6.

The CO_2 curve used for *Figure 2.9* was determined following the protocol described in Montañez et al. (2016). Data from the compilation of Foster et al. (2017), as well as Montañez et al. (2016), Witkowski et al. (2018) and Dahl et al. (2022) were used. The input data used by Dahl et al. (2022) were modified to correct for pore depth parameterisation and $\delta^{13}C$ and rerun in the Franks model as outlined in the Materials and Methods section. A 0.3 span (i.e. smoothing) was chosen for the loess curve to avoid curve overfitting, as CO_2 data for the Devonian is more sparse than more high resolution studies such as that of Montañez et al. (2016). Comparison of the loess curves obtained by using a span of 0.1, 0.2 and 0.3. *Figure A2.6.1* shows the overlap of curves obtained using a span of 0.1, 0.2 and 0.3. The robustness of the 0.3 span was then evaluated by carrying out a series of loess runs excluding 10% of data from each run (as per Montañez et al. (2016)). *Figure A2.6.2* shows the overlap of these curves, which overlap well, indicating that this estimate is robust.

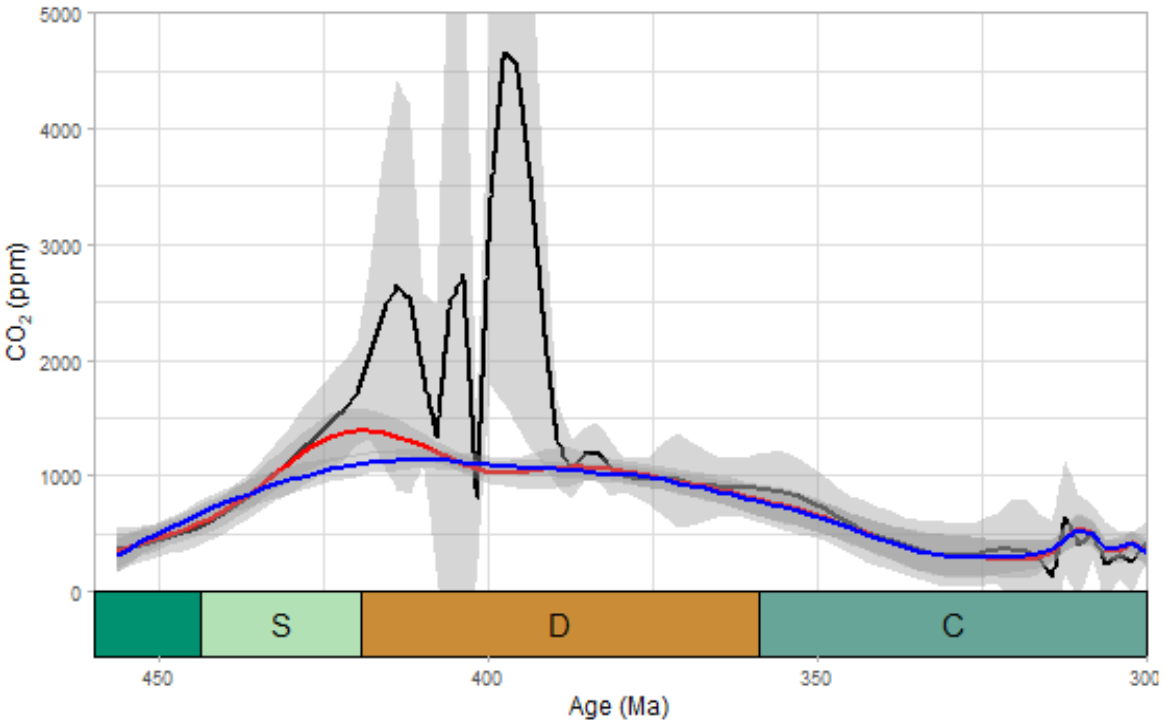

Figure A2.6.1. Comparison of loess results from fossil plant-, palaeosol- and phytoplankton-based CO_2 estimates using different smoothing parameters. A span of 0.1 (back), 0.2 (red) and 0.3 (blue) were compared, with the span of 0.3 being selected.

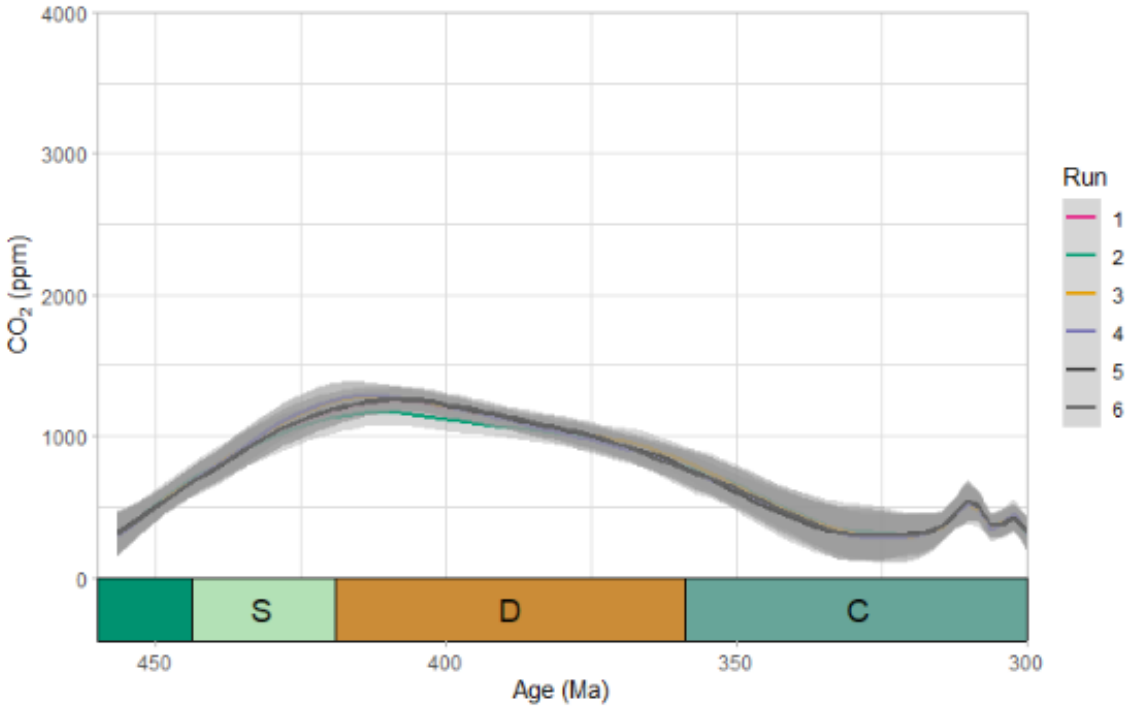

Figure A2.6.2. Comparison of loess results from running six different loess runs with 10% of the data excluded each time. Data subsets were defined by removing every 10th point starting from the 2nd ('Run 2'), 4th ('Run 3'), 6th ('Run 4'), 8th ('Run 5') and 10th ('Run 6') data points as per Montañez *et al.* (2016). 'Run 1' corresponds to the loess curve obtained when no data was removed.

Appendix 3.1

Table A3.1.1. A table of the flora found at Kiltorcan Hill to date.

Taxon	Synonyms	Plant type/ organ	General Affinities	Location	References
Archaeopteris hibernica	*Cyclopteris hibernicus, Cyclopteris hibernica, Adiantites hibernica, Palaeopteris hibernica*	leaves, stems, sporangia	Archaeopteridales	Old Plant Quarry (chlorite compression; probable Famennian)	(Baily, 1858, Baily, 1861, Baily, 1869a, Baily, 1869b, Baily, 1872, Baily, 1875b, Baily, 1875a, Brongniart, 1857, Carruthers, 1872, Forbes, 1853, Griffith and Brongniart, 1857, Haughton, 1855, Haughton, 1860, Jarvis, 1990, Jarvis, 1992, Jarvis, 2000, Johnson, 1911a, Johnson, 1911b, Johnson, 1917, Wang, 2011)
Bythotrephis sp.		stems	Alga	Roadstone Quarry (chlorite compression; IV Miospore Biozone)	(Jarvis, 1990, Jarvis, 1992, Jarvis, 2000)

Taxon	Synonyms	Plant type/ organ	General Affinities	Location	Reference(s)
Cyclostigma kiltorkense	*Bothodendron kiltorkense, Cyclostigma minutum, Cyclostigma griffithi, Knorria acicularis* Gopp. var. *bailyana, Knorria bailyana, Lepidodendron bailyana, Lepidodendron minutum, Lepidodendron griffithii, Lepidodendron velthemianum, Lepidostrobus bailyana* (cone)*, Sagenaria bailyana, Sigillaria dichotoma.*	leaves, stems, cones	Lepidodendrales (Lycophyta)	Old Plant Quarry and New Quarry (chlorite compression and coalified compression; Probable Famennian, and LE Miospore Biozone)	(Baily, 1861, Baily, 1869a, Baily, 1875b, Baily, 1875a, Brongniart, 1857, Chaloner, 1968, Chaloner and Meyer-Berthaud, 1983, Cleal and Thomas, 2018, Doweld, 2017b, Doweld, 2017a, Forbes, 1853, Griffith and Brongniart, 1857, Haughton, 1855, Haughton, 1860, Heer, 1872, Herendeen, 2020, Jarvis, 1990, Jarvis, 1992, Jarvis, 2000, Johnson, 1911b, Johnson, 1913, Johnson, 1914a, Schimper, 1870)

Taxon/Taxa	Synonyms	Plant type/ organ	General Affinities	Location	Reference(s)
Kiltorkensia devonica	*Gingkophyllum kiltorkense*	leaves	Unknown	Old Plant Quarry (chlorite compression; probable Famennian)	(Jarvis, 1990, Johnson, 1914b, Johnson, 1917)
Lepodendropsis sp., aff. *L. Hirmeri*	Misidentified as *C. kiltorkense* in Chaloner (1968)	stems	Lepidodendrales (Lycophyta)	Roadstone Quarry (chlorite compression; IV Miospore Biozone)	(Jarvis, 1990, Jarvis, 1992, Jarvis, 2000)
Noeggerathia ? *foliosa*	Possibly *Archaeopteris hibernica*	unknown	Unknown; possible synonym for *Archaeopteris*	Old Plant Quarry (chlorite compression; probable Famennian)	(Chagnoux, 2021, Dawson, 1871)
Rhacophyton sp.		leaves	Lyginopteridales (Pteridosperm)	Roadstone Quarry (chlorite compression; IV Miospore Biozone)	(Jarvis, 1990, Jarvis, 1992)
Rhacopteris sp.		Fertile pinna	Lyginopteridales (Pteridosperm)	Roadstone Quarry (chlorite compression; IV Miospore Biozone)	(Fairon-Demaret, 1986, Jarvis, 2000)

Taxon/Taxa	Synonyms	Plant type/organ	General Affinities	Location	Reference(s)
Spermolithus devonicus		seeds	unknown	Old Plant Quarry (chlorite compression; probable Famennian)	(Chaloner et al., 1977, Jarvis, 1990, Jarvis, 1992, Jarvis, 2000, Johnson, 1917)
Sphenopteridium ? *tschermaki*	*Archaeopteris* ? *tschermaki,* Possibly *Archaeopteris hibernica*	leaves	Unknown; possibly a poorly preserved *A. hibernica* specimen	Old Plant Quarry (chlorite compression; probable Famennian)	(Jarvis, 1990, Johnson, 1911b, Johnson, 1917, Kidston, 1923, Kräusel and Weyland, 1941)
Sphenopteris hookeri		leaves	Lyginopteridales (Pteridosperm)	Old Plant Quarry (chlorite compression; probable Famennian)	(Baily, 1861, Baily, 1875b, Jarvis, 1990, Jarvis, 1992, Jarvis, 2000, Johnson, 1913)
Sphenopteris humphresiana		leaves	Lyginopteridales (Pteridosperm)	Old Plant Quarry (chlorite compression; probable Famennian)	(Baily, 1875b, Jarvis, 1990)

Taxon/Taxa	Synonyms	Plant type/organ	General Affinities	Location	Reference(s)
Stigmaria		rhizomorph	Lepidodendrales (Lycophyta)	Old Plant and New Quarry (chlorite compression and coalified compression; Probable Famennian, and LE Miospore Biozone)	(Forbes, 1853, Jarvis, 1990, Johnson, 1914a)
Sublepidodendropsis c.f. *isachseni*		stems	Lepidodendrales (Lycophyta)	Roadstone Quarry (chlorite compression; IV Miospore Biozone)	(Chaloner and Meyer-Berthaud, 1983)
Cuticular remains		cuticle	unknown	Roadstone and New Quarry (LE and IV Miospore Biozones)	(Jarvis, 1990, Jarvis, 1992, Jarvis, 2000)
Plant debris		debris	unknown	Roadstone and New Quarry (LE and IV Miospore Biozones)	(Jarvis, 1990, Jarvis, 1992, Jarvis, 2000)

Appendix 4.1.

Different petiole width – leaf area scaling relationships with LMA have been found using different calibration datasets. The different equations that were used to compare LMA estimates for *Archaeopteris hibernica* are shown below. The fern calibration dataset of Peppe et al. (2014) was not used as the leaves of *Archaeopteris* are simple leaves (Carluccio et al., 1966).

Petiole width-leaf area relationship with LMA based on the gymnosperm calibration dataset of Royer et al. (2010):

$$log_{10}\left(LMA_{Gymno}\right) = 0.3076\, log_{10}\left(\frac{PW^2}{A}\right) + 3.015; N = 93, r^2 = 0.44, p < 0.0001 \quad (17)$$

Petiole width-leaf area relationship with LMA based on the angiosperm calibration dataset of Royer et al. (2007):

$$log_{10}\left(LMA_{Angio}\right) = 0.3820\, log_{10}\left(\frac{PW^2}{A}\right) + 3.070; N = 667, r^2 = 0.55, p < 0.0001 \quad (18)$$

Petiole width-leaf area relationship with LMA based on the Ginkgo calibration dataset of Haworth and Raschi (2014):

$$log_{10}\left(LMA_{Ginkgo}\right) = 0.285\, log_{10}\left(\frac{PW^2}{A}\right) + 2.882; N = 36, r^2 = 0.212, p < 0.05 \quad (19)$$

Appendix 4.2

Table A4.2.1. Summary of LMA data obtained from the TRY database (Kattge et al., 2020).

Data used in *Figure 4.3*.

Group	Median ($g\ m^{-2}$)	Q1 ($g\ m^{-2}$)	Q3 ($g\ m^{-2}$)	n	Data Source
Archaeopteris	**233.7**	176.0	289.0	83	This study
Baiera	**145.0**	116.7	159.1	7	Soh et al. (2017)
Ginkgoites	**126.8**	106.5	142.5	25	Soh et al. (2017)
Evergreen fern	**55.0**	41.1	74.5	51	TRY database
Deciduous shrub	**60.19**	40.6	88.0	498	TRY database
Deciduous shrub/tree	**59.3**	38.8	90.4	287	TRY database
Deciduous tree	**57.4**	38.4	88.9	957	TRY database
Evergreen shrub	**95.0**	46.9	171.2	1151	TRY database
Evergreen shrub/tree	**79.8**	43.9	143.0	452	TRY database
Evergreen tree	**96.6**	46.0	106.114	3308	TRY database
Deciduous gymnosperms	**61.0**	33.7	71.1	18	TRY database
Evergreen gymnosperms	**75.7**	20.2	181.7	279	TRY database

Review

New Phytologist

Tansley review

Functional traits of fossil plants

Author for correspondence:
Jennifer McElwain
Email: jmcelwai@tcd.ie

Received: *10 September 2023*
Accepted: *19 December 2023*

Jennifer C. McElwain[1], William J. Matthaeus[1], Catarina Barbosa[1], Christos Chondrogiannis[1], Katie O' Dea[1], Bea Jackson[1], Antonietta B. Knetge[1], Kamila Kwasniewska[1], Richard Nair[1], Joseph D. White[2], Jonathan P. Wilson[3], Isabel P. Montañez[4,5], Yvonne M. Buckley[6], Claire M. Belcher[7] and Sandra Nogué[8,9]

[1]School of Natural Sciences, Botany, Trinity College Dublin, Dublin, D02 PN40, Ireland; [2]Department of Biology, Baylor University, Waco, 76798-7388, TX, USA; [3]Department of Environmental Studies, Haverford College, Haverford, Pennsylvania 19041 PA, USA; [4]UC Davis Institute of the Environment, University of California, Davis, CA 95616, USA; [5]Department of Earth and Planetary Sciences, University of California, Davis, CA 95616, USA; [6]School of Natural Sciences, Zoology, Trinity College Dublin, Dublin, D02 PN40, Ireland; [7]wildFIRE Lab, University of Exeter, Exeter, EX4 4PS, UK; [8]Universitat Autònoma de Barcelona, Bellaterra (Cerdanyola del Vallès), 08193, Catalonia, Spain; [9]CREAF, Bellaterra (Cerdanyola del Vallès), 08193, Catalonia, Spain

Contents

New Phytologist (2024) **242:** 392–423
doi: 10.1111/nph.19622

Key words: earth system processes, fossil plant preservation modes, functional traits, leaf economic spectrum, paleobiology, paleobotany, plant fossil record, taphonomy.

Summary

A minuscule fraction of the Earth's paleobiological diversity is preserved in the geological record as fossils. What plant remnants have withstood taphonomic filtering, fragmentation, and alteration in their journey to become part of the fossil record provide unique information on how plants functioned in paleo-ecosystems through their traits. Plant traits are measurable morphological, anatomical, physiological, biochemical, or phenological characteristics that potentially affect their environment and fitness. Here, we review the rich literature of paleobotany, through the lens of contemporary trait-based ecology, to evaluate which well-established extant plant traits hold the greatest promise for application to fossils. In particular, we focus on fossil plant functional traits, those measurable properties of leaf, stem, reproductive, or whole plant fossils that offer insights into the functioning of the plant when alive. The limitations of a trait-based approach in paleobotany are considerable. However, in our critical assessment of

over 30 extant traits we present an initial, semi-quantitative ranking of 26 paleo-functional traits based on taphonomic and methodological criteria on the potential of those traits to impact Earth system processes, and for that impact to be quantifiable. We demonstrate how valuable inferences on paleo-ecosystem processes (pollination biology, herbivory), past nutrient cycles, paleobiogeography, paleo-demography (life history), and Earth system history can be derived through the application of paleo-functional traits to fossil plants.

I. Introduction

To date, the predominant focus of enquiry in paleobotany has been to document plant diversity and evolution (taxonomy and systematics), and through the development of climatic and atmospheric proxies (paleoclimatology), to examine how long-term environmental change has influenced plant form and diversity across time and space (paleoecology, evolutionary biology). Fewer studies have focused on the capacity of vegetation to 'force' the Earth system through its heterogeneous alteration of the hydrological cycle, weathering rates, and elemental fluxes between land and ocean. It is hypothesized that the magnitude of plant-driven forcing of the Earth system is influenced by the evolution of new plant groups that possess novel traits and trait combinations (Bonan, 1995; Boyce *et al.*, 2010; Boyce & Lee, 2010; Franks *et al.*, 2017; White *et al.*, 2020), yet to date, we lack a robust foundation of functional data on extinct plants to test these hypotheses in sufficient detail.

In this paper, we review a rich resource of paleobotanical and plant trait literature and outline a methodology for bringing fossil and extinct plants 'to life' using a functional trait-based approach pioneered by contemporary plant trait ecologists. We present a critical assessment of fossil plant functional traits that influence Earth system processes in particular. Such traits are referred to as 'effect traits' (Lavorel & Garnier, 2002; Chapin 3rd, 2003; Violle *et al.*, 2007) and are well-established in contemporary ecology. These traits have an 'effect' on ecosystem-scale processes such as carbon sequestration, chemical weathering, and decomposition. In addition to modulating local processes differently across the globe, variation in these traits is a key determinant of global biogeography. Our overarching aim is thus to identify and semi-quantitatively rank a set of fossil plant functional traits that are robust to taphonomic constraints, are relatively easy to measure across various fossil plant preservation modes and which have played a role in shaping Earth's environment, climate, and atmosphere through time via their effect on the carbon, oxygen, nutrient, and hydrological cycles (Fig. 1). We do not focus on 'response traits', such as leaf area, leaf physiognomy and wood growth rings (Lavorel & Garnier, 2002; Chapin 3rd, 2003; Violle *et al.*, 2007; Wright *et al.*, 2017), which are plant traits predominantly shaped by local environmental factors, because they have been extensively used as the fundamental underpinning of fossil plant paleo-climate proxies and reviewed in depth elsewhere (Peppe *et al.*, 2011, 2014; Yang *et al.*, 2011, 2014; Allen *et al.*, 2020; Spicer *et al.*, 2021).

For each paleo-functional trait, we: (1) provide some brief examples of how fossil plant functional traits can elucidate population and ecosystem processes, plant–climate, and plant–atmosphere interactions in Earth's deep past. (2) We highlight relationships between traits and trade-offs that have been robustly established within contemporary global datasets and that could be applied to fossil plants to obtain additional, indirect paleo-functional trait data. In cases where no suitable direct methods or trait–trait relationships have been established, (3) we present opportunities for future research to address these paleo-ecological gaps. Finally, (4) we assess how modes of fossil plant preservation and relevant taphonomic factors may potentially influence paleo-functional trait fidelity to the original trait value and its variability. Using these criteria, the author team has semi-quantitatively scored 26 fossil plant functional traits out of 30 initially assessed (Fig. 1) as a starting point for broader community engagement and to illustrate the relative ranking of paleo-functional traits based on our review.

We have organized the review using the contemporary trait selection in the 'New handbook for standardized measurement of plant functional traits worldwide' (Pérez-Harguindeguy *et al.*, 2013) with a focus first on regenerative traits that can be obtained from fossil palynomorphs and seeds followed by an appraisal of paleo-functional traits of fossil leaves and stems. In the last sections of the paper, we evaluate whole plant traits and trait syndromes that provide critical insights into extant plant ecological strategy and assess which can robustly be applied to plant fossils given their often fragmentary nature. Traits presented by Pérez-Harguindeguy *et al.* (2013) without potential application as paleo-functional traits (4 out of 30 traits) are included along with our assessment and reasoning in Supporting Information Notes S1–S7.

II. Toward the development of fossil plant functional traits

Current Earth system models (ESMs) incorporate vegetation, and biosphere feedbacks and drivers, but generally have not considered how plant-driven feedbacks and forcing over time may have changed with the emergence of new plant evolutionary groups and their associated functional traits (Matthaeus *et al.*, 2023). On geological timescales, the primary drivers of plant trait selection and filtering such as Earth's global mean annual temperature and precipitation, atmospheric composition, wildfire ecology, biota of herbivores, pathogens, symbionts, mutualists, dispersers, pollinators have all changed dramatically. Marked filtering and selection of 'response traits' in an evolving Earth may in turn have changed the forcing strength or capacity of plant traits to have an 'effect' on processes within their ecosystems. For instance, increasing atmospheric CO_2 in the earliest Jurassic selected for plants with lower stomatal conductance (g_{max}). Changes in g_{max} trait values halved evapotranspiration rates of early Jurassic forests impacting run-off in the hydrological cycle, a key Earth system process

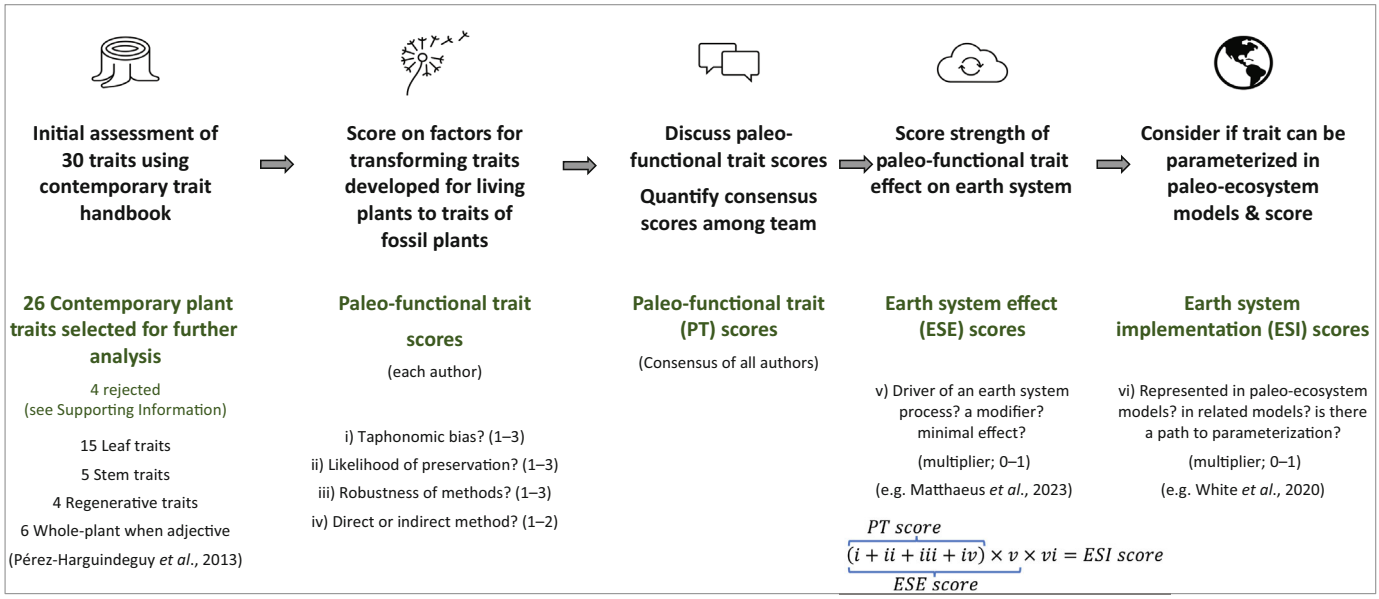

Fig. 1 Methodological framework used to critically evaluate 30 contemporary plant traits (from Pérez-Harguindeguy *et al*., 2013) for their potential application to the plant fossil record as paleo-functional traits. Four traits (leaf water potential, leaf dry matter content, leaf and litter PH, and seedling functional morphology, see Supporting Information Notes S1–S7) were deemed to have low potential applicability to fossil plants and were not evaluated beyond the initial assessment step. The 26 remaining traits were reviewed (Sections V–VII) and semi-quantitatively evaluated by the authors to produce an initial list of paleo-functional traits (Table S1), which we then ranked according to taphonomic bias (i, ii), ease and robustness of trait measurement in fossil plants (iii, iv), strength of the trait's impact on the Earth system (v) and capacity to quantify the impact of the trait on an Earth system process within paleo-ecosystem models (vi; Figs 3, 4).

(Steinthorsdottir *et al*., 2012). We propose, therefore, that a paleo-functional trait approach in paleobotany will provide an improvement to the representation of vegetation–ESM interactions that is evidence-based, provides testable hypotheses, and is scalable. For example, a linear multiplier has historically been used to account for enhanced plant-driven chemical weathering over geological time (reviewed in Goddéris *et al*., 2023). This assumption could be tested using fossil functional traits that likely influence weathering rates such as photosynthetic rate, litter decomposability, and xylem conductivity and by tracking changes in their trait values over time. Terrestrial productivity exerts critical influence on the carbon and nutrient cycles (N, P; Lenton *et al*., 2018), in large part via weathering rates, and is hypothesized to have undergone step-change increases over geological time with more recently derived plant groups (angiosperms) generally being more productive than their ancestors (gymnosperms; Boyce & Zwieniecki, 2012; Boyce *et al*., 2023). These ideas, however, are challenged by the observation that long-extinct plants (Carboniferous) had similar rates of photosynthesis and transpiration as modern angiosperms (Wilson *et al*., 2017, 2020; Yiotis & McElwain, 2019) and are ripe for further testing using multiple paleo-functional traits – but which ones should we focus on? The uncertain trajectory of plant functional trait evolution over geological time thereby introduces uncertainty to key Earth system processes (e.g. hydrological cycle and weathering) that exert substantial control on the long-term carbon and oxygen cycles, global temperature, and the habitability of the planet.

A wealth of contemporary ecological studies demonstrates that the functional diversity of plant traits does not map simply to plant evolutionary groups (Diaz *et al*., 2016; Bruelheide *et al*., 2018). Global trait-based ecology has emerged in the field of contemporary ecology as a powerful tool to categorize how plants influence their abiotic and biotic environment based on their morphological, anatomical, chemical, physiological, demographic, and/or reproductive traits rather than their species identity or evolutionary relationships (Wright *et al*., 2004; Cornwell *et al*., 2008; Diaz *et al*., 2016; but see van der Plas *et al*., 2020). A trait-based ecology approach in paleobotany, where species identities are often uncertain compared with contemporary taxonomy, would thus allow the functional characterization of plants, whether long extinct or living, by their functional traits preserved in fossils. In order to critically evaluate the potential of different plant functional traits to inform Earth system science, we have semi-quantitatively evaluated every trait we review in the ensuing sections on the strength of its impact on the Earth system (Earth system effect (ESE) score, Fig. 1) and on the current capacity to quantify this impact using paleo-ecosystem models (Earth System implementation (ESI) score; Fig. 1).

III. Taphonomic constraints for a paleo-functional trait approach

A tree fell in a forest 200 million years ago; no one was there to observe it. Depending on plant type and circumstances, we might

still infer how it functioned based on its traits. The plant fossil record is mostly composed of fragmented plant parts (e.g. spores, seeds, leaves, and shoots) that are preserved separately. Broadly, tissue type, preservation mode, and taphonomy (reviewed in Collinson, 1983; Greenwood & Donovan, 1991; Gastaldo, 2001; Ferguson, 2005; Sims & Cassara, 2009) determine the availability of different plant parts on which functional trait measurements can be obtained. Furthermore, each combination of tissue type, preservation mode, and trait requires a unique set of considerations regarding the bias of the resulting trait values (Fig. 1). All fossil preservation types depend on the presence of water, introducing a taphonomic mega-bias favoring plants that grew in or near wet locations or that can survive transport by water to a depositional environment (Ferguson, 2005). Furthermore, because fossil preservation is a rare outcome, robust estimates of the distribution of trait values, and extreme values (i.e. maxima) are likely unavailable most of the time, and require exceptionally preserved floras where thousands of fossil plant parts, including the most delicate (e.g. fossil flowers, pollen tubes, and fern fiddleheads), are available for study. In combination with fragmentation, taphonomy also makes disentangling trait variation from development difficult but not impossible. Part of the solution to the filtering of original trait values by the fossil record is integrating an understanding of the taphonomic factors that transform a living community of plants at some past instance in geological time to a dead assemblage of fossil plant parts, each with their measurable trait values. Taphonomic processes are very well understood for fossil plants and what is required now is that this field is extended to explicitly consider functional traits.

Most often, plant parts are preserved when they are buried quickly, enter anaerobic conditions that hinder decomposition, and are then further altered where the sediment around them becomes rock. This produces compression fossils when original organic material remains, and still-valuable impression fossils when the original matter is lost. Compression/impression fossils allow for the measurement of gross morphological trait values, but deformation due to compression may alter individual traits. Chemical traits may be measured from compressions, though they may be altered in diagenesis (Box 1; Ferguson, 2005) and biased by fossilization potential (Spicer, 1989; Tegelaar *et al*., 1991; Bacon *et al*., 2016) likely imposing artifacts in trait values at the plant community/ fossil assemblage scale. This mode of preservation is more likely to preserve tissues that are resistant to fragmentation, deformation, and decomposition, suggesting that functional traits measured from compression/impression fossils will more likely be biased toward trait values of more robust plants and plant parts with dense and/or tough lignin-rich, suberin-rich, or polymer-rich tissues.

In a few special circumstances, anatomy can be preserved in plant fossils. Plant tissues that are flooded with mineral-saturated water or inundated *in situ* by volcanic ash falls (e.g. Wuda Tuff flora), or partially burned in forest fires produce permineralization (see Box 1) and charcoalified fossils, respectively (Schopf, 1975; Wang *et al*., 2012). These allow measurement of cellular-scale and morphological traits that can be obtained with minimal alteration due to deformation but in most cases, little unaltered organic material remains, precluding ready access to functional traits based on plant chemistry or stoichiometry. Permineralization of fossils allows preservation with less fragmentation, and occasionally of

Box 1 Definition of terms.

Demographic traits: vital rates for the processes of growth, survival, and reproduction that are calculated at a population level. Demographers use life-history traits measured at population levels to model complex attributes of vital rates such as lifespan and maximum age at reproductive maturity.

Diagenesis: the physical and chemical alterations to plants and plant parts and their surrounding sediments that occur during the process of fossilization (before deep metamorphic processes under high temperatures and pressures) and ultimately determine whether the plant/ plant part and its trait values are preserved or destroyed.

Fossil plant (paleo-) functional traits: a measurable property of a plant fossil that is inferred to have influenced the function of the plant while it was alive, and which likely affected its environment or its fitness. These inferences are usually made through relationships between structure or chemistry, and plant function that have been established, and continue to be developed in modern plants.

Fossil plant preservation modes: types of plant fossil preservation are determined by the matrix type (and grain size) the fossil is embedded in as well as the specimens' paleoenvironmental setting. There are six broad preservation categories. Those of two-dimensional preservation are compressions and impressions (Schopf, 1975); the latter lacking any remaining organic material. Three-dimensional preservations are permineralization, casts/molds, and compactions, with permineralizations lacking organic material (except cell walls) as the plant tissue is infiltrated by mineral deposits during formation. These modes have been abundantly described in the literature by case-to-case scenarios and much descriptive work was initially addressed by Schopf (1975). Lastly and of more recent application, molecular preservation retains organic compounds though lack structural remains.

Life-history traits: metrics or quantities that are integrated over a plant's life cycle and usually calculated at population levels (e.g. maximum age at reproductive maturity). Some life-history traits can also be considered as plant functional traits when measured at the level of individual rather than population. Our focus here is on those which can be measured on individuals.

Plant functional traits: broadly defined as any measurable morphological, anatomical, physiological, biochemical, or phenological trait of an individual plant that potentially affects its environment or its fitness (from Pérez-Harguindeguy *et al*., 2013). For the purpose of this review, we focus more on plant functional traits which affect their local, regional and/or global environment (Chapin 3rd's (2003) 'effect' traits) as these are important for Earth system modelling (*sensu* Lavorel *et al*., 2007) in the present and past (Matthaeus *et al*., 2023).

Taphonomy: the fossil record of plants presents a biased representation of living vegetation that once existed. Taphonomy is defined as the processes and factors involved in the transformation of these once-living plant communities to an assemblage of fossil plants preserved within the rock record. According to Greenwood & Donovan (1991), 'plant taphonomy incorporates the processes of the initial abscission of plant parts, their transport (by air and/or water) to a place of eventual deposition, entrapment and eventual burial, and subsequent lithification'.

Trait syndrome: suite of consistently coordinated/correlated traits that occur across multiple scales of biological organization and environmental gradients that result from evolutionary processes (e.g. plant flammability, litter decomposability, and photosynthetic pathway).

herbaceous plants and delicate structures, depending on the process of initial burial. In some exceptional cases, for example, the Rhynie Chert (Trewin, 1994) and Chemnitz Fossil Forest (Rößler *et al.*, 2012) communities are preserved in growth position, allowing measurement of multiple functional traits from the same fossil plant, and whole plant traits in an ecosystem context. In sections V–VIII, we evaluate the research potential of reproductive, leaf, stem, and whole fossil plant functional traits in the context of some of the biases and limitations imposed by preservation mode and taphonomy (i and ii in Fig. 1).

IV. Methodological constraints for a paleo-functional trait approach

The form, development, and taxonomy of plants are increasingly uncertain for extinct plants in deep time. Whereas modern plant ecologists generally begin their investigations with whole plants of known species, plant paleobiologists must start from plant parts. Understanding plant form from a mostly fragmented fossil record requires conceptual reconstruction of plants from fossils containing attachments of one organ to a different kind of organ (e.g. a shoot with an attached seed). Whole plant reconstructions represent a best-case scenario, requiring a comprehensive collection of attachments, often from different fossiliferous beds (e.g. Matsunaga & Tomescu, 2017). The core experimental grouping of the plant paleobiologist, therefore, is not an individual plant, but the plant part available to measure. Furthermore, the co-variation of traits in whole plants is generally unavailable on an individual fossil specimen due to fragmentation and separation of stems, leaves and fruits due to taphonomic processes (Box 1). However, information on the co-variation of traits is often available within a fossil assemblage at the bed level where tens to thousands of different plant organs that originally occurred as litter within the living community are preserved in the same relative abundance ranking as was present in the living vegetation (Burnham *et al.*, 1992). Fossil plant assemblages of this nature enable deep investigation into trait variance within- and between species, assessments of appropriate sample sizes needed to achieve stable trait means, and ultimately the calculation of community-weighted mean trait values.

The limitations of using a paleo-functional trait approach are considerable and multifaceted. Nonetheless, plant fossils represent the one ground-truth record of the foundation of terrestrial ecosystems across deep time. Inferences of trait values from fossil plants may be made more robust by combining estimates from multiple plant parts and using direct measurement alongside biophysical and biochemical relationships between sub-tissue properties and function (e.g. C3/C4 photosynthetic pathways may be distinguished directly using anatomy when it is preserved, and indirectly using C isotopic signatures). Furthermore, the integration of contemporary plant ecology regarding trait trade-offs and economics with the plant fossil record allows for the inference of additional trait values by analogy or through observed trait–trait correlations. For example, six leaf traits (photosynthetic capacity (A_{mass}), dark respiration rate (R_{mass}), leaf mass per area (LMA), leaf lifespan (LL), leaf nitrogen (N_{mass}), and phosphorous content (P_{mass})) co-vary strongly in contemporary global datasets across thousands of species and climate zones; they collectively describe the 'leaf economic spectrum' – the economics of constructing and maintaining a leaf and the trade-offs involved (Wright *et al.*, 2004). Because correlations between some functional traits are so well constrained for extant plants, this opens a window of possibility in paleobotany to infer traits that cannot be measured in fossils, such as P_{mass}, from those that can using multiple methods (e.g. LMA; see leaf economic traits). Variation in trait inferences may then be studied across scales (i.e. within and among fossiliferous bed, horizon, region, biome, and age) to form a picture of vegetation–climate interactions across deep time. We take these methodological considerations (iii and iv in Fig. 1) into account in a semi-quantitative evaluation of every trait in the following sections to ultimately calculate a '-Paleo-functional trait score' for each trait we review. A ranked list of paleo-functional traits is finally produced in the conclusion section by weighting Paleo-functional trait scores for each trait by its ESE and Implementation Scores (see Fig. 1).

V. Functional traits of fossil spores, pollen, and seeds

1. Spores and pollen

The study of functional traits of fossil pollen and spores provides key insights into persistence and resilience of plants, fungi, and ecosystems under environmental change, in particular drought (Abrego *et al.*, 2017; Brussel *et al.*, 2018; Sande *et al.*, 2019; Table 1) as well as inferences on dispersal syndrome and pollination success. Thicker spore walls in forest edge fungi are likely linked to UV-light tolerance, and/or harsher environmental conditions (Norros *et al.*, 2015; Abrego *et al.*, 2017) and habitat characteristics (e.g. moisture) have likely played a substantial role in the evolution of pollen morphology (Ackerman, 2000; Franchi *et al.*, 2011). The presence of pollen wall apertures is related to environments characterized by dry seasons or occasional droughts (Franchi *et al.*, 2011). Although much pollen trait-based research to date tends to be reliant on recently collected data (*c.* 20 yr; Franchi *et al.*, 2011; Nogué *et al.*, 2022), several studies have shown the importance of the incorporation of paleo-ecological and paleontological data into trait frameworks to understand plant performance, fitness, and/or functioning (Reitalu *et al.*, 2015; Brussel *et al.*, 2018; van der Sande *et al.*, 2023). The microscopic size of pollen and spores and their low taxonomic resolution create a challenge to their incorporation as functional traits into global trait analysis. However, potential methodologies have been proposed (reviewed in Reitalu & Nogué, 2023; Table 1). Taphonomic biases in the pollen and spore record are very well constrained compared with other fossilized plant parts, and there is a high likelihood of their fossilization. For these reasons, together with a high potential for direct measurement of trait values from pollen and spores, we attributed a relatively high overall Paleo-functional trait score to spores and pollen (10) (Fig. 3; Table S1). However, lower ESE (3) and ESI (0.3) scores were however assigned (Fig. 1), because although dispersal is a key determinant of biogeographic units, which in turn influence climate and biogeochemical cycles, realized dispersal also relies on vegetative traits. Furthermore, dispersal is

Table 1 Functional traits of fossil pollen.

Trait	Life history/ dispersal syndrome*/climate preference Trait description in relation to drought tolerance and dispersal
Pollen size Small (S), 10–25 μm Medium (M), 26–50 μm Large (L), 51–100 μm	*Tolerance to drought*: Larger pollen grains should have an advantage over smaller ones when desiccation intensity increases: to minimize the rate of water loss due to desiccation, a plant produces larger grains that also have a lower surface-to-volume ratio (Ejsmond *et al*., 2011) *Dispersal*: We expect small and medium pollen grains (e.g. 20-40 μm) to disperse better than those with larger pollen grain (> 40 μm; Vonhof & Harder, 1995). We also expect that small and medium pollen grains to be wind-pollinated and that larger pollen grains to be mostly animal-pollinated. But this is controversial. Smaller sizes are suggested to reduce the settling velocity and, thus, increase the dispersal distance of the pollen (Niklas, 1992). However, various mechanisms exist to increase dispersal distances by reducing pollen mass, such as the presence of air sacs of many conifers (Ackerman, 2000; Schwendemann *et al*., 2007) Pollen size has been found to be affected by chromosome ploidy level, environmental factors, and flower characters, among others (Muller, 1979; Stroo, 2000) and may determine reproductive and seed-siring success as large pollen grains have higher chances of successful fertilization because their size determines the growth rate of pollen tubes (Cruzan, 1990; Ejsmond *et al*., 2011)
Shape oblate, prolate, spheroidal	*Dispersal*: There is evidence that suggests that spherical pollen grains are more present in wind-pollinated plants (Niklas, 1985b; Vaknin *et al*., 2008). In addition, spherical pollen grains dispersed further (Niklas, 1985b; Jackson & Myford, 1999; Ackerman, 2000). The relationship between oblate and prolate pollen grain shapes and dispersal type is not clear. Pollen shape does not seem to play a major role in preferences of forage sources (e.g. honeybees on *Gossypium Hirsutum*; Vaissière & Vinson, 1994)
Aperture types and number Innaparture (0) Colpate (1, 2, 3, > 3) Porate (1, 2, 3, > 3) Colporate (1, 2, 3, > 3)	*Tolerance to drought*: Pollen tolerance to drought may be indicated by the presence of apertures (furrows, pores; Fig. 2; Moore *et al*., 2008, Franchi *et al*., 2011). Apertures are structural elements that allow variation in the pollen volume with changing moisture conditions (Franchi *et al*., 2011) Pollen grains with low desiccation tolerance ('recalcitrant') and furrows are usually absent and there may be an absence of pores (Franchi *et al*., 2011). Recalcitrant plant species are more likely to occur in moist habitats. Pollen grains with high desiccation tolerance ('orthodox'), furrows are usually present
Presence of sculptures (exine) Psilate, Perforate (micro- and macro-); Reticulate; Rugulate; Striate; Gemmate; Verrucate; Echinate	*Dispersal*: Pollen wall sculptures (e.g. perforate, reticulate, and rugulate) may be affected by pollination syndrome (reviewed in Hesse *et al*., 2000; Konzmann *et al*., 2019). Rich ornamentation is associated with entomophily (Vaknin *et al*., 2000; Hu *et al*., 2008). Sculpturing plays an important role in attachment to insect pollinators and to the stigma of the flower Wind-pollinated species often lack elaborate sculptures and appear smooth (i.e. psilate). But, this is controversial as the presence of sculptures on the pollen wall is suggested to be a specific feature for each plant taxon (Pacini & Hesse, 2012)
Dispersal unit (e.g. monad, tetrad)	*Dispersal*: Pollen grains are generally dispersed as monads (single grains) and tetrads (four grains derived from the same meiocyte; Pacini & Franchi, 1999). In addition, some pollen grains present a fluid called pollenkitt. This fluid glues the pollen grains together and forms clumps of both monads and tetrads (e.g. Ericaceae) Monad pollen is a common characteristic for both entomophilous and anemophilous taxa (Chaloner, 1986). However, pollenkitt is typically present in almost all zoophilous plants (Pacini & Hesse, 2005)
Wall thickness (exine) < 2 μm > 2 μm	*Tolerance to drought*: The function of the wall is considered to be mainly protection against adverse environmental conditions such as desiccation and UV radiation (found in fungal spores also). Reduced wall thickness has been considered to be an advantage for taxa living in humid, moist, or even wet environments. The advantage consists of a rapid germination due to the short rehydration time (Pacini & Hesse, 2012)

Terminology used for the six pollen traits (pollen size, shape, apertures, sculptures, dispersal unit, and wall thickness) follows the Palynological Database-PalDat (https://paldat.org) and Halbritter *et al*. (2018).
*We use the concept pollen dispersal to refer to how far for example airborne pollen grains may travel before being deposited (Yao *et al*., 2022).

not currently parameterized within paleo-ecosystem models. Furthermore, many of the key functional traits conferring resilience to drought highlighted below (Table 1) are stronger 'response' traits than 'effect' traits.

2. Seed size and shape

Here, we consider the traits of seeds as they enter the soil or a suitable depositional environment and do not include the fruit or dispersal structures (Fig. 2) associated with the seed as these are much less likely to be preserved in the fossil record. There is an enormous (11 orders of magnitude) variation in seed size among extant plants (Moles *et al*., 2005a). Still, biases imposed by the fossilization process and factors that influence the movement of seeds into suitable depositional environments are all likely to filter the full range of paleo-seed diversity (Sims & Cassara, 2009). Despite the fact that the fossil record is imperfect, the function of seeds to protect and transport the embryo means that of all plant parts, seeds are very well represented as fossils. Seed size is one of six plant traits selected for its global significance in defining the functional bauplan of extant plants (Diaz *et al*., 2016); it defines a trade-off between the seedling survival and colonization potential and is strongly correlated with plant height (Diaz *et al*., 2016). Seeds are usually discrete units but there are exceptions. Seed size, shape, and structure, especially, have been shown to be good indicators of seed persistence in the soil in some biomes

(Thompson *et al.*, 1993; Diaz & Cabido, 1997; Leishman & Westoby, 1998; Peco *et al.*, 2003), which in turn plays a major role in the survival of species in time and space (Christoffoleti & Caetano, 1998). For example, rounder seeds with lower shape values (closer to 0 than to 1) tend to be buried deeper into the soil and seed bank and persist longer (Pérez-Harguindeguy *et al.*, 2013). Interestingly, small seed size is likely underrepresented in the fossil record (Sims & Cassara, 2009), and fossil seed

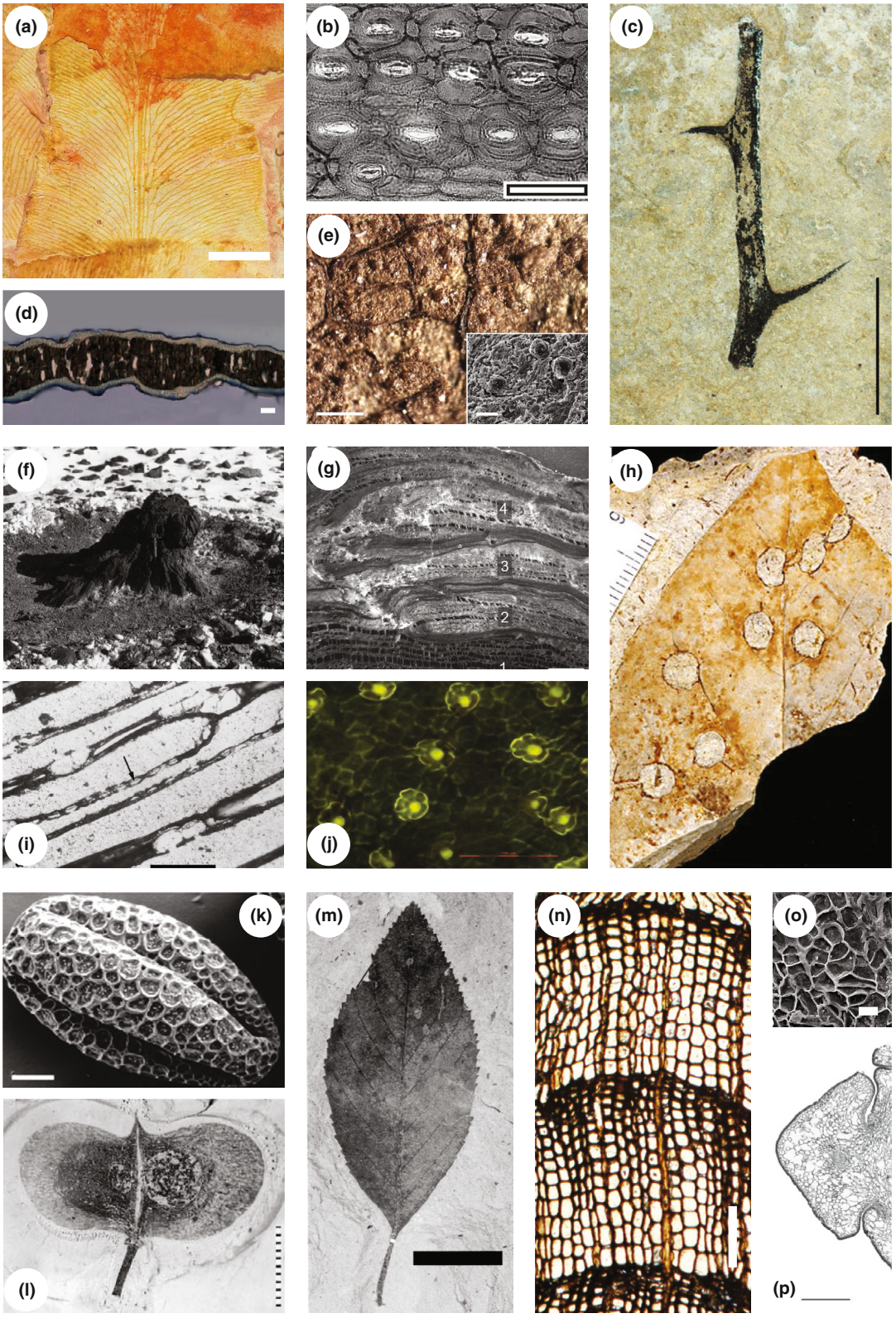

Fig. 2 Examples of fossil plant functional traits. (a) Vein density trait illustrated for Permian *Glossopteris* from Esperança Júnior *et al*. (2023, reused with permission) Bar, 5 mm. (b) Leaf g_{max} trait (a function of stomatal density and pore geometry) illustrated on Cretaceous aged Podocarpaceae compression fossils (Pole & Philippe, 2010, reused with permission) Bar, 50 μm. (c) Spinescence trait (SI) illustrated for Eocene fossil twigs from Tibet (Zhang *et al*., 2022, reused under the terms of a CC-BY 4.0 license) Bar, 10 mm. (d) Leaf mass per area (LMA) trait illustrated on cross-section of Jurassic fossil *Ginkgo* leaf estimated from measurements of cuticle thickness (Soh *et al*., 2017, reused with permission) Bar, 10 μm. (e) Salinity trait illustrated by the ghost presence of CaOx globules (interpreted as druses) on late Oligocene aged *Quercus neriifolia* impression fossils (Malekhosseini *et al*., 2022, reused under the terms of a CC-BY 4.0 license) Bar, 200 μm, inset = 40 μm. (f) Plant height trait can be estimated from fossil trunk diameter on *in situ* fossil tree stumps such as illustrated from the Triassic of Antarctica (Cúneo *et al*., 2003, reused with permission) pen Bar, 14 cm. (g) Bark thickness trait illustrated on Early Carboniferous fossil tree from Australia (Decombeix, 2013, reused with permission) showing successive zones of periderm layers, Bar, 2 mm. (h) Palatability trait measured from the ratio of presence of feeding damage as illustrated by large circular hole feeding on fossil dicot leaf species (Currano *et al*., 2008, reused with permission, copyright (2008) National Academy of Sciences) Bar, 11 mm. (i) Xylem conductivity trait measured from xylem pit membrane (arrow), pit orientation, and abundance shown here on longitudinal sections of polished pyritized Eocene fossil twigs of *Pityoxylon* (Grimes *et al*., 2002, reused with permission). (j) Cuticle trait illustrated using auto-fluorescent properties of Cretaceous aged Angiosperm cuticles (LK-B-55) from West Greenland highlighting secretory trichomes (pellucid dots; C Fay, JC McElwain, & S Robinson, unpublished) Bar, 100 μm. (k) Pollen trait indicating resistance to drought by the presence of furrows illustrated here for recent *Citrus lanatus* (Franchi *et al*., 2011, reused with permission) Bar, 10 μm . (l) Dispersal syndrome illustrated in winged fossil fruits of Eocene aged *Bridgesia bovayensis* (Manchester & O'Leary, 2010, reused with permission) scale bar in mm. (m) LMA trait based on petiole thickness illustrated for Eocene *Alnus parvifolia* from Royer *et al*. (2007), reused with permission) Bar, 1 cm. (n) Life history and maximum plant lifespan can be indirectly inferred from fossil ring width measurements illustrated here in Jurassic permineralized fossil wood *Protophyllocladoxylon* from Vajda *et al*. (2016, reused under the terms of a CC-BY 3.0 license) Bar, 100 μm; (o) Photosynthetic pathway is a syndrome of traits, one of which, cuticle pegs (spandrels) are observed here on the inner surface of the adaxial leaf epidermis of Cretaceous *Frenelopsis teixeirae* compression fossils (Mendes *et al*., 2010; reused with permission) Bar, 200 μm. (p) Mesophyll conductance (g_m) trait can be inferred from mesophyll cell wall thickness within anatomically preserved fossil leaves as illustrated here in a permineralized conifer scale leaf of *Cunninghamia lanceolata* from Brink *et al*. (2009), reused with permission) Bar, 0.5 mm.

assemblages often contain seeds from species that have travelled long distances and are not therefore representative of the local flora (Collinson, 1983; Burnham, 1990), suggesting considerable taphonomic filtering at play.

In extant plants, seed size (sometimes referred to as mass) is measured by oven-dry mass (Moles *et al*., 2005a; Pérez-Harguindeguy *et al*., 2013) and seed shape is defined by its variance in three dimensions (x, y, z – thickness, width, length; Pérez-Harguindeguy *et al*., 2013). In fossil plants, seed shape can still be defined by its variance in two to three dimensions using a range of microscopy and micro-CT methods (DeVore *et al*., 2006). Once characterized, seed size and shape can be used beyond taxonomic characterization (DeVore *et al*., 2006; Matsunaga *et al*., 2019) and open a window on the functional ecology of the whole plant in the absence of other articulated fossil plant parts. However, taphonomic biases should be considered (Sims & Cassara, 2009). For example, seed mass is strongly correlated with genome size (Beaulieu *et al*., 2007), growth form (Moles *et al*., 2005a,b; Beaulieu *et al*., 2007), dispersal syndrome (Moles *et al*., 2005a,b), plant lifespan (Moles *et al*., 2005b), and weakly correlated with net primary production (Moles *et al*., 2005a). Seed size and shape trait yielded a relatively high paleo-functional trait score in our semi-qualitative analyses (10) but low ESE and ESI scores due to the fact that correlations between this trait and Earth system processes such as photosynthesis are weak and because the functional attributes that correlate strongly with seed size such as dispersal and plant lifespan are not currently parameterized within paleo-ecosystem models (Fig. 3; Table S1).

3. Dispersal syndrome

Dispersal syndromes (Pérez-Harguindeguy *et al*., 2013) are seed, fruit, or spore morphologies (referred to collectively as disseminules) and the associated modifications that enhance the probability of being dispersed away from the parent plant and characterize a distinct mode of dispersal (Hughes *et al*., 1994). Such syndromes are known to facilitate dispersal via flotation in water, by animal consumption, or by wind, among other modes. Dispersal by gravity will be excluded from this review as no specialized adaptations are required for this mode (Castro *et al*., 2010; McLoughlin & Pott, 2019). Where dispersal syndrome can be distinguished based on fossil disseminule morphology, it potentially provides useful insights into fossil species biogeographic limits and biotic interactions within paleo-ecosystems even in the absence of body fossils of the disperser (Robledo-Arnuncio *et al*., 2014; Aslan *et al*., 2019; Wojewódzka *et al*., 2019; Rojas *et al*., 2022).

Dispersal syndrome can be directly inferred from morphological observations of fossils and comparisons with relevant extant examples. Reproductive architectures like the rain-splash cups that accommodate water dispersal seen in liverworts are also found in *Cooksonia*, one of the earliest land plants, although the dispersal syndromes of the spores themselves remain unspecified (Briggs & Crowther, 2008; Murray, 2012; Medina & Estebanez, 2014). Hypothesized plant–insect mutualism is proposed for Permian lycopsid megaspores based on the presences of external starch structures (elaiosomes; Liu *et al*., 2018). Dispersal syndrome at the ecosystem scale can be indirectly inferred from dental adaptations (Norconk *et al*., 1998; Guimarães *et al*., 2008), and coprolites (Habgood *et al*., 2003). Spore phytophagy in insects is hypothesized for some Carboniferous lycopsids (Chaloner, 1984), providing early evidence for the potential evolution of a dispersal syndrome based on plant–animal interaction. Combinations of direct and indirect evidence, seed morphology, and availability, inferred from the coprolite record, have helped identify deep-time frugivore diets (Dutta & Ambwani, 2007) and contextualize ecological shifts in more recent ecosystems (Boast *et al*., 2018; Heinen *et al*., 2023).

Spatial resolution poses a problem for inference of dispersal syndrome. Any disseminule can be transported accidentally via a prevalent dispersal type regardless of the disseminule's adaptive

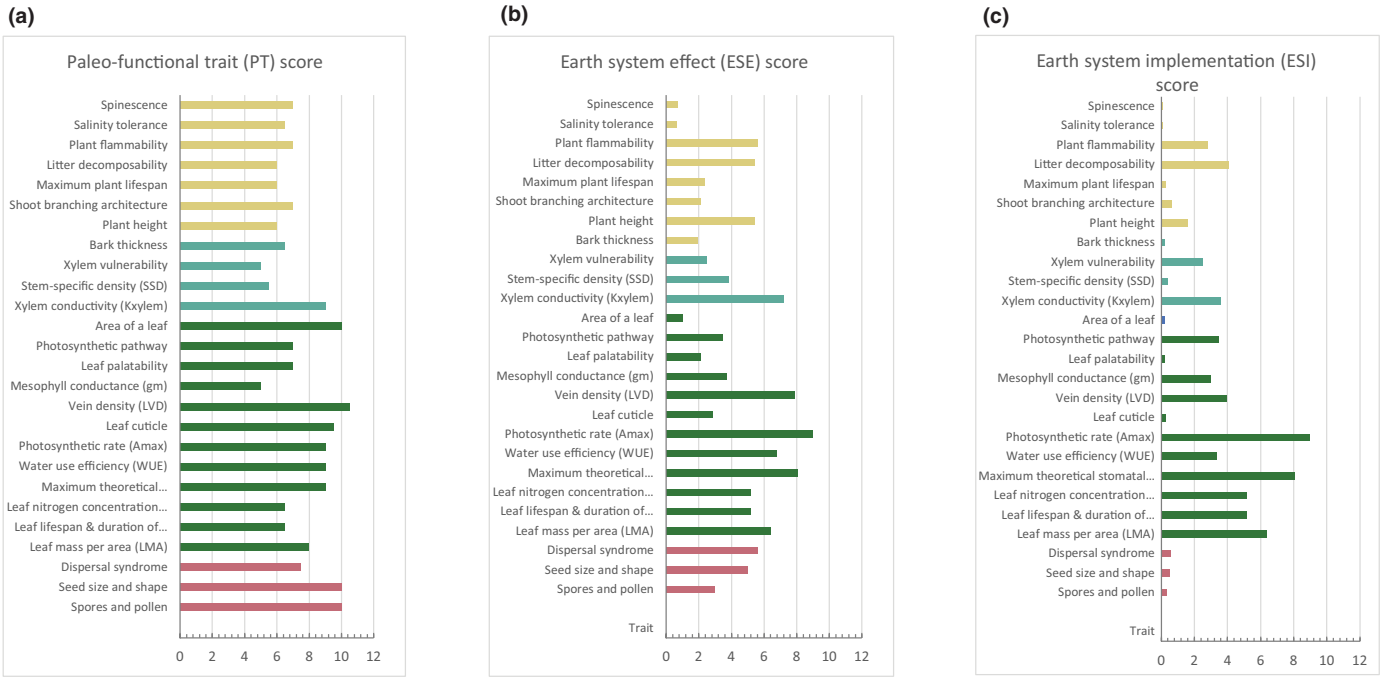

Fig. 3 Comparison of paleo-functional trait scores according to different weighting criteria. (a) Paleo-functional trait (PT in Fig. 1; Supporting Information Table S1) score plots the consensus results of the author team's semi-quantitative evaluation (Fig. 1; Table S1) of how taphonomic bias and methodology of trait measurement influence trait values in fossil plants. Higher PT scores indicate less taphonomic bias and more robust methods of trait estimation. (b) Earth System effect (ESE in Fig. 1; Table S1; ESE = PT × v) score plots the results of the PT score weighted by the author team's semi-quantitative evaluation of the strength of effect of the paleo-trait on the Earth system, with higher scores indicating greater impact. (c) Earth system implementation (Earth system implementation (ESI) in Fig. 1; Table S1; ESI = ESE × vi) score adjusts the results of the ESE score according to the current capacity to parameterize the paleo-trait and its impact on the Earth system within paleo-ecosystem models. Higher ESI scores indicate greater potential application of the paleo-trait to address questions in relation to Earth system processes.

morphology (Pérez-Harguindeguy *et al.*, 2013), and this limitation is magnified for fossils. For example, nonfrugivorous animals consume a wide array of plants and unintentionally disperse fleshy seeds, carrying them long distances regardless of whether the dispersal syndrome is adapted for long or short distances, biasing inferences from the fossil record (Green *et al.*, 2021). Other taphonomic processes such as preburial filtering, reworking, and transport (allochthonous assemblages) can also make the time and place of origin of fossil disseminules unclear. Fossil disseminules may be disintegrated or ruptured, requiring reconstruction, and interfering with syndrome inferences. Nonetheless, evidence of ornamentation or detachment scars from detached fossil appendages (e.g. wings; Fig. 2) can aid in classification (McLoughlin & Pott, 2019). However, even direct morphological inferences of paleo-ecological function may be prone to error (Green *et al.*, 2021). For example, dissimilar fern spore morphologies are anemochorous (Gómez-Noguez *et al.*, 2017), are unexpectedly endozoochorous in certain ecosystems (Lovas-Kiss *et al.*, 2018), and may function in other components of life history (see Table 1). Some important features of dispersal syndromes may be irrecoverable from fossils (i.e. smell, color, sticky textures/substances; Tiffney, 2004). However, successful development of fossil color biomarkers in dinosaur feathers (McNamara *et al.*, 2021) and the observation that nano-surface structures on extant flowers influence petal color (Moyroud *et al.*, 2017) suggest that future advances may allow inference on some of these usually hidden features. In the absence of direct observation of dispersal *per se*, inference of the function of particular structures and dispersal syndromes in the fossil record may therefore be unclear in many cases. This complexity is reflected by the fact that multiple dispersal syndromes have been proposed for some plant groups including Permian *Glossopteris* (Klavins *et al.*, 2001; McLoughlin & Prevec, 2021), fossil *Cycas* (Murray, 2012; Liu *et al.*, 2021), and fleshy seeds in general (e.g. *Ginkgo*; van der Pijl, 1969; Tiffney, 1984; Mack, 2000; Bolmgren & Eriksson, 2005; Del Tredici, 2007; Valenta & Nevo, 2020, 2022). Based on these considerations, we assigned modest paleo-functional trait (7.5) and ESE (5.6) scores for the trait 'dispersal syndrome' and low scores for ESI (0.56), because although undoubtedly the evolution of new dispersal traits through geological time (e.g. the first seed plants in the Devonian and angiosperms in the Cretaceous) influenced biotic interactions and dispersal potential, the 'effect' of such traits on Earth system processes cannot explicitly be quantified within paleo-ecosystem models (Fig. 3; Table S1). This is an interesting research gap that warrants further study.

VI. Fossil leaf functional traits

1. Leaf mass per area

Leaf mass per area (in g m^{-2}), also referred to as specific leaf area (SLA = 1/LMA), is calculated for extant plants by dividing the dry mass by the area of one side of a fresh leaf (Pérez-Harguindeguy *et al.*, 2013). LMA is a leaf economic trait, which, together with LL, leaf nitrogen concentration (LNC), photosynthetic rate (A_{mass}), and respiration rate collectively, reflect the spectrum of ways in which a leaf can be constructed, maintained, and operated as primary photosynthetic structure (Wright *et al.*, 2004; Reich, 2014). LMA is one of the most readily measured and useful plant functional traits within the leaf economic spectrum. Broadly speaking, low LMA leaves such as those of extant deciduous trees (median = 75 g m^{-2}) tend to grow faster, have higher A_{mass} and stomatal conductance (g_s), have less carbon investment in structural tissues, shorter LL, and higher LNC; the corollary is observed for leaves with high LMA such as evergreen gymnosperms (median = 227 g m^{-2}), which invest heavily in structural tissues, have long LLs but the trade-off is lower LNC and A_{mass} per mass (Wright *et al.*, 2004; Poorter *et al.*, 2009). Collectively, leaf economic spectrum traits, including LMA, are important predictors of ecosystem-scale processes such as productivity (Chapin 3rd, 2003; Poorter & Bongers, 2006), decomposition and nutrient cycling (see Decomposition; Cornwell *et al.*, 2008), herbivory (see Leaf Palatability; Currano *et al.*, 2008), and water use efficiency (WUE; Soh *et al.*, 2019). They have already been utilized in fossil plants to infer paleo-life history (e.g. pace of life; Blonder *et al.*, 2014) and whole plant ecological strategy (e.g. stress tolerator, Soh *et al.*, 2019), but such inferences are complex (Kelly *et al.*, 2021; see Section VII).

Fresh leaf area and dry mass cannot be directly measured in fossils due to dehydration, shrinkage, compression, and selective loss of internal leaf tissues that occur during fossilization. Furthermore, taphonomic factors likely strongly bias the fossil record against the preservation of low LMA taxa due to the low abundance of carbon-rich structural compounds resulting in greater mechanical damage during transport to a depositional environment (Bacon *et al.*, 2016). Despite these challenges, numerous independent proxy methods have been developed to quantify paleo-LMA from adaxial epidermal density (Haworth & Raschi, 2014), leaf petiole width (Royer *et al.*, 2007, 2010; Peppe *et al.*, 2014; Fig. 2), and leaf cuticle thickness (Soh *et al.*, 2017; Fig. 2), all of which scale positively with LMA. Multiple trait models that include leaf ^{13}C, petiole width, and epidermal cell area have also been developed to predict paleo-LMA and paleo-canopy position (Cheesman *et al.*, 2020). High LMA leaves have a greater investment in structural tissues, higher densities of smaller cells, larger petioles to mechanically support leaves that have thicker tissue layers (including cuticle), and/or more dense tissue. Application of paleo-LMA methods to fossil plants has enabled functional classification of extinct genera (Soh *et al.*, 2017; Wilson *et al.*, 2017), assessment of extinction selectivity associated with mass extinction events (Blonder *et al.*, 2014; Soh *et al.*, 2017; Butrim *et al.*, 2022), and appraisal of herbivore-plant interactions (Currano *et al.*, 2008) among many others. Not surprisingly, therefore, LMA scored highly as a paleo-functional trait (8) and ESE Trait (6.4) and yielded high ESI scores in our evaluation as it is among a few functional traits currently parameterized in paleo-ecosystem models (Fig. 3; Table S1).

2. Leaf lifespan and duration of green foliage

Leaf lifespan, or the period of time for which a leaf is alive and physiologically active, as well as duration of green foliage, is useful in understanding a plant's nutrient use strategy, life history, leaf decomposability, palatability, and canopy position (Aerts, 1995; Wright *et al.*, 2004). Leaf lifespan covaries with LMA, A_{mass}, and g_s (Wright *et al.*, 2004; Poorter *et al.*, 2009). The duration of green foliage is important in the hydrological cycle, for productivity and Earth albedo effects, and should be included where possible within paleo-ecosystem models (Matthaeus *et al.*, 2023). Shorter-lived leaves tend to show resource allocation toward high photosynthetic rates and have lower investment in C-rich lignified tissues, whereas longer-lived leaves are often lignin-rich and tend to allocate resources toward leaf protection (Reich *et al.*, 1991). Longer-lived leaves decompose more slowly due to a higher proportion of structurally complex tissue, but they tend to sink in water faster than leaves with lower LMA (Greenwood & Donovan, 1991; Gastaldo, 2001). This may provide a taphonomic bias toward leaves with a long lifespan in fossil litter deposits preserved *in situ* (Bacon *et al.*, 2016; e.g. volcanic ash deposits) but toward leaves with a much shorter lifespan in fossil assemblages filtered by transport via water (e.g. lake deposits).

Leaf physiognomy (size and shape) and abscission scars (Thomas & Cleal, 1999) have traditionally been used to characterize whether a fossil leaf is deciduous or evergreen; however, these parameters provide mixed signals in relation to LL. Thick leaves, small leaf surface area, and thick cuticles in combination are typically associated with an evergreen habit (Thomas & Cleal, 1999; Falcon-Lang & Cantrill, 2001), but there are many exceptions and leaf thickness cannot be measured easily in fossils. Entire margins, drip tips, and leaf size are associated with tropical rainforests, which have an evergreen canopy but with varied LL (Burnham & Johnson, 2004). Fossil growth ring anatomy may be a better way to assess LL in fossils; leaf traces within the rings of juvenile stems or branches differ between deciduous and evergreen conifers (Falcon-Lang & Cantrill, 2001). In some cases, anatomically preserved leaf traces can show a number of growth ring increments indicating the longevity of a particular leaf (Falcon-Lang & Cantrill, 2001). However, this method is not widely applicable due to difficulties associated with preservation and sample preparation (Falcon-Lang & Cantrill, 2001). Furthermore, a precise age estimate is not possible for LLs of < 1 yr. The markedness of the growth ring boundary in trunk woods may also be used to estimate LL in anatomically preserved coniferopsids (Falcon-Lang, 2000a,b; Falcon-Lang & Cantrill, 2001), but the method requires well-preserved specimens, which lack growth abnormalities (Falcon-Lang & Cantrill, 2001). Both methods using growth ring anatomy also require the assumption that distinct growth rings represent annual increments, which may not be the case.

The most fruitful route for obtaining LL estimates from fossils comes from leaf trait relationships within the leaf economics

spectrum; in particular with LMA (Wright *et al.*, 2004; Poorter *et al.*, 2009; see LMA section above). While the leaf LL–LMA relationship is significant (positive), it is also noisy, showing a shallower response along an environmental gradient (e.g. increasing aridity, temperature, and irradiance; Wright *et al.*, 2004; Royer *et al.*, 2010). Therefore, it is more appropriate to infer LL from LMA at an assemblage level to avoid over-interpreting LMA estimates of individual taxa (Royer *et al.*, 2010; Soh *et al.*, 2017). Chemical characterization of fossil leaf waxes may also prove useful in the development of novel LL proxies in the future (García-Plazaola *et al.*, 2015; Leide *et al.*, 2020). Large differences are observed between n-alkane abundance in angiosperms and gymnosperms, and within these groups, a higher abundance of n-alkanes is associated with longer-lived leaves (Diefendorf *et al.*, 2011). However, when considered in a broader phylogenetic context, these differences appeared to be less pronounced (Diefendorf *et al.*, 2015). Further work incorporating more detailed descriptors of LL (as opposed to just 'evergreen' or 'deciduous'; Diefendorf *et al.*, 2015), as well as a more comprehensive leaf chemical characterization (Leide *et al.*, 2020) are thus needed. High scores were assigned to LL across all the categories in our semi-quantitative analyses as although taphonomic biases toward certain LL trait values are highly probable, because these biases are well known for different depositional environments, associated errors can be constrained (Fig. 3; Table S1). Overall, the potential of using LL as a paleo-functional trait (score = 5.2) ranked slightly lower than LMA because the methods of estimating LL trait values from fossils are not as well developed as those for LMA despite both traits having equal strength of impact on the Earth system (Figs 3, 4; Table S1).

3. Leaf nitrogen concentration

Leaf nitrogen concentration (LNC) refers to the total amount of N per unit dry leaf mass expressed in mg g^{-1} (or sometimes as % dry leaf mass; Pérez-Harguindeguy *et al.*, 2013). N is essential for protein (such as photosynthetic enzymes) and nucleotide synthesis (Moreau *et al.*, 2019). Despite its abundance in the environment, N is one of the most limiting plant nutrients, often existing as forms inaccessible to plants such as N_2, NO_3^-, and NH_4^+ (Aerts & Chapin, 1999; Jia & von Wiren, 2020). As such, LNC measurements can provide valuable insights into plant ecology and physiology (Chapin, 1980) and it is considered an important plant functional trait. Leaf N concentration correlates negatively with LL (Reich *et al.*, 1992; Wright *et al.*, 2004), positively with A_{mass} (Field & Mooney, 1986; Wright *et al.*, 2004), and negatively with LMA (Wright *et al.*, 2004). These relationships within the leaf economic spectrum represent the trade-off between investment in structural tissue and allocation of N to RuBisCO, though long-lived leaves tend to have lower LNC and vice versa (Wright *et al.*, 2004; Luo *et al.*, 2021).

LNC can be measured directly from extant and compression fossil plant material using elemental analysis (White *et al.*, 2020). Currently, however, the fate of LNC during diagenesis and fossilization is not well known. Loss of internal leaf structures and leaching of solutes during the fossilization process (Haworth & Raschi, 2014) could severely alter the original trait values. Pyrolysis experiments have been used to simulate the chemical changes that take place within leaves due to diagenesis (Mosle *et al.*, 1997) and would be equally valuable to assess the fate of LNC during fossilization. Pilot LNC measurements on compression fragments of Late Pennsylvanian fossil taxa have yielded promising results that plot within the trait values of modern LNC (Matthaeus *et al.*, 2023) and are in line with expectations based on their other paleo-leaf economic spectrum traits but further systematic investigation is required. A likely future challenge in establishing direct protocols for measuring fossil LNC will be to collect adequate amounts of compression fossil material (a minimum of 1 mg of ground-up sample material is required; Aslam *et al.*, 2012). Fossil LNC could also be estimated indirectly using trait relationships with LMA. However, paleo-LMA is also subject to diagenetic effects and reliance on indirect inference could mask the detection of unusual trait combinations that may have arisen during plant evolution but are no longer present in extant plants Based on these considerations, the authors attributed paleo-functional trait, ESE, and ESI scores of 6.5, 5.2, and 5.2, respectively (Figs 3, 4; Table S1).

4. Maximum theoretical stomatal conductance

Maximum theoretical stomatal conductance (g_{max}, sometimes referred to as G_{max} or g_{smax}) is a measure of the total diffusive stomatal area available for the exchange of CO_2 and water vapor into and out of the leaf respectively and assumes that all stomatal pores on the leaf (or photosynthetic stem) are open to their maximum geometry (circle or ellipse). g_{max} can be calculated from extant and fossil plants by combining measurements of stomatal density, stomatal pore length (to calculate maximum pore area), and guard cell width into the equation of Parlange & Waggoner (1970) modified by Franks & Beerling (2009; Fig. 2). Maximum geometry of the stomatal pore is estimated by fitting an ellipse (Lawson *et al.*, 1998) or circle, using stomatal pore length (m) as the long axis (diameter) and m/2 as the short axis. Because all stomata on a leaf surface are never fully open to a maximum circular or elliptic geometry in field conditions, g_{max} is considered a theoretical maximum rate (Dow *et al.*, 2014; McElwain *et al.*, 2016). Stomatal opening behavior is dynamic (Lawson & Vialet-Chabrand, 2019) and patchy (Weyers & Lawson, 1997) across the leaf surface and the degree of dynamism, coordination, and patchiness varies across evolutionary groups (Brodribb & McAdam, 2011), meaning that no living plant operates at its theoretical maximum. Extensive field surveys of woody angiosperm trees and laboratory-based measurements of a broad range of evolutionary groups demonstrate that living plants operate (g_{op} and referred to as g_s) at around from 25% (Franks) to 26% (Murray *et al.*, 2020) of their g_{max} value. It is therefore possible to estimate the operational stomatal conductance (g_{op}) of extinct fossil plants to both CO_2 (g_{CO2}) and water vapor (g_{H2O}; 1.6 times g_{CO2}) using the g_{max} trait (McElwain *et al.*, 2016). As functional plant traits, g_{max} and g_{op} provide vital insights into a fossil plant's likely ecological strategy within a paleo-community as g_{op} correlates strongly with photosynthetic rate (reviewed in Berry *et al.*, 2010; Medlyn *et al.*, 2011) and other key traits in the leaf economic spectrum (Kröber *et al.*, 2015) including LMA (Soh

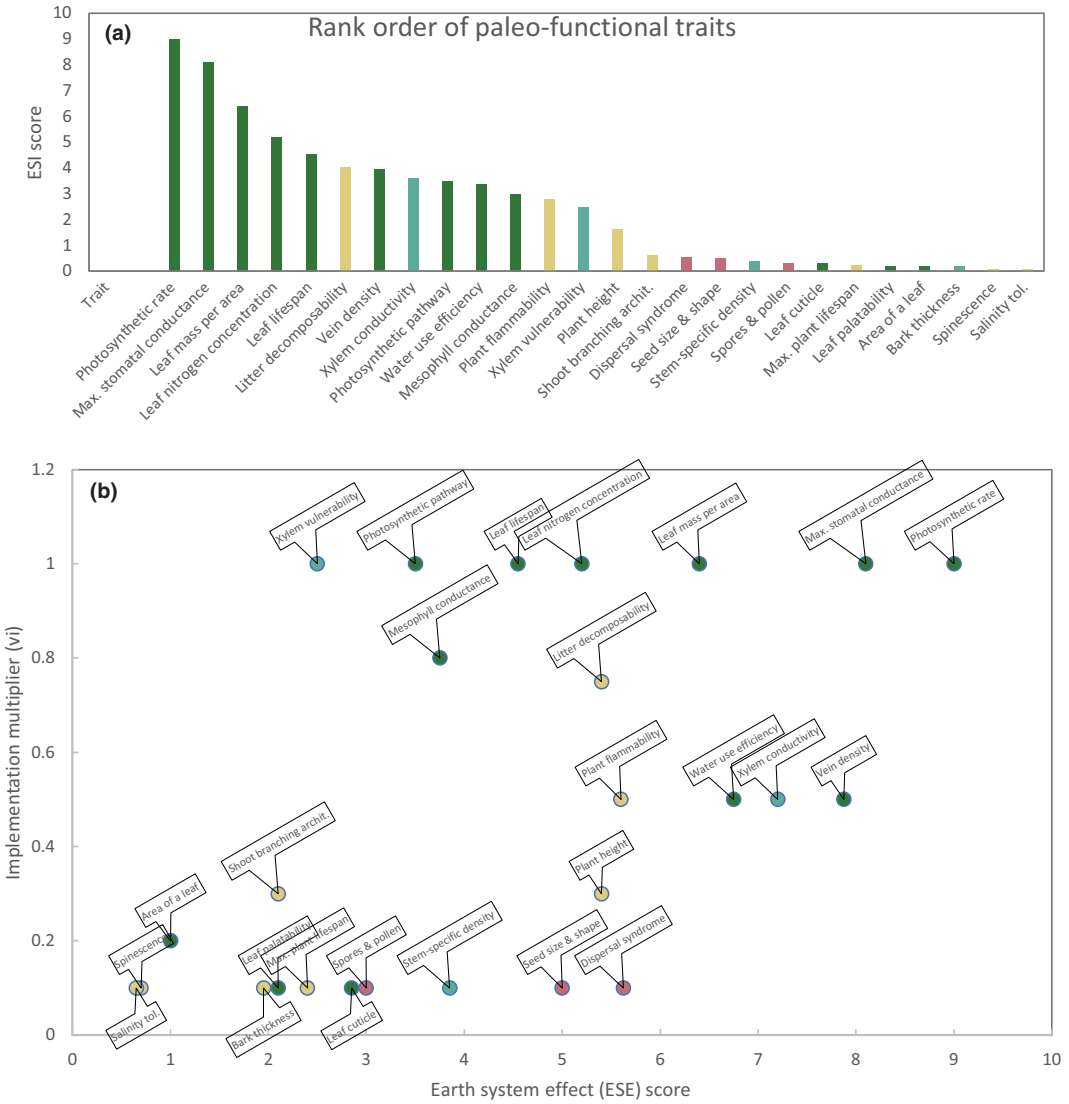

Fig. 4 A ranked list of paleo-functional traits that can be applied to fossil plants. (a) Ranked list of paleo-functional traits based on Earth system implementation (ESI) scores illustrating the rank order of traits with the highest (photosynthetic rate) to lowest (salinity tolerance) potential application to the plant fossil record as evaluated by the author team. (b) Bi-plot illustrating the breakdown of components within the final trait ranking shown in panel a, where the horizontal axis shows the Earth system effect (ESE) score (in Fig. 1; Supporting Information Table S1; ESE = PT × v) and the vertical axis is the implementation multiplier (vi in Fig. 1; Table S1).

et al., 2019; Wu *et al.*, 2020), LNC (Schulze *et al.*, 1994; Juhrbandt *et al.*, 2004), and LL (Poorter & Bongers, 2006), and also whole plant WUE (Soh *et al.*, 2019). Based on the relative ease with which g_{max} can be measured across various modes of plant fossil preservation (McElwain & Steinthorsdottir, 2017) and the fact that it constrains understanding of paleo-productivity (Franks & Beerling, 2009; Wilson *et al.*, 2015; McElwain *et al.*, 2016), the hydrological cycle at local to global levels (Steinthorsdottir *et al.*, 2012; Jasechko *et al.*, 2013; White *et al.*, 2020), and fossil plant WUE (Reichgelt *et al.*, 2020), we evaluate it here as a paleo-plant functional trait with strong potential application to a range of research questions relating to plant–climate and plant–atmosphere evolution and Earth system processes in general (Matthaeus *et al.*, 2023). Paleo-functional trait, ESE, and ESI scores of 9, 8.1, and 8.1 were, respectively assigned (Fig. 3; Table S1).

5. Water use efficiency

Water use efficiency is a measure of how water saving a plant is in relation to photosynthesis. Low values in the 20 to 40 µmol mol^{-1} range are typically observed in modern angiosperm trees of tropical everwet forest biomes while higher values (60 to 80 µmol mol^{-1}) are recorded from desert plants and those from seasonally dry biomes (Soh *et al.*, 2019).Water use efficiency is an informative functional trait in relation to the hydrological cycle and hydroclimate generally in the deep past (White *et al.*, 2020) and allows broad characterization of paleo-biomes from fossil iWUE estimates of dominant taxa within paleo-ecosystems (Matthaeus *et al.*, 2023). Intrinsic water use efficiency (iWUE) is expressed as the ratio of photosynthesis (A) and leaf conductance to water vapor transfer (g) of which g_s is the dominant component. It

can be calculated using stable carbon isotope ratios of modern and fossil plants according to the equation of Farquhar *et al.* (1982) below. However, in the case of fossils both the concentration and $\delta^{13}C_{air}$ of CO_2 cannot be measured directly and need to be inferred from proxies. Furthermore, differential preservation of fossil plant tissue can bias $\delta^{13}C_{plant}$ samples toward lighter or heavier values and must also be taken into account along with other sources of variability (Sheldon *et al.*, 2020). $\delta^{13}C_{air}$ in the geological past is estimated from temperature-sensitive equations (Romanek *et al.*, 1992) applied to measurements of $\delta^{13}C_{calcite}$ of marine brachiopods and their estimated paleo-temperature at the time of growth. Paleo-CO_2 concentration can be obtained from stomatal-based proxies applied to the same leaf or fossils within the same assemblage (McElwain & Steinthorsdottir, 2017) or other proxy CO_2 methods (CenCO$_2$PIP Consortium, 2023).

An isotope ratio mass spectrometer is used to determine the ratio of $C^{13}:C^{12}$ in a living and fossil plant sample ($\delta^{13}C_{plant}$) (Farquhar *et al.*, 1982).

$$\begin{aligned} \text{iWUE} = A/g &= c_a(1-c_i/c_a)/1.6 \\ &= c_a\left(1-\left(\Delta_{plant}-a\right)/\left(b-a\right)\right)/1.6 \end{aligned}$$

where $\Delta_{plant} = (\delta 13C_{air}-\delta 13C_{plant})/1 + (\delta 13C_{plant}/1000)$; c_i/c_a is calculated according to $\Delta_{plant} = a + (b-a)\ (c_i/c_a)$, where a is fractionation due to diffusion in air (=4.4‰) and b is net fractionation caused by carboxylation (=27‰); $\delta^{13}C_{air}$ = the stable isotope ratio of CO_2 in the air at the time the leaf developed; $c_a = CO_2$ concentration of the atmosphere at the time of leaf development.

An alternative method of estimating iWUE of fossil taxa is from model estimates of photosynthesis (A) and stomatal conductance (g_s) (A/g_s = WUE) that can be derived from biochemical proxy CO_2 models (Franks *et al.*, 2014) using a methodology fully described in Reichgelt *et al.* (2020) or inferred from multiple traits that are directly measurable on fossilized stems (stem hydraulic conductance; Wilson *et al.*, 2015) and leaves (vein density (VD) to infer A and G_{max}; McElwain *et al.*, 2016; Murray *et al.*, 2019, 2020) and integrated to get a picture of the whole plant WUE (see detailed discussion in Wilson *et al.*, 2015). Our semi-quantitative analysis of iWUE yielded high paleo-functional trait scores (9) as this trait can be measured using multiple independent methods but lower ESE scores (6.75) because the trait is a ratio, and it is difficult to quantify its impact on the Earth system as this requires disentangling the combined impacts of photosynthesis and transpiration. A lower ESI score (3.37) reflects the fact that the trait is an output of paleo-ecosystem models rather than an input.

6. Photosynthetic rate

The light-saturated CO_2 assimilation rate (A_{max}) represents the theoretical potential of a leaf's photosynthetic capacity. Canopy-scale assimilation, which influences the organic C cycle, is proportional to A_{max} (Wilson *et al.*, 2017). Well-established correlations with other parameters of the world-wide leaf economics spectrum (Wright *et al.*, 2004), such as LMA (see leaf mass per area) and N_{mass} (see leaf nitrogen concentration) allow indirect estimation of A_{max} from plant fossils. The mechanistic model proposed by Franks *et al.* (2014) may also be used to estimate A_{max} from plant fossils based on the photosynthetic activity of a modern ecophysiological analog (A_0) under ambient conditions (C_{a0}), diffusive estimates of g_{max} (see Section V), and c_i/c_a as estimated from fossil carbon isotopes. Methods of estimating paleo-functional trait values which do not rely on the use of, or comparison with, modern ecophysiological analogs are preferable, however, especially for extinct species with unusual trait combinations that have no appropriate modern equivalents. Alternatively, A_0 can be indirectly estimated from fossils by measuring leaf venation properties (D_v, D_m; McElwain *et al.*, 2016) and g_{max}. The Franks model relies on a linear correlation between photosynthetic carbon gain and C_a, which may not be physiologically accurate in some cases (McElwain, 2018). This trait was identified as the trait with the highest potential as a paleo-functional trait (score = 9) as it can be estimated from multiple methods and is currently parameterized in paleo-ecosystem models, yielding a high ESI score (9) (Figs 3, 4; Table S1).

7. Leaf cuticle traits

The leaf cuticle membrane is denser than wood (Onoda *et al.*, 2012) and because of its unique acid and enzymatic-resistant qualities is exceptionally well preserved in the plant fossil record (McElwain & Chaloner, 1996). The cuticle of all plants functions to protect the plant against water loss via transpiration (Zeisler & Schreiber, 2016). Although cuticular conductance (g_{min}) is low relative to stomatal conductance (g_{op}), it varies widely among extant plants (Duursma *et al.*, 2019; Slot *et al.*, 2021) and is critical to whole plant function and survival during heatwaves and drought when stomata are closed but low quantities of transpiration water loss still occur. Ultimately, the permeability of cuticle to water molecules and resistance of cuticles to water loss is dependent on both physical and chemical (e.g. waxes) attributes, which can be readily determined in fossils. The chemical composition of waxes and their distribution are considered the most important determinants of cuticular water loss, with long-chain n-alkanes playing a particularly important role (Leide *et al.*, 2007), and both can be measured in compression fossils. Additional cuticular traits can be determined for fossil cuticle samples using their autofluorescent properties (Fig. 2j); these analyses yield chemo-ecological data in relation to plant–insect interactions via chemical signaling to pollinators, seed dispersers, and prey and on secondary metabolites defense against UV-B radiation (reviewed in García-Plazaola *et al.*, 2015; Leide *et al.*, 2020). For example, strong autofluorescence in the blue (emission at 475 nm) under excitation with UV light (360 nm) can signal the presence of UV-protecting compounds such as coumarin (García-Plazaola *et al.*, 2015; Jardine *et al.*, 2019).

Physical cuticle traits including thickness, density, and mechanical properties (tensile strength and modulus of elasticity) vary substantially across evolutionary groups (Onoda *et al.*, 2012) and show strong correlations with whole-leaf functional traits such as LMA and LL. Interesting trait trade-offs have been observed for cuticle alone. For example, cuticle thickness is not correlated with

cuticular conductance, suggesting that thickness does not play a role in reducing water loss; however, thick cuticles have higher tensile strength (Onoda *et al.*, 2012) and are positively correlated with LL. This suggests that thick cuticles contribute to the overall mechanical strength of long-lived leaves (Onoda *et al.*, 2012) and could therefore be a route to estimating LL of fossils from cuticle fragments. Despite the fact that the cuticle membrane of leaves is thin compared with the total leaf thickness, because it is dense, it contributes substantially to overall LMA (Onoda *et al.*, 2012). It is unsurprising, therefore, that cuticle thickness has been developed as a paleo-LMA proxy (Soh *et al.*, 2017; Fig. 2d). Techniques for extracting and observing fossil cuticle are reviewed in Kerp & Bomfleur (2011). The abundance of cuticle in the fossil record and the range of significant functional characteristics that can be inferred for the whole plant from fossil cuticle fragments resulted in a high paleo-functional trait score (9.5) but low ESE score (2.85) because its influence on reflectivity and water relations cannot be easily quantified currently, nor are these attributes parametrized within paleo-ecosystem models (Fig. 3; Table S1).

8. Vein density

Venation architecture shows diverse patterns across different phylogenetic groups and across evolutionary time, applying functional constraints on hydraulic conductance and indirectly on photosynthetic rate, as well as providing mechanical stability (Roth-Nebelsick *et al.*, 2001; Boyce *et al.*, 2009; Pérez-Harguindeguy *et al.*, 2013; Sack *et al.*, 2013). Leaf VD (the length of veins per unit leaf area) is therefore a functional, measurable leaf trait in megaphyll leaves playing an important role in ecosystem processes such as transpiration and productivity. On a global scale, VD influences the carbon and hydrological cycle (Boyce *et al.*, 2009). Vein density shows a high degree of phenotypic plasticity, showing adaptations to resource gradients (e.g. light, nutrient, and soil water availability) and environmental conditions (e.g. humidity and wind speed; Roth-Nebelsick *et al.*, 2001; Sack & Scoffoni, 2013), and emerging work has demonstrated that vein conductivity can compensate for lower VD (Rockwell & Holbrook, 2017). Given these caveats, taphonomic biases should be taken into consideration when measuring VD traits in the geological past. The paleobotanical record is biased toward the preservation of certain leaf types (e.g. sun leaves) and toward the preservation of plants growing near lacustrine or fluvial environments (Van der Burgh, 1994; Ferguson, 2005). As VD is affected by both light and soil water availability, these taphonomic factors may lead to an overrepresentation of certain vein network traits in the fossil record. These can be controlled for, in part, by using proxies for leaf canopy placement such as epidermal undulation index (Kürschner, 1997), leaf ^{13}C (Carvalho *et al.*, 2021), and number of vein endings per leaf perimeter (Boyce, 2009).

Vein density is measurable on compression/impression leaf fossils and has been used extensively in taxonomic work and to infer paleoecophysiology (Uhl & Mosbrugger, 1999; Boyce *et al.*, 2009; Boyce *et al.*, 2010; Esperança Júnior *et al.*, 2023; Fig. 2a). VD can also be estimated on cross-sections of anatomically preserved leaf specimens from trait correlations with interveinal distance (Uhl & Mosbrugger, 1999). However, this is a less reliable parameter than leaf vein length per area (Uhl & Mosbrugger, 1999). Relatively unaltered fossil leaf remains can be prepared for VD measurements by clearing, following similar methods for modern material (Dilcher, 1974; Evans-FitzGerald *et al.*, 2016). For compression/impression fossils, various photography and lighting techniques can be employed (Kerp & Bomfleur, 2011) as well as latex or silicone molds (Barbosa & Muchagata, 2021) and transfers (Dilcher, 1974; Kouwenberg *et al.*, 2007). Vein density can be measured from photographed fossil specimens using digital tracing in image processing software provided there is sufficient contrast between the leaves' nonvenal tissue and vein network (Sack *et al.*, 2014). Additional difficulties can be caused by the surrounding matrix not being sufficiently fine to preserve small morphological features.

A denser vein network provides greater mechanical stability (Roth-Nebelsick *et al.*, 2001). Therefore, VD may be useful to consider in the context of leaf strength and palatability traits (Vincent, 1990; Sack & Scoffoni, 2013). VD measurements are also used to model assimilation rates of fossil plants (Boyce & Zwieniecki, 2012; Blonder *et al.*, 2014; McElwain *et al.*, 2016; Wilson *et al.*, 2017), to reconstruct paleo hydroclimate, to infer canopy position (Carvalho *et al.*, 2021), and to estimate leaf size from fossil fragments (Sack *et al.*, 2012). Vein density may also have some application as a paleo-functional trait in distinguishing different photosynthetic pathways as it is generally higher for C4 than C3 and crassulacean acid metabolism (CAM) plants (Sack & Scoffoni, 2013). Vein networks can however be highly three-dimensional in the succulent leaves of CAM plants suggesting that VD would likely underestimate their conductive capacity (Ogburn & Edwards, 2013). Overall, VD is a thoroughly useful trait and our semi-quantitative assessment yielded high paleo-functional trait (10.5) and ESE scores (7.8) but lower ESI scores (3.9) (Fig. 1) because although this trait is important for the hydrological cycle/productivity, it is not currently directly parameterized within paleo-ecosystem models (Fig. 3; Table S1).

9. Mesophyll conductance

Mesophyll conductance (g_m; mol CO_2 m^{-2} s^{-1}) is the measure of CO_2 diffusion from the substomatal cavity through the mesophyll tissue to the site of carboxylation. Low mesophyll conductance can limit photosynthesis, and its relative importance varies significantly between different phylogenetic lineages and under different atmospheric compositions (Gago *et al.*, 2019; Yiotis & McElwain, 2019). In bryophytes, lycophytes, and in some CAM plants, g_m is the predominant limiting factor in photosynthetic capacity, whereas more evolutionarily recent lineages show a co-limitation between g_m and g_{op} (Males & Griffiths, 2017; Gago *et al.*, 2019; Yiotis & McElwain, 2019). As a functional trait, therefore, g_m has a bearing on the productivity of past ecosystems that depends on prevailing climatic and atmospheric conditions and dominant plant evolutionary group.

It should be measured using multiple different approaches in modern-day plants to obtain robust trait values (Flexas *et al.*, 2013). The principal methods to estimate g_m in living plants include chlorophyll fluorescence and gas exchange (Harley *et al.*, 1992), carbon isotope analysis (Evans *et al.*, 1986), and A/Ci curve fitting

(Ethier & Livingston, 2004), none of which can be applied to fossils. However, anatomical features, such as leaf mesophyll cell wall thickness and exposure of chloroplasts to cell perimeter (S_c/S), play an important role in constraining g_m and have been used as a basis to develop g_m proxies for permineralized and charcoalified fossil plants (Tomas *et al.*, 2013; Veromann-Jurgenson *et al.*, 2017; Carriqui *et al.*, 2019; Fig. 2p).

Anatomical data such as porosity, mesophyll cell width, cell wall thickness, and thickness of mesophyll tissue have also been used to model mesophyll conductance for well-preserved fossils (Roth-Nebelsick & Konrad, 2003; White *et al.*, 2020). However, this type of preservation is exceptionally rare, and anatomically preserved specimens may also have undergone postburial deformation. Furthermore, while there is a good correlation between anatomy-based models and chlorophyll fluorescence/gas exchange approaches for extant plants, there are some discrepancies. Anatomical modelling tends to overestimate g_m in species with high LMA and underestimate it in species with low LMA (Tomas *et al.*, 2013). In addition, uncertainties with anatomical approaches are increased when applied to fossils, as fewer parameters can be directly measured, and must be inferred from extant plants (e.g. using a scaling relationship between S_c/S and mesophyll surface area exposed to intercellular air spaces per unit of leaf area (S_m/S) in White *et al.* (2020)).

Other methods include the use of scaling relationships between g_m and photosynthetic rate (A_n) to estimate g_m from paleo-assimilation rate (see A_n; Niinemets *et al.*, 2009; Franks *et al.*, 2014; Veromann-Jurgenson *et al.*, 2017; Gago *et al.*, 2019), carbon isotopic technique which require measurements of g_{max} and $\delta^{13}C$ of a leaf fossil and $\delta^{13}C$ of the prevailing atmospheric CO_2 (Pons *et al.*, 2009), and neurofuzzy logic model approaches for defining g_m from the inputs of leaf hydraulic conductance (K_{leaf}) and LMA (Flexas *et al.*, 2013). Isotopic approaches may be too difficult to resolve in the fossil record given that discrimination by g_m is so small compared with other drivers of variability in leaf $\delta^{13}C$. In the case of the latter method as more traits (K_{leaf} and LMA and VD) are required to model g_m and those traits are typically observed in different fossil plant preservation modes, they may have weak predictive power (Flexas *et al.*, 2013). Given some of the limitations to inferring g_m in fossils and its indirect impact on the Earth system (via photosynthesis), our analysis yielded relatively low scores for the g_m trait across all of the indicators developed (Fig. 3; Table S1).

10. Leaf palatability

Leaf palatability is one of the most widely studied functional traits in fossils (Royer *et al.*, 2007; Currano *et al.*, 2008). It is important for understanding biotic interaction, ecosystem productivity, and nutrient recycling in the deep past because palatable leaves are usually more nitrogen-rich (Currano & Jacobs, 2021). In modern plants, palatability is the measure of a model herbivore's preference for the leaves of certain plants, or the proportion of leaf area eaten (Dostalek *et al.*, 2020). This preference is affected by numerous underlying leaf-quality traits (Pérez-Harguindeguy *et al.*, 2003, 2013). The suite of leaf traits that influence palatability also affect decomposability due to their similar constraints (low LNC, high concentration of lignin, and secondary metabolites); as a result, they are positively correlated (Grime *et al.*, 1996; Pérez-Harguindeguy *et al.*, 2013). There is a correlation between LMA and palatability: high LMA has been linked to lower nutrient concentrations and tougher leaves, which makes them less palatable to herbivores (Coley & Barone, 1996; Wright *et al.*, 2004; Royer *et al.*, 2007; Currano *et al.*, 2008).

It is important that herbivory damage in fossils is first distinguished from detritivory before palatability measurements are undertaken (Labandeira & Allen, 2007), as palatability only concerns the former. The four main criteria used to differentiate between the two are reviewed in Labandeira (1998). Palatability is quantified by the percentage or ratio of leaf area consumed vs total leaf area and then compared between species (Pérez-Harguindeguy *et al.*, 2013; Dostalek *et al.*, 2020). Williams & Abbott (1991) proposed using the total proportion damaged for a tree or stand instead of the average proportion damaged:

$$\mathrm{TPD} = \sum_{i=1}^{n} D_i / \sum_{i=1}^{n} T_i,\ D = \text{Damaged area},\ T = \text{Total area}$$

Alternatively, for fossil leaves, Currano *et al.* (2008) calculated the ratio of leaves with/without feeding damage instead of measuring the consumed leaf area ratio. This metric can be compared among fossil species for assemblages with diverse and well-preserved fossil floras, and between assemblages from the same depositional environments and likely similar taphonomic filtering of palatable/unpalatable leaf categories. The Currano *et al.* (2008) method is better suited to paleobotanical studies due to the general incompleteness of the fossil record and because true preference tests on leaf palatability cannot be undertaken for extinct herbivores.

On average, gap demanders are more palatable than shade-tolerant plants, due to lower concentrations of tannins, lower tensile strength, and lower fiber content (Coley, 1987), whereas taxa with high LMA and LL are more well-defended (Wright *et al.*, 2004). Ultraviolet-B absorbing compounds can also make plants unpalatable (Liu *et al.*, 2023) and because UV-B dosage has changed dramatically in the geological past, especially at mass extinction boundaries and before the establishment of an ozone layer, it is important to couple palatability traits with those that allow inferences on canopy position (e.g. Carvalho *et al.*, 2021) and UV-B dose (Jardine *et al.*, 2019). Leaf palatability scored relatively highly in our analysis as a paleo-functional trait (7) because the taphonomic processes which can under- or overrepresent certain leaf categories in the fossil record are well studied. A lower ESE score was assigned because its impact on Earth system processes is difficult to quantify and implement within paleo-ecosystem models (Figs 3, 4; Table S1).

11. Photosynthetic pathway

There are three well-recognized photosynthetic pathways in terrestrial plants, C3, C4, and CAM, each of which is characterized by a broadly distinctive suite of associated biochemical, physiological, anatomical, and carbon isotopic traits that are collectively

referred to as trait syndromes (reviewed in Sage, 2017; Edwards, 2019, Box 1). CAM and C4 are carbon-concentrating photosynthetic pathways that originated and diversified in the Cenozoic according to molecular clock estimates (Sage, 2017; Edwards, 2019) but may have had multiple pre-Cenozoic origins in extinct lineages (Raven & Spicer, 1996; Green, 2010; Looy *et al.*, 2021). Identifying the likely photosynthetic pathway of fossil plants relies mainly on anatomical (C4, C3, and CAM) and carbon isotopic (C4 and C3) traits; however, these can only rarely be measured from the same fossil sample and distinguishing CAM from C4 in fossils remains a challenge. Determining photosynthetic pathway is important from a functional traits perspective, because as a trait syndrome, it has consequences for overall productivity within the paleo-ecosystem, the timing and magnitude of water flux to the atmosphere (at night for CAM and in the day for C4 and C3), and for both the timing (in the day for C3 and C4 and night for CAM) and optimal conditions for photosynthesis (Sage, 2017; Edwards, 2019). C4 photosynthesis is found in hot, high-light, and dry environments, where photorespiration is increased due to high temperatures, while CAM photosynthesis is found in arid environments where mesophyll CO_2 concentrations are low due to stomatal closure and tissue succulence. In general, C4 plants have higher photosynthetic rates and productivity than C3 plants, while the opposite trend is found in CAM plants (Sage, 2017).

C4 photosynthesis takes place in modified, thickened bundle sheath cells that surround veins, which are rarely observable in fossils. High leaf bundle sheath : mesophyll ratio in C4 plants (Christin *et al.*, 2013; Edwards, 2019) could be indirectly inferred from high vein densities (see section V). C4 plants can also be distinguished from C3 plants based on their distinctive carbon isotopic signatures which range from − 10‰ to −14‰ under modern atmospheric $\delta^{13}C$ values of *c.* −8‰ compared with the C3 plants range of −21‰ to −35‰ (Pérez-Harguindeguy *et al.*, 2013).

Detecting CAM plants in the fossil record is more complex because their C isotopic values overlap with the ranges of both C3 and C4 depending on whether they are obligate (−10‰ to −15‰) or facultative CAM (−10‰ to −30‰; Winter *et al.*, 2015; Edwards, 2019). Extant CAM plants typically have very high LMA values, which overlap with those of evergreen gymnosperms (Poorter *et al.*, 2009). Despite this apparent complexity in definitively detecting CAM in the fossil record, there is a suite of leaf traits associated with obligate and 'strong' CAM plants (i.e. those with C3 + CAM that predominantly use CAM), which are potentially highly recognizable in a myriad of fossilization modes that warrant future coordinated research. These traits are functionally associated with either reducing water loss in arid environments (high iWUE) or facilitating water transport from water storage tissue and veins in succulent leaves and stems that have low leaf and/or stem g_m (Edwards, 2019). They include leaf succulence, long LL, large mesophyll cell size, low stomatal density, low intercellular air space and low g_m, thick cuticles with high hydrophobicity, thick inter-epidermal cuticular pegs (spandrels; Fig. 2o) and intra-cuticular wax and often with Calcium oxalate crystals (druses), 3D leaf venation, leaves that are terete or oblong in cross-section, extra-xylary vascular bundles (xylem and phloem tissue that are grouped into units of vascular tissue occurring in the pith outside of the main grouping of vascular bundles that occur in the stele) and photosynthetic phylloclades (modified flattened, usually photosynthetic, stem that is often subtended by a scale-like leaf; Bernardino-Nicanor *et al.*, 2012; Ogburn & Edwards, 2013; Males & Griffiths, 2017; Edwards, 2019; Niechayev *et al.*, 2019; Fig. 2). The extinct Cheirolepidiaceae conifers that were widespread in saline, arid, and humid environments in the Jurassic and Cretaceous (Gomez *et al.*, 2002; Mendes *et al.*, 2023) possess a number of potential CAM functional traits and may be a good target for further research. This syndrome of traits scored highly as paleo-functional traits and moderately as ESE traits in our semi-quantitative analysis (Fig. 3; Table S1).

VII. Fossil stem functional traits

1. Xylem conductivity

Xylem conductivity (K) is a measure of the capacity of xylem tissue to transport and supply water from roots to leaves. It is considered a master regulator of photosynthesis and plant productivity (Sperry *et al.*, 2008; Brodribb, 2009) and damage to stem water-transport capacity plays an outsized role in plant mortality. Many plants can survive the temporary loss of conductivity in leaf and branch xylem, whereas stem damage can be fatal (Choat *et al.*, 2012). The movement of water through xylem is a function of the anatomy of the xylem conduits and how resistant they are to flow (measured as plant, stem, or leaf conductance) and the negative water potential gradient between soil and leaves (Sperry *et al.*, 2008). As water potential cannot be measured or inferred from fossil plants and multiple studies on extant plants have demonstrated the importance of xylem anatomy for whole plant water movement (Hacke *et al.*, 2004; Pittermann *et al.*, 2005, 2011; Feild *et al.*, 2009, 2011; Schulte & Hacke, 2021), it follows that xylem conductivity (*K*) has emerged as a key functional trait in paleobotany (Cichan, 1986; Wilson & Knoll, 2010). Fossilized xylem conduits provide a timeline on both the evolution of xylem conductivity and on the appearance of novel safety-giving anatomies, which evolved to maintain water flow under changing environmental stressors (Niklas, 1985a; Kenrick & Crane, 1991, 1997; Friedman & Cook, 2000; Edwards *et al.*, 2006; Wilson & Fischer, 2011; Strullu-Derrien *et al.*, 2013; Wilson, 2016; Decombeix *et al.*, 2019; Olson *et al.*, 2021). Fossilized xylem anatomy has also been measured to infer potential vulnerability in water-conducting tissues to drought, aridity, and freezing (Wilson & Knoll, 2010; Matthaeus *et al.*, 2022).

Xylem conductivity (*K*) describes water flow through the vascular system, and it can be expressed on several anatomical or spatial scales. For example, *K* can be expressed as either *Ks* (stem-specific conductivity) or *Kl* (conductivity including selected leaf area measured *Kl* = *Ks*/leaf area : sapwood cross-sectional area) per unit of pressure gradient ($kg\ m^{-1}\ s^{-1}\ MPa^{-1}$) in living plants. Detailed guidance on how to perform measurements of K in living plants can be found in Jarvis & Whitehead (1981), Gleason

et al. (2012) and Pérez-Harguindeguy *et al.* (2013). Although *K* cannot be directly measured in fossil plants, xylem cells are well preserved and common in the fossil record dating back to the early Devonian (Kenrick & Crane, 1997; Kenrick *et al.*, 2012). Moreover, mature xylem conduits are dead cells in living plants; therefore, estimating *K* for fossil specimens is facilitated with less taphonomic filtering than for live tissues. Estimating *K* in paleobotany is broadly achieved by measurements of xylem conduit area, diameter, and length, paired with cell wall morphology/dimensions, while considering decay, and diagenesis (Cichan, 1986; Kenrick & Crane, 1991; Wilson *et al.*, 2008; Strullu-Derrien *et al.*, 2013). Estimations of *K* in all plants are grounded in adaptations of the Hagen–Poiseuille equation (Cichan, 1986; Wilson *et al.*, 2008) and Ohm's Law (van den Honert, 1948), applied at the cellular level rather than per whole plant. This is also ideal for paleobotanical research given the frequent disarticulation of plant specimens (Wilson *et al.*, 2008; Wilson & Knoll, 2010; Wilson & Fischer, 2011; Wilson, 2013, 2016). In these, xylem flow is estimated as conductance on a single-cell scale, where *Ksc* (cross-section conductivity) and *Ksp* (conduit-specific conductivity) represent *K*, normalized by transverse lumen and tracheid wall areas rather than by rate of flow, allowing for quantitative functional comparison of plants across genera independent of individual pressure gradients and environmental conditions.

Ultimately, the objective of representing conductance in extinct plants requires models and theory capable of piecing together the missing and perhaps *unknown* anatomical features of the whole plant. Therefore, a prominent focus in deep-time xylem conductivity studies over the past decade has been the role of pits, their membranes, and how their resistance and safety ultimately impact *K* and xylem transport. Pit membranes and pit apertures are preserved in the fossil record (Fig. 2i), and can be of use in estimating extinct plant hydraulics (Jones & Chaloner, 1991; Duerden, 1993; Wilson *et al.*, 2008; Pittermann, 2010; Wilson, 2013; Matthaeus *et al.*, 2022; Wilson *et al.*, 2023); xylem conductivity scored highly in our semi-quantitative assessment as a paleo-functional trait (9) and as an ESE trait (7.2) but achieved lower scores for ESI because it cannot currently be parameterized in a paleo-ecosystem model (Table S1; Figs 3, 4).

2. Stem-specific density

Stem-specific density (SSD) is the dry mass of a stem segment divided by the fresh volume of the same segment (Pérez-Harguindeguy *et al.*, 2013) and is of primary importance in the herbaceous-woody plant divide in global plant trait variation (Diaz *et al.*, 2016). Most of the carbon in the extant biosphere is incorporated into the stems of woody plants (Zanne *et al.*, 2010), and although the carbon concentration of stems is generally *c.* 50% across species and climates, the total carbon stocks stored in an individual tree is largely a function of the diameter of the tree at chest height and SSD (Chave *et al.*, 2005, 2009). Large-scale changes in SSD over geological time and space therefore influence the long-term carbon cycle. Burial of woody biomass with different SSD values would in turn influence the long-term oxygen cycle by preventing decomposition and oxidation processes. Increased SSD is associated with stem resistance to biomechanical and hydraulic failure (King *et al.*, 2006; Diaz *et al.*, 2016; Meinzer *et al.*, 2016; Fu *et al.*, 2019), at the cost of decreased growth rate due to increased stem carbon requirements. Plants with higher SSD tend to be more resilient to environmental stressors, have lower mortality rates, wider ecological niches, and achieve greater heights. In paleobotany, manoxylic (low SSD), and pycnoxylic (high SSD) wood types correspond to the two end members of the SSD continuum (Galtier & Meyer-Berthaud, 2006), and opportunities remain to tease out finer paleo-ecological strategies of fossil taxa using quantitative proxies for SSD (proposed below). Applying standard techniques for direct measurement of modern SSD (*sensu stricto*) to stem fossils is not possible due to the inaccessibility of fresh volume. Morphological distortions during fossilization (e.g. compression) further complicate the direct measurement of SSD. However, SSD and related quantities like wood density might be reconstructed based on stem biochemistry, anatomy (xylem lumen diameter), and compared with SSD in modern plant taxa to develop paleoproxies for this trait.

Stem-specific density can be decomposed into wood and bark density. These tissues serve different functions and are expected to have different chemical compositions, physical structures, and densities (Pérez-Harguindeguy *et al.*, 2013). In woody plants, structural support is provided by the secondary xylem, necessitating enrichment with biomolecules like lignin, while phloem and stem parenchyma perform biochemical functions, bark protects the tree from water loss, herbivory, and fire (Rosell, 2019). Because wood density is a commercially important property, a considerable body of literature exists on the patterns and causes of wood density variation in commercial forestry species. This literature might be leveraged to establish relationships between areal fractions of wood tissues and density, which could then be applied to the fossil record. In tropical angiosperm trees, for example, wood density is positively correlated to vessel wall fraction, and negatively correlated to fiber lumen fraction, vessel area, and pith area (Ziemińska *et al.*, 2013; Zieminska *et al.*, 2015).

SSD may be inaccessible for fossil tissues where there is a high degree of density variation, or for which function is expected to be different between extinct and modern plants. For example, lycopsids were likely structurally supported by bark rather than secondary xylem (DiMichele *et al.*, 2013), and medullosan stelar and parenchyma arrangements are unlike any modern tree (Wilson *et al.*, 2017). In such cases, biochemical analyses combined with inferences about potential tissue function may be applied as an additional lens for estimating SSD. For example, modern-stem bulk C : N is associated with the proportion of the tissue in various structural and functional tissue types that have well-characterized densities. A database of these associations would allow bulk stem compression C : N ratios to serve as a proxy for SSD that is more broadly applicable to the fossil record. Taphonomy experiments would however be required to test the robustness of the original stem C : N signal through temperature and pressure changes associated with fossilization (*sensu* McNamara *et al.*, 2021). In summary, therefore, although SSD is undoubtedly important for Earth system processes and woody fossils are well preserved in the

fossil record, given the highly preliminary nature of methodology to estimate this trait from fossils, SSD achieved relatively low paleo-functional (5.5), ESE (3.85), and ESI scores (0.38) (Table S1; Figs 3, 4).

3. Xylem vulnerability

Xylem of vascular plants facilitates the transport of water to plant tissues from the soil and the maintenance of plant function (Zanne *et al.*, 2014). Water is drawn from soil through tracheary conduits in xylem by negative water potential (Ψ) induced by transpiration from leaves. During dry periods, water potential may exceed the physiological limits of xylem, causing water-transport failure, also known as hydraulic failure. The primary mode of failure is thought to be embolism via air-seeding (Venturas *et al.*, 2017): Under extreme negative potential air is pulled into water-filled conduits from adjacent tissues resulting in conduit blockage and reduction of total xylem water-transport capacity (Mayr *et al.*, 2014). Ecosystem functions like transpiration and photosynthesis depend on xylem water transport, and the physiological limitations of xylem are associated with tree mortality and vegetation distribution in modern ecosystems (Sperry, 2000; Sperry *et al.*, 2002; McDowell *et al.*, 2008; Choat *et al.*, 2012; Adams *et al.*, 2017). Therefore, xylem vulnerability to failure has likely had an impact on ecosystems and Earth surface processes since the initial diversification of vascular plants in the Devonian (Banks, 1975; Chaloner & Sheerin, 1979; Niklas, 1980, 1983, 1985a; Bouda *et al.*, 2022).

Xylem physiology has been inferred from morphological and anatomical measurements of deep-time fossils (e.g. Niklas, 1985a; Wilson *et al.*, 2008; Wilson & Knoll, 2010; Wilson, 2013), and has largely focused on the conductivity allowed by conduits and pit apertures. Pits are openings in the xylem secondary cell wall that leave only the middle lamella between adjacent conduits (i.e. the pit membrane; Choat *et al.*, 2008). Pit characteristics are a good target for estimating xylem hydraulic vulnerability from fossil conduit anatomy. Recent work has shown that the pit-membrane area-to-thickness ratio is a strong predictor of the hydraulic limitations of xylem (Kaack *et al.*, 2021). Unfortunately, pit membranes are challenging to measure, and measurements at the nanometer scale (i.e. of pit-membrane thickness) would be subject to considerable preservation biases. Though this has not yet been tested, fossil pit-membrane thickness may not be representative of *in vivo*-pit thickness. Another anatomical character, pit-area per conduit, also informative on xylem vulnerability to embolism (Pittermann *et al.*, 2006; Hacke *et al.*, 2007; Brodersen *et al.*, 2014), has been applied to late Pennsylvanian-aged fossil plants (Matthaeus *et al.*, 2022; Wilson *et al.*, 2023). Inferring absolute water-transport properties and ecosystem impacts based on conduit anatomy, however, requires assumptions about tissue-scale properties – of xylem as a whole (e.g. size distribution of conduits and sapwood area), which is accessible from stem permineralizations based on network connectivity (Bouda *et al.*, 2022) – along with the whole plant architecture and the whole plant coordination of traits. We evaluated xylem vulnerability as having lower potential as a paleo-functional trait because of the reliance on fossilized pit-membrane anatomy, the difficulty of obtaining trait values from fossilized pit membranes and due to the complexity of incorporating the trait within paleo-ecosystem models (Figs 3, 4; Table S1).

4. Bark thickness

Bark is a complex tissue with diverse physiological and ecological functions (Rosell, 2019). In extant plants, bark thickness is simply measured with calipers. There is a robust relationship between bark thickness and stem diameter in many tree taxa (Borger, 1973; Williams *et al.*, 2007; Rosell *et al.*, 2017), suggesting that it might be used as a proxy for stem diameter in fossil plants where whole stems are not preserved. However, the relationship between bark thickness and stem diameter varies among taxa, bark types, and between main stem and twigs – as bark thickness is also associated with a number of different environmental factors and physiological functions (Rosell *et al.*, 2017; Rosell, 2019; see flammability). In the most extreme cases – for species with decorticating bark (Gill & Ashton, 1968; Borger, 1973) or bark shed in strips (Williams *et al.*, 2007) – there may be little or no allometric relationship between bark thickness and stem diameter. Attempts to account for the factors influencing bark thickness in contemporary ecology have considered different parts of bark (e.g. inner and outer) and varied environments (e.g. tropical rainforest, temperate forest, or savannah), and they have made progress in disentangling interactions (Paine *et al.*, 2010; Hempson *et al.*, 2014; Rosell *et al.*, 2015, 2017). These studies have also laid the foundations for using fossil bark thickness as a paleo-functional trait to infer wildfire frequency and intensity (Uhl & Kauffman, 1990; Hoffmann *et al.*, 2003; Lawes *et al.*, 2013; Pausas, 2015). Stem photosynthesis and herbivory defense may be inferred from the proportion of inner and outer bark, and the presence or absence of rhytidome (outermost bark which is characterized by multiple layers of periderm tissue interspersed by phloem-rich layers; Rosell *et al.*, 2015; Rosell, 2019). Bark (wound periderm) has also been observed in extant CAM plants as a defense against high UV-B flux (dos Santos Nascimento *et al.*, 2015).

The fossil record contains bark components (i.e. periderm; Fig. 2g; vascular cambium) as early as the Lower Devonian, and may coincide with the earliest appearance of secondary growth (Banks, 1981; Hoffman & Tomescu, 2013). Functional inferences based on bark thickness traits and constituent structures require the preservation of complete sections of bark which can be achieved when the bark type (i.e. its physiology) is known, and the delimiting structures are identifiable (e.g. vascular cambium and periderm). Even in these cases, the actual thickness of the outermost structures will likely be thinner than *in vivo* due to alteration during burial. These processes may be indistinguishable from normal, *in vivo* shedding from periderm. Furthermore, the considerable differences in the physiological function of bark in some extinct taxa that completely lack any living structural analogs (e.g. all extant lycopsids are herbaceous but many ancestral taxa were arborescent with extensive bark) may make high-confidence inferences difficult for those taxa. Chemical components of fossil bark (dos Santos Nascimento *et al.*, 2015; Angyalossy *et al.*, 2016) may, however, provide broadly useful information on the paleo-function of the individual even in the absence of phylogenetically related modern

analogs. Considering all of the factors reviewed above, we assessed bark thickness as having lower potential as a paleo-functional and ESE trait relative to many of the other traits reviewed here with scores of 6.5 and 1.95 respectively (Figs 3, 4; Table S1).

5. Plant height

Plant height is the shortest distance between the upper boundary of the main photosynthetic tissues and the ground level, expressed in meters (Pérez-Harguindeguy *et al.*, 2013). Direct measurement of height is not usually possible within the fossil record due to fragmentation (Niklas, 1994). Rare fossilization events can lead to whole tree stumps being preserved *in situ* (Cúneo *et al.*, 2003; Wang *et al.*, 2012) and whole-body fossils being preserved intact (Sun *et al.*, 1998; Fig. 2f). In such cases, fossil plant height can be measured directly. For the most part, fossil plant stems and trunks are not intact. However, their height can be estimated indirectly. Niklas has developed formulae for estimating fossil plant height based on the allometric scaling relationships of diameter at chest height across phylogenetic and ontogenetic differences (Niklas, 1994; Enquist & Niklas, 2001). Height has also been estimated based on the shape of permineralized logs by projecting to vanishing point (Falcon-Lang & Scott, 2000). However, this methodology may underestimate tree height where the base width of trunks is unknown (Falcon-Lang & Scott, 2000).

Height is a key trait in the global spectrum of plant form and function (Diaz *et al.*, 2016). It represents the economic trade-off between investment in structural tissues, stem maintenance, and access to light (Falster & Westoby, 2003). Taller plants are linked to increased biomass, acting as carbon sinks (Moles *et al.*, 2009), and woody debris of taller plants such as trees slows decomposition (Gora *et al.*, 2019 and references therein). Taller canopies provide niche partitioning by opening up understory and aerial habitats. Increased plant height is therefore associated with greater plant and animal diversity in contemporary ecosystems (August, 1983; Moles *et al.*, 2009). Maximum plant height is also associated with an ability to disperse reproductive propagules and can thus provide useful insights on reproductive success (Beckman *et al.*, 2018). Therefore, particularly since the acquisition of arborescence in the late Devonian (Stein *et al.*, 2007), plant height can tell us a great deal about total ecosystem function (Moles *et al.*, 2009), and has been used extensively to provide key ecological contexts for swamp dwelling plants of the Carboniferous (Philips & DiMichele, 1992; DiMichele *et al.*, 2013). However, the light-competitive advantage of height depends on the relative height of other species within the paleo- or modern plant community rather than the absolute height of a species (Falster & Westoby, 2003), complicating inferences for fossil communities. Although plant height scored modestly as a potential paleo-functional trait (6) in our semi-quantitative evaluation, because of its importance in affecting ecosystem-scale and Earth system processes outlined above it ranked relatively highly as an ESE trait (score = 5.4; Figs 3, 4; Table S1). We suggest this paleo-functional trait has good potential for further development of methods to quantify trait values from fossils and to parameterize within paleo-ecosystem models.

VIII. Whole plant functional traits applied to fossils

1. Life history and maximum plant lifespan

Life-history strategies are described by the timing and intensity of the demographic processes of growth, survival, and reproduction (Stearns, 1992). Life-history strategies are indicators of ecological strategy and give insights into how populations respond to abiotic and biotic drivers, including climate (Csergo *et al.*, 2017) and variation in these traits is strongly associated with environmental stress (Pérez-Harguindeguy *et al.*, 2013). As an example, extant gymnosperm and angiosperm trees with high longevity (high maximum lifespan) are slow-growing and usually occupy sites that are harsh (cold, nutrient-poor, frequently flooded etc.) but are subject to little storm disturbance (reviewed in Di Filippo *et al.*, 2015). Quantification of life-history strategies thus informs potential responses of populations to environmental change (Buckley *et al.*, 2019). Contemporary life-history metrics, however, cannot usually be calculated directly for extinct populations, as demography is usually unavailable. Nonetheless, life history has been considered for even the oldest, most basal plants using whole plant concepts (Matsunaga & Tomescu, 2017).

Direct morphological and anatomical evidence of life-history strategies for fossils are generally lacking. For instance, counting permineralized annual growth rings of woody stems and roots merely elucidates a plant's age at the time of death (Creber & Chaloner, 1984; Weaver *et al.*, 1997; Luthardt *et al.*, 2017) not the tree or species potential longevity. Long sequences of fossil growth rings are also rare (Chapman, 1994; Luthardt *et al.*, 2017). Growth rate estimates based on mean annual ring widths from the same fossil trunks/roots (Fig. 2n) could however, be used to infer longevity using scaling relationships between mean ring width and longevity that have been developed for living taxa (Di Filippo *et al.*, 2015), although they are biome specific. Population-level surveys of mean ring width from *in situ* preserved fossil forests provide some of the best data sources to model the longevity of fossil taxa (e.g. Cúneo *et al.*, 2003) but it is acknowledged that these are exceptionally rare. For taxa that lack annual growth rings (e.g. most wet tropical taxa), plant lifespan is more difficult to interpret (Chaloner & McElwain, 1997; Boyce & DiMichele, 2016).

Counting the mean size of the annual increments on the stolon or rhizome may be the only way to indirectly assess maximum lifespan via growth rate in nonwoody fossil plants (Hotton *et al.*, 2001; Gensel & Berry, 2016). In cases without clear annual increments, detailed analysis of morphology, including the presence of perennating roots and shoots, counting the number of annual stem growth increments in woody shoots, presence of leaf scars on shoots and shoot scars on roots, will at least determine whether the fossil is an annual or perennial. Alternatively, if LL and plant height can be estimated for the fossil taxon, and leaves with axial attachment are available, a rough estimate of axial growth rate can be compared with overall tree height to estimate age at death (Boyce & DiMichele, 2016).

Most current inferences of paleo-life-history rest on plant form (e.g. woodiness and seed size), leaf economics, and trait–climate

associations (e.g. leaf shape). However, interpretation of lifespan for taxa that lack living relatives or equivalents (NLEs) or those that have extinct combinations of physiological traits can result in vastly different estimates for the plant's lifespan (Philips & DiMichele, 1992; Cleal & Thomas, 2005; Boyce & DiMichele, 2016; Thomas & Cleal, 2018). For example, lifespan estimates for the iconic late Pennsylvanian *Lepidodendron*, which reached an estimated height of 45 m, range from decades (Thomas & Cleal, 2018) to centuries (Boyce & DiMichele, 2016). For fossil taxa with no obvious NLEs, studies have relied on observations that extant plant life histories are structured by two major axes – a 'pace of life' axis and a reproductive axis (Salguero-Gomez *et al.*, 2016). Furthermore, maximum plant lifespan is strongly aligned with the pace of life dimension of life-history strategies (Salguero-Gomez *et al.*, 2016). These principles have been applied to early angiosperms, where a fast-paced 'weedy' life strategy has been inferred from single paleo-functional traits such as seed size (Wing & Boucher, 1998) and LMA (Royer *et al.*, 2010). Recent studies, however, demonstrate the complexity of inferring demography from individual functional traits; seed size and plant height are positively correlated with maximum lifespan in extant plants but only in hot relatively invariable climates (Kelly *et al.*, 2021). Furthermore, very different life forms, such as herbs and trees, can give rise to similar life histories (Salguero-Gomez *et al.*, 2016), and divergent life forms can converge on similar trait and life-history profiles depending on environment and phylogeny (Kelly *et al.*, 2021). Thus, combinations of paleo-functional traits, with information from multiple plant organs as well as the sedimentary and paleo-climatic environment context of the fossils may improve our understanding of the life-history strategy of fossil plants in the future. Based on these myriad considerations and obvious complexity, we assessed this syndrome of traits with a relatively high Paleo-functional trait value (6) but low ESE (2.4) and even lower ESI scores (0.24) due to the difficulty of integrating ecosystem models and demography models for current living vegetation let alone developing a paleo-demography model for fossils (Figs 3, 4; Table S1).

2. Litter decomposability

Decomposition of plant litter is important for nutrient recycling, soil fertility, and productivity. It regulates terrestrial biogeochemical cycles at both a global and local ecosystem scale (Zhang *et al.*, 2021) by restoring nutrients from dead plant parts into the soil and CO_2 to the atmosphere, while slow decomposition provides fuel for wildfires (Cornwell *et al.*, 2008). Decomposition involves the breakdown of plant litter, both physically and chemically, into its elements through progressively simpler compounds (Aerts, 2006). In contemporary ecosystems, the majority of aboveground litter is leaf litter, and broadly, chemical trait–decomposability relationships are preserved both across organs (leaves, roots, and stems) of different species and within organs in the same species (Freschet *et al.*, 2012).

Experimentally, the rate of decomposition is the percentage of mass loss over time with k (decomposition constant) defining a mass loss curve (Pérez-Harguindeguy *et al.*, 2013). Litter decomposition is the result of interactions between climate and the community of decomposers (Berg & McClaugherty, 2008). Global litter decomposition is primarily driven by environmental conditions such as temperature and precipitation (Aerts, 1997), which are relevant to environmental change in geological time. Plant traits affect decomposition rate, primarily via their influence on usefulness as a resource for decomposer organisms (i.e. chemical composition and morphology), referred to as litter quality. Litter quality varies significantly among living plant lineages, so patterns of plant effects on nutrient cycling probably varied through deep time (Liu *et al.*, 2014). For instance, the leaves of gymnosperms generally decompose 44% slower than eudicots, and ferns and bryophytes decompose more slowly again (Liu *et al.*, 2014).

The most important traits contributing to litter quality are chemical traits that can be assessed in fossils. These are N content, lignin content, toughness (can be inferred from VD and cuticle thickness), and LMA (see section V; Cornwell *et al.*, 2008; Freschet *et al.*, 2012). Other leaf traits that go beyond the scope of fossil taxa such as N form (Rosenfield *et al.*, 2020) and phenolics also influence the decomposition rate. Morphological traits further impact decomposability. At the very least size/volume (S/V), ratios affect the area exposed to decomposers in the early stages of decomposition. Consequently, overall prediction of decomposition relies on a relatively full picture of taxon traits. Litter quality is, therefore, a trait syndrome that is relevant for past environmental change but accessible from fossils only via correlations with chemical traits (available from compression fossils and coal balls) and morphological and anatomical traits (available from most fossil preservation modes). Detailed taphonomic studies suggest that most compression leaf fossils and leaves preserved in carbonaceous coal balls were likely preserved rapidly by covering recent falls of undecomposed leaf litter (Greenwood & Donovan, 1991; Gastaldo, 2001), making them the best targets for relatively unbiased assessment of paleo-litter decomposability in future studies.

For litter decomposition and biomass turnover, it is important to note that plants are made up of multiple organs that may have different geochemical effects; for instance, stem and root litter typically decompose slower and contain more lignin, so they have a disproportionate role in humus formation (Swift, 1977). Particular traits may also vary in their contribution to litter quality per organ; for instance, lignin content is important for wood decomposition. The effect of chemical traits may also change due to differing access to decomposers; for instance, N is found in enzymes in leaves and roots for CO_2 assimilation/absorptive capacity, while it is primarily found in storage and defense compounds in stems (Freschet *et al.*, 2012). Lignin is in itself notable because it is a complex polymer fundamental to the lignin–cellulose structural matrix of wood and relevant to co-evolution of enzymatic mechanisms in decomposers. It is hypothesized that the evolution of wood-degrading enzymes was a key event ending coal formation at the end of the Carboniferous (Floudas *et al.*, 2012) although this is disputed based on evidence of from the fossil record of fungi and plants (Nelsen *et al.*, 2016). Chemical derivatives of lignin are readily preserved and extractable from fossils (Niklas, 1981; Logan & Thomas, 1987) throughout the geological record although to our knowledge no paleo-decomposability metric for fossil lignin

content has been developed. Overall, interactions with both decomposers and other species in litter mixtures (Porre *et al.*, 2020) are a key modulator of the effects of traits on decomposition and may act differently on different traits. Hence, litter decomposability should be cautiously inferred from the fossil record and we have attributed relatively low paleo-functional trait scores accordingly (6), although the Earth system score (5.4) and ESI (4.05) scores are high because of the quantifiable impacts on biogeochemical cycling (Figs 3, 4; Table S1). Our assessment is that this paleo-functional trait syndrome is a good target for further study because of its high potential value to address interesting questions on plant evolution–Earth system interaction.

3. Plant flammability

Wildfire has occurred for > 400 million years (Ma; Edwards & Axe, 2004; Glasspool *et al.*, 2004; Belcher, 2016) and has likely been relevant to Earth system processes for at least 350 Ma (Scott & Glasspool, 2006). Plants host many traits that either influence fire or respond to fire, many of which can be, or have the potential to be, observed in the fossil record. These can be linked to variations in environmental conditions such as weather, seasonality, climate, and the abundance of oxygen in the atmosphere and therefore, have the potential to clarify a broad range of Earth system processes across deep time (Archibald *et al.*, 2018). Of critical importance and often overlooked in deep-time research is the influence of plant traits on flammability (the propensity of plant material to ignite, given an ignition source, and then propagate a fire) and the nature of the subsequent fire behavior (rate of spread and intensity), which interacts with ecosystem processes to determine the effects that a fire may have. While other proxies such as charcoal abundance may serve as indicators of fire frequency, we can utilize fire-linked plant traits to make the best-informed interpretations of fire effects (*sensu* the 'effect' trait concept) in the ancient past (Belcher, 2016).

Plant traits influence flammability and fire behavior at the leaf level, the whole plant level, and the physiological/phenological level (Archibald *et al.*, 2018) and act together to determine whether fires may burn in the canopy of forests, in the surface fuels (the understory) in litter or in ground fuels (such as organic soils and peat). There is a considerable literature describing the variety of plant traits that impact fire regimes (Kane *et al.*, 2008; Schwilk & Caprio, 2011; Cornwell *et al.*, 2015; Grootemaat *et al.*, 2015), many of which are observable in the fossil record. Perhaps the most obvious are the leaf morphological traits of leaf length and leaf area (Notes S1), which are particularly important in determining the nature of fires in leaf litter because they influence the bulk density of the litter. The bulk density of leaf litter decreases with leaf area and length such that litters that have leaves with larger areas or longer needles will carry more rapidly spreading fires (de Magalhães & Schwilk, 2012). Such measurements have been linked to the energy production from paleo-litter fires where leaves that pack tightly in high bulk density litter beds will burn more slowly but with an overall high total energy release that can damage soils and seed banks, while those of larger leaves or longer needles that pack less densely will run rapidly through litter beds but impart little heat downward (Belcher, 2016).

The opposite tends to be true for tree or shrub canopies, where small leaves increase the ease of heat transfer and tend to form dense canopies (Schwilk & Ackerly, 2001; Archibald *et al.*, 2018). LMA likely also influences flammability, where higher LMA leaves ought to contain overall more energy to give to a fire (both crown, surface, and litter fires) but will also affect litter fires via their influence on rates of decomposition (Cornwell *et al.*, 2008). Other traits that enhance canopy flammability include dead branch retention (Bond & Midgley, 1995; Schwilk & Ackerly, 2001) and the retention of dead leaves (He *et al.*, 2011). Low canopy base heights and dead branch retention influence the ability of surface fires to climb into the canopy. Hence, whole plant reconstructions are of importance to understanding the likely potential fire behavior that might exist in an ancient ecosystem. Other observations – such as branch or shoot shedding, a trait observed in many extant Pinaceae – tend to be associated with surface fire regimes. This trait has been noted using careful observations of Permian age conifer fossils (Looy, 2013). Similarly, thick bark tends to be associated with survival in surface fire regimes, where thick bark protects the trees' cambium from the heat of surface fires, while thinner bark is associated with traits such as canopy seed storage (serotiny) and tends to be linked to crown fire regimes (Pausas, 2014). The evolution of thick bark and serotiny in *Pinus* appears to date back to the Cretaceous, a time of enhanced flammability (He *et al.*, 2012). It has also been suggested that a woody rachis that supports a compact cone with bracts/scales covering winged seeds are traits that might be considered as characteristic of serotinous cones (He *et al.*, 2016). Such observations demonstrate the potential of using paleo-functional traits to indicate the likely fire regime operating in ancient ecosystems. Similarly, variations in leaf biochemical traits (such as terpene content) have been linked to flammability and being capable of driving different fire regimes. For example, conifers in surface fire regimes appear to have higher needle terpene contents, which appears to enhance litter flammability, encouraging frequent surface fires (Dewhirst *et al.*, 2020).

Ancient ecosystems have been reconstructed using plant traits and included in models that make fire behavior predictions for time periods such as the Permian (He *et al.*, 2016), the Triassic–Jurassic (Belcher *et al.*, 2010; Belcher, 2016; Baker *et al.*, 2022), the Cretaceous (Belcher & Hudspith, 2017), and the Miocene (Boulton & Belcher, 2019). More recently, global dynamic vegetation models have been used to answer deep-time questions regarding atmospheric oxygen that rely on consideration of plant functional types (Vitali *et al.*, 2022). Therefore, the study of fossil plant traits has a significant potential to inform novel understanding of paleo wildfires and their effects, and we have scored this trait highly as a paleo-functional trait (7) accordingly (Table S1). Flammability has significant but complex impacts on the carbon and oxygen cycles, resulting in an ESE score of 5.6 (Figs 3, 4). Furthermore, although paleofire can be modelled currently within paleo-ecosystem models, flammability is a trait syndrome made up of many individual traits and it is not a simple task to parameterize at individual trait level, thus resulting in a lower ESI score (2.8) (Figs 3, 4; Table S1).

4. Salinity tolerance

Salinity tolerance is a complex trait consisting of the ability of plants to grow in saline environments. Saline-tolerant plants (halophytes) appear to be present as early as the Devonian (Channing & Edwards, 2009); however, the fossil record of halophytes is often based on the sedimentary context indicating a marine influence (Vakrahmeev, 1991; Gomez *et al.*, 2002; Mendes *et al.*, 2023) rather than more direct evidence based on fossil plant functional traits. Stable carbon isotopic analysis of leaf compression fossils has been used to indicate likely salinity gradients among fossil plant taxa from the same depositional setting (Nguyen Tu *et al.*, 1999) with greater discrimination against C^{13} (less negative ^{13}C values) used to indicate higher salinity sub-environments. Variability in stable carbon isotopes can also be influenced by photosynthetic syndrome (see section V), light intensity, aridity, and many other factors, so it is not a straightforward salinity indicator (Arens *et al.*, 2000; Diefendorf *et al.*, 2011; Cernusak *et al.*, 2013). Nowadays, only a small fraction of terrestrial plants exhibit salinity tolerance. Plants use three main mechanisms by which they deal with excess environmental NaCl: (1) salt exclusion, (2) salt excretion, and (3) salt compartmentalization.

Roots of many salt-tolerant plants maintain K^+ uptake, discriminating against Na^+, resulting in an increased K^+/Na^+ ratio compared with the growing medium. K : Na selectivity (S) can be calculated as: $S = ([K^+]/[Na^+])_{plant}/([K^+]/[Na^+])_{soil}$ (Pérez-Harguindeguy *et al.*, 2013). Ion concentrations in living plants and modern soils can be measured by atomic emission spectrometry (AES) and atomic absorption spectrometry (AAS) but are not currently available in fossils due to unknown effects of diagenesis on the original K/Na ratios. Other salt-tolerant plants excrete salt through special salt glands. These glands, found mostly on leaves and sometimes on stems, show different structural and functional diversity (Dassanayake & Larkin, 2017; Grigore & Toma, 2020). Microscopic observation of fossil plant cuticle with epifluorescence (see Cuticle Traits) may reveal their presence as many have auto-fluorescent properties and are superficially similar in size and structure to ordinary trichome bases which are readily observed on fossil leaves. Some salt-tolerant species compartmentalize Na^+ in vacuoles and these are often succulent. Although direct observation of this type of compartmentalization is currently not possible to study in fossils, which typically lack cellular level preservation, LMA (reviewed in detail in section V) is a good general predictor of succulence (Poorter *et al.*, 2009). However, LMA cannot be used in isolation as values for evergreen gymnosperms and succulent overlap (Poorter *et al.*, 2009). Traits associated with salt excretion which are observable in fossils include the presence of regularly spaced crystals (salt recreation) and their anatomical excretory structures (sclereids, tracheo-ideoblasts; Grigore & Toma, 2020). For example, salt tolerance is often associated with the presence of calcium oxalate (CaOx) crystals in idioblasts of leaves and roots (Santos *et al.*, 2016; Karabourniotis *et al.*, 2020). SEM EDX analysis of Oligocene fossil leaves has confirmed the presence of ghost accumulations of CaOx crystals (druses; Malekhosseini *et al.*, 2022), suggesting that additional underutilized traits are now available to study paleo salinity tolerance in fossil plants (Fig. 2e).

Overall, however, salinity tolerance achieved low scores across all categories (Table S1; Figs 3, 4), suggesting that it ranks low in terms of future development potential as a paleo-functional trait compared with others reviewed here.

IX. Concluding remarks

Measurement of fossils forms the primary record of vegetation–climate interactions across deep time. Traditionally, fossil plants have been used to document paleodiversity and plant evolution and as proxies of past environmental change. Less often have individual fossils been used to measure trait values as a means to evaluate their functioning within paleo-ecosystems. Incorporation of trait values within paleo-ecosystem models provides a powerful tool with which to evaluate the impact of newly evolved traits and suites of traits on the Earth system. Our critical review and semi-quantitative assessment of plant traits have resulted in a ranked list of paleo-functional traits (Fig. 4) that we identify as having the greatest potential to use in further studies investigating how plant evolution has shaped their environment, Earth surface, and Earth system processes through deep time. We have focused on and attempted to rank 'effect' traits; however, we view our ranked list as a working hypothesis and preliminary rather than a final and definitive outcome. Our methodological framework outlined in Fig. 1 provides a means for others to re-assess our scores and re-evaluate our ranking or to develop new paleo-functional trait evaluations that align better with the specific questions being asked. For example, we expect that an entirely different paleo-functional trait ranking will emerge if the traits are evaluated for their 'response' to rather than 'effect' on their paleo-environment. Response traits that have been strongly filtered by paleo-environment are the foundation stone of paleo-climate and paleo-atmospheric proxies. Pollen, spore, and leaf area traits would rank highly under a 'response to environment' evaluation.

Where relevant in the review, we highlighted particular traits that are ripe for further development but have scored relatively low under our ranking criteria because they require systematic approaches to quantify their trait values from fossils and further control for bias and error (e.g. plant height, CAM photosynthesis, LNC, SSD). Our critical assessment of paleo-functional traits has also revealed a constellation of traits (flammability, iWUE, xylem conductivity, VD, plant height, and dispersal syndrome) that are measurable in the fossil record and critically important for Earth system processes but are not yet parameterized within paleo-ecosystem models (Fig. 4). We highlight these, in particular, as excellent targets for future data-model integration. Perhaps somewhat unsurprisingly, leaf traits in the leaf economic spectrum rank among the highest paleo-functional traits (Figs 3, 4), which is encouraging as their application to fossil plant assemblages is growing and methodologies for their estimation are improving.

While individual paleo-functional traits provide interesting quantitative insight into the function of individual plant parts, a paleo-ecosystem-scale network of traits using multiple traits from different organs and community-weighted plant trait values (calculated as the product of relative taxon abundance and average trait values; e.g. Soh *et al.*, 2017) should be our ultimate goal. Trait-

based whole-plant understanding of plant function should incorporate existing knowledge about architecture, growth form, life history, and phenology from the rich literature of paleo-ecological inference as a framework for checking the robustness of individual trait values. Synthesizing all available paleo-functional traits in this way also provides a framework for integration with processes, global constraints, and trade-offs observed in modern plant ecology to allow the understanding of global vegetation effects across deep time and plant evolution.

Inference of vegetation function across deep time is a major outcome of interest for paleo-functional trait analysis. A parallel goal is obtaining a deeper understanding of the tempo of plant trait evolution and an overview of the functional traits that confer ecological resilience in a changing global climate (e.g. through xylem vulnerability, spore, and pollen traits). The impact of improving the resolution of trait spaces within phylogenetic and ecological groupings, as well as clarification of plant and ecosystem processes by modern plant scientists will expand understanding of deep-time vegetation processes. Coordination between paleo- and contemporary plant scientists is warranted, for example, to promote the measurement of traits that have a high degree of ecological impact and are measurable from both living and fossil plants (Fig. 4). We hope that our review and semi-quantitative assessment of fossil plant functional traits will provide ideas and 'fossil for thought' toward this endeavor. Equally, we hope that our proposed methodological framework to evaluate paleo-functional traits will provide a useful basis for the development of new paleo-functional trait metrics and trait rankings in the future that are aligned with the specific questions being asked.

Acknowledgements

JM and SN acknowledge support from H2020 European Research Council funded Grants TERRAFORM ERC-ADG-2020-101020824 and TIME-LINES ERC-CoG-2021-101045309, respectively. IPM acknowledges funding from NSF EAR 1338281. YB acknowledges an Irish Research Council Laureate Awards 2017/2018 IRCLA/2017/60. Sincere thanks to four anonymous reviewers who provided a wealth of ideas and insights toward the improvement of our contribution. Open access funding provided by IReL.

Competing interests

None declared.

Author contributions

JCM and SN conceived the project. JCM and WJM designed the review structure and approach. JCM, WJM, BJ, AK, CC, SN, CB, KO'D, KK, CMB, IPM, JDW, YMB and RN drafted the manuscript. JCM, WJM, CC, YMB, JPW, JDW and SN prepared the figures and tables. KK, AK, KO'D and CB prepared the bibliography. All authors participated in the discussion and editing of the manuscript, figures, and tables.

ORCID

Catarina Barbosa https://orcid.org/0000-0003-1179-6553
Claire M. Belcher https://orcid.org/0000-0003-3496-8290
Yvonne M. Buckley https://orcid.org/0000-0001-7599-3201
Christos Chondrogiannis https://orcid.org/0000-0003-4586-5537
Bea Jackson https://orcid.org/0000-0002-3914-3661
Antonietta B. Knetge https://orcid.org/0000-0002-2493-8250
Kamila Kwasniewska https://orcid.org/0000-0003-3446-413X
William J. Matthaeus https://orcid.org/0000-0002-0117-4059
Jennifer C. McElwain https://orcid.org/0000-0002-1729-6755
Isabel P. Montañez https://orcid.org/0000-0003-0492-3796
Richard Nair https://orcid.org/0000-0002-6293-3610
Sandra Nogué https://orcid.org/0000-0003-0093-4252
Joseph D. White https://orcid.org/0000-0002-9249-5009
Jonathan P. Wilson https://orcid.org/0000-0002-8586-171X

References

Abrego N, Norberg A, Ovaskainen O, Aerts R. 2017. Measuring and predicting the influence of traits on the assembly processes of wood-inhabiting fungi. *Journal of Ecology* **105**: 1070–1081.

Ackerman JD. 2000. Abiotic pollen and pollination: ecological, functional, and evolutionary perspectives. *Plant Systematics and Evolution* **222**: 167–185.

Adams HD, Zeppel MJB, Anderegg WRL, Hartmann H, Landhausser SM, Tissue DT, Huxman TE, Hudson PJ, Franz TE, Allen CD *et al.* 2017. A multi-species synthesis of physiological mechanisms in drought-induced tree mortality. *Nature Ecology & Evolution* **1**: 1285–1291.

Aerts R. 1995. The advantages of being evergreen. *Trees* **10**: 402–405.

Aerts R. 1997. Climate, leaf litter chemistry and leaf litter decomposition in terrestrial ecosystems: a triangular relationship. *Oikos* **79**: 439–449.

Aerts R. 2006. The freezer defrosting: global warming and litter decomposition rates in cold biomes. *Journal of Ecology* **94**: 713–724.

Aerts R, Chapin FS. 1999. The mineral nutrition of wild plants revisited: a re-evaluation of processes and patterns. *Advances in Ecological Research* **30**: 1–67.

Allen SE, Lowe AJ, Peppe DJ, Meyer HW. 2020. Paleoclimate and paleoecology of the latest Eocene Florissant flora of central Colorado, USA. *Palaeogeography, Palaeoclimatology, Palaeoecology* **551**: 109678.

Angyalossy V, Pace MR, Evert RF, Marcati CR, Oskolski AA, Terrazas T, Kotina E, Lens F, Mazzoni-Viveiros SC, Angeles G *et al.* 2016. IAWA list of microscopic bark features. *IAWA Journal* **37**: 517–615.

Archibald S, Lehmann CER, Belcher CM, Bond WJ, Bradstock RA, Daniau AL, Dexter KG, Forrestel EJ, Greve M, He T *et al.* 2018. Biological and geophysical feedbacks with fire in the Earth system. *Environmental Research Letters* **13**: 33003.

Arens NC, Jahren AH, Amundson R. 2000. Can C3 plants faithfully record the carbon isotopic composition of atmospheric carbon dioxide? *Paleobiology* **26**: 137–164.

Aslam TJ, Johnson SN, Karley AJ. 2012. Plant-mediated effects of drought on aphid population structure and parasitoid attack. *Journal of Applied Entomology* **137**: 136–145.

Aslan C, Beckman NG, Rogers HS, Bronstein J, Zurell D, Hartig F, Shea K, Pejchar L, Neubert M, Poulsen J *et al.* 2019. Employing plant functional groups to advance seed dispersal ecology and conservation. *AoB Plants* **11**: plz006.

August PV. 1983. The role of habitat complexity and heterogeneity in structuring tropical mammal communities. *Ecology* **64**: 1495–1507.

Bacon KL, Haworth M, Conroy E, McElwain JC. 2016. Can atmospheric composition influence plant fossil preservation potential via changes in leaf mass per area? A new hypothesis based on simulated palaeoatmosphere experiments. *Palaeogeography, Palaeoclimatology, Palaeoecology* **15**: 51–64.

Baker SJ, Dewhirst RA, McElwain JC, Haworth M, Belcher CM. 2022. CO_2-induced biochemical changes in leaf volatiles decreased fire-intensity in the run-up to the Triassic-Jurassic boundary. *New Phytologist* **235**: 1442–1454.

Banks HP. 1975. The oldest vascular land plants: a note of caution. *Review of Palaeobotany and Palynology* **20**: 13–25.

Banks HP. 1981. Peridermal activity (Wound repair) in an Early Devonian (Emsian) Trimerophyte from the Gaspe Peninsula, Canada. *Palaeobotanist* **28**: 20–25.

Barbosa C, Muchagata J. 2021. The use of latex moulds as a complement for studying paleobotanical specimens. *Comunicações Geológicas* **108**: 21–26.

Beaulieu JM, Moles AT, Leitch IJ, Bennett MD, Dickie JB, Knight CA. 2007. Correlated evolution of genome size and seed mass. *New Phytologist* **173**: 422–437.

Beckman NG, Bullock JM, Salguero-Gómez R, Violle C. 2018. High dispersal ability is related to fast life-history strategies. *Journal of Ecology* **106**: 1349–1362.

Belcher CM. 2016. The influence of leaf morphology on litter flammability and its utility for interpreting palaeofire. *Philosophical Transactions of the Royal Society of London. Series B, Biological Sciences* **371**: 20150163.

Belcher CM, Hudspith VA. 2017. Changes to Cretaceous surface fire behaviour influenced the spread of the early angiosperms. *New Phytologist* **213**: 1521–1532.

Belcher CM, Mander L, Rein G, Jervis FX, Haworth M, Hesselbo SP, Glasspool IJ, McElwain JC. 2010. Increased fire activity at the Triassic/Jurassic boundary in Greenland due to climate-driven floral change. *Nature Geoscience* **3**: 426–429.

Berg B, McClaugherty C. 2008. Decomposition, hummus formation, carbon sequestration. In: Springer, ed. *Plant litter*. Berlin Heidelberg, Germany: Springer, 315 p.

Bernardino-Nicanor A, Mora-Escobedo R, Montañez-Soto JL, Filardo-Kerstupp S, González-Cruz L. 2012. Microstructural differences in Agave atrovirens Karw leaves and pine by age effect. *African Journal of Agricultural Research* **7**: 3550–3559.

Berry JA, Beerling DJ, Franks PJ. 2010. Stomata: key players in the Earth system, past and present. *Current Opinion in Plant Biology* **13**: 232–239.

Blonder B, Royer DL, Johnson KR, Miller I, Enquist BJ. 2014. Plant ecological strategies shift across the Cretaceous–Paleogene boundary. *PLoS Biology* **12**: e1001949.

Boast AP, Weyrich LS, Wood JR, Metcalf JL, Knight R, Cooper A. 2018. Coprolites reveal ecological interactions lost with the extinction of New Zealand birds. *Proceedings of the National Academy of Sciences, USA* **115**: 1546–1551.

Bolmgren K, Eriksson O. 2005. Fleshy fruits – origins, niche shifts, and diversification. *Oikos* **109**: 255–272.

Bonan GB. 1995. Sensitivity of a GCM simulation to inclusion of inland water surfaces. *Journal of Climate* **11**: 2691–2704.

Bond WJ, Midgley JJ. 1995. Kill thy neighbour: an individualistic argument for the evolution of flammability. *Oikos* **73**: 79–85.

Borger GA. 1973. In: Kozlowski TT, ed. *Shedding of plants parts*. New York, NY, USA: Academic Press.

Bouda M, Huggett BA, Prats KA, Wason JW, Wilson JP, Brodersen CR. 2022. Hydraulic failure as a primary driver of xylem network evolution in early vascular plants. *Science* **378**: 642–646.

Boulton CA, Belcher CM. 2019. A novel approach for predicting the probability of ignition of palaeofires using fossil leaf assemblages. *Palaeontology* **62**: 715–730.

Boyce CK. 2009. Seeing the forest with the leaves – clues to canopy placement from leaf fossil size and venation characteristics. *Geobiology* **7**: 192–199.

Boyce CK, Brodribb TJ, Feild TS, Zwieniecki MA. 2009. Angiosperm leaf vein evolution was physiologically and environmentally transformative. *Proceedings of the Biological Sciences* **276**: 1771–1776.

Boyce CK, DiMichele WA. 2016. Arborescent lycopsid productivity and lifespan: constraining the possibilities. *Review of Palaeobotany and Palynology* **227**: 97–110.

Boyce CK, Ibarra DE, Nelsen MP, D'Antonio MP. 2023. Nitrogen-based symbioses, phosphorus availability, and accounting for a modern world more productive than the Paleozoic. *Geobiology* **21**: 86–101.

Boyce CK, Lee J, Field TS, Brodribb TJ, Zwieniecki MA. 2010. Angiosperms helped put the rain in the rainforests: the impact of plant physiological evolution on tropical biodiversity. *Annals of the Missouri Botanical Garden* **97**: 527–540.

Boyce CK, Lee JE. 2010. An exceptional role for flowering plant physiology in the expansion of tropical rainforests and biodiversity. *Proceedings of the Biological Sciences* **277**: 3437–3443.

Boyce CK, Zwieniecki MA. 2012. Leaf fossil record suggests limited influence of atmospheric CO_2 on terrestrial productivity prior to angiosperm evolution. *Proceedings of the National Academy of Sciences, USA* **109**: 10403–10408.

Briggs DE, Crowther PR. 2008. *Palaeobiology II*. Oxford, UK: Blackwell Science.

Brink KS, Stockey RA, Beard G, Wehr WC. 2009. *Cunninghamia hornbyensis* sp. nov.: permineralized twigs and leaves from the Upper Cretaceous of Hornby Island, British Columbia, Canada. *Review of Palaeobotany and Palynology* **155**: 89–98.

Brodersen C, Jansen S, Choat B, Rico C, Pittermann J. 2014. Cavitation resistance in seedless vascular plants: the structure and function of interconduit pit membranes. *Plant Physiology* **165**: 895–904.

Brodribb TJ. 2009. Xylem hydraulic physiology: the functional backbone of terrestrial plant productivity. *Plant Science* **177**: 245–251.

Brodribb TJ, McAdam SA. 2011. Passive origins of stomatal control in vascular plants. *Science* **4**: 582–585.

Brodribb TJ, McAdam SAM, Jordan GJ, Feild TS. 2009. Evolution of stomatal responsiveness to CO_2 and optimization of water-use efficiency among land plants. *New Phytologist* **183**: 839–847.

Bruelheide H, Dengler J, Purschke O, Lenoir J, Jimenez-Alfaro B, Hennekens SM, Botta-Dukat Z, Chytry M, Field R, Jansen F *et al.* 2018. Global trait-environment relationships of plant communities. *Nature Ecology & Evolution* **2**: 1906–1917.

Brussel T, Minckley TA, Brewer S, Long CJ. 2018. Community-level functional interactions with fire track long-term structural development and fire adaptation. *Journal of Vegetation Science* **29**: 450–458.

Buckley J, Widmer A, Mescher MC, De Moraes CM, van Dam N. 2019. Variation in growth and defence traits among plant populations at different elevations: implications for adaptation to climate change. *Journal of Ecology* **107**: 2478–2492.

Burnham RJ. 1990. Paleobotanical implications of drifted seeds and fruits from modern mangrove litter, Twin Cays, Belize. *PALAIOS* **5**: 364–370.

Burnham RJ, Johnson KR. 2004. South American palaeobotany and the origins of neotropical rainforests. *Philosophical Transactions of the Royal Society of London. Series B: Biological Sciences* **359**: 1595–1610.

Burnham RJ, Wing SL, Parker GG. 1992. The reflection of deciduous forest communities in leaf litter: implications for autochthonous litter assemblages from the fossil record. *Paleobiology* **18**: 30–49.

Butrim MJ, Royer DL, Miller IM, Dechesne M, Neu-Yagle N, Lyson TR, Johnson KR, Barclay RS. 2022. No consistent shift in leaf dry mass per area across the Cretaceous—Paleogene boundary. *Frontiers in Plant Science* **13**: 894690.

Carriqui M, Douthe C, Molins A, Flexas J. 2019. Leaf anatomy does not explain apparent short-term responses of mesophyll conductance to light and CO_2 in tobacco. *Physiologia Plantarum* **165**: 604–618.

Carvalho MR, Jaramillo C, de la Parra F, Caballero-Rodríguez D, Herrera F, Wing S, Turner BL, D'Apolito C, Romero-Báez M, Narváez P *et al.* 2021. Extinction at the end-Cretaceous and the origin of modern Neotropical rainforests. *Science* **372**: 63–68.

Castro S, Ferrero V, Loureiro J, Espadaler X, Silveira P, Navarro L. 2010. Dispersal mechanisms of the narrow endemic Polygala vayredae: dispersal syndromes and spatio-temporal variations in ant dispersal assemblages. *Plant Ecology* **207**: 359–372.

Cenozoic CO_2 Proxy Integration Project (CenCO_2PIP) Consortium, Hönisch B, Royer DL, Breecker DO, Polissar PJ, Bowen GJ, Henehan MJ, Cui Y, Steinthorsdottir M, McElwain JC *et al.* 2023. Toward a Cenozoic history of atmospheric CO_2. *Science* **382**: eadi5177.

Cernusak LA, Ubierna N, Winter K, Holtum JA, Marshall JD, Farquhar GD. 2013. Environmental and physiological determinants of carbon isotope discrimination in terrestrial plants. *New Phytologist* **200**: 950–965.

Chaloner WG. 1984. 13th Birbal Sahni Memorial lecture: plants animals and time. *Journal of Palaeosciences* **32**: 197–202.

Chaloner WG. 1986. Electrostatic forces in insect pollination and their significance in exine ornament. In: Blackmore S, Ferguson IK, eds. *Pollen and spores. Form and function, Vol. 2*. London, UK: Academic Press, 103–108.

Chaloner WG, McElwain JC. 1997. The fossil plant record and global climatic change. *Review of Palaeobotany and Palynology* **95**: 73–82.

Chaloner WG, Sheerin A. 1979. Devonian macrofloras. *Special Papers in Palaeontology* **23**: 145–161.

Channing A, Edwards D. 2009. Yellowstone hot spring environments and the palaeo-ecophysiology of Rhynie chert plants: towards a synthesis. *Plant Ecology and Diversity* **2**: 111–143.
Chapin FS 3rd. 2003. Effects of plant traits on ecosystem and regional processes: a conceptual framework for predicting the consequences of global change. *Annals of Botany* **91**: 455–463.
Chapin FS. 1980. The mineral nutrition of wild plants. *Annual Review of Ecology and Systematics* **11**: 233–260.
Chapman JL. 1994. Distinguishing internal developmental characteristics from external palaeoenvironmental effects in fossil wood. *Review of Palaeobotany and Palynology* **81**: 19–32.
Chave J, Andalo C, Brown S, Cairns MA, Chambers JQ, Eamus D, Fölster H, Fromard F, Higuchi N, Kira T *et al.* 2005. Tree allometry and improved estimation of carbon stocks and balance in tropical forests. *Oecologia* **145**: 87–99.
Chave J, Coomes D, Jansen S, Lewis SL, Swenson NG, Zanne AE. 2009. Towards a worldwide wood economics spectrum. *Ecology Letters* **12**: 351–366.
Cheesman AW, Duff H, Hill K, Cernusak LA, McInerney FA. 2020. Isotopic and morphologic proxies for reconstructing light environment and leaf function of fossil leaves: a modern calibration in the Daintree Rainforest, Australia. *American Journal of Botany* **107**: 1165–1176.
Choat B, Cobb AR, Jansen S. 2008. Structure and function of bordered pits: new discoveries and impacts on whole-plant hydraulic function. *New Phytologist* **177**: 608–626.
Choat B, Jansen S, Brodribb TJ, Cochard H, Delzon S, Bhaskar R, Bucci SJ, Feild TS, Gleason SM, Hacke UG *et al.* 2012. Global convergence in the vulnerability of forests to drought. *Nature* **491**: 752–755.
Christin PA, Osborne CP, Chatelet DS, Columbus JT, Besnard G, Hodkinson TR, Garrison LM, Vorontsova MS, Edwards EJ. 2013. Anatomical enablers and the evolution of C4 photosynthesis in grasses. *Proceedings of the National Academy of Sciences, USA* **110**: 1381–1386.
Christoffoleti P, Caetano RSX. 1998. Soil seed banks. *Scientia Agricola* **55**: 74–78.
Cichan MA. 1986. Conductance in the wood of selected Carboniferous plants. *Paleobiology* **12**: 302–310.
Cleal CJ, Thomas BA. 2005. Palaeozoic tropical rainforests and their effect on global climates: is the past the key to the present? *Geobiology* **3**: 13–31.
Coley PD. 1987. Patrones en las defensas de las plantas por qué. *Revista de Biología Tropical* **35**: 151–164.
Coley PD, Barone JA. 1996. Herbivory and plant defenses in tropical forests. *Annual Review of Ecology and Systematics* **27**: 305–335.
Collinson ME. 1983. Accumulations of fruits and seeds in three small sedimentary environments in southern England and their palaeoecological implications. *Annals of Botany* **52**: 583–592.
Cornwell WK, Cornelissen JH, Amatangelo K, Dorrepaal E, Eviner VT, Godoy O, Hobbie SE, Hoorens B, Kurokawa H, Perez-Harguindeguy N *et al.* 2008. Plant species traits are the predominant control on litter decomposition rates within biomes worldwide. *Ecology Letters* **11**: 1065–1071.
Cornwell WK, Elvira A, van Kempen L, van Logtestijn RS, Aptroot A, Cornelissen JH. 2015. Flammability across the gymnosperm phylogeny: the importance of litter particle size. *New Phytologist* **206**: 672–681.
Creber GT, Chaloner WG. 1984. Influence of environmental factors on the wood structure of living and fossil trees. *The Botanical Review* **50**: 357–448.
Cruzan MB. 1990. Variation in pollen size, fertilization ability, and postfertilization siring ability in *Erythronium grandiflorum*. *Evolution* **44**: 843–856.
Csergo AM, Salguero-Gomez R, Broennimann O, Coutts SR, Guisan A, Angert AL, Welk E, Stott I, Enquist BJ, McGill B *et al.* 2017. Less favourable climates constrain demographic strategies in plants. *Ecology Letters* **20**: 969–980.
Cúneo NR, Taylor EL, Taylor TN, Krings M. 2003. *In situ* fossil forest from the upper Fremouw Formation (Triassic) of Antarctica: paleoenvironmental setting and paleoclimate analysis. *Palaeogeography, Palaeoclimatology, Palaeoecology* **197**: 239–261.
Currano ED, Jacobs BF. 2021. Bug-bitten leaves from the early Miocene of Ethiopia elucidate the impacts of plant nutrient concentrations and climate on insect herbivore communities. *Global and Planetary Change* **207**: 103655.
Currano ED, Wilf P, Wing SL, Labandeira CC, Lovelock EC, Royer DL. 2008. Sharply increased insect herbivory during the Paleocene-Eocene Thermal Maximum. *Proceedings of the National Academy of Sciences, USA* **105**: 1960–1964.
Dassanayake M, Larkin JC. 2017. Making plants break a sweat: the structure, function, and evolution of plant salt glands. *Frontiers in Plant Science* **8**: 406.
Decombeix AL. 2013. Bark anatomy of an Early Carboniferous tree from Australia. *IAWA Journal* **34**: 183–196.
Decombeix A-L, Boura A, Tomescu AMF. 2019. Plant hydraulic architecture through time: lessons and questions on the evolution of vascular systems. *IAWA Journal* **40**: 387–420.
Del Tredici P. 2007. The phenology of sexual reproduction in ginkgo biloba: ecological and evolutionary implications. *Botanical Review* **73**: 267–278.
DeVore ML, Kenrick P, Pigg KB, Ketcham RA. 2006. Utility of high resolution x-ray computed tomography (HRXCT) for paleobotanical studies: an example using London Clay fruits and seeds. *American Journal of Botany* **93**: 1848–1851.
Dewhirst RA, Smirnoff N, Belcher CM. 2020. Pine species that support crown fire regimes have lower leaf-level terpene contents than those native to surface fire regimes. *Firehouse* **3**: 17.
Di Filippo A, Pederson N, Baliva M, Brunetti M, Dinella A, Kitamura K, Knapp HD, Schirone B, Piovesan G. 2015. The longevity of broadleaf deciduous trees in Northern Hemisphere temperate forests: insights from tree-ring series. *Frontiers in Ecology and Evolution* **3**: 46.
Diaz S, Cabido M. 1997. Plant functional types and ecosystem function in relation to global change. *Journal of Vegetation Science* **8**: 463–474.
Diaz S, Kattge J, Cornelissen JH, Wright IJ, Lavorel S, Dray S, Reu B, Kleyer M, Wirth C, Prentice IC *et al.* 2016. The global spectrum of plant form and function. *Nature* **529**: 167–171.
Diefendorf AF, Freeman KH, Wing SL, Graham HV. 2011. Production of n-alkyl lipids in living plants and implications for the geologic past. *Geochimica et Cosmochimica Acta* **75**: 7472–7485.
Diefendorf AF, Leslie AB, Wing SL. 2015. Leaf wax composition and carbon isotopes vary among major conifer groups. *Geochimica et Cosmochimica Acta* **170**: 145–156.
Dilcher DL. 1974. Approaches to the identification of angiosperm leaf remains. *Botanical Review* **40**: 1–157.
DiMichele WA, Elrick SD, Bateman RM. 2013. Growth habit of the late Paleozoic rhizomorphic tree-lycopsid family Diaphorodendraceae: phylogenetic, evolutionary, and paleoecological significance. *American Journal of Botany* **100**: 1604–1625.
Dostalek T, Rokaya MB, Munzbergova Z. 2020. Plant palatability and trait responses to experimental warming. *Scientific Reports* **10**: 10526.
Dow GJ, Bergmann DC, Berry JA. 2014. An integrated model of stomatal development and leaf physiology. *New Phytologist* **201**: 1218–1226.
Duerden H. 1993. On the xylem elements of certain fossil pteridophyta. *Annals of Botany* **47**: 187–195.
Dutta D, Ambwani K. 2007. Capers: a food for Upper Cretaceous dinosaurs of Pisdura, India. *Current Science* **92**: 897–899.
Duursma RA, Blackman CJ, Lopéz R, Martin-StPaul NK, Cochard H, Medlyn BE. 2019. On the minimum leaf conductance: its role in models of plant water use, and ecological and environmental controls. *New Phytologist* **221**: 693–705.
Edwards D, Axe L. 2004. Anatomical evidence in the detection of the earliest wildfires. *PALAIOS* **19**: 113–128.
Edwards D, Geng BY, Li CS. 2016. New plants from the lower Devonian Pingyipu Group, Jiangyou County, Sichuan Province, China. *PLoS ONE* **11**: e0163549.
Edwards D, Li CS, Raven JA. 2006. Tracheids in an early vascular plant: a tale of two branches. *Botanical Journal of the Linnean Society* **150**: 115–130.
Edwards EJ. 2019. Evolutionary trajectories, accessibility and other metaphors: the case of C4 and CAM photosynthesis. *New Phytologist* **223**: 1742–1755.
Ejsmond MJ, Wrońska-Pilarek D, Ejsmond A, Dragosz-Kluska D, Karpińska-Kołaczek M, Kołaczek P, Kozłowski J. 2011. Does climate affect pollen morphology? Optimal size and shape of pollen grains under various desiccation intensity. *Ecosphere* **2**: art117.
Enquist BJ, Niklas KJ. 2001. Invariant scaling relations across tree-dominated communities. *Nature* **410**: 655–660.
Esperança Júnior MG, Cybis GB, Iannuzzi R. 2023. An efficient method for estimating vein density of Glossopteris and its application. *Palaeontology* **66**: e12640.

Ethier GJ, Livingston NJ. 2004. On the need to incorporate sensitivity to CO_2 transfer conductance into the Farquhar-von Caemmerer-Berry leaf photosynthesis model. *Plant, Cell and Environment* **27**: 137–153.

Evans JR, Sharkey TD, Berry JA, Farquhar GD. 1986. Carbon isotope discrimination measured concurrently with gas exchange to investigate CO_2 diffusion in leaves of higher plants. *Australian Journal of Plant Physiology* **13**: 281–292.

Evans-FitzGerald C, Porter AS, Yiotis C, Elliott-Kingston C, McElwain JC. 2016. Co-ordination in morphological leaf traits of early diverging angiosperms is maintained following exposure to experimental palaeo-atmospheric conditions of sub-ambient O_2 and elevated CO_2. *Frontiers in Plant Science* 7: 1368.

Falcon-Lang HJ. 2000a. A method to distinguish between woods produced by evergreen and deciduous coniferopsids on the basis of growth ring anatomy: a new palaeoecological tool. *Palaeontology* **43**: 785–793.

Falcon-Lang HJ. 2000b. The relationship between leaf longevity and growth ring markedness in modern conifer woods and its implications for palaeoclimatic studies. *Palaeogeography, Palaeoclimatology, Palaeoecology* **160**: 317–328.

Falcon-Lang HJ, Cantrill DJ. 2001. Gymnosperm woods from the Cretaceous (mid-Aptian) Cerro Negro Formation, Byers Peninsula, Livingston Island, Antarctica: the arborescent vegetation of a volcanic arc. *Cretaceous Research* **22**: 277–293.

Falcon-Lang HJ, Scott AC. 2000. Upland ecology of some Late Carboniferous cordaitalean trees from Nova Scotia and England. *Palaeogeography, Palaeoclimatology, Palaeoecology* **156**: 225–242.

Falster DS, Westoby M. 2003. Plant height and evolutionary games. *Trends in Ecology & Evolution* **18**: 337–343.

Farquhar GD, O'Leary MH, Berry JA. 1982. On the relationship between carbon isotope discrimination and the intercellular carbon dioxide concentration in leaves. *Australian Journal of Plant Physiology* **9**: 121–137.

Feild TS, Chatelet DS, Balun L, Schilling EE, Evans R. 2011. The evolution of angiosperm lianescence without vessels–climbing mode and wood structure-function in *Tasmannia cordata* (Winteraceae). *New Phytologist* **193**: 229–240.

Feild TS, Chatelet DS, Brodribb TJ. 2009. Ancestral xerophobia: a hypothesis on the whole plant ecophysiology of early angiosperms. *Geobiology* **7**: 237–264.

Ferguson DK. 2005. Plant taphonomy: ruminations on the past, present, and the future. *PALAIOS* **20**: 418–428.

Field C, Mooney HA. 1986. The photosynthesis-nitrogen relationship in wild plants. In: Givnish TJ, ed. *On the economy of plant form*. Cambridge, UK: Cambridge University Press, 25–55.

Flexas J, Scoffoni C, Gago J, Sack L. 2013. Leaf mesophyll conductance and leaf hydraulic conductance: an introduction to their measurement and coordination. *Journal of Experimental Botany* **64**: 3965–3981.

Floudas D, Binder M, Riley R, Barry K, Blanchette RA, Henrissat B, Martinez AT, Otillar R, Spatafora JW, Yadav JS *et al.* 2012. The Paleozoic origin of enzymatic lignin decomposition reconstructed from 31 fungal genomes. *Science* **336**: 1715–1719.

Franchi GG, Piotto B, Nepi M, Baskin CC, Pacini E. 2011. Pollen and seed desiccation tolerance in relation to degree of developmental arrest, dispersal, and survival. *Journal of Experimental Botany* **65**: 5267–5281.

Franks PJ, Beerling DJ. 2009. Maximum leaf conductance driven by CO_2 effects on stomatal size and density over geologic time. *Proceedings of the National Academy of Sciences, USA* **106**: 10343–10347.

Franks PJ, Berry JA, Lombardozzi DL, Bonan GB. 2017. Stomatal function across temporal and spatial scales: deep-time trends, land-atmosphere coupling and global models. *Plant Physiology* **174**: 583–602.

Franks PJ, Royer DL, Beerling DJ, Van de Water PK, Cantrill DJ, Barbour MM, Berry JA. 2014. New constraints on atmospheric CO_2 concentration for the Phanerozoic. *Geophysical Research Letters* **41**: 4685–4694.

Freschet GT, Aerts R, Cornelissen JHC. 2012. A plant economics spectrum of litter decomposability. *Functional Ecology* **26**: 56–65.

Friedman WE, Cook ME. 2000. The origin and early evolution of tracheids in vascular plants: integration of palaeobotanical and neobotanical data. *Philosophical Transactions of the Royal Society of London. Series B: Biological Sciences* **355**: 857–868.

Fu X, Meinzer FC, Woodruff DR, Liu YY, Smith DD, McCulloh KA, Howard AR. 2019. Coordination and trade-offs between leaf and stem hydraulic traits and stomatal regulation along a spectrum of isohydry to anisohydry. *Plant, Cell & Environment* **42**: 2245–2258.

Gago J, Carriqui M, Nadal M, Clemente-Moreno MJ, Coopman RE, Fernie AR, Flexas J. 2019. Photosynthesis optimized across land plant phylogeny. *Trends in Plant Science* **24**: 947–958.

Galtier J, Meyer-Berthaud B. 2006. The diversification of early arborescent seed ferns. *The Journal of the Torrey Botanical Society* **133**: 7–19.

García-Plazaola JI, Fernández-Marín B, Duke SO, Hernández A, López-Arbeloa F, Becerril JM. 2015. Autofluorescence: biological functions and technical applications. *Plant Science* **236**: 136–145.

Gastaldo RA. 2001. Terrestrial plants. In: Briggs DEG, Crowther PR, eds. *Palaeobiology II*. Oxford: Blackwell Scientific, 312–315.

Gensel PG, Berry CM. 2016. Sporangial morphology of the early Devonian zosterophyll *Sawdonia ornata* from the type locality (Gaspé). *International Journal of Plant Sciences* **177**: 618–632.

Gill AM, Ashton DH. 1968. The role of bark type in relative tolerance to fire of three central Victorian Eucalypts. *Australian Journal of Botany* **16**: 491–498.

Glasspool IJ, Edwards D, Axe L. 2004. Charcoal in the Silurian as evidence for the earliest wildfire. *Geology* **32**: 381.

Gleason SM, Butler DW, Ziemińska K, Waryszak P, Westoby M. 2012. Stem xylem conductivity is key to plant water balance across Australian angiosperm species. *Functional Ecology* **26**: 343–352.

Goddéris Y, Donnadieu Y, Mills BJW. 2023. What models tell us about the evolution of carbon sources and sinks over the phanerozoic. *Annual Review of Earth and Planetary Sciences* **51**: 471–492.

Gomez B, Martin-Closas C, Barale G, Solé de Porta N, Thévenard F, Guignard G. 2002. Frenelopsis (Coniferales: Cheirolepidiaceae) and related male organ genera from the Lower Cretaceous of Spain. *Palaeontology* **45**: 997–1036.

Gómez-Noguez F, León-Rossano LM, Mehltreter K, Orozco-Segovia A, Rosas-Pérez I, Pérez-García B. 2017. Experimental measurements of terminal velocity of fern spores. *American Fern Journal* **107**: 59–71.

Gora EM, Lucas JM, Gonzalez A. 2019. Dispersal and nutrient limitations of decomposition above the forest floor: evidence from experimental manipulations of epiphytes and macronutrients. *Functional Ecology* **33**: 2417–2429.

Green AJ, Baltzinger C, Lovas-Kiss Á. 2021. Plant dispersal syndromes are unreliable, especially for predicting zoochory and long-distance dispersal. *Oikos* **2**: 1–11.

Green WA. 2010. The function of the aerenchyma in arborescent lycopsids: evidence of an unfamiliar metabolic strategy. *Proceedings of the Royal Society B: Biological Sciences* **277**: 2257–2267.

Greenwood DR, Donovan SK. 1991. *The taphonomy of plant macrofossils. The processes of fossilization*. New York, NY, USA: Columbia University Press.

Grigore MN, Toma C. 2020. *Integrative anatomy of halophytes from Mediterranean climate. Handbook of halophytes: from molecules to ecosystems towards biosaline agriculture*. Springer.

Grime JP, Cornelissen JHC, Thompson K, Hodgson JG. 1996. Evidence of a causal connection between anti-herbivore defence and the decompositionrate of leaves. *Oikos* 77: 489–494.

Grimes ST, Davies KL, Butler IB, Brock F, Edwards D, Rickard D, Briggs DEG, Parkes RJ. 2002. Fossil plants from the Eocene London Clay: the use of pyrite textures to determine the mechanism of pyritization. *Journal of the Geological Society* **159**: 493–501.

Grootemaat S, Wright IJ, Bodegom PM, Cornelissen JHC, Cornwell WK. 2015. Burn or rot: leaf traits explain why flammability and decomposability are decoupled across species. *Functional Ecology* **29**: 1486–1497.

Guimarães PR, Galetti M, Jordano P. 2008. Seed dispersal anachronisms: rethinking the fruits extinct megafauna ate. *PLoS ONE* **3**: e1745.

Habgood KS, Hass H, Kerp H. 2003. Evidence for an early terrestrial food web: coprolites from the Early Devonian Rhynie chert. *Earth and Environmental Science Transactions of the Royal Society of Edinburgh* **94**: 371–389.

Hacke UG, Sperry JS, Feild TS, Sano Y, Sikkema EH, Pittermann J. 2007. Water transport in vesselless angiosperms: conducting efficiency and cavitation safety. *International Journal of Plant Sciences* **168**: 1113–1126.

Hacke UG, Sperry JS, Pittermann J. 2004. Analysis of circular bordered pit function II. Gymnosperm tracheids with torus-margo pit membranes. *American Journal of Botany* **91**: 386–400.

Halbritter H, Ulrich S, Grímsson F, Weber M, Zetter R, Hesse M, Buchner R, Svojtka M, Frosch-Radivo A. 2018. *Illustrated pollen terminology.* Springer.

Harley PC, Loreto F, Di Marco G, Sharkey TD. 1992. Theoretical considerations when estimating the mesophyll conductance to CO_2 flux by the analysis of the response of photosynthesis to CO_2. *Plant Physiology* **98**: 1429–1436.

Haworth M, Raschi A. 2014. An assessment of the use of epidermal micro-morphological features to estimate leaf economics of Late Triassic–Early Jurassic fossil Ginkgoales. *Review of Palaeobotany and Palynology* **205**: 1–8.

He T, Belcher CM, Lamont BB, Lim SL. 2016. A 350-million legacy of fire adaptation among conifers. *Journal of Ecology* **104**: 352–363.

He T, Lamont BB, Downes KS. 2011. Banksia born to burn. *New Phytologist* **191**: 184–196.

He T, Pausas JG, Belcher CM, Schwilk DW, Lamont BB. 2012. Fire-adapted traits of Pinus arose in the fiery Cretaceous. *New Phytologist* **194**: 751–759.

Heinen JH, Florens FBV, Baider C, Hume JP, Kissling WD, Whittaker RJ, Rahbek C, Borregaard MK. 2023. Novel plant-frugivore network on Mauritius is unlikely to compensate for the extinction of seed dispersers. *Nature Communications* **14**: 1019.

Hempson GP, Midgley JJ, Lawes MJ, Vickers KJ, Kruger LM. 2014. Comparing bark thickness: testing methodswith bark– stem data from two South African fire-prone biomes. *Journal of Vegetation Science* **25**: 1247–1256.

Hesse M, Vogel S, Halbritter H. 2000. Thread-forming structures in angiosperm anthers: their diverse role in pollination ecology. *Plant Systematics and Evolution* **222**: 281–292.

Hoffman LA, Tomescu AM. 2013. An early origin of secondary growth: *Franhueberia gerriennei* gen. et sp. nov. from the Lower Devonian of Gaspé (Quebec, Canada). *American Journal of Botany* **100**: 754–763.

Hoffmann WA, Orthen B, Nascimento PKVD. 2003. Comparative fire ecology of tropical savanna and forest trees. *Functional Ecology* **17**: 720–726.

van den Honert TH. 1948. Water transport in plants as a catenary process. *Discussions of the Faraday Society* **3**: 146.

Hotton CL, Hueber FM, Griffing DH, Bridge JS. 2001. Early terrestrial plant environments: an example from the Emsian of Gaspé, Canada. In: Gensel PG, Edwards D, eds. *Plants invade the land: evolutionary and environmental perspectives.* New York, NY, USA: Columbia University Press, 179–212.

Hu S, Dilcher DL, Jarzen DM, Winship Taylor D. 2008. Early steps of angiosperm pollinator coevolution. *Proceedings of the National Academy of Sciences, USA* **105**: 240–245.

Hughes L, Dunlop M, French K, Leishman MR, Rice B, Rodgerson L, Westoby M. 1994. Predicting dispersal spectra: a minimal set of hypotheses based on plant attributes. *The Journal of Ecology* **82**: 933.

Jackson ST, Myford ME. 1999. Pollen dispersal models in quaternary plant ecology: assumptions, parameters, and prescriptions. *Botanical Review* **65**: 39–75.

Jardine PE, Kent M, Fraser WT, Lomax BH. 2019. Ginkgo leaf cuticle chemistry across changing pCO_2 regimes. *PalZ* **93**: 549–558.

Jarvis SC, Whitehead DC. 1981. The influence of some soil and plant factors on the concentration of copper in perennial ryegrass. *Plant and Soil* **60**: 275–286.

Jasechko S, Sharp ZD, Gibson JJ, Birks SJ, Yi Y, Fawcett PJ. 2013. Terrestrial water fluxes dominated by transpiration. *Nature* **496**: 347–350.

Jia Z, von Wiren N. 2020. Signaling pathways underlying nitrogen-dependent changes in root system architecture: from model to crop species. *Journal of Experimental Botany* **71**: 4393–4404.

Jones TP, Chaloner WG. 1991. Fossil charcoal, its recognition and palaeoatmospheric significance. *Palaeogeography, Palaeoclimatology, Palaeoecology* **97**: 39–50.

Juhrbandt J, Leuschner C, Hölscher D. 2004. The relationship between maximal stomatal conductance and leaf traits in eight Southeast Asian early successional tree species. *Forest Ecology and Management* **202**: 245–256.

Kaack L, Weber M, Isasa E, Karimi Z, Li S, Pereira L, Trabi CL, Zhang Y, Schenk HJ, Schuldt B *et al.* 2021. Pore constrictions in intervessel pit membranes provide a mechanistic explanation for xylem embolism resistance in angiosperms. *New Phytologist* **230**: 1829–1843.

Kane JM, Varner JM, Hiers JK. 2008. The burning characteristics of southeastern oaks: discriminating fire facilitators from fire impeders. *Forest Ecology and Management* **256**: 2039–2045.

Karabourniotis G, Horner HT, Bresta P, Nikolopoulos D, Liakopoulos G. 2020. New insights into the functions of carbon-calcium inclusions in plants. *New Phytologist* **228**: 845–854.

Kelly R, Healy K, Anand M, Baudraz MEA, Bahn M, Cerabolini BEL, Cornelissen JHC, Dwyer JM, Jackson AL, Kattge J *et al.* 2021. Climatic and evolutionary contexts are required to infer plant life history strategies from functional traits at a global scale. *Ecology Letters* **24**: 970–983.

Kenrick P, Crane PR. 1991. Water-conducting cells in early fossil land plants: implications for the early evolution of tracheophytes. *Botanical Gazette* **152**: 335–356.

Kenrick P, Crane PR. 1997. The origin and early evolution of plants on land. *Nature* **389**: 33–39.

Kenrick P, Wellman CH, Schneider H, Edgecombe GD. 2012. A timeline for terrestrialization: consequences for the carbon cycle in the Palaeozoic. *Philosophical Transactions of the Royal Society of London. Series B, Biological Sciences* **367**: 519–536.

Kerp H, Bomfleur B. 2011. Photography of plant fossils – new techniques, old tricks. *Review of Palaeobotany and Palynology* **166**: 117–151.

King DA, Davies SJ, Tan S, Noor NSM. 2006. The role of wood density and stem support costs in the growth and mortality of tropical trees. *Journal of Ecology* **94**: 670–680.

Klavins S, Taylor EL, Krings M, Taylor T. 2001. An unusual, structurally preserved ovule from the Permian of Antarctica. *Review of Palaeobotany and Palynology* **115**: 107–117.

Konzmann S, Kluth M, Karadana D, Lunau K. 2019. Pollinator effectiveness of a specialist bee exploiting a generalist plant—tracking pollen transfer by *Heriades truncorum* with quantum dots. *Apidologie* **51**: 201–211.

Kouwenberg LLR, Hines RR, McElwain JC. 2007. A new transfer technique to extract and process thin and fragmented fossil cuticle using polyester overlays. *Review of Palaeobotany and Palynology* **145**: 243–248.

Kröber W, Plath I, Heklau H, Bruelheide H. 2015. Relating stomatal conductance to leaf functional traits. *Journal of Visualized Experiments* **12**: 52738.

Kürschner WM. 1997. The anatomical diversity of recent and fossil leaves of the durmast oak (*Quercus petraea* Lieblein/*Q. pseudocastanea* Goeppert)—implications for their use as biosensors of palaeoatmospheric CO_2 levels. *Review of Palaeobotany and Palynology* **96**: 1–30.

Labandeira CC. 1998. Early history of arthropod and vascular plant associations. *Annual Review of Earth and Planetary Sciences* **26**: 329–377.

Labandeira CC, Allen EG. 2007. Minimal insect herbivory for the Lower Permian Coprolite Bone Bed site of north-central Texas, USA, and comparison to other Late Paleozoic floras. *Palaeogeography, Palaeoclimatology, Palaeoecology* **247**: 197–219.

Lavorel S, Diaz S, Hans J, Cornelissen C, Garnier E, Harrison SP, McIntyre S, Pausas JG, Pérez-Harguindeguy N, Roumet C *et al.* 2007. *Terrestrial ecosystems in a changing world.* Berlin, Heidelberg, Germany: Springer.

Lavorel S, Garnier E. 2002. Predicting changes in community composition and ecosystem functioning from plant traits: revisiting the Holy Grail. *Functional Ecology* **16**: 545–556.

Lawes MJ, Midgley JJ, Clarke PJ, Jones R. 2013. Costs and benefits of relative bark thickness in relation to fire damage: a savanna/forest contrast. *Journal of Ecology* **101**: 517–524.

Lawson T, Vialet-Chabrand S. 2019. Speedy stomata, photosynthesis and plant water use efficiency. *New Phytologist* **221**: 93–98.

Lawson T, Weyers JD, A'Brook R. 1998. The nature of heterogeneity in the stomatal behaviour of *Phaseolus vulgaris* L. primary leaves. *Journal of Experimental Botany* **49**: 1387–1395.

Leide J, Hildebrandt U, Reussing K, Riederer M, Vogg G. 2007. The developmental pattern of tomato fruit wax accumulation and its impact on cuticular transpiration barrier properties: effects of a deficiency in a b-ketoacyl-coenzyme A synthase (LeCER6). *Plant Physiology* **144**: 1667–1679.

Leide J, Nierop KG, Deininger AC, Staiger S, Riederer M, de Leeuw JW. 2020. Leaf cuticle analyses: implications for the existence of cutan/non-ester cutin and its biosynthetic origin. *Annals of Botany* **126**: 141–162.

Leishman MR, Westoby M. 1998. Seed size and shape are not related to persistence in soil in Australia in the same way as in Britain. *Functional Ecology* **12**: 480–485.

Lenton TM, Daines SJ, Mills BJW. 2018. COPSE reloaded: an improved model of biogeochemical cycling over Phanerozoic time. *Earth-Science Reviews* **178**: 1–28.

Liu F, Bomfleur B, Peng H, Li Q, Kerp H, Zhu H. 2018. 280-m.y.-old fossil starch reveals early plant–animal mutualism. *Geology* **46**: 423–426.

Liu F, Peng H, Marshall JEA, Lomax BH, Bomfleur B, Kent MS, Fraser WT, Philip EJ. 2023. Dying in the sun: direct evidence for elevated UV-B radiation at the end-Permian mass extinction. *Science Advances* **9**: eabo6102.

Liu G, Cornwell WK, Pan X, Cao K, Ye X, Huang Z, Dong M, Cornelissen JHC, Austin A. 2014. Understanding the ecosystem implications of the angiosperm rise to dominance: leaf litter decomposability among magnoliids and other basal angiosperms. *Journal of Ecology* **102**: 337–344.

Liu J, Lindstrom AJ, Chen Y, Nathan R, Gong X. 2021. Congruence between ocean-dispersal modelling and phylogeography explains recent evolutionary history of *Cycas* species with buoyant seeds. *New Phytologist* **232**: 1863–1875.

Logan KJ, Thomas BA. 1987. The distribution of lignin derivatives in fossil plants. *New Phytologist* **105**: 157–173.

Looy CV. 2013. Natural history of a plant trait: branch-system abscission in Paleozoic conifers and its environmental, autecological, and ecosystem implications in a fire-prone world. *Paleobiology* **39**: 235–252.

Looy CV, van Konijnenburg-van Cittert JH, Duijnstee IA. 2021. Proliferation of isoëtalean lycophytes during the Permo-Triassic biotic crises: a proxy for the state of the terrestrial biosphere. *Frontiers in Earth Science* **9**: 615370.

Lovas-Kiss Á, Vizi B, Vincze O, Attila Molnár V, Green AJ. 2018. Endozoochory of aquatic ferns and angiosperms by mallards in Central Europe. *Journal of Ecology* **106**: 1714–1723.

Luo X, Keenan TF, Chen JM, Croft H, Colin Prentice I, Smith NG, Walker AP, Wang H, Wang R, Xu C *et al.* 2021. Global variation in the fraction of leaf nitrogen allocated to photosynthesis. *Nature Communications* **12**: 4866.

Luthardt L, Rößler R, Schneider JW. 2017. Tree-ring analysis elucidating palaeo-environmental effects captured in an *in situ* fossil forest – the last 80 years within an early Permian ecosystem. *Palaeogeography, Palaeoclimatology, Palaeoecology* **487**: 278–295.

Mack AL. 2000. Did fleshy fruit pulp evolve as a defence against seed loss rather than as a dispersal mechanism? *Journal of Biosciences* **25**: 93–97.

de Magalhães RMQ, Schwilk DW. 2012. Leaf traits and litter flammability: evidence for non-additive mixture effects in a temperate forest. *Journal of Ecology* **100**: 1153–1163.

Malekhosseini M, Ensikat HJ, McCoy VE, Wappler T, Weigend M, Kunzmann L, Rust J. 2022. Traces of calcium oxalate biomineralization in fossil leaves from late Oligocene maar deposits from Germany. *Scientific Reports* **12**: 15959.

Males J, Griffiths H. 2017. Stomatal biology of CAM plants. *Plant Physiology* **174**: 550–560.

Manchester SR, O'Leary EL. 2010. Phylogenetic distribution and identification of fin-winged fruits. *The Botanical Review* **76**: 1–82.

Matsunaga KK, Manchester SR, Srivastava R, Kapgate DK, Smith SY. 2019. Fossil palm fruits from India indicate a Cretaceous origin of Arecaceae tribe Borasseae. *Botanical Journal of the Linnean Society* **190**: 260–280.

Matsunaga KK, Tomescu AM. 2017. An organismal concept for *Sengelia radicans* gen. et sp. nov.–morphology and natural history of an Early Devonian lycophyte. *Annals of Botany* **119**: 1097–1113.

Matthaeus WJ, Macarewich SI, Richey J, Montañez IP, McElwain JC, White JD, Wilson JP, Poulsen CJ. 2023. A systems approach to understanding how plants transformed earth's environment in deep time. *Annual Review of Earth and Planetary Sciences* **51**: 551–580.

Matthaeus WJ, Montañez IP, McElwain JC, Wilson JP, White JD. 2022. Stems matter: xylem physiological limits are an accessible and critical improvement to models of plant gas exchange in deep time. *Frontiers in Ecology and Evolution* **10**: 955066.

Mayr S, Kartusch B, Kikuta S. 2014. Evidence for air-seeding: watching the formation of embolism in conifer xylem. *Journal of Plant Hydraulics* **1**: e004.

McDowell N, Pockman WT, Allen CD, Breshears DD, Cobb N, Kolb T, Plaut J, Sperry J, West A, Williams DG *et al.* 2008. Mechanisms of plant survival and mortality during drought: why do some plants survive while others succumb to drought? *New Phytologist* **178**: 719–739.

McElwain JC. 2018. Paleobotany and global change: important lessons for species to biomes from vegetation responses to past global change. *Annals of Botany* **69**: 761–787.

McElwain JC, Chaloner WG. 1996. The fossil cuticle as a skeletal record of environmental change. *PALAIOS* **11**: 376–388.

McElwain JC, Steinthorsdottir M. 2017. Paleoecology, ploidy, paleoatmospheric composition, and developmental biology: a review of the multiple uses of fossil stomata. *Plant Physiology* **174**: 650–664.

McElwain JC, Yiotis C, Lawson T. 2016. Using modern plant trait relationships between observed and theoretical maximum stomatal conductance and vein density to examine patterns of plant macroevolution. *New Phytologist* **209**: 94–103.

McLoughlin S, Pott C. 2019. Plant mobility in the mesozoic: disseminule dispersal strategies of Chinese and Australian Middle Jurassic to Early Cretaceous plants. *Palaeogeography, Palaeoclimatology, Palaeoecology* **515**: 47–69.

McLoughlin S, Prevec R. 2021. The reproductive biology of glossopterid gymnosperms — a review. *Review of Palaeobotany and Palynology* **295**: 104527.

McNamara ME, Rossi V, Slater TS, Rogers CS, Ducrest AL, Dubey S, Roulin A. 2021. Decoding the evolution of Melanin in vertebrates. *Trends in Ecology & Evolution* **36**: 430–443.

Medina NG, Estebanez B. 2014. Does spore ultrastructure mirror different dispersal strategies in mosses? A study of seven iberian orthotrichum species. *PLoS ONE* **9**: e112867.

Medlyn BE, Duursma RA, Eamus D, Ellsworth DS, Prentice IC, Barton CVM, Crous KY, De Angelis P, Freeman M, Wingate L. 2011. Reconciling the optimal and empirical approaches to modelling stomatal conductance. *Global Change Biology* **17**: 2134–2144.

Meinzer FC, Woodruff DR, Marias DE, Smith DD, McCulloh KA, Howard AR, Magedman AL. 2016. Mapping 'hydroscapes' along the iso- to anisohydric continuum of stomatal regulation of plant water status. *Ecology Letters* **19**: 1343–1352.

Mendes MM, Dinis JL, Gomez B, Pais J. 2010. Reassessment of the cheirolepidiaceous conifer Frenelopsis teixeirae Alvin et Pais from the Early Cretaceous (Hauterivian) of Portugal and palaeoenvironmental considerations. *Review of Palaeobotany and Palynology* **161**: 30–42.

Mendes MM, Kvaček J, Doyle JA. 2023. *Pseudofrenelopsis dinisii*, a new species of the extinct conifer family Cheirolepidiaceae from the probable lower Hauterivian (Cretaceous) of western Portugal. *Review of Palaeobotany and Palynology* **315**: 104905.

Moles AT, Ackerly DD, Webb CO, Tweddle JC, Dickie JB, Pitman AJ, Westoby M. 2005a. Factors that shape seed mass evolution. *Proceedings of the National Academy of Sciences, USA* **102**: 10540–10544.

Moles AT, Ackerly DD, Webb CO, Tweddle JC, Dickie JB, Westoby M. 2005b. A brief history of seed size. *Science* **307**: 576–580.

Moles AT, Warton DI, Warman L, Swenson NG, Laffan SW, Zanne AE, Pitman A, Hemmings FA, Leishman MR. 2009. Global patterns in plant height. *Journal of Ecology* **97**: 923–932.

Moore JP, Vicré-Gibouin M, Farrant JM, Driouich A. 2008. Adaptations of higher plant cell walls to water loss: drought vs desiccation. *Physiologia Plantarum* **134**: 237–245.

Moreau D, Bardgett RD, Finlay RD, Jones DL, Philippot L, Power S. 2019. A plant perspective on nitrogen cycling in the rhizosphere. *Functional Ecology* **33**: 540–552.

Mosle B, Finch P, Collinson ME, Scott AC. 1997. Comparison of modern and fossil plant cuticles by selective chemical extraction monitored by flash pyrolysis-gas chromatography-mass spectrometry and electron microscopy. *Journal of Analytical and Applied Pyrolysis* **40-41**: 585–597.

Moyroud E, Wenzel T, Middleton R, Rudall PJ, Banks H, Reed A, Mellers G, Killoran P, Westwood MM, Steiner U *et al.* 2017. Disorder in convergent floral nanostructures enhances signalling to bees. *Nature* **550**: 469–474.

Muller J. 1979. Form and function in angiosperm pollen. *Annals of the Missouri Botanical Garden* **66**: 593–632.

Murray DR. 2012. *Seed dispersal*. Sydney, Australia: Academic Press.

Murray M, Soh WK, Yiotis C, Batke S, Parnell AC, Spicer RA, Lawson T, Caballero R, Wright IJ, Purcell C *et al.* 2019. Convergence in maximum stomatal conductance of C(3) woody angiosperms in natural ecosystems across bioclimatic zones. *Frontiers in Plant Science* **10**: 558.

Murray M, Soh WK, Yiotis C, Spicer RA, Lawson T, McElwain JC. 2020. Consistent relationship between field-measured stomatal conductance and theoretical maximum stomatal conductance in C3 woody angiosperms in four major biomes. *International Journal of Plant Sciences* **181**: 142–154.

Nelsen MP, DiMichele WA, Peters SE, Boyce CK. 2016. Delayed fungal evolution did not cause the Paleozoic peak in coal production. *Proceedings of the National Academy of Sciences, USA* **113**: 2442–2447.

Nguyen Tu TT, Bocherens H, Mariotti A, Baudin F, Pons D, Broutin J, Derenne S, Largeau C. 1999. Ecological distribution of Cenomanian terrestrial plants based on C13/C12 ratios. *Palaeogeography, Palaeoclimatology, Palaeoecology* **145**: 79–93.

Niechayev NA, Pereira PN, Cushman JC. 2019. Understanding trait diversity associated with crassulacean acid metabolism (CAM). *Current Opinion in Plant Biology* **49**: 74–85.

Niinemets Ü, Díaz-Espejo A, Flexas J, Galmés J, Warren CR. 2009. Role of mesophyll diffusion conductance in constraining potential photosynthetic productivity in the field. *Journal of Experimental Botany* **60**: 2249–2270.

Niklas KJ. 1980. Evidence for lignin-like constituents in early Silurian (Llandoverian) plant fossils. *Science* **28**: 396–397.

Niklas KJ. 1981. The chemistry of fossil plants. *Bioscience* **31**: 820–825.

Niklas KJ. 1983. Organelle preservation and protoplast partitioning in fossil angiosperm leaf tissues. *American Journal of Botany* **70**: 543–548.

Niklas KJ. 1985a. The evolution of tracheid diameter in early vascular plants and its implications on the hydraulic conductance of the primary xylem strand. *Evolution* **39**: 1110–1122.

Niklas KJ. 1985b. The aerodynamics of wind pollination. *Botanical Review* **51**: 328–386.

Niklas KJ. 1992. *Plant biomechanics: an engineering approach to plant form and function.* Chicago, IL, USA: Univeristy of Chicago Press.

Niklas KJ. 1994. Predicting the height of fossil plant remains: an allometric approach to an old problem. *American Journal of Botany* **81**: 1235–1242.

Nogué S, de Nascimento L, Graham L, Brown LA, González LAG, Castilla-Beltrán A, Penuelas J, Fernández-Palacios JM, Willis K. 2022. The spatiotemporal distribution of pollen traits related to dispersal and desiccation tolerance in Canarian laurel forest. *Journal of Vegetation Science* **33**: e13147.

Norconk MA, Grafton BW, Conklin-Brittain NL. 1998. Seed dispersal by neotropical seed predators. *American Journal of Primatology* **45**: 103–126.

Norros V, Karhu E, Norden J, Vahatalo AV, Ovaskainen O. 2015. Spore sensitivity to sunlight and freezing can restrict dispersal in wood-decay fungi. *Ecology and Evolution* **5**: 3312–3326.

Ogburn MR, Edwards EJ. 2013. Repeated origin of three-dimensional leaf venation releases constraints on the evolution of succulence in plants. *Current Biology* **23**: 722–726.

Olson ME, Anfodillo T, Gleason SM, McCulloh KA. 2021. Tip-to-base xylem conduit widening as an adaptation: causes, consequences, and empirical priorities. *New Phytologist* **229**: 1877–1893.

Onoda Y, Richards L, Westoby M. 2012. The importance of leaf cuticle for carbon economy and mechanical strength. *New Phytologist* **196**: 441–447.

Pacini E, Hesse M. 2005. Pollenkitt – its composition, forms and functions. *Flora* **200**: 399–415.

Pacini E, Hesse M. 2012. Uncommon pollen walls: reasons and consequences. *Verhandlungen der Zoologisch-Botanischen Gesellschaft in Österreich* **148-149**: 291–306.

Pacini EF, Franchi GG. 1999. Pollen grain sporoderm and types of dispersal units. *Acta Societatis Botanicorum Poloniae* **68**: 299–305.

Paine CET, Stahl C, Courtois EA, Patiño S, Sarmiento C, Baraloto C. 2010. Functional explanations for variation in bark thickness in tropical rain forest trees. *Functional Ecology* **24**: 1202–1210.

Parlange JY, Waggoner PE. 1970. Stomatal dimensions and resistance to diffusion. *Plant Physiology* **46**: 337–342.

Pausas JG. 2014. Bark thickness and fire regime. *Functional Ecology* **29**: 315–327.

Pausas JG. 2015. Evolutionary fire ecology: lessons learned from pines. *Trends in Plant Science* **20**: 318–324.

Peco B, Traba J, Levassor C, Sánchez AM, Azcárate FM. 2003. Seed size, shape and persistence in dry Mediterranean grass and scrublands. *Seed Science Research* **13**: 87–95.

Peppe DJ, Lemons CR, Royer DL, Wing SL, Wright IJ, Lusk CH, Rhoden CH. 2014. Biomechanical and leaf–climate relationships: a comparison of ferns and seed plants. *American Journal of Botany* **101**: 338–347.

Peppe DJ, Royer DL, Cariglino B, Oliver SY, Newman S, Leight E, Enikolopov G, Fernandez-Burgos M, Herrera F, Adams JM *et al.* 2011. Sensitivity of leaf size and shape to climate: global patterns and paleoclimatic applications. *New Phytologist* **190**: 724–739.

Pérez-Harguindeguy N, Díaz S, Garnier E, Lavorel S, Poorter H, Jaureguiberry P, Bret-Harte MS, Cornwell WK, Craine JM, Gurvich DE *et al.* 2013. New handbook for standardised measurement of plant functional traits worldwide. *Australian Journal of Botany* **61**: 167.

Pérez-Harguindeguy N, Díaz S, Vendramini F, Cornelissen JHC, Gurvich DE, Cabido M. 2003. Leaf traits and herbivore selection in the field and in cafeteria experiments. *Austral Ecology* **28**: 642–650.

Philips TL, DiMichele WA. 1992. Comparative ecology and life-history biology of arborescent lycopsids in late carboniferous swamps of Euramerica. *Annals of the Missouri Botanical Garden* **79**: 560–588.

van der Pijl L. 1969. *Principles of dispersal in higher plants.* Berlin, Germany: Springer.

Pittermann J. 2010. The evolution of water transport in plants: an integrated approach. *Geobiology* **8**: 112–139.

Pittermann J, Limm E, Rico C, Christman MA. 2011. Structure-function constraints of tracheid-based xylem: a comparison of conifers and ferns. *New Phytologist* **192**: 449–461.

Pittermann J, Sperry JS, Hacke UG, Wheeler JK, Sikkema EH. 2005. Torus-margo pits help conifers compete with angiosperms. *Science* **310**: 1924.

Pittermann J, Sperry JS, Hacke UG, Wheeler JK, Sikkema EH. 2006. Inter-tracheid pitting and the hydraulic efficiency of conifer wood: the role of tracheid allometry and cavitation protection. *American Journal of Botany* **93**: 1265–1273.

van der Plas F, Schroder-Georgi T, Weigelt A, Barry K, Meyer S, Alzate A, Barnard RL, Buchmann N, de Kroon H, Ebeling A *et al.* 2020. Plant traits alone are poor predictors of ecosystem properties and long-term ecosystem functioning. *Nature Ecology & Evolution* **4**: 1602–1611.

Pole M, Philippe M. 2010. Cretaceous plant fossils of Pitt Island, the Chatham group, New Zealand. *Alcheringa* **34**: 231–263.

Pons TL, Flexas J, von Caemmerer S, Evans JR, Genty B, Ribas-Carbo M, Brugnoli E. 2009. Estimating mesophyll conductance to CO_2: methodology, potential errors, and recommendations. *Journal of Experimental Botany* **60**: 2217–2234.

Poorter H, Niinemets Ü, Poorter L, Wright IJ, Villar R. 2009. Causes and consequences of variation in leaf mass per area (LMA): a meta-analysis. *New Phytologist* **182**: 565–588.

Poorter L, Bongers F. 2006. Leaf traits are good predictors of plant performance across 53 rain forest species. *Ecology* **87**: 1733–1743.

Porre RJ, van der Werf W, De Deyn GB, Stomph TJ, Hoffland E. 2020. Is litter decomposition enhanced in species mixtures? A meta-analysis. *Soil Biology and Biochemistry* **145**: 107791.

Raven JA, Spicer RA. 1996. The evolution of crassulacean acid metabolism. In: Winter K, Smith JAC, eds. *Crassulacean acid metabolism: biochemistry, ecophysiology and evolution.* Berlin, Heidelberg, Germany: Springer, 360–385.

Reich PB. 2014. The world-wide 'fast–slow' plant economics spectrum: a traits manifesto. *Journal of Ecology* **102**: 275–301.

Reich PB, Uhl C, Walters MB, Ellsworth DS. 1991. Leaf lifespan as a determinant of leaf structure and function among 23 amazonian tree species. *Oecologia* **86**: 16–24.

Reich PB, Walters MB, Ellsworth DS. 1992. Leaf life-span in relation to leaf, plant, and stand characteristics among diverse ecosystems. *Ecological Monographs* **62**: 365–392.

Reichgelt T, D'Andrea WJ, Valdivia-McCarthy AD, Fox BR, Bannister JM, Conran JG, Lee WG, Lee DE. 2020. Elevated CO_2, increased leaf-level productivity, and water-use efficiency during the early Miocene. *Climate of the Past* **16**: 1509–1521.

Reitalu T, Gerhold P, Poska A, Pärtel M, Väli V, Veski S. 2015. Novel insights into post-glacial vegetation change: functional and phylogenetic diversity in pollen records. *Journal of Vegetation Science* **26**: 911–922.

Reitalu T, Nogué S. 2023. Functional vegetation change over millennia. *Nature Ecology & Evolution* **7**: 174–175.

Robledo-Arnuncio JJ, Klein EK, Muller-Landau HC, Santamaría L. 2014. Space, time and complexity in plant dispersal ecology. *Movement Ecology* **2**: 16.

Rockwell FE, Holbrook NM. 2017. Leaf hydraulic architecture and stomatal conductance: a functional perspective. *Plant Physiology* **174**: 1996–2007.

Rojas TN, Zampini IC, Isla MI, Blendinger PG. 2022. Fleshy fruit traits and seed dispersers: which traits define syndromes? *Annals of Botany* **129**: 831–838.

Romanek CS, Grossman EL, Morse JW. 1992. Carbon isotopic fractionation in synthetic aragonite and calcite: effects of temperature and precipitation rate. *Geochimica et Cosmochimica Acta* **56**: 419–430.

Rosell JA. 2019. Bark in woody plants: understanding the diversity of a multifunctional structure. *Integrative and Comparative Biology* **59**: 535–547.

Rosell JA, Castorena M, Laws CA, Westoby M. 2015. Bark ecology of twigs vs. main stems: functional traits across eighty-five species of angiosperms. *Oecologia* **178**: 1033–1043.

Rosell JA, Olson ME, Anfodillo T, Martinez-Mendez N. 2017. Exploring the bark thickness-stem diameter relationship: clues from lianas, successive cambia, monocots and gymnosperms. *New Phytologist* **215**: 569–581.

Rosenfield MV, Keller JK, Clausen C, Cyphers K, Funk JL. 2020. Leaf traits can be used to predict rates of litter decomposition. *Oikos* **129**: 1589–1596.

Rößler R, Zierold T, Feng Z, Kretzschmar R, Merbitz M, Annacker V, Schneider JW. 2012. A snapshot of an early Permian ecosystem preserved by explosive volcanism: new results from the Chemnitz Petrified Forest, Germany. *PALAIOS* **27**: 814–834.

Roth-Nebelsick A, Uhl D, Mosbrugger V, Kerp H. 2001. Evolution and function of leaf venation architecture: a review. *Annals of Botany* **87**: 553–566.

Roth-Nebelsick A, Konrad W. 2003. Assimilation and transpiration capabilities of rhyniophytic plants from the Lower Devonian and their implications for paleoatmospheric CO_2 concentration. *Palaeogeography, Palaeoclimatology, Palaeoecology* **202**: 153–178.

Royer DL, Miller IM, Peppe DJ, Hickey LJ. 2010. Leaf economic traits from fossils support a weedy habit for early angiosperms. *American Journal of Botany* **97**: 438–445.

Royer DL, Sack L, Wilf P, Lusk CH, Jordan GJ, Niinemets Ü, Wright IJ, Westoby M, Cariglino B, Coley PD *et al.* 2007. Fossil leaf economics quantified: calibration, Eocene case study, and implications. *Paleobiology* **33**: 574–589.

Sack L, Caringella M, Scoffoni C, Mason C, Rawls M, Markesteijn L, Poorter L. 2014. Leaf vein length per unit area is not intrinsically dependent on image magnification: avoiding measurement artifacts for accuracy and precision. *Plant Physiology* **166**: 829–838.

Sack L, Scoffoni C. 2013. Leaf venation: structure, function, development, evolution, ecology and applications in the past, present and future. *New Phytologist* **198**: 983–1000.

Sack L, Scoffoni C, John GP, Poorter H, Mason C, Mendez-Alonzo R, Donovan LA. 2013. How do leaf veins influence the worldwide leaf economic spectrum? Review and synthesis. *Journal of Experimental Botany* **64**: 4053–4080.

Sack L, Scoffoni C, McKown AD, Frole K, Rawls M, Havran JC, Tran H, Tran T. 2012. Developmentally based scaling of leaf venation architecture explains global ecological patterns. *Nature Communications* **3**: 837.

Sage RF. 2017. A portrait of the C4 photosynthetic family on the 50th anniversary of its discovery: species number, evolutionary lineages, and Hall of Fame. *Journal of Experimental Botany* **68**: 11–28.

Salguero-Gomez R, Jones OR, Jongejans E, Blomberg SP, Hodgson DJ, Mbeau-Ache C, Zuidema PA, de Kroon H, Buckley YM. 2016. Fast-slow continuum and reproductive strategies structure plant life-history variation worldwide. *Proceedings of the National Academy of Sciences, USA* **113**: 230–235.

van der Sande MT, Bush MB, Akesson CM, Berrio JC, Correia Metrio A, Flantua SGA, Hooghiemstra H, Maezumi SY, McMichael CNH, Montoya E *et al.* 2023. Warming, drought, and disturbances lead to shifts in functional composition: a millennial-scale analysis for Amazonian and Andean sites. *Global Change Biology* **29**: 4775–4792.

Sande MT, Gosling W, Correa-Metrio A, Prado-Junior J, Poorter L, Oliveira RS, Mazzei L, Bush MB. 2019. A 7000-year history of changing plant trait composition in an Amazonian landscape; the role of humans and climate. *Ecology Letters* **22**: 925–935.

Santos J, Al-Azzawi M, Aronson J, Flowers TJ. 2016. eHALOPH a database of salt-tolerant plants: helping put halophytes to work. *Plant & Cell Physiology* **57**: e10.

dos Santos Nascimento LB, Leal-Costa MV, Menezes EA, Lopes VR, Muzitano MF, Costa SS, Tavares ES. 2015. Ultraviolet-B radiation effects on phenolic profile and flavonoid content of Kalanchoe pinnata. *Journal of Photochemistry and Photobiology. B* **148**: 73–81.

Schopf JM. 1975. Modes of fossil preservation. *Review of Palaeobotany and Palynology* **20**: 20–53.

Schulte PJ, Hacke UG. 2021. Solid mechanics of the torus-margo in conifer intertracheid bordered pits. *New Phytologist* **229**: 1431–1439.

Schulze ED, Kelliher FM, Korner C, Lloyd J, Leuning R. 1994. Relationships among maximum stomatal conductance, ecosystem surface conductance, carbon assimilation rate, and plant nitrogen nutrition: a global ecology scaling exercise. *Annual Review of Ecology and Systematics* **25**: 629–660.

Schwendemann AB, Wang G, Mertz ML, McWilliams RT, Thatcher SL, Osborn JM. 2007. Aerodynamics of saccate pollen and its implications for wind pollination. *American Journal of Botany* **94**: 1371–1381.

Schwilk DW, Ackerly DD. 2001. Flammability and serotiny as strategies: correlated evolution in pines. *Oikos* **94**: 326–336.

Schwilk DW, Caprio AC. 2011. Scaling from leaf traits to fire behaviour: community composition predicts fire severity in a temperate forest. *Journal of Ecology* **99**: 970–980.

Scott AC, Glasspool IJ. 2006. The diversification of Paleozoic fire systems and fluctuations in atmospheric oxygen concentration. *Proceedings of the National Academy of Sciences, USA* **103**: 10861–10865.

Sheldon ND, Smith SY, Stein R, Ng M. 2020. Carbon isotope ecology of gymnosperms and implications for paleoclimatic and paleoecological studies. *Global and Planetary Change* **184**: 103060.

Sims HJ, Cassara JA. 2009. The taphonomic fidelity of seed size in fossil assemblages: a live-dead case study. *PALAIOS* **24**: 387–393.

Slot M, Nardwattanawong T, Hernández GG, Bueno A, Riederer M, Winter K. 2021. Large differences in leaf cuticle conductance and its temperature response among 24 tropical tree species from across a rainfall gradient. *New Phytologist* **232**: 1618–1631.

Soh WK, Wright IJ, Bacon KL, Lenz TI, Steinthorsdottir M, Parnell AC, McElwain JC. 2017. Palaeo leaf economics reveal a shift in ecosystem function associated with the end-Triassic mass extinction event. *Nature Plants* **3**: 17104.

Soh WK, Yiotis C, Murray M, Pernell A, Wright IJ, Spicer RA, Lawson T, Caballero R, McElwain JC. 2019. Rising CO_2 drives divergence in water use efficiency of evergreen and deciduous plants. *Science Advances* **5**: eaax7906.

Sperry JS. 2000. Hydraulic constraints on plant gas exchange. *Agricultural and Forest Meteorology* **104**: 13–23.

Sperry JS, Hacke UG, Oren R, Comstock JP. 2002. Water deficits and hydraulic limits to leaf water supply. *Plant, Cell & Environment* **25**: 251–263.

Sperry JS, Meinzer FC, McCulloh KA. 2008. Safety and efficiency conflicts in hydraulic architecture: scaling from tissues to trees. *Plant, Cell & Environment* **31**: 632–645.

Spicer RA. 1989. The formation and interpretation of plant fossil assemblages. *Advances in Botanical Research* **16**: 95–191.

Spicer RA, Yang J, Spicer TE, Farnsworth A. 2021. Woody dicot leaf traits as a palaeoclimate proxy: 100 years of development and application. *Palaeogeography, Palaeoclimatology, Palaeoecology* **562**: 110138.

Stearns SC. 1992. *The evolution of life histories.* Oxford, UK: Oxford University Press.

Stein WE, Mannolini F, Hernick LV, Landing E, Mays C. 2007. A new high-paleolatitude late Permian permineralized peat flora from the Sydney Basin, Australia. *Nature* **446**: 904–907.

Steinthorsdottir M, Woodward FI, Surlyk F, McElwain JC. 2012. Deep-time evidence of a link between elevated CO_2 concentrations and perturbations in the hydrological cycle via drop in plant transpiration. *Geology* **40**: 815–818.

Stroo A. 2000. Pollen morphological evolution in bat pollinated plants. *Plant Systematics and Evolution* **222**: 225–242.

Strullu-Derrien C, Kenrick P, Badel E, Cochard H, Tafforeau P. 2013. An overview of the hydraulic systems in early land plants. *IAWA Journal* **34**: 333–351.

Sun G, Dilcher DL, Zheng S, Zhou Z. 1998. In search of the first flower: a Jurassic angiosperm, Archaefructus, from northeast China. *Science* **27**: 1692–1695.

Swift MJ. 1977. The ecology of wood decomposition. *Science Progress* **64**: 175–199.

Tegelaar EW, Kerp H, Visscher H, Schenck P, de Leeuw JW. 1991. Bias of the paleobotanical record as a consequence of variations in the chemical composition of higher vascular plant cuticles. *Paleobiology* **17**: 133–144.

Thomas BA, Cleal CJ. 1999. Abscission in the fossil record. In: Kurmann MH, Hemsley AR, eds. *The evolution of plant architecture.* Kew, UK: Royal Botanic Gardens, 183–203.

Thomas BA, Cleal CJ. 2018. Arborescent lycophyte growth in the late Carboniferous coal swamps. *New Phytologist* **218**: 885–890.
Thompson K, Band SR, Hodgson JG. 1993. Seed size and shape predict persistence in soil. *Functional Ecology* **7**: 236–241.
Tiffney BH. 1984. Seed size, dispersal syndromes, and the rise of the angiosperms: evidence and hypothesis. *Annals of the Missouri Botanical Garden* **71**: 551.
Tiffney BH. 2004. Vertebrate dispersal of seed plants through time. *Annual Review of Ecology, Evolution, and Systematics* **35**: 1–29.
Tomas M, Flexas J, Copolovici L, Galmes J, Hallik L, Medrano H, Ribas-Carbo M, Tosens T, Vislap V, Niinemets U. 2013. Importance of leaf anatomy in determining mesophyll diffusion conductance to CO_2 across species: quantitative limitations and scaling up by models. *Journal of Experimental Botany* **64**: 2269–2281.
Trewin NH. 1994. Depositional environment and preservation of the biota in the lower Devonian hot springs of Rhynie, Aberdeenshire, Scotland. *Transactions of the Royal Society of Edinburgh: Earth Sciences* **84**: 433–442.
Uhl C, Kauffman JB. 1990. Deforestation, fire susceptibility, and potential tree responses to fire in the Eastern Amazon. *Ecology* **71**: 437–449.
Uhl D, Mosbrugger V. 1999. Leaf venation density as a climate and environmental proxy: a critical review and new data. *Palaeogeography Palaeoclimatology Palaeoecology* **149**: 15–26.
Vaissière BE, Vinson SB. 1994. Pollen morphology and its effect on pollenl collection by honey bees, *Apis mellifera* L. (Hymenoptera: Apidae), with special Reference to Upland Cotton, *Gossypium Hirsutum* L. (Malvaceae). *Grana* **33**: 128–138.
Vajda V, Linderson H, McLoughlin S. 2016. Disrupted vegetation as a response to Jurassic volcanism in southern Sweden. *Geological Society, London, Special Publications* **434**: 127–147.
Vaknin Y, Gan-Mor S, Bechar A, Ronen B, Eisikowitch D. 2000. The role of electrostatic forces in pollination. *Plant Systematics and Evolution* **222**: 133–142.
Vaknin Y, Hadas R, Schafferman D, Murkhovsky L, Bashan N. 2008. The potential of milk thistle (*Silybum marianum* L.), an Israeli native, as a source of edible sprouts rich in antioxidants. *International Journal of Food Sciences and Nutrition* **59**: 339–346.
Vakrahmeev VA. 1991. *Jurassic and Cretaceous floras and climates of the earth.* Cambridge, UK: Cambridge University Press.
Valenta K, Nevo O. 2020. The dispersal syndrome hypothesis: how animals shaped fruit traits, and how they did not. *Functional Ecology* **34**: 1158–1169.
Valenta K, Nevo O. 2022. The illusiveness of seed dispersal syndromes. A commentary on: fleshy fruit traits and seed dispersers: which traits define syndromes? *Annals of Botany* **129**: vi–vii.
Van der Burgh J. 1994. Differences in fossil seed/fruit-, wood-, and leaf-floras, taphonomy and ecological implications. *Review of Palaeobotany and Palynology* **83**: 119–129.
Venturas MD, Sperry JS, Hacke UG. 2017. Plant xylem hydraulics: what we understand, current research, and future challenges. *Journal of Integrative Plant Biology* **59**: 356–389.
Veromann-Jurgenson LL, Tosens T, Laanisto L, Niinemets U. 2017. Extremely thick cell walls and low mesophyll conductance: welcome to the world of ancient living! *Journal of Experimental Botany* **68**: 1639–1653.
Vincent JFV. 1990. Fracture properties of plants. In: Callow JA, ed. *Advances in botanical research incorporating advances in plant pathology, vol. 17*. Cambridge, MA, USA: Academic Press, 235–287.
Violle C, Navas M-L, Vile D, Kazakou E, Fortunel C, Hummel I, Garnier E. 2007. Let the concept of trait be functional! *Oikos* **116**: 882–892.
Vitali R, Belcher CM, Kaplan JO, Watson AJ. 2022. Increased fire activity under high atmospheric oxygen concentrations is compatible with the presence of forests. *Nature Communications* **13**: 7285.
Vonhof MJ, Harder LD. 1995. Size-number trade-offs and pollen production by papilionaceous legumes. *American Journal of Botany* **82**: 230–238.
Wang J, Pfefferkorn HW, Zhang Y, Feng Z. 2012. Permian vegetational Pompeii from Inner Mongolia and its implications for landscape paleoecology and paleobiogeography of Cathaysia. *Proceedings of the National Academy of Sciences, USA* **109**: 4927–4932.
Weaver L, McLoughlin S, Drinnan A. 1997. Fossil woods from the Upper Permian Bainmedart Coal Measures, northern Prince Charles Mountains, East Antarctica. *AGSO Journal of Australian Geology and Geophysics* **16**: 655–676.
Weyers JD, Lawson T. 1997. Heterogeneity in stomatal characteristics. *Advances in Botanical Research* **26**: 317–352.
White JD, Montañez IP, Wilson JP, Poulsen CJ, McElwain JC, DiMichele WA, Hren MT, Macarewich S, Richey JD, Matthaeus WJ. 2020. A process-based ecosystem model (Paleo-BGC) to simulate the dynamic response of Late Carboniferous plants to elevated O_2 and aridification. *American Journal of Science* **320**: 547–598.
Williams MR, Abbott I. 1991. Quantifying average defoliation using leaf-level measurements. *Ecology* **72**: 1510–1511.
Williams VL, Witkowski ETF, Balkwill K. 2007. Relationship between bark thickness and diameter at breast height for six tree species used medicinally in South Africa. *South African Journal of Botany* **73**: 449–465.
Wilson JP. 2013. Modeling 400 million years of plant hydraulics. *The Paleontological Society Papers* **19**: 175–194.
Wilson JP. 2016. Hydraulics of Psilophyton and evolutionary trends in plant water transport after terrestrialization. *Review of Palaeobotany and Palynology* **227**: 65–76.
Wilson JP, Fischer WW. 2011. Hydraulics of *Asteroxylon mackei*, an early Devonian vascular plant, and the early evolution of water transport tissue in terrestrial plants. *Geobiology* **9**: 121–130.
Wilson JP, Knoll AH. 2010. A physiologically explicit morphospace for tracheid-based water transport in modern and extinct seed plants. *Paleobiology* **36**: 335–355.
Wilson JP, Knoll AH, Holbrook M, Marshall CR. 2008. Modeling fluid flow in Medullosa, an anatomically unusual carboniferous seed plant. *Paleobiology* **34**: 472–493.
Wilson JP, Montañez IP, White JD, DiMichele WA, McElwain JC, Poulsen CJ, Hren MT. 2017. Dynamic Carboniferous tropical forests: new views of plant function and potential for physiological forcing of climate. *New Phytologist* **215**: 1333–1353.
Wilson JP, Oppler G, Reikowski E, Smart J, Marquardt C, Keller B. 2023. Physiological selectivity and plant–environment feedbacks during middle and Late Pennsylvanian plant community transitions. *Geological Society, London, Special Publications* **535**: 361–382.
Wilson JP, White JD, Dimichele WA, Hren MT, Poulsen CJ, McElwain JC, Montañez IP. 2015. Reconstructing extinct plant water use for understanding vegetation–climate feedbacks: methods, synthesis, and a case study using the Paleozoic-era medullosan seed ferns. *The Paleontological Society Papers* **21**: 167–196.
Wilson JP, White JD, Montanez IP, DiMichele WA, McElwain JC, Poulsen CJ, Hren MT. 2020. Carboniferous plant physiology breaks the mold. *New Phytologist* **227**: 667–679.
Wing SL, Boucher LD. 1998. Ecological aspects of the Cretaceous flowering plant radiation. *Annual Review of Earth and Planetary Sciences* **26**: 379–421.
Winter K, Holtum JA, Smith JAC. 2015. Crassulacean acid metabolism: a continuous or discrete trait? *New Phytologist* **208**: 73–78.
Wojewódzka A, Baczyński J, Banasiak Ł, Downie SR, Czarnocka-Cieciura A, Frankiewicz K, Spalik K. 2019. Evolutionary shifts in fruit dispersal syndromes in Apiaceae tribe Scandiceae. *Plant Systematics and Evolution* **305**: 401–414.
Wright IJ, Dong N, Maire V, Prentice IC, Westoby M, Díaz S, Gallagher RV, Jacobs BF, Kooyman R. 2017. Global climatic drivers of leaf size. *Science* **357**: 917–921.
Wright IJ, Reich PB, Westoby M, Ackerly DD, Baruch Z, Bongers F, Cavender-Baress J, Chapin T, Cornelissen JHC, Diemer M *et al.* 2004. The worldwide leaf economics spectrum. *Nature* **428**: 821–827.
Wu J, Serbin SP, Ely KS, Wolfe BT, Dickman LT, Grossiord C, Michaletz ST, Collins AD, Detto M, McDowell NG *et al.* 2020. The response of stomatal conductance to seasonal drought in tropical forests. *Global Change Biology* **26**: 823–839.
Yang B, Qin C, Wang J, He M, Melvin TM, Osborn TJ, Briffa KR. 2014. A 3,500-year tree-ring record of annual precipitation on the northeastern Tibetan Plateau. *Proceedings of the National Academy of Sciences, USA* **111**: 2903–2908.
Yang J, Spicer RA, Spicer TEV, Li CS. 2011. 'CLAMP Online': a new web-based palaeoclimate tool and its application to the terrestrial Paleogene and Neogene of North America. *Palaeobiodiversity and Palaeoenvironments* **91**: 163–183.
Yao L, Ogle K, Lichstein JW, Jackson ST. 2022. Estimation of pollen productivity and dispersal: how pollen assemblages in small lakes represent vegetation. *Ecological Monographs* **92**: e1513.
Yiotis C, McElwain JC. 2019. A novel hypothesis for the role of photosynthetic physiology in shaping macroevolutionary patterns. *Plant Physiology* **181**: 1148–1162.

Zanne AE, Tank DC, Cornwell WK, Eastman JM, Smith SA, FitzJohn RG, McGlinn DJ, O'Meara BC, Moles AT, Reich PB *et al.* 2014. Three keys to the radiation of angiosperms into freezing environments. *Nature* **506**: 89–92.

Zanne AE, Westoby M, Falster DS, Ackerly DD, Loarie SR, Arnold SE, Coomes DA. 2010. Angiosperm wood structure: global patterns in vessel anatomy and their relation to wood density and potential conductivity. *American Journal of Botany* **97**: 207–215.

Zeisler V, Schreiber L. 2016. Epicuticular wax on cherry laurel (*Prunus laurocerasus*) leaves does not constitute the cuticular transpiration barrier. *Planta* **243**: 65–81.

Zhang J, Li H, Zhang H, Zhang H, Tang Z. 2021. Responses of litter decomposition and nutrient dynamics to nitrogen addition in temperate shrublands of North China. *Frontiers in Plant Science* **11**: 618675.

Zhang X, Gelin U, Spicer RA, Wu F, Farnsworth A, Chen P, Del Rio C, Li S, Liu J, Huang J *et al.* 2022. Rapid Eocene diversification of spiny plants in subtropical woodlands of central Tibet. *Nature Communications* **13**: 3787.

Ziemińska K, Butler DW, Gleason SM, Wright IJ, Westoby M. 2013. Fibre wall and lumen fractions drive wood density variation across 24 Australian angiosperms. *AoB Plants* **5**: plt046.

Zieminska K, Westoby M, Wright IJ. 2015. Broad anatomical variation within a narrow wood density range – a study of twig wood across 69 Australian angiosperms. *PLoS ONE* **10**: e0124892.

Supporting Information

Additional Supporting Information may be found online in the Supporting Information section at the end of the article.

Notes S1 Area of a leaf.

Notes S2 Leaf water potential.

Notes S3 Leaf dry matter content.

Notes S4 Leaf and leaf litter PH.

Notes S5 Seedling functional morphology trait.

Notes S6 Spinescence.

Notes S7 Shoot branching architecture.

Table S1 Assessment of contemporary plant traits for potential utilization as paleo-traits.

Please note: Wiley is not responsible for the content or functionality of any Supporting Information supplied by the authors. Any queries (other than missing material) should be directed to the *New Phytologist* Central Office.